COLUMN CALIBRATION FACTOR AND FORCE PARAMETERS TO PREDICT TEMPERATURE AND COMPOSITION DEPENDENCE OF THERMAL DIFFUSION FACTOR OF SOME SIMPLE MOLECULES

THESIS SUBMITTED FOR
THE DEGREE OF DOCTOR OF PHILOSOPHY (SCIENCE) OF THE
UNIVERSITY OF NORTH BENGAL
JANUARY 1999

By

Goutam Dasgupta, M.Sc., B.Ed.

ST - VERF

Dedicated to my
Mother Smt. Reba Dasgupta
and
Father Late Amaresh Dasgupta

List of Published and Communicated Research Work

1. A.K. Datta, G. Dasgupta and S. Acharyya, J. Phys. Soc. Japan, **59** (1990) 3602.
2. G. Dasgupta, A.K. Datta and S. Acharyya, Pramana J. Phys. **43** (1994) 81.
3. G. Dasgupta, N. Ghosh, N. Nandi, A. K. Chatterjee and S. Acharyya, J. Phys. Soc. Japan, **65** (1996) 2506.
4. G. Dasgupta, N. Ghosh, N. Nandi and S. Acharyya, J. Phys. Soc. Japan, **66** (1997) 108.
5. G. Dasgupta and S. Acharyya, J. Phys. D: Appl. Phys. **31** (1998) 1092.
6. G. Dasgupta and S. Acharyya, J. Phys. D: Appl. Phys. Communicated for Publication.

ACKNOWLEDGEMENT

At the outset I express my deepest sense of gratitude to Dr. S. Acharyya, M.Sc, D. Phil; Reader, Department of Physics, Raiganj College (University College), Raiganj, Uttar Dinajpur (W.B) for his kind guidance, whole hearted cooperation and active supervision towards the progress of the research works presented in this thesis.

I am grateful to Dr. T.K. Chatterjee, Registrar, Dr. R. Paul and Dr. B. Bhattacharyya Professors of Physics of North Bengal University and Dr. A. K. Datta, Reader, Raiganj B.Ed College, for their constant inspiration towards the progress of the research works.

I also thankfully acknowledge the enormous help of Dr. S.K. Sit, Lecturer in Physics, Raiganj Polytechnic Institute in reading the manuscript carefully.

I am indebted to all my teachers, colleagues and friends without whom my higher education might have ceased.

Finally the persistent support and encouragement offered by all my family members including my uncles : Sri Aparesh, Animesh, Kamalesh, Promothes and Samaresh Dasgupta, my elder brother Mr. Debasish Dasgupta M.Sc, B.Ed, my sister Chandana Bhattacharjee and my wife Mitra during the length of my entire education and research works will remain ever memorable in my mind.

Goutam Dasgupta 8.1.99.

(Goutam Dasgupta)
Asst teacher (Department of Physics)
Sudarsanpur D.P. U. Vidyachakra,
Sudarsanpur, Raiganj, Uttar Dinajpur,
West Bengal, INDIA, 733134

Preface

Thermal diffusion is a process in which partial separation of an isotopic or nonisotopic component occurs in a homogeneous binary or ternary gas mixture under the influence of temperature gradient. The phenomenon is well known for its wide applicability in gases, liquids and solids. It is also important in the study of various types of physicochemical natural phenomena like flames, planetary atomosphere, stellar interiors and nabulae. Moreover, thermal diffusion phenomenon being a second order effect, is concerned with the relative motions of the components in a homogeneous gas mixture under temperature gradient. It is thus important to separate ordinary and rare isotopes from technical point of view.

The main purpose of the thesis entitled "Column Calibration Factor and Force Parameters to Predict Temperature and Composition Dependence of Thermal Diffusion Factor of some Simple Molecules," is concerned with the estimation of Thermal diffusion factor α_T and force parameters of the isotopic gas mixture by thermal diffusion column measurement. The theory of thermal diffusion column (TDC) is a very complicated phenomenon. In order to improve the column theory a scaling factor F_s called the column calibration factor (CCF) as a function of cold and hot wall radii r_c and r_h, geometrical length L of a column and mean temperature $\bar{T}$ is introduced. F_s is, however, related to TD factor α_T and $\ln q_{max}$ of a TD column. q_{max} is the maximum value of separation factor q_e defined by:

$$q_e = (x_i / x_j)_{top} / (x_i / x_j)_{bottom}$$

x_i and x_j are the mass or mole fractions of the lighter (i) and the heavier (j) components of a gas mixture to be investigated.

The first chapter of the thesis is concerned with the general introduction of various experimental techniques involved in thermal diffusion. Various aspects of all the experimental techniques have widely been discussed under the heading "General introduction: Experimental details". A brief review of work on thermal diffusion column measurements has been made in chapter 2 entitled, "Brief review of the previous theoretical and experimental works".

"The scope and objective of the present works" of chapter 3 deals with the role of column calibration factor in determining α_T of a gas mixture. It is also interesting to note that α_T is a sensitive parameter to investigate intermolecular

forces like ε_{ij}/k and σ_{ij} of the molecules. Here, an attempt is made to determine the force parameters of the interacting molecules by α_T through F_s of the column.

The thermal diffusion factor α_T is of much importance to examine whether elastic or inelastic collisions occurs among the experimental molecules. So in chapter 4 different theoretical aspects to determine α_T as well as experimental α_T by the existing methods have been discussed under the title" Estimation of theoretical and experimental thermal diffusion factor."

Chapter 5 of the thesis deals with composition dependence of TDF of some inert gas mixtures at a given experimental temperature where as chapter 6 is related to the estimation of α_T of hydrogenic trace mixtures like He- T_2, He- HT and He- HD. In both cases α_T's are calculated from F_s and $\ln q_{max}$.

Chapter 7 and 8 of the thesis are concerned with the determination of the force parameters of some isotopic inert gas mixtures from their temperature dependence of α_T's obtained by the CCF method. Further the model independency of the CCF is established in chapter 8.

Thus, it becomes necessary to derive a functional relationship of F_s with r_c, r_h, L and $\bar{T}$. From the Navier- Stokes hydrodynamical equation an approximate formulation of F_s is, however, derived in chapter 9 of "The functional relationship of the column calibration factor in thermal diffusion column measurement." Approximate F_s of four different column geometries is found to be in good agreement with the respective experimental F_s. Further, the molecular force parameters of Ne as obtained from α_T by the CCF method agree well with the literature values.

The column parameters as formulated in chapter 9 are again used to get the optimum pressure of the light isotopic gas mixture like He^3- He^4. The experimental F_s when plotted against $\bar{T}$ in chapter 10 of the thesis shows the similar magnitudes and trends with respect to theoretical F_s.

To have a clear birds- eye view on the subject matter of the thesis "The summary and conclusion" is presented in chapter11.

Thus the thesis provides one with the important aspect of the column calibration factor to obtain thermal diffusion factor. Subsequently, molecular force parameters are obtained from thermal diffusion phenomenon. Moreover, an attempt is made to explain the thermal diffusion column behaviour explicitly by formulation of F_s, derived from Navier- Stokes hydrodynamical equation.

Contents

CHAPTER 1

General Introduction : Experimental Details

General Introduction : Experimental Details

Thermal diffusion in gases was first theoretically predicted by Enskog and Chapman[1]. But the existence of thermal diffusion in gases was experimentally detected by Dootson[2] in 1917 with H_2-CO_2 binary gas mixture in a Thermal diffusion column (TDC). Since then it has been drawing the attention of a large number of workers. The instrument of TD column was devised by Clusius and Dickel[3]. The elementary effect of separation of a component in a gas mixture caused by thermal diffusion in a TDC is multiplied in a simple way.

However, TD experiments can be performed with three different types of apparatuses. These are:

(i) the two bulb apparatus

(ii) the swing separator or trennschaukel and

(iii) the thermal diffusion column (TDC).

1.1) Two Bulb Apparatus : A two bulb apparatus consists of two metal brass bulbs of volumes V_1 and V_2 maintained at two different experimental temperatures. The temperature of the hot bulb is T_h and that of the cold bulb is T_c. A schematic diagram of the two bulb apparatus is shown in Fig 1.1. To prevent gravitational convective flow of the gas mixture the apparatus is held in a vertical position with its hot bulb at the top. The bulbs are usually connected by a narrow metal tube of length L and cross sectional area Q.

Under the influence of temperature gradient upon the gas mixture of uniform pressure, there is always a diffusion flow of a gas in a binary gas mixture. The equation of diffusion which governs the transport of the desired component of a gas mixture is :

$$\vec{J} = \frac{-p}{RT}\left[D_{ij} \text{ grad } x - D_T \frac{1}{T} \text{ grad } T \right] \qquad \ldots.(1.1)$$

where $\vec{J}$ is the flux density and x is the molefraction of a component in a mixture at any given pressure p. D_T and D_{ij} are the thermal diffusion coefficient

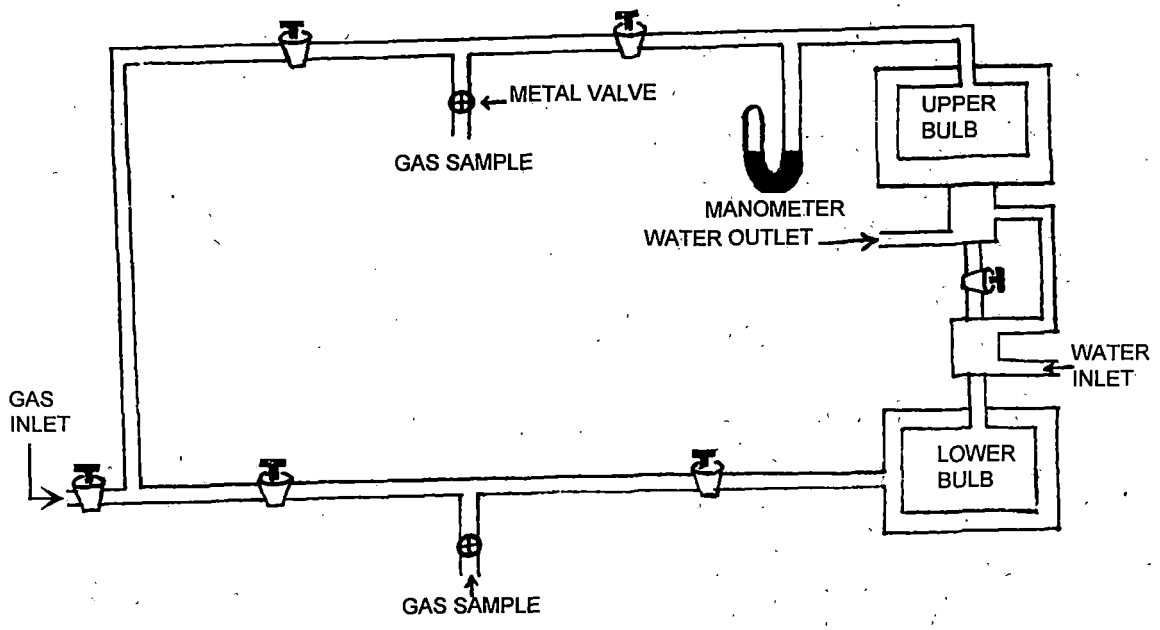

Fig. 1.1. Schematic diagram of the Two Bulb Apparatus

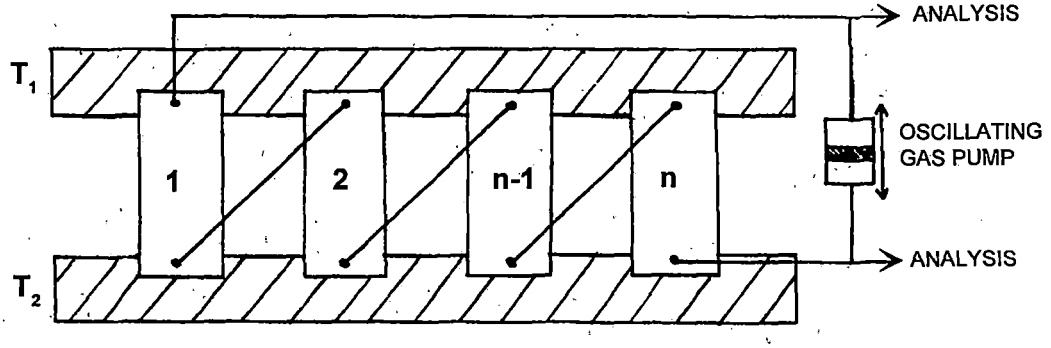

Fig. 1.2. Schematic diagram of the Swing Separator or Trennschaukel

and diffusion coefficient respectively. The partial separation of the components under temperature gradient is determined by D_T at any temperature T K. The thermal diffusion ratio K_T on the other hand, defined by $K_T = D_T/D_{ij}$, is strongly dependent on the composition of the gas mixture. It is thus desirable to introduce a composition independent factor, called the Thermal Diffusion Factor (TDF), denoted by α_T given by

$$\alpha_T = \frac{K_T}{x(1-x)} \qquad \text{.....(1.2)}$$

The flux density $\vec{J}$ is finally given by

$$\vec{J} = \frac{-pD_{ij}}{RT}[\text{grad } x - \alpha_T x (1-x) \text{ grad } \ln T]. \qquad \text{.....(1.3)}$$

At steady state condition $\vec{J}$ = O.Eq (1.3) can then be integrated to yield $\ln q_e$ where it becomes :

$$\ln q_e = \int_{T_c}^{T_h} \alpha_T \, d \ln T \qquad \text{..... (1.4)}$$

The equilibrium separation factor q_e is defined by

$$q_e = \frac{(x_i / x_j)_{top}}{(x_i / x_j)_{bottom}}.$$

Thus the TDF α_T depends strongly on the temperature, but slowly on the compositions of a gas mixture. The integration of the right hand side of eq (1.4) gives only an average thermal diffusion factor α_T at any intermediate temperature $\overline{T}$. Here, the concentration dependence of the trace components of any gas mixture is, neglected.

The α_T can also be found out from the slope of the curve of $\ln q_e$ against $\ln(T_h/T_c)$ by the relation :

$$\alpha_T = \frac{d \ln q_e}{d \ln (T_h/T_c)}, \qquad \text{..... (1.5)}$$

α_T is taken to be positive if the lighter component concentrates in the hotter part of the system.

1.2. The Swing Separator or Trennschaukel

The Swing separator or trennschaukel consists of a series of two bulbs connected by small capillary tubes as shown in Fig.1.2. The capillaries connect the bottom of stage 1 to the top of stage 2, the bottom of stage 2 to the top of stage 3 and so on. A wobbling mercury pump is used to maintan equilibrium between the hot part of stage 1 and the cold part of stage 2. The pump produces an oscillating motion of the gas mixture in the swing separator. Thus the gas composition becomes equal at the bottom and the top of the adjacent stages and over-all separation factor Q is given by

$$Q = q_e^n \qquad \text{..... (1.6)}$$

where q_e is the equlibrium separation factor of the individual stage and n is the number of stages.

Due to oscillation in the gas mixture, the volume of the gas will disturb the steady state separation in the individual separation tube. The back diffusion through the capillaries will thus reduce the oscillating effect with respect to high or low speed of the pump. The optimum speed of the pump can, however, be estimated from the theory developed by Wearden[4].

Finally, in a swing separator, eq (1.5) becomes :

$$\alpha_T = \frac{1}{n} \frac{d \ln q_e}{d \ln (T_h/T_c)} \qquad \text{.....(1.7)}$$

The swing separator has been recognised as a valuable instrument specially designed to measure α_T of isotopic mixture when the separation is very small in a two bulb apparatus. Wearden [4] had argued that the simple relation $Q = q_e^n$ are not sufficient enough for the swing separator. Here, the equality of composition at the ends of the capillary connectors are not attained in finite pumping time. Although the swing separator is a useful device to yield more accurate results, it is susceptible to various types of errors in comparison to the simple two bulb apparatus.

1.3. Thermal Diffusion Column

Thermal Diffusion Column (TDC) is a unique device to concentrate impurities of a gas mixture. The column consists of two cylindrical surfaces of which one is kept at higher temperature T_h and the other at lower temperature T_c. Unlike two bulb apparatus and swing separator in a thermal diffusion column a temperature gradient is arranged horizontally to cause convection, as a result cumulative effect occurs. To produce separation in the binary mixture by a TDC it is thus subjected to two effects. These are :

a) thermal diffusion in a horizontal direction due to temperature gradient between hot wall or wire and the cold wall of a TDC and

b) convective motion of the lighter component of a gas mixture upward near the hot wall or wire and downward for the heavier component near the cold wall of a TDC.

From the equation of continuity the differential equation in vector notation for the separation of a gas mixture in a TDC is given by :

$$\vec{\tau}_o = - \rho_{ij} D_{ij} \{\text{grad } x + \alpha_T x (1-x) \text{ grad } \ln T\} + \rho \vec{v} x \qquad \ldots\ldots (1.8)$$

where τ_0 is the transport of the desired component through a cross section of the column per unit time, x is the molefraction of the component, D_{ij} is the diffusion coefficient and ρ_{ij} is the density of the binary gas mixture. Now, considering the thermal diffusion column as a square cascade, the column equation is given by:

$$\mu \frac{\delta x}{\delta t} = (K_c + K_d) \frac{\delta^2 x}{\delta z^2} - \frac{\delta}{\delta z} \{ Px + Hx(1-x) \} \qquad \ldots\ldots\ldots (1.9)$$

where μ is the mass of the gas transported per unit length of the column, H is the initial transport coefficient which determines the enrichment of a component of the gas mixture in a TDC, K_c is the loss of enrichment due to axial counter current and K_d represents the axial back diffusion. The product stream is P in the vertical z direction. In the steady state condition $\vec{\tau}_0$ is no longer a function

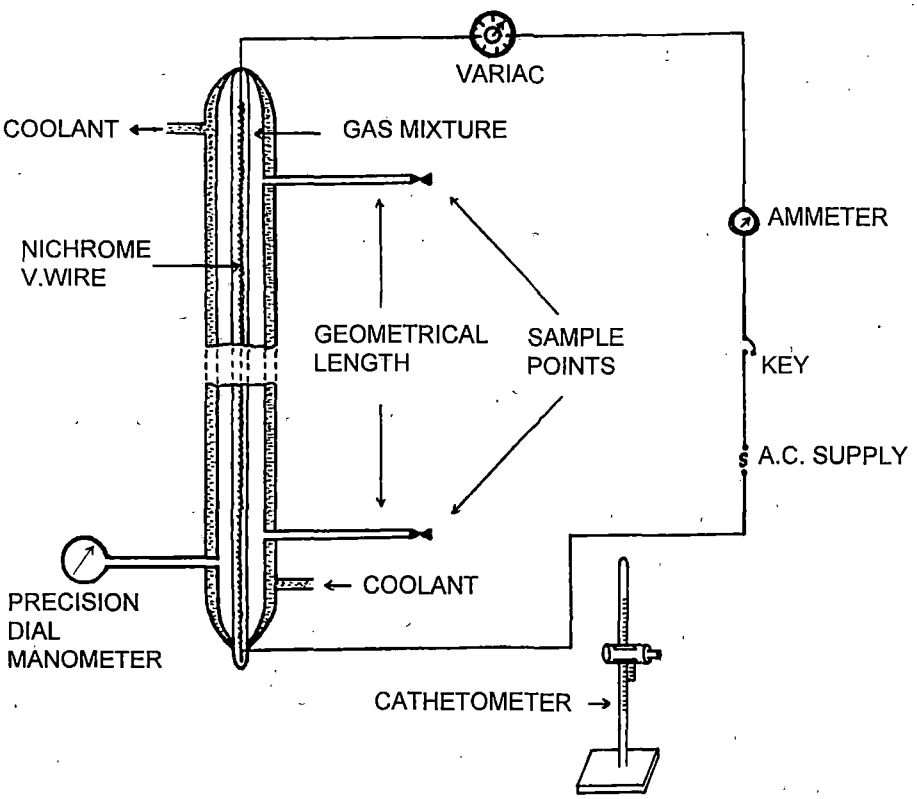

Fig. 1.3. One Stage Thermal Diffusion Column

of z and is equal to Px_p, where x_p is the molefraction of the product. Using Cohens equation[5] i.e.,

$$\frac{\delta \vec{\tau}_o}{\delta z} = - \mu \frac{\delta x}{\delta t} .$$

eq (1.9) after integration becomes :

$$\vec{\tau}_o = Px + Hx\,(1-x) - (K_c+K_d)\,\frac{\delta x}{\delta z} \qquad \ldots\ldots\ldots\ldots (1.10)$$

At total reflux i.e., with zero production rate we have P = 0. The eq (1.10) thus yields

$$\vec{\tau}_o = Hx\,(1-x) - (K_c+K_d)\,\frac{\delta x}{\delta z} .$$

As the TDC starts to work, the concentration gradient in a uniform gas mixture contained in a column is zero everywhere. This leads to

$$(\vec{\tau}_o)_{t=0} = Hx\,(1-x)$$

which represents the initial transport. At the steady state the concentration in the reservoir of the column is time independent and the net transport becomes zero. Thus for a thermal diffusion column working at total reflux we have,

$$Hx\,(1-x) = (K_c + K_d)\,\frac{\delta x}{\delta z} \qquad \ldots\ldots\ldots (1.11)$$

Introducing the equilibrium separation factor q_e and integrating eq (1.11) for a TDC of length L one gets

$$\ln q_e = \frac{HL}{K_c + K_d} , \qquad \ldots\ldots\ldots\ldots\ldots (1.12)$$

x_i and x_j are the molefractions of the lighter and the heavier components respectively at the steady state condition.

When the temperature difference between the walls of a TDC is small, the expressions for the column parameters H, K_c and K_d are given by Jones and Furry[6], Fleischmann and Jenson [7], Slieker [8], and others. The coefficient of viscosity η_{ij}, the coefficient of thermal conductivity λ_{ij}, the diffusion coefficient D_{ij}, thermal diffusion factor α_T and the density ρ_{ij} occuring in the formulae for H, K_c and K_d are taken at the mean temperature $\bar{T} = (T_h + T_c)/2$. The convective

velocity v which specify the flow of a component of a gas mixture in the TDC can be obtained from the well known Navier - Stokes equation. For a square cascade TD column the equation which describes the vertical flow of a gas as a function of horizontal x - coordinate is given by [8]

$$v = -\frac{1}{12}\frac{\rho_{ij} g}{\eta_{ij}}\frac{\Delta T}{\bar{T}}\frac{x}{d}(2x\text{-}d)(x\text{-}d). \qquad \text{..... (1.13)}$$

With some suitable boundary conditions the column parameters are finally given by [8] :

$$\left.\begin{aligned} H &= \frac{d^3 \rho_{ij}^{\,2} \alpha_T g}{6|\eta_{ij}} B \left(\frac{\Delta T}{\bar{T}}\right)^2, \\ K_c &= \frac{d^7 \rho_{ij}^{\,3} g^2}{9|\eta_{ij}^{\,2} D_{ij}} B \left(\frac{\Delta T}{\bar{T}}\right)^2 \text{and} \\ K_d &= \rho_{ij} D_{ij} B d. \end{aligned}\right\} \qquad \text{..... (1.14)}$$

Here, B is the mean circumference of the parallel plates of a TDC at a distance d apart and g is the acceleration due to gravity.

From eqs (1.12) and (1.14) for a plane parallel plate type thermal diffusion column we have

$$\ln q_e = \frac{L}{1.2d}\alpha_T \left(\frac{\Delta T}{\bar{T}}\right)\frac{m}{1+m^2} \qquad \text{..... (1.15)}$$

$$\text{where } m = \frac{d^3 \rho_{ij} g}{602.4\,\eta_{ij} D_{ij}}\left(\frac{\Delta T}{\bar{T}}\right). \qquad \text{..... (1.16)}$$

η_{ij} is independent of pressure p while ρ_{ij} and D_{ij} are proportional to p and p^{-1} respectively. α_T is pressure independent function and hence $\ln q_e$ is only a function of pressure through m, m is proportional to p^2.

From eq (1.15) it is obvious that as pressure p increases $\ln q_e$ increases

and eventually assumes a maximum value for m = 1. Thus on maximization eq (1.15) becomes

$$\ln q_{max} = \frac{L}{2.4d}\alpha_T \left(\frac{\Delta T}{\bar{T}}\right) \qquad \text{..... (1.17)}$$

and the optimum pressure p_{opt} can be obtained as :

$$p^2_{opt} = 602.4 \frac{\eta_{ij} D'_{ij}}{d^3 \rho'_{ij} g} \left(\frac{\bar{T}}{\Delta T}\right) p_0^2$$

where the transport coefficients are to be evaluated at any reference pressure p_0.

In order to develop the theory of a plane parallel type TDC[9-10] it is assumed that there is a nonturbulent convective flow of gas mixture in the column. In a thermal diffusion column it depends upon the Grashof - Prandtl number[9]. The authors are in the habit to express the Grashof - Prandtl number, Gr. Pr, as the Reynolds number R_e where

$$R_e = \frac{\rho_{ij}^2 g\, d^3}{384 \eta_{ij}^2} \left(\frac{\Delta T}{\bar{T}}\right).$$

It follows that

$$\text{Gr. Pr.} = \frac{C_p \eta_{ij}}{\lambda_{ij}} \quad 384\, R_e. \qquad \text{.....(1.18)}$$

It had been shown experimentally by Onsager and Watson[11] in a TDC that the maximum possible value of R_e<25.According to Donaldson and Watson[12] and Jones and Furry[6] R_e<14 and R_e<10 respectively. Grew and Ibbs[13] argued that spacing should be so adjusted that $5<K_c/K_d<25$. Summarizing all these facts for laminar flow in a TDC we have

$$5<R_e<10.$$

For diffusion of trace components where R_e = 0.78 the condition for laminar flow becomes

$$2.5\, P_{opt} < P < 3.6\, P_{opt}$$

The other limitations of the theory of concentric cylindrical type TDC can

be summarized as follows :

(a) the concentration and temperature dependence of the transport coefficients like ρ_{ij} . η_{ij} . D_{ij} λ_{ij} and α_T are not taken into account,

(b) for a concentric cylindrical type TDC the coefficients are measured at the mean gas temperature[9] $\bar{T}$ where

$$\bar{T} = T_c + \frac{0.56}{\ln (r_c/r_h)} \Delta T \text{ and}$$

(c) the temperature distribution along the x - axis of the TDC is determined by the conduction of heat energy alone.

For the concentric cylinder type TDC the expressions for the column parameters are given by Jones and Furry[6], Fleischman and Jenson[7], Slieker[8] and others. Velds et al[9] have, however, used these column parameters for column of cold wall radius r_c=10 mm and hot wall radii r_h=4mm, 6.7 mm and 8.3 mm respectively with cold wall temperature T_c=293K and hot wall temperature T_h=633K. The calculated values of column parameters H, K_c and K_d for concentric cylinder type columns were compared with the values for the expressions of plane parallel plates[9]. There is a clear difference between the results of column parameters H, K_c and K_d for concentric cylinder type and plane parallel plate type columns. The column parameters using Jones and Furry[6] column shape factors (CSF) were larger in magnitude than the parallel plate type in contrast with those by using either Fleischmann and Jensons[7] CSF or Slieker's CSF. However, for simplicity many of the authors [9-10] had used the plane parallel type column behaviour.

It is assumed that the approximations for the theoretical developments of a plane parallel plate type TDC do not give serious deviations between the theory and experiment. Further, the deviations are caused by the imperfectness of the TDC such as nonverticallity of the TDC and non uniformity in the diameter of the tubes. These usually invite remixing. Jones and Furry[6,14] had added a term K_p proportional to p^4 to the denominator of eq (1.12) for this remixing effects. However, different authors have made different approximations in the

formulation for H, K_c and K_d of the concentric cylinder type TDC. The agreement between the theoretical and experimental results are still not satisfactory. Better experimental results of interesting pair of molecules are, therefore, needed for the column parameters H, K_c and K_d of a concentric cylinder type TDC.

Reference

[1] S. Chapman and T. G .Cowling, (1952) The Mathematical theory of non-uniform gases (London : Cambridge University Press).

[2] S. Chapman and F. W. Dootson, Phil. Mag, **33** (1917) 248.

[3] K. Clusius and G. Dickel, Z. Ph. Chem. B **44** (1939) 397.

[4] B. L. Vander Wearden, Z. Naturf **12a** (1957) 587.

[5] K. Choen, The Theory of Isotope Separation, NNES, Ser III, vol IB, New York, Mc Graw-Hill Book Cy. Inc. (1951).

[6] R. C. Jones and W. H. Furry, Rev. Mod. Phys. **18** (1946) 151.

[7] R. Fleischmann and H. Jensen, Erg Exakt, Naturw, **20** (1942) 121.

[8] C. J. G. Slieker, Ph. D thesis, Techn, Hogeschool, Delft (1964).

[9] C.A. Velds, H.W. Grotendorst, J Los and A.E. de Vries, at at D. P. Report 392, AEE Winfrith, Dorchester, Dorset,England (1966).

[10] W. M. Rutherford and K. J. Kaminsky, J. Chem. Phys. **47** (1967) 1527.

[11] L. Onsager and W.W. Watson, Phys. Rev. **56** (1939) 474.

[12] J. Donaldson and W. W. Watson, Phys. Rev. **82** (1951) 909.

[13] K. E. Grew and T. L. Ibbs, Thermal diffusion in gases, Cambridge University Press (1952).

[14] S. Acharyya, A. K Das, P Acharyya, S. K. Datta and I.L Saha, J. Phys. Soc. Jpn. **50** (1981) 1603.

Brief Review of the Previous Theoretical and Experimental Works

Since 1911 onward a large number of workers had devoted themselves to the theoretical and experimental developments on the phenomenon of thermal diffusion in a thermal diffusion column. As a result, the literature of the subject has now become so vast that a separate monograph is required to review it properly. Here, an attempt has been made to accumulate some of the essential and important experimental and theoretical works on thermal diffusion column by different authors in different times.

The effect of thermal diffusion in liquid was discovered by Dufour[1] and Soret[2] in the middle of the 19th century. But thermal diffusion in gases was theoretically predicted in 1911 by Enskog[3] and Chapman[4]. In 1917 Chapman and Dootson[5] established the existence of thermal diffusion in gases with H_2-CO_2 gas mixture. Interests on thermal diffusion was largely increased when Clusius and Dickel[6] invented thermal diffusion column (TDC) in which the elementary effect of separation could be multiplied in a simpler way. This discovery, however, made it possible to enrich rare isotopes in amount of gram per day in multistage installation of TD columns called cascade designed by Väsaru et al[7].

The analysing technique of the two bulb apparatus were much more refined during the middle of the twentith century. With a two bulb apparatus designed by Mason[8] it becomes possible to get reliable results of thermal diffusion coefficients from the rate of approach to the steady state. In 1955 Clusius and Huber[9] have invented the swing separator in which the elementary effects of thermal diffusion can be multiplied with a known factor. However, to avoid errors much care might be taken in such measurements.

Thermal diffusion column on the other hand is easy to construct and can produce enriched isotopes in a relatively short time. With special techniques Clusius[10] had produced highly enriched rare stable isotopes by TDC. The most striking theoretical work on thermal diffusion column was done by Furry, Jones and Onsager[11], Furry and Jones[12] and Jones and Furry[13] in their classic papers. Subsequently the theory was extended by different authors [14-15]. But

only a qualitative agreement with the experimental data was observed.

Meanwhile using spherically symmetric intermolecular potential, Chapman and Enskog[16] succeeded very well in predicting the transport properties of the symmetrical molecules. Wang Chang, Uhlenbeck and de Boer[17] developed the formal kinetic theory in order to include the existence of internal degrees of freedom and inelastic collisions among molecules. Monchick, Yun and Mason[18] extended this theory to include the binary molecular interactions. In spite of its great theoretical significance, these advances failed to put forth the required improvement. Van de Ree[19] made an attempt to give a reason for such theoretical failure and contributed a more adequate calculation of the thermal diffusion factor of the asymmetric molecules.

Grew and Ibbs[20] had attempted to develop the theory of separation in a TD column. Still the theory of separation by the TD column is understood semiquantitatively perhaps due to involvement of both the convective and diffusion flow between the column surfaces. Further, discrepancies are caused due to deviation of the experimental column from the idealised one. Moran and Watson[21], Corbett and Watson[22] had however, shown that many of the discrepancies disappeared in a carefully constructed column.

The characteristics of separation of the gas mixtures like Ne-Ar, He-Ar etc. in a thermal diffusion column was investigated by Saxena and Saxena[23], Raman and Saxena[24] had computed the thermal diffusion column shape factors to explain the proper behaviour of gas mixtures in a TD column. Rutherford et al [25,26] had constructed a large number of TDC with various column geometries to enrich rare isotopic binary molecular mixtures. Many precautions had been taken into account in performing their experiments so that preliminary experimental errors could be removed. Column experiments were performed with different binary monatomic or polyatomic gas mixtures like He, Ne, Ar, Kr, CO, CH_4, N_2, CH_3Cl etc. The experimental results as obtained are of much importance to those who are investigating thermal diffusion column behaviours.

Saviron et al[27] had tried to give a simplified formulation for the steady state maximum separation factor and optimum pressure of a TD column. A

flow pattern weighted average temperature as a reference temperature is introduced. Starting from the classical FJO theory and introducing the reference temperature attempts have been made to obtain the formulation in which the influence of the nature of the gas appears only through transport coefficients. A proportionality relationship of the logarithmic of maximum separation factor $\ln q_{max}$ with the thermal diffusion factor α_T of the mixture is obtained. The proportionality constant is supposed to be molecular model independent parameter.

The influence of thermodynamic parameter of any binary gas mixture in a TDC, the geometry of TDC on the degree of separation and the energy consumption of a gas in a TDC is interestingly investigated by Leyarovski et al[28]. To explain the gas behaviour under the influence of temperature gradient in a TD column an effective transfer unit height (TUH) is introduced. Evaluation of the degree of enrichment of the heavy to the light gas molecules of the mixture is made possible only if the initial concentration, the geometry of the column, the cold wall and the hot wall temperatures of the TD column are known.

An approximate formulation for the desired column constants are, however, derived by Yamamoto et al[29]. The constants are expressed explicitly in terms of the geometry of the column and physical properties of the gases to be separated. Attempts are made to estimate the optimum pressure of a gas mixture in the TD column. Theoretical predictions as obtained are systematically compared with experimental results for binary, multicomponent monatomic and for isotopically substituted polyatomic gas mixtures. Moreover, optimum pressures were studied for H_2-HT, D_2-HT binary molecular mixture where the mass difference between the components are practically nil. It is found that even for mixture of unlike gases or systems of low atomic weights the predicted optimum pressure are in good agreement with the experimental data.

The theory actually advanced by Furry-Jones and Onsager[11] was later on developed by different authors in different times. The theories are, however, useful for roughly predicting the column behaviour. The analysis is not so simple and it requires numerical calculations with computer.

Under such context, Acharyya et al[30] and Datta et al[31] introduced a column calibration factor F_s so that the thermal diffusion column behaviour can be understood in a simpler way. Thermal diffusion factors α_T of different isotopic, nonisotopic and monatomic molecules were evaluated by the CCF method and compared with experimental α_T by the existing methods. Role of the CCF in determining the temperature or composition dependence of α_T are carefully examined by Acharyya et al[30] and Datta et al[31]. The reliable α_T's for He - HT, He-HD, Ne, Ar, Kr, Xe isotopic mixtures and other like or unlike molecules are obtained. The application of the CCF in thermal diffusion column and its wide significance inspired the present author[32] to derive the functional relationship of F_s with the geometry of the TD column from the Navier-Stokes hydrodynamical equation.

References

[1] L. Dufour, Ann; Physik **148** (1873) 490.

[2] C. Soret, Arch. Sci. (Geneva) **2** (1879) 48.

[3] D. Enskog, Z. Physik **12** (1911) 533.

[4] S. Chapman, Proc. Roy Soc. **A 93** (1916) 1.

[5] S. Chapman and F. W Dootson, Phil. Mag. **33** (1917) 248.

[6] K. Clusius and G. Dickel, Z. Ph. Chem. **B 44** (1939) 397.

[7] G. Vasaru, G. Muller, G. Reinhold and T. Fodor, Thermal Diffusion Column, (1969) VED Deutscher Verlag Der Wissenschaften, Berlin.

[8] S. C. Saxena and E.A. Mason, Mol. Phys. **2** (1959) 264, 379.

[9] K. Clusius and M Huber, Z Naturf 19 a (1955) 230.

[10] K.Clusius, J. Chem. Phys. **60** (1963) 163.

[11] W. H. Furry, R. C. Jones and L. Onsagar, Phys. Rev. **55** (1939) 1083.

[12] W. H. Furry and R. C. Jones, Phy. Rev. **60** (1946) 459

[13] R. C. Jones and W. H. Furry. Rev. Mod. Phys. **18** (1946) 151

[14] K. Cohen, The Theory of Isotope Separation (McGraw Hill Book Cy. Inc. New York, 1951).

[15] C. J. G. Slieker, Z Naturforsch. **20** (1965) 591.

[16] S. Chapman and T. G. Cowling, The Mathematical theory of nonuniform gases (cambridge 1939).

[17] C. S. Wang Chang, G.E. Uhlenbeck and J. de Boer, "Studies in Statistical Mechanics". (New York 1964) 2, 241.

[18] L. Monchick, K. S. Yun and E. A. Mason, J. Chem. Phys. **39.** (1963) 654.

[19] J. Van dee Ree, Ph.D. Dissertation thesis (1967).

[20] K. E. Grew and T.L. Ibbs, Thermal Diffusion in Gases, Cambridge University Press (1952).

[21] T. I. Moran and W.W. Watson, Phy. Rev. **111** (1957) 380.

[22] J.W. Corbett and W.W. Watson, Phy. Rev. **101** (1956) 519.

[23] V. K. Saxena and S.C. Saxena, Z. Naturforsch **24a** (1969) 1378.

[24] S. Raman and S.C. Saxena, J. Chem. Phys. **26** (1962) 3345.

[25] W. J. Roos and W.M. Rutherford, J. Chem. Phys. **50** (1969) 3936.

[26] W. M. Rutherford and K. J. Kaminski, J. Chem. Phys. **47** (1967) 5427.

[27] J. L. Navarro, J.A. Madariage and J.M. Saviron, J. Phys. Soc. Japan **50** (1967) 5427.

[28] E. I. Leyarovski, J.K. Georgiev and A.L. Zahariev. Int. J of Thermophysics **9** (1988) 391.

[29] I. Yamamoto, H. Makino and A. Kanagawa, J. Nucl. Sci. technol **27** (1990) 156.

[30] S. Acharyya, I.L. Saha, P. Acharyya, A.K. Das and S.K. Datta, J Phys. Soc. Japan **51** (1982) 1469.

[31] A. K. Datta and S. Acharyya, J. Phys. Soc. Japan, **62** (1993) 1527.

[32] G. Dasgupta and S. Acharyya, J. Phys. D. Applied Phys. (London) **31** (1998) 1092.

CHAPTER 3

Scope and Objective of the Present Work

Scope and Objective of the Present Work

Earlier elementary theory of thermal diffusion column was first put forward by Furth. The theories developed so far are either complicated or have missed one or more essential physical points. Further, the development of the classical thermal diffusion column theory is based on the rigorous mathematical concept of hydrodynamics mixed with a net transfer of components of a gas mixture up and down the column under the temperature gradient. As a results, the column constants are evaluated analytically. The analysis needs calculations with high speedy computer. Still it is found that there is a wide disagreement between the theoretical formulations of the column parameters with their experimental results.

3.1. General theory

An ideal column with two concentric cylinders is shown in Fig 1.3. The cold and hot walls of radii r_c and r_h are kept at temperatures T_c and T_h respectively. The hydrodynamical equation in cylindrical coordinates for a given gas mixture confined in the column is

$$\frac{1}{r}\frac{\delta}{\delta r}\left(\eta r\frac{dv}{dr}\right)=\frac{dp}{dz}-\rho g. \qquad \text{.....(3.1)}$$

where v is the convective velocity parallel to z axis of the column. Now the rate of heat flow per unit area per unit length of the TD column is given by $2\pi Q$ where $2\pi Q = 2\pi r\lambda\left(-\frac{\delta T}{\delta r}\right)$

Thus we have

$$\frac{\delta}{\delta r}=-\frac{Q}{r\lambda}\frac{\delta}{\delta T}, \qquad \text{.....(3.2)}$$

establishing the fact that the operator $\frac{\delta}{\delta r}$ is replaced by the operator $\frac{\delta}{\delta T}$.

The equation for the transport of the lighter component (J_1) along the tube of the column is

$$J_1=\rho c_1 v_1+\rho D_{12}\,(-\text{grad}\, c_1+\alpha_T c_1 c_2\,\text{grad}\,\ln T) \qquad \text{.....(3.3)}$$

where c_1 is the mass fractions and v_1 is the velocity of the lighter component

along the z axis of a TDC. Here, v_1 is not a function of z. For the steady state condition $\frac{\delta\rho}{\delta z}$ =0, thus eq (3.3) becomes.

$$\frac{\delta}{\delta T}\left(\frac{\rho D_{12}}{\lambda}\right)\left[\frac{\delta c_1}{\delta T}-\frac{\alpha_T c_1 c_2}{T}\right]=\frac{r^2\lambda}{Q^2}\rho v_1\frac{\delta c_1}{\delta z}\,, \qquad \text{.....(3.4)}$$

For simplicity the term which gives rise to the longitudinal diffusion is omitted here. This will be taken into account later on.

Introducing a new function G(z,T) which is defined by :

$$\frac{\delta c_1}{\delta z}\,G(z,T)=\frac{r\,\lambda Q^3}{[\rho D_{12}]}J_{1r}$$

where J_{1r} is the radial flux of the lighter component per unit area per unit time, eq. (3.4) becomes

$$v_1=\frac{1}{\lambda r^2 Q^2\rho}\frac{\delta}{\delta T}\left[\frac{\delta D_{12}}{\lambda}\,G(z,T)\right]. \qquad \text{..... (3.5)}$$

Neglecting the term $\frac{\delta^2 p}{\delta T\delta z}$ which is supposed to be very small, the hydrodynamical equation in terms of v_1 becomes

$$\frac{\delta}{\delta T}\left(\frac{1}{r^2\lambda}\right)\frac{\delta}{\delta T}\left(\frac{\eta}{\lambda}\right)\frac{\delta}{\delta T}\left(\frac{1}{\lambda r^2\rho}\right)\frac{\delta}{\delta T}\left[\frac{\rho D_{12}}{\lambda}G(T)\right]=-g\,\frac{\delta\rho}{\delta T}, \qquad \text{.....(3.6)}$$

with the boundary conditions :

$$G(T_c)=G(T_h)=G'(T_c)=G'(T_h)=0\,. \qquad \text{..... (3.7)}$$

To find out the total upward transport of the lighter component let us suppose

$$\tau_1=-\frac{2\pi}{Q^3}\int_{T_c}^{T_h} c_1\rho\,\lambda v_1 r^2\,dT.$$

Using $G(T_c)=G(T_h)=0$, total upward transport becomes

$$\tau_1=\frac{2\pi}{Q^3}\int_{T_c}^{T_h}\frac{dc_1}{dT}\left(\frac{\rho D_{12}}{\lambda}\right)G(T)\,dT. \qquad \text{..... (3.8)}$$

The net transport of the lighter component finally becomes :

$$\tau_1 = H\, c_1\, c_2 + K_c \frac{dc_1}{dz} \quad . \qquad \text{..... (3.9)}$$

Taking into account of the longitudinal diffusion effect the exact transport equation is

$$\tau_1 = H\, c_1\, c_2 - (K_c + K_d) \frac{dc_1}{dz} \quad . \qquad \text{..... (3.10)}$$

The initial transport coefficient H, convective remixing coefficient K_c and the diffusive remixing coefficient K_d are respectively given by :

$$H = \frac{2\pi}{Q^3} \int_{T_c}^{T_h} \left(\frac{\rho D_{12}}{\lambda}\right) \frac{\alpha_T}{T}\, G(T)\, dT,$$

$$K_c = \frac{2\pi}{Q^7} \int_{T_c}^{T_h} \left(\frac{\rho D_{12}}{\lambda}\right) G^2(T)\, dT \qquad \text{and}$$

$$K_d = \frac{2\pi}{Q} \int_{T_c}^{T_h} r^2 \lambda \rho D_{12}\, dT$$

If the steady state situation is acheived in a TDC the net transport τ_1 of the lighter component of a gas mixture up the column is zero. Eq. (3.10) thus becomes:

$$\ln q_e = \frac{HL}{K_c + K_d} \qquad \text{..... (3.11)}$$

where $$q_e = \frac{[c/(1-c)]_{z=L}}{[c/(1-c)]_{z=0}} = \frac{(c_i / c_j)_{top}}{(c_i / c_j)_{bottom}}$$

is called the equilibrium separation factor of the lighter and the heavier components of a gas mixture in a TDC of geometrical length L.

The column theory developed by Furry, Jones and Onsager[1] was further extended both theoretically and experimentally by Mason, Munn and Smith[2].

Since then most of the current experimental works are directed to estimate the experimental α_T of isotopic, isobaric and non-isotopic binary gas mixture as a function of temperature or composition. The experimental results thus obtained are compared with the theoretical α_T by both the elastic or inelastic collision theories of thermal diffusion derived by Chapman-Cowling[3] and Monchick-Munn and Mason[4] respectively. Unfortunately, the experimental results obtained so far could hardly be explained by the existing theories[3,4]

3.2. Column Calibration Factor

Under such context, Acharyya et al[5], Datta et al[6] and other workers[7-8] have introduced a scaling factor F_s called Column Calibration Factor (CCF) to determine α_T of any binary gas mixture in a thermal diffusion column (TDC). The role of the CCF was extensively studied and the CCF is now regarded as the best experimental parameter to determine α_T of any binary gas mixture.

In absence of reliable theoretical possibility to estimate the actual experimental α_T through the use of rigorous column theory Acharyya et al[5] used this F_s to get temperature as well as composition dependence of α_T of any binary gas mixture. The experimental α_T obtained by the CCF method from the available data are found to be of the same order of magnitudes maintaning almost the same trend with respect to temperature or composition. Thus it become necessary to derive the functional relationship of F_s with the geometry of the TD column.

In order to modify the existing column theory of Furry, Jones and Onsager[1] and to get the reliable α_T of a binary gas mixture, the CCF which is a apparatus constant is introduced. It is defined as[5,6].

$$\ln q_{max} = \alpha_T F_s (r_c, r_h, L \text{ and } \bar{T}) \quad \ldots\ldots\ldots\ldots (3.12)$$

The eq (3.12) was widely used by A. K.Datta to establish the role of F_s in his Ph. D dissertation[6]. F_s is really a useful parameter in thermal diffusion column experiments to estimate the actual experimental α_T of any binary gas mixture.

From eq (3.12) it is clear that the logarithmic of the maximum separation

factor $\ln q_{max}$ is related with F_s which solely depends on the column geometry and the mean gas temperature of the TD column. Further, it is free from binary molecular interaction model and is purely an apparatus constant. The temperature dependence of F_s for a large number of columns of different column geometries were extensively studied by a large number of workers[5,6] from the available experimental data.

As the transport coefficients H, K_c and K_d are proportional to p^2, p^4 and p^0 respectively, p being the pressure in atmosphere, eq (3.11) can be written as:

$$\ln q_e = ap^2/(b+p^4) \qquad \text{..... (3.13)}$$

where $a = (HL/K_c)\, p^2$ and $b = (K_d/K_c)\, p^4$. As there exists asymmetry in the column geometry, Jones and Furrry[9] simply added a term K_p called the remixing coefficient proportional to p^4 to the denominator of eq (3.11). The eq(3.13) takes the form :

$$(p^2 / \ln q_e) = (b'/a') + (1/a')p^4 \qquad \text{..... (3.14).}$$

where a' and b' are related with a and b as

$$a = a' (1+K_p/K_c) \text{ and } b = b' (1+K_p/K_c).$$

Thus a' and b' are the parameters governing the nature of variation of experimental $\ln q_e$ against pressure p at any mean gas temperature or composition of the binary or ternary gas mixture. It is also evident from eq (3.14) that as the pressure p increases $\ln q_e$ increases and eventually reaches a maximum value of $\ln q_e$ at $p = (b')^{1/4}$ for which $\frac{\delta}{\delta p}(\ln q_e) = 0$. Thus

$$\ln q_{max} = \frac{a'}{2\sqrt{b'}}, \qquad \text{..... (3.15)}$$

a' and b' of eq (3.14) can, however, be calculated by solving the following equations satisfying the experimental data of $\ln q_e$ against p in atmosphere:

$$\Sigma p^4 \ln q_e = a' \Sigma p^2 - b' \Sigma \ln q_e$$

$$\Sigma p^6 \ln q_e = a' \Sigma p^4 - b' \Sigma p^2 \ln q_e$$

Using known and reliable α_T of any calibrating gas mixture and their

$\ln q_{max}$ in a TDC, F_s of that column can be obtained from eq (3.12). The obtained F_s are always found to satisfy an empirical formula of the type :

$$F_s = A + B\,\bar{T} + C\,\bar{T}^2 \qquad \text{..... (3.16)}$$

where A, B and C are three coefficients depending on the geometry of the column. The relations of F_s with $\bar{T}$ for a large number of columns were extensively studied by Acharyya et al[5] and Datta et al[6] and following equations were arrived at :

(i) $r_c = 1.37$ cm; $r_h = 0.6$ cm; L = 149 cm

$$F_s = 68.9480 - 0.3175\,\bar{T} + 3.7138 \times 10^{-4}\,\bar{T}^2$$

(ii) $r_c = 2.15$ cm; $r_h = 0.5$cm; L=120 cm.

$$F_s = -66.5220 + 0.3502\,\bar{T} - 4.1879 \times 10^{-4}\,\bar{T}^2$$

(iii) $r_c = 0.943$ cm; $r_h = 0.319$ cm; L=154.4 cm.

$$F_s = 91.153 - 0.3156\,\bar{T} + 3.3446 \times 10^{-4}\,\bar{T}^2$$

(iv) $r_c = 0.9525$ cm; $r_h = 0.0795$ cm; L = 487.7 cm.

$$F_s = 67.194 - 8.5052 \times 10^{-2}\,\bar{T} + 1.0993 \times 10^{-4}\,\bar{T}^2$$

(v) $r_c = 0.943$ cm ; $r_h = 0.08$ cm ; L = 152 cm.

$$F_s = -56.7230 + 0.2462\,\bar{T} - 0.7497 \times 10^{-4}\,\bar{T}^2$$

From the above equations of F_s against $\bar{T}$ it is obvious that F_s's of different columns are the same except their coefficients A, B and C of eq (3.16) are of varying magnitudes and signs. This is probably due to different values of r_h/r_c with varying geometrical length of the TD column. Temperature dependence of F_s for different TD columns[5-6] are, however, illustrated in Figs 3.1 and 3.2.

Thus keeping in mind that F_s plays a vital role in thermal diffusion column experiment, a rigorous study of experimental $\ln q_{max}$ of different interesting pair of molecules with reliable α_T are needed to arrive at the temperature dependence of F_s for a TD column. A large number of experimental values of F_s so far obtained in TD columns of different geometries may be used to arrive

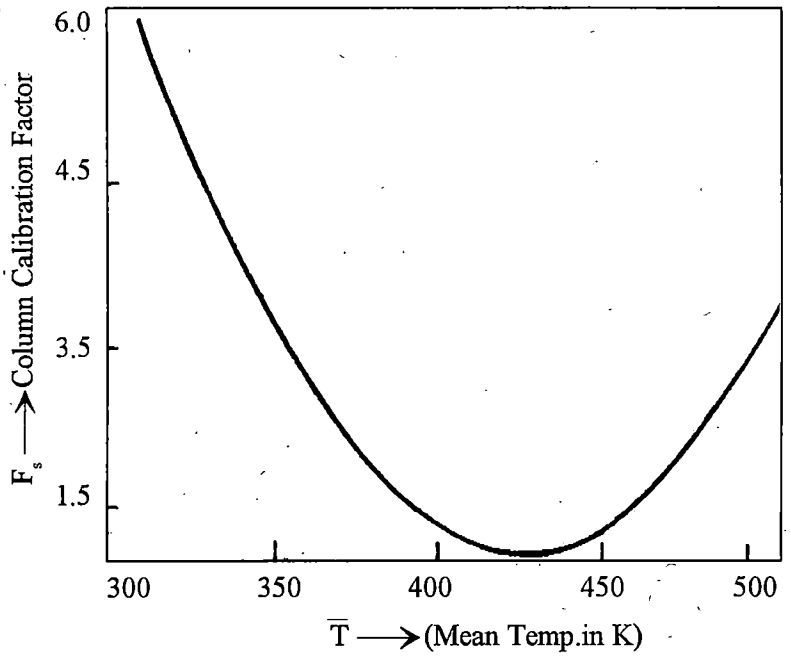

Fig. 3.1. Column Calibration Factor Against Mean Temperature in K.

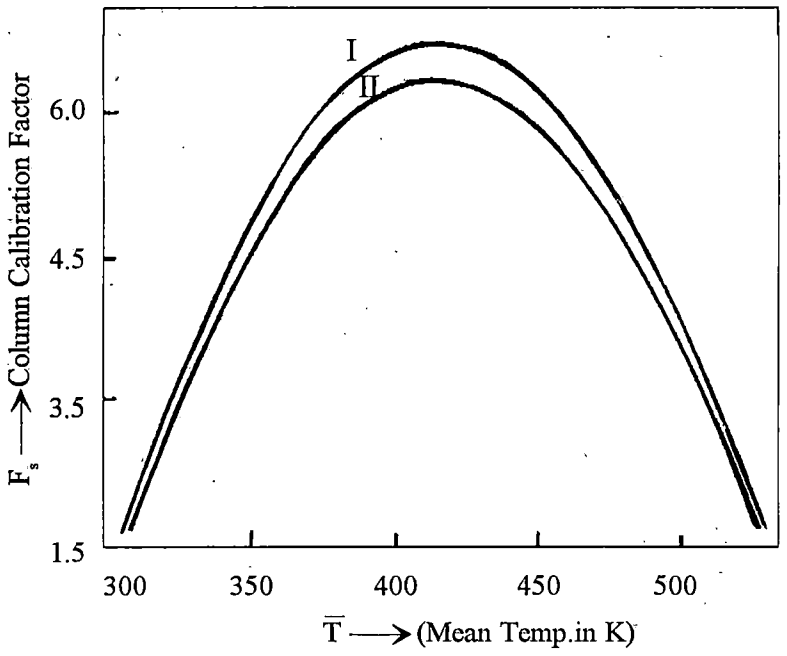

Fig. 3.2. Expt. and theor. plot (curve I & II) of F_s against mean temp.

at a unique expression of F_s in terms of r_c, r_h, L and $\bar{T}$. This study also observes how far F_s is a simple and useful parameter to determine the existence of elastic or inelastic collision effects[10] among molecules in thermal diffusion.

The column thus calibrated by using reliable α_T and $\ln q_{max}$ are now used simply to determine α_T of other binary molecules from their available $\ln q_{max}$'s in the same column. Obtained α_T's are necessarily compared with other α_T's by the existing methods using column shape factors (CSF) of Lennard - Jones binary molecular interaction model, Maxwell's model and Slieker's molecular model independent methods. The α_T's obtained from the CCF method are compared with the theoretical α_T's due to elastic or inelastic collision theory according to their needs. The comparisons are well displayed graphically in Figs. 3.3 and 3.4 for some systems under investigations[6]. It is clear that the α_T's by the CCF method are in close agreement with the theoretical α_T's. Although, the α_T's based on the Maxwell's molecular model are continuous with respect to $\bar{T}$, still in most of the cases they are found to be one order of magnitude less than those by the other methods. As the cold wall temperature held fixed Lennard - Jones binary molecular interaction model is inapplicable in most of the cases. The molecular model independent Slieker shape factors (CSF) were also used[5,6] to get α_T's. These α_T's can hardly explain the theoretical values. On the other hand, the experimental α_T's by the CCF method maintain the same trends and magnitudes with respect to their theoretical values. The experimental α_T's as obtained from the CCF method for He-T_2, He-HT and He-HD molecules when compared with the theoretical ones revealed the fact that F_s plays an important role to yield the actual α_T's with respect to $\bar{T}$ for the molecules under investigation.

Elastic collision effect is usually expected on a symmetric diatomic molecules like T_2 where the angle dependent part of molecular potential is trivial in comparison to eccentrically loaded sphere molecules like HT and DT. Interestingly the magnitudes and their trends of α_T's with respect to $\bar{T}$ as obtained from the CCF method for He-T_2 mixture are in accordance with the theoretical α_T's due to elastic collision effect. This study, however, observes inelastic collision effect in He-HT and He-DT molecules.

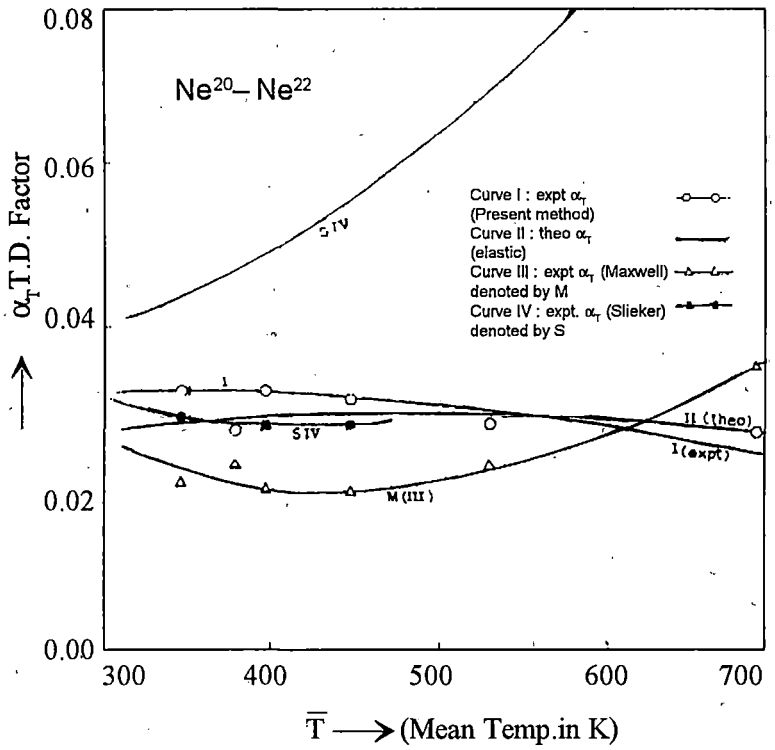

Fig. 3.3. Temperature dependence of α_T of Ne^{20} – Ne^{22} isotopic mixture.

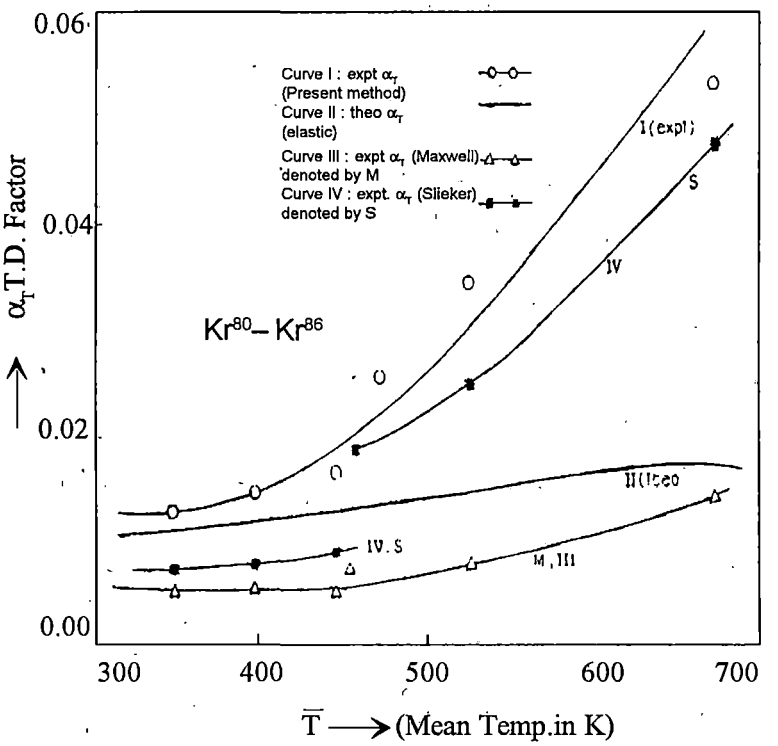

Fig. 3.4. Temperature dependence of α_T of Kr^{80} – Kr^{86} isotopic mixture.

Attention to the transport coefficients, H, K_c and K_d, through rigorous formulation of the column theory is, therefore, shifted to a simple F_s which is supposed to be free from binary molecular interaction model. Rather F_s depends entirely on the geometry of the column. Consequently it becomes necessary to explore the functional relationship of F_s with r_c, r_h, L and $\bar{T}$ of the TD column.

3.3. Molecular Force Parameters

The intermolecular force potentials for different molecules had already been determined by a large number of workers[11] where various equilibrium and nonequilibrium properties of gases and gas mixture have been used. The properties of the gas mixture rather depends on the interaction potentials between the like or unlike molecules which tends to musk the dependence of this property on the unlike potential parameters. Musking effect was much greater in case of viscosity, thermal conductivity and virial coefficient while in thermal diffusion it is much reduced. The available experimental α_T data of the gas mixture may thus be used to determine the force parameters of the interacting molecules undergoing thermal diffusion.

Using the method of graphical translation Mason and Rice[12], Srivastava and Madan[13] had estimated the molecular force parameters. The method was further refined by Saxena and Srivastava[14] on the basis of molecular exp-6 model.

The theoretical expression of α_T for a binary gas mixture due to Chapman and Cowling[3] is :

$$\alpha_T = (6C^*_{ij} - 5)\,\frac{S_i x_i - S_j x_j}{x^2_i Q_i + x_i x_j Q_{ij} + x^2_j Q_j} \qquad \ldots\ldots\ldots\ldots (3.17)$$

S_i, S_j, x_i, x_j, and C^*_{ij} are explicitly explained elsewhere[5]. The principal contribution to the temperature dependence of α_T comes from the factor ($6C_{ij}^*$ -5) of eq (3.17). The other terms of eq (3.17), say 'g', depends strongly on the composition of the gas mixture and very weekly on its temperature. Thus assuming the temperature dependence of α_T comes from the factor (6 C_{ij}^*-5) alone, one can obtain the potential parameters of the molecules. It is

obvious from eq (3.17) that

$$\log \alpha_T = \log (6C_{ij}^* - 5) + \log g \quad . \qquad \ldots\ldots\ldots\ldots (3.18)$$

Further since $\bar{T}^* = \bar{T}/(\varepsilon_{ij}/k)$ one may have

$$\log \bar{T}^* = \log \bar{T} - \log (\varepsilon_{ij}/k) \quad . \qquad \ldots\ldots\ldots\ldots (3.19)$$

In order to have suitable translation along the x and y axes $(6C^*_{ij} - 5)$ against $\bar{T}$ and logarithmic of reliable experimental values of α_T against log $\bar{T}$ are plotted on the same graph paper. Experimental curve can thus be made to coincide with the theoretical curve and the translation gives ε_{ij}/k and 'g'. By taking into account the small variation of 'g' with temperature evaluation of ε_{ij}/k can, further, be refined using the values of ε_{ij}/k and 'g' obtained earlier.

Using the translational method Srivastava and Srivastava[15] had determined the potential parameter of the unlike interaction between the pair of molecules like Ne-Ar, Ne-Kr and Ar-N_2. The method of translation actually given by Mason and Rice[12] was employed to determine ε_{ij}/k by the method of successive approximations. Using expressions for binary viscosity molecular diameter σ_{ij}'s were determined. The unlike force parameters (ε_{ij}/k)'s and σ_{ij}'s were then utilised by Srivastava and Srivastava[15] to calculate the temperature dependence of α_T's of the binary molecules. Although the obtained results were not always close to the experimental data, the potential parameters obtained by them are close to the literature values[15]. This lead to interesting fact that the temperature dependence of α_T has become an important tool to investigate the potential parameters of the like or unlike molecules.

On the other hand, the graphical translation procedure is complicated and lengthy. In the course of evaluation of ε_{ij}/k the procedure often invites personal judgement. A simple mathematical relationship has, therefore, been developed to yield the force parameter of molecule from thermal diffusion.

The principal contribution to the temperature dependence of α_T comes from the factor $(6C^*_{ij} - 5)$ while the other term 'g' is a composition dependence factor, depends very weekly on temperature. Thus 'g' can be assumed fairly constant for a short range of temperature and for fixed composition. Paul

et al[10] had shown that

$$(\alpha_T)_{expt} = A+B / \bar{T} \quad \text{..... (3.20)}$$

where A and B are two arbitrary constants. Similarly, it is easy to assume that C^*_{ij} is a function of $\bar{T}^*$ like

$$C^*_{ij} = C + D / \bar{T}^* \quad \text{..... (3.21)}$$

where C and D are two new constants and $\bar{T}^* = \bar{T}/(\varepsilon_{ij}/k)$. Substituting C^*_{ij} in eq (3.18) one may have

$$(\alpha_T)_{ther} = (6C-5)g + 6Dg/ \bar{T}^*. \quad \text{..... (3.22)}$$

Using the fact that $(\alpha_T)_{ther} = (\alpha_T)_{expt}$ we can have from eq (3.20) and eq (3.22) that

$$g = A /(6C-5) \quad \text{..... (3.23)}$$

Experimental α_T at any two temperatures can give the constants A and B of eq (3.20). To evaluate C and D of eq (3.21) any two arbitrary $\bar{T}^*$ is chosen. Corresponding C^*_{ij} for (12-6) L-J potential[17] is used to determine the constants C and D. Finally C^*_{ij} can be expressed in term of A and C of eqs (3.20) and (3.21) respectively as :

$$C^*_{ij} = \frac{1}{6}\left\{\frac{(\alpha_T)_{expt}}{A}(6C-5)+5\right\} \quad \text{..... (3.24)}$$

C^*_{ij} thus fixes $\bar{T}^*$ and the molecular force parameter (ε_{ij}/k) can be obtained from the relation :

$$(\varepsilon_{ij}/k) = \bar{T} / \bar{T}^* \quad \text{..... (3.25)}$$

Taking into account the small variation of 'g' with temperature the entire procedure as explained above repeated again to yield more correct (ε_{ij}/k).

The mathematical procedure as mentioned above was employed in this thesis to determine ε_{ij}/k and σ_{ij} of the binary molecules like Ne^{20}-Ne^{22}, Ar^{36}-Ar^{40}, Kr^{80}-Kr^{86}, Xe^{129}-Xe^{136}, CO^{28}-CO^{29}, $CH_4{}^{16}$-$CH_4{}^{17}$ and $N_2{}^{28}$-$N_2{}^{29}$ from the temperature dependence of the experimental α_T by the CCF method of the aforesaid molecules. The excellent agreement of the estimated ε_{ij}/k with the literature values at once establishes the fact that the method of predicting α_T by the CCF method is a reliable one.

REFERENCES

[1] W.H. Furry, R.C. Jones and L. Onsagar, Phy. Rev **55** (1939) 1083.

[2] E.A. Mason, R.J. Munn and F.J. Smith, Advances in atomic molecular Physics Vol II (1966) 31.

[3] S. Chapman and T.G. Cowling : The mathematical theory of nonuniform gases and liquids (John Wiley and Sons N.Y. 1964).

[4] L. Monchick, R. J. Munn and E.A. Mason : J. Chem. Phys. **45** (1966) 3051.

[5] S. Acharyya, I.L. Saha, A.K. Datta and A.K. Chattarjee, J. Phys. Soc. Japan **56** (1987) 105.

[6] A.K. Datta, Ph.D. Dissertation (1990) North Bengal University.

[7] J. A. Madariage, J.L. Navarro, J.M. Saviron and J.L. Brun, J. Phys. A : Math. Gen. **16** (1983) 1947.

[8] G. Vasaru, Thermal Diffusion column, supplied by S. Raman (Bombay BARC).

(9) R. C. Jones and W.H. Furry, Rev. Mod. Phys. **18** (1946) 151.

[10] T. K. Chattopadhyay and S Acharyya, Atomic and Mol. Phys. J. Phys. **B7**(1974) 2277.

[11] J.O. Hirschfelder, C.F. Curtiss and R.B. Bird, Molecular theory of gases and liquids, John. Willey and Sons, INC New York 1964.

[12] E.A. Mason and W.E. Rice, J. Chem. Phys. **22** (1954) 522.

[13] B. N. Srivastava and M.P. Madan, Proc. Phys. Soc. London **66** (1953) 277.

[14] S.C. Saxena and B.N. Srivastava, J. Chem. Phys. **23** (1955) 1571.

[15] B. N. Srivastava and K.P. Srivastava, Physic **23** (1957) 103.

[16] R. Paul, A.J. Howard and W.W. Watson : J.Chem. Phys. **39** (1963) 3053.

[17] M. Klein and F. J. Smith, A.E.D.C., Air Force System, Command Arnold, Air Force Station, Tennessee, 1968.

CHAPTER 4

Estimation of Theoretical and Experimental Thermal Diffusion factor

Estimation of Theoretical and Experimental Thermal Diffusion Factor

4.1 Introduction

Theoretical α_T of any binary gas mixture is derived from the Chapman-Enskog[1] gas kinetic theory. The theory is based on the elastic collisions among the molecules associated with the distribution function. The distribution function gives the number of molecules with position coordinates and translational velocities in a particular range at a given time. The theory is, therefore, suitable for a gas mixture of monatomic molecules colliding each other elastically.

For polyatomic molecules such a distribution function is inadequate because it requires a knowledge of the number of molecules in a particular internal state. The classical theory for such molecules has been given by Taxman[2]. A semiclassical theory has further been developed by Wang-Chang, Uhlenbeck and de Boer[3]. Based on such theories Monchick et al[4] derived the theoretical α_T for molecules with inelastic collisions among them.

4.2. Theoretical α_T Due to Elastic Collisions Among Molecules

α_T due to Chapman-Enskog[1] gas kinetic theory is derived as the solution of an infinite set of coupled algebraic equations whose coefficients are functions of molefractions, molecular masses and collision integrals. For convenience, in numerical calculations it is customary to select some molecular diameter σ and define the dimensionless collision integrals as :

$$\Omega^{(l,s)^*} = \frac{4}{\sigma^2(s+1)!}\left[1-\frac{1+(-1)^l}{2(1+l)}\right]^{-1}\left(\frac{\mu}{2\pi kT}\right)^{1/2}\Omega^{(l)}(s) \quad \text{.....(4.1)}$$

The reduced collision integrals are so defined as to be unity for rigid elastic spheres of molecular diameter σ . The solution of the infinite set of equations can formally be written as the ratio of two infinite determinants. In Chapman-Cowling[1] procedure this is replaced by the ratio of two finite determinants.

The coefficients a_{ij} in these determinants can be expressed in terms of the collision integrals. But explicit expressions are available only to the third order of approximation.

Another successive approximation procedure has been derived by Kihara[5] and extended by Mason[6]. Although Kihara's approximation for the transport coefficients are usually simpler than the Chapman-Cowling[1] expression, they may not be more accurate depending on the specific system under consideration. Following Chapman-Enskog[1] procedure the expression for α_T of a binary gas mixture can be given by :

$$\alpha_T = \frac{1}{6[\lambda_{ij}]_1} \frac{S_i^{(1)} x_i - S_j^{(1)} x_j}{X_\lambda + Y_\lambda} (6C^*_{ij} - 5) \qquad \ldots\ldots\ldots\ldots (4.2)$$

where C_{ij}^* is the ratio of the collision integral and it strongly depends on the temperature of the gas mixture. λ_{ij} is the coefficient of thermal conductivity, x_i and x_j are respectively the molefractions of the lighter (i) and heavier (j) components of the mixture. $S_i^{(1)}$ is given by :

$$S_i^{(1)} = \frac{M_i + M_j}{2M_j} \left(\frac{\lambda_{ij}}{\lambda_i}\right)_1 - \frac{15}{4 A^*_{ij}} \left(\frac{M_j - M_i}{2M_i}\right) - 1 \qquad \ldots\ldots\ldots\ldots (4.3)$$

where A_{ij}^* is the collision integral which depends upon ε_{ij}/k of the binary mixture. M_i and M_j are the masses of the lighter and the heavier components of the molecules of thermal conductivities $(\lambda_i)_1$ and $(\lambda_j)_1$ respectively. The usual values of thermal conductivities are computed by the relation :

$$[\lambda_{ij}]_1 = \frac{15}{4} \frac{R}{M} [\eta_{ij}]_1 \qquad \ldots\ldots\ldots\ldots (4.4)$$

instead of $[\lambda_{ij}]_1 = 1989.1 \times 10^{-7} \dfrac{[T (M_i+M_j)/2 M_iM_j]^{1/2}}{\sigma^2 \Omega_{ij}^{(2,2)^*}(T^*_{ij})}$

X_λ and Y_λ of eq (4.2) are calculated using the relations :

$$X_\lambda = \frac{x_i^2}{(\lambda_i)_1} + \frac{2x_ix_j}{(\lambda_{ij})_1} + \frac{x_j^2}{(\lambda_j)_1} \qquad \ldots\ldots\ldots\ldots (4.5)$$

and $$Y_\lambda = \frac{x_i^2}{(\lambda_i)_1} U^{(1)} + \frac{2x_i x_j}{(\lambda_{ij})_1} U^{(Y)} + \frac{x_j^2}{(\lambda_j)_1} U^{(2)} \quad \text{..... (4.6)}$$

where $$U^{(1)} = \frac{4}{15} A^*_{ij} - \frac{1}{12}\left(\frac{12}{5} B^*_{ij} + 1\right)\frac{M_i}{M_j} + \frac{1}{2}\frac{(M_i - M_j)^2}{M_i M_j} \quad \text{, ... (4.7)}$$

$$U^{(2)} = \frac{4}{15} A^*_{ij} - \frac{1}{12}\left(\frac{12}{5} B^*_{ij} + 1\right)\frac{M_j}{M_i} + \frac{1}{2}\frac{(M_j - M_i)^2}{M_i M_j} \quad \text{..... (4.8)}$$

and $$U^{(Y)} = \frac{4}{15} A^*_{ij} \frac{(M_i + M_i)^2}{4 M_i M_j} \frac{(\lambda^2_{ij})_1}{(\lambda_i)_1 (\lambda_j)_1} - \frac{1}{12}\left(\frac{12}{5} B^*_{ij} + 1\right)$$

$$- \frac{5}{32 A^*_{ij}}\left(\frac{12}{5} B^*_{ij} - 5\right)\frac{(M_i - M_j)^2}{M_i M_j} \quad \text{, ... (4.9)}$$

B_{ij}^* is another collision integral. For different binary molecular mixtures α_Ts' can be evaluated using eqs (4.2) to (4.9). The present investigation includes binary gas mixtures like CH_4[16] - CH_4[17], N_2[28]-N_2[29] and CO[28]-CO[29], hydrogenic gases in trace concentration in Helium (He[4]) and inert gas molecules. The purpose is to compare the theoretical α_T with the experimental α_T obtained by the CCF method and to examine whether elastic or inelastic collisions occur among the experimental molecules. Here, it is to be noted that thermal diffusion is a second order effect in the sense that its existence depends on the nature of molecular collisions, whereas the other transport properties like viscosity, heat conductivity and ordinary diffusion arise due to occurrence of collisions and secondarily on their nature.

4.3. Theoretical α_T Due to Inelastic Collisions Among Molecules

The most satisfactory theory of α_T based on inelastic collisions among the molecules was given by Monchick, Munn and Mason[7]. It is as follows :

$$\alpha_T = \frac{\mu_{ij}(6C^*_{ij} - 5)}{5nk(D_{ij})_1}\left(\frac{\lambda_{ji}}{x_j M_j} - \frac{\lambda_{ij}}{x_i M_i}\right) \quad \text{.....(4.10)}$$

where x_i and M_i are the molefraction and molecular mass of the component i, μ_{ij} is the reduced mass of the molecules and n is the number density of the mixture. For the polyatomic gas molecules the standard ratio of the collision integral C^*_{ij} is given by[8]

$$(6\,C^*_{ij} - 5) = \frac{2\langle(\gamma^2 - {}^5/_2)(\gamma^2 - \gamma\gamma' \cos\chi)\rangle_{ii}}{\langle(\gamma^2 - \gamma\gamma' \cos\chi)\rangle_{ij}}$$

where the angle bracket notation $\langle\ldots\ldots\ldots\ldots\rangle_{ij}$ is the standard notation for a collision integral. Primed and unprimed quantities are used after and before collisions of the colliding molecules and χ is a dynamic variable for the scattering angle.

Assuming the entrance and the exit channels are not the same except for an angle independent factor equal to the probability of a change in the internal energy state, Monchick, Sandlar and Mason[9] removed certain approximations of the previous work[8]. Under this assumption the partial thermal conductivity λ_{ij} becomes the steady state translational thermal conductivity $\lambda_i{}^{\alpha}{}_{trans}$ of species i in the mixture. Using the relations of $\lambda_i{}^{\alpha}{}_{trans}$ and $\lambda_i{}^{\alpha}{}_{int}$ and retaining the spin isotropic approximations it is found that

$$\alpha_T = \frac{(6C^*_{ij} - 5)\mu_{ij}}{5nk\,(D_{ij})_1}\left[\frac{\lambda_j{}^{\alpha}{}_{trans}}{x_j m_j} - \frac{\lambda_i{}^{\alpha}{}_{trans}}{x_i m_i}\right]$$

$$+ \quad \frac{1}{5nk\,(D_{ij})_1}\left[\frac{(6\tilde{C}_{ij} - 5)\lambda_{j\,int}}{x_j} - \frac{(6\tilde{C}_{ij} - 5)\lambda_{i\,int}}{x_i}\right].$$

The collision integral ratio $\tilde{C}_{ij}$ is not symmetric with respect to interchanges of the indices i and j and is very sensitive to inelastic collisions among molecules. $\lambda_i{}^{\alpha}{}_{trans}$ and $\lambda_j{}^{\alpha}{}_{trans}$ are also influenced by inelastic collisions and they are expressed as[10] :

$$\lambda^{\alpha}_{i\,trans} = \frac{\eta}{M}\left[\left(\frac{5}{2}\, C_{v\,trans} + \frac{\rho D_{int}}{\eta} C_{int}\right) - \left(\frac{2}{\pi}\frac{C_{int}}{Z_{rot}}\right)\left(\frac{5}{2} - \frac{\rho D_{int}}{\eta}\right)^{2}\left\{1 + \frac{2}{\pi Z_{rot}}\left(\frac{5}{3}\frac{C_{int}}{R} + \frac{\rho D_{int}}{\eta}\right)\right\}^{-1}\right].$$

Partial internal thermal conductivity is given as below[11]

$$\lambda^{\alpha}_{i\,trans} = \frac{n\,(D_{ij})_1\, C_{i\,int}}{1+(x_i / x_j)\,(D_{ii} / D_{ij})_1} \quad .$$

It is observed by many workers[12,13] that this theory is successful in predicting both temperature and composition dependence of α_T in such system where one of the components of the binary mixtures is eccentrically loaded sphere molecule. In other cases the theory fails to explain the experimental results. However, Chattopadhyay and Acharyya[14] extended this part of the theory with the nonspherical part of the potential in the following way :

$$(6\,\widetilde{C}_{ji} - 5) = \frac{5}{2}\left(\frac{W_j^{(1)} - W_j^{(2)}}{W_j^{(1)}}\right) \qquad \text{..... (4.11)}$$

where $$W_j^{(1)} = 2\,\epsilon_j^{-1/2}\,\sin^{-1}\left(\frac{\epsilon_j}{1+\epsilon_j}\right)^{1/2} \qquad \text{..... (4.12)}$$

and $$W_j^{(2)} = \frac{2}{(1+\epsilon_j)} \quad . \qquad \text{..... (4.13)}$$

ϵ_j is the molecular eccentricity given by

$$\epsilon_j = \frac{m\,\xi_j^{\,2}}{2\,I_j} \quad ,$$

the subscript j refers to the eccentrically loaded sphere molecule, ξ_j is the distance between the centre of mass of the molecule from its centre of symmetry and I_j is the moment of inertia about the centre of mass of the molecule.

However, the rotational translational collision number Z_{rot} is approximately inversely proportional to $(6\widetilde{C}_{ij} - 5)$. Thus from eqs (4.11) to (4.13) we have

$$\sin \frac{5K^{1/2}}{(K+I)\,[5-2\,(C_{ji}-5)]} = \frac{1}{(K+I)^{1/2}} \quad .$$

Since $\xi_j = \frac{C}{I_j}$ then $K=I_j/C$. This K can be found out from the method of successive approximation. The distance ξ_j is calculated from the knowledge of structure and bond lengths of different types of molecules of varying sizes and shapes.

Moments of inertia of different molecules from inelastic theory of thermal diffusion has been shown elsewhere[11]. On comparison with experimental values of moment of inertia it reveals that for molecules like HT, DT, HD, CH_3Cl, NH_3 etc, there is a good agreement while in case of other molecules like NO, CO, HCl, HBr, N_2O, H_2O etc wide disagreement occurs. It is thus obvious that experimental α_T for molecules like HT, DT, HD, CH_3Cl etc as one of the components in a binary mixture will give reasonable good agreement with theoretical α_T due to inelastic collision.

In case of NO, CO molecules with very small eccentricity and N_2O whose eccentricity is comparable to that of HT there is wide disagreement between theoretical and experimental α_T's. Also disagreement are there for other molecules whose eccentricities are larger. Thus the eccentricity parameter does not appear to be an important factor in determining the validity of this theory. Any rationalisation of the disagreement or any inference regarding the types of molecules for which the theory is valid can not be made at present[14].

However, the composition dependence of α_T due to elastic collision theory of He^4 - Ar^{40}, Ne^{20}-Xe^{132} and Ne^{20}-Ne^{22} binary molecular mixtures have been determined theoretically and discussed in chapter 5 of the thesis. Theoretical α_T due to elastic collision theory for different experimental molecules are presented in different tables as well as in different graphical plots of α_T against $\bar{T}$ curves in the thesis chapterwise. α_T for He-HT, He-HD, He-T_2, CH_4^{16}-CH_4^{17}, N_2^{28}-N_2^{29} and CO^{28}-CO^{29} molecules based on elastic collision theory fails to explain experimental α_T's. Consequently, α_T based on inelastic collision theory for these molecules are worked out and

compared with their respective experimental α_T. It reveals that inelastic collision plays an important role in case of binary molecular mixtures like He-HT, He-HD and He-T_2 molecules.

4.4. Experimental α_T by the Existing and the Present Method

For an ideal column of length L with a gas mixture at any mean temperature $\bar{T}$ the separation factor q_e is given by the relation[11)]

$$\ln q_e = \frac{HL}{K_c + K_d}$$

where H, K_c and K_d are proportional to p^2, p^4 and p^0 respectively, p being the pressure in atmosphere of the gas mixture. It is obvious that as pressure p increases $\ln q_e$ increases and eventually becomes maximum at $K_c = K_d$ for which the maximum separation factor q_{max} is given by the relation :

$$\ln q_{max} = \frac{HL}{2(K_c K_d)^{1/2}} \qquad \text{.....(4.14)}$$

Writing $(HL/K_c) = a'/p^2$ and $(K_d / K_c) = b' / p^4$ we have

$$\ln q_{max} = \frac{a'}{2\sqrt{b'}} \qquad \text{.....(4.15)}$$

where a' and b' are the parameters governing the nature of experimental $\ln q_e$ against pressure p at any constant temperature or composition. Experimental $\ln q_{max}$ in terms of a' and b' can thus be obtained from eq (4.15).

Further, the expressions for the column coefficients H, K_c and K_d are as the followings[11)] :

(i) Maxwellian case (n = 1, α_T is assumed to be temperature independent)

$$H = \frac{2\pi}{6l} \quad (\alpha_T \rho^2 g/\eta)_1 \frac{1}{2}(r_c + r_h)(r_c - r_h)^3 (2u)^2 h',$$

$$K_c = \frac{2\pi}{9|}(\rho^3 g^2 / \eta^2 D)_1 \frac{1}{2}(r_c+r_h)(r_c-r_h)^7 (2u)^2 k'_c$$

and $$K_d = 2\pi (\rho D)_1 \frac{1}{2}(r_c+r_h)(r_c-r_h) k'_d.$$

(ii) Slieker's case (Interaction model independent) :

$$H = [S.F]_1 r_c^4 (\rho^2 g \alpha_T/\eta)_1 (\frac{\Delta T}{T})^2$$

$$K_c = [S.F]_3 r_c^8 (\rho^3 g^2 / \eta^2 D)_1 (\frac{\Delta T}{T})^2 \quad \text{and}$$

$$K_d = \pi (1-a^2) r_c^2 (\rho D)_1.$$

(iii) Lennard - Jones case (Interaction model dependent)

$$H = \frac{2\pi}{6|} (\alpha_T \rho^2 g / \eta)_1 r_c^2 h,$$

$$K_c = \frac{2\pi}{9|} (\rho^3 g^2 / \eta^2 D)_1 r_c^8 k_c \quad \text{and}$$

$$K_d = 2\pi (\rho D)_1 r_c^2 k_d.$$

Here { h', k_c', k_d' }, {$[S.F]_1$;$\pi(1-a^2)$, $[S.F.]_3$ } and { h, k_c and k_d } are the dimensionless Maxwell, Slieker and Lennard-Jones shape factor (CSF) respectively, $u = \frac{\Delta T}{2\bar{T}}$ and $a = r_h / r_c$. Evaluation of experimental α_T by the existing methods thus involved with column shape factors. The Lennard-Jones case is, however, inapplicable where the cold wall temperature T_c is held fixed. The mass density ρ, the coefficient of viscosity η and the diffusion coefficient D may be found out from the experimental results or theoretical formulations reported elsewhere[15]. Now, using the expressions for H, K_c and K_d the experimental α_T by the existing method can be obtined from eq (4.14). The α_T's thus obtained are :

$$\alpha_T \text{(Maxwell model)} = 2.39 \frac{r_c-r_h}{L} \frac{\bar{T}}{\Delta T} \frac{\sqrt{k'_c k'_h}}{h'} \ln q_{max} \qquad \text{.....(4.16)}$$

$$\alpha_T \text{(Lennard Jones case)} = 2.39 \frac{r_c}{L} \frac{\bar{T}}{\Delta T} \frac{\sqrt{k_c k_h}}{h} \ln q_{max} \qquad \text{..... (4.17)}$$

$$\alpha_T \text{(Slieker model)} = 2.00 \frac{r_c}{L} \frac{\bar{T}}{\Delta T} \frac{\sqrt{\pi(1-a^2)[S.F.]_3}}{[S.F]_1} \ln q_{max} \qquad \text{..... (4.18)}$$

Actually, the column shape factors depends on the geometry of the column. Experimental value of lnq_{max} is obtained from eq (4.15). Thus the α_T by the existing methods are worked out from eqs (4.16) to (4.18).

The determination of α_T by the present CCF method deals with the column calibration factor F_s of the column. The temperature or composition variation of α_T is simply found out from the relation. :

$$lnq_{max} = \alpha_T F_s (r_c, r_h, L \text{ and } \bar{T}) \quad \text{..... (4.19)}$$

where F_s depends on the geometry of the thermal diffusion column and can be obtained by the calibration method. Determination of α_T by the CCF method is well discussed in different chapters of this thesis.

We are now in a position to compare the α_T's by the CCF method with those by the existing methods as well as with the theoretical α_T. The comparison is well displayed in different tables and also in different graphs of α_T against composition or temperature in chapters 5 to 10 of the thesis. Further, estimation of molecular force parameters of the experimental molecules from α_T by the CCF method have been made in chapters 7 to 9 of the thesis. This is to ensure the reliability of the composition or temperature dependence of α_T by the present CCF method.

References

[1] S. Chapman and T.G Cowling, The Mathematical theory of non uniform gases (Cambridge University press NY. 1952)

[2] N. Taxman, Phy. Rev. **110** (1958) 1235.

[3] C. S. Wang Chang, G. E. Uhlenbeck and J. de Boer "Studies in Statistical Mechanics" (New York 1964) 2,241.

[4] L. Monchick, K.S. Yun and E. A. Mason, J. Chem.Phys. **39** (1963)654.

[5] T. Kihara, "Imperfect Gases" (Tokyo, 1949).

[6] E. A. Mason, J. Chem. Phys. **27** (1957) 75.

[7] L.Monchick, R. J. Munn and E. A. Mason, J. Chem. Phys. **45** (1966) 3051

[8] L.Monchick, A.N.G Pereira and E.A. Mason, J. Chem. Phys. **42**(1965) 3241

[9] L.Monchick, S.I. Sandlar and E.A. Mason, J. Chem. Phys. **49** (1968) 1178

[10] C. Neyland, E.A. Mason and L.Monchick, J. Chem. Phys. **56** (1972) 6180

[11] A.K. Datta Ph. D Dissertation (thesis) (1990) North Bengal University.

[12] S. Acharyya, I.L. Saha, A.K. Datta and A.K. Chattarjee, J. Phys. Soc. Japan **56** (1987) 105

[13] G. Dasgupta and S. Acharyya, Pramana, J. Phys. **43** (1994) 81

[14] T.K. Chattopadhyay and S. Acharyya, J. Phys. B. **7** (1974) 2277

[15] J.O. Hirschfelder, C.F. Curtiss and R.B. Bird, Molecular theory of gases and liquids (John Wiley, New York, 1964).

CHAPTER 5

Column Calibration Factor to Study the Composition Dependence of the Thermal Diffusion Factors of Inert Gas Mixtures.

Column Calibration Factor to Study the Composition Dependence of the Thermal Diffusion Factors of Inert Gas Mixtures

5.1. Introduction

Nowadays the study of thermal diffusion is mostly directed to measuring the equilibrium separation factor q_e defined by

$$q_e = (C_i/C_j)_{top} / (C_i/C_j)_{bottom} \quad \text{..... (5.1)}$$

for isotopic and nonisotopic binary gas mixtures of different compositions at a fixed temperature, or for a binary gas mixture of fixed composition at different temperatures, in a thermal diffusion (TD) column first introduced by Clusius and Dickel[1]. Here C_i and C_j are the mass fractions of the lighter and heavier components of a gas mixture respectively, and the subscripts 'top' and 'bottom' denote the values at the top and bottom of a TD column. The experimental values of q_e are measured usually at different pressures below and around one atmosphere with the help of a precision type mass spectrometer and hence the TD factor α_T of a binary gas mixture as a function of the composition or the temperature is estimated by using various molecular models such as those of Maxwell and Lennard-Jones[2] and sometimes by using Slieker's model-independent method[3], which is, however, a crude one. In an attempt to get the actual α_T, we,[4-6] however, introduced a factor F_s called the column calibration factor of a TD column, by the relation

$$\ln q_{max} = \alpha_T F_s (r_c, r_h, L \text{ and } \bar{T}) \quad \text{..... (5.2)}$$

where q_{max} is the maximum value of q_e measured experimentally in a TD column, r_c are r_h are the cold wall and hot wall radii of the column of geometrical length L and $\bar{T}$ is the mean temperature in K of the gas mixture in the column, defined by $\bar{T} = (T_h + T_c)/2$, T_h and T_c being the temperatures of the hot and cold walls of the column, respectively. The column calibration factor F_s which is purely an apparatus quantity, is supposed to be independent of a molecular interaction model and depends only on the geometry of the column at any mean temperature $\bar{T}$.

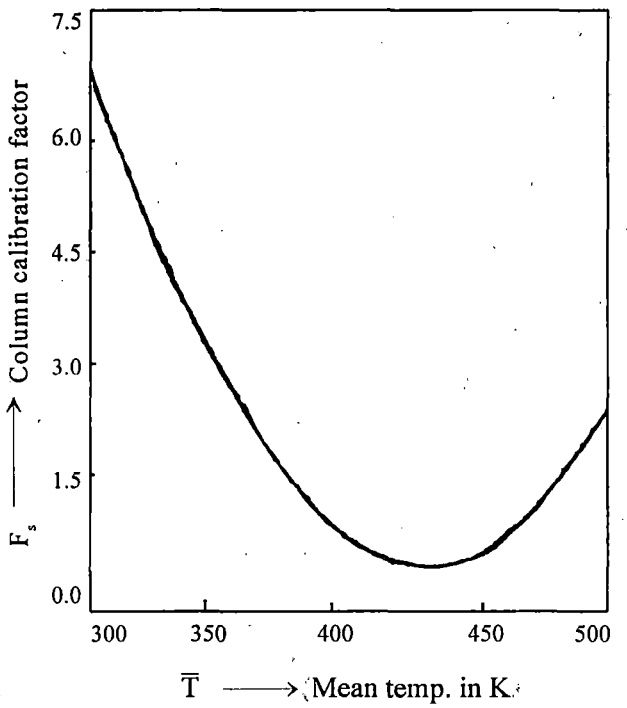

Fig. 5.1. Plot of the column calibration factor against $\overline{T}$, the mean temperature in K.

The column calibration factor F_s of a column with L = 149 cm, r_c = 1.37 cm and r_h = 0.6 cm has already been studied elsewhere[5], and the empirical relation of F_s to $\overline{T}$ has been found to be

$$F_s = 68.94796 - 0.3174514\,\overline{T} + 3.71383 \times 10^{-4}\,\overline{T}^2$$

yielding the value of F_s = 3.946 at $\overline{T}$ = 340 K. The F_s for this column is plotted against $\overline{T}$ in Fig 5.1. Fortunately J. M. Saviron et al[7] have recently studied the pressure dependence of the reduced logarithmic separation factors for two binary inert gas mixtures of He^4 - Ar^{40} and Ne^{20} - Xe^{132} and also an isotopic natural mixture of Ne^{20} - Ne^{22} for different compositions of the lighter components in the respective mixtures in this column at the experimental mean temperature $\overline{T}$ = 340 K, the hot wall and cold wall temperatures being $\overline{T}_h$ = 380 K and T_c = 300K respectively. From these results we estimate $\ln q_e$ of the mixtures for different concentrations of the lighter components at different pressures in atmosphere and the data thus obtained are found to satisfy the hydrodynamical part of the column theory, as developed by Furry and Jones[8] and Furry, Jones and Onsager[9], so excellently shown in Figs 5.2 and 5.3 that we have at once the following relations of $p^2/\ln q_e$ to p^4 for these mixtures at different concentrations:

$$p^2/\ln q_e = 3.09752 + 177.30496\ p^4$$
$$p^2/\ln q_e = 8.52467 + 66.65334\ p^4$$
$$p^2/\ln q_e = 17.20000 + 41.70213\ p^4$$
$$p^2/\ln q_e = 19.65238 + 16.78669\ p^4$$
$$p^2/\ln q_e = 18.74249 + 12.92235\ p^4$$

for the He^4 - Ar^{40} mixture for the concentrations 8.76%, 21.63%, 30.14%, 49.30% and 64.46% of He^4 respectively;

$$p^2/\ln q_e = 0.59848 + 3156.6\ p^4$$
$$p^2/\ln q_e = 2.39745 + 327.3\ p^4$$
$$p^2/\ln q_e = 3.03368 + 133.3\ p^4$$

for the Ne^{20} - Xe^{132} mixture for 15%, 66% and 90% of Ne^{20}, and finally

$$p^2/\ln q_e = 13.3 + 89.06\ p^4,$$

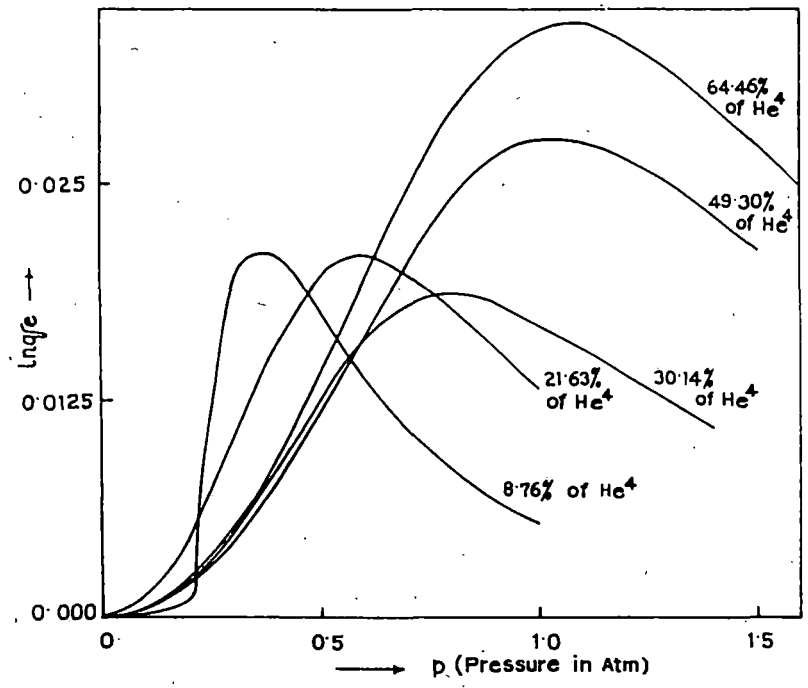

Fig. 5.2. Plot of $\ln q_e$ of He^4–Ar^{40} (binary inert gas mixture) against pressure p in atm at different concentrations of He^4 at temperature $\overline{T}$=340 K.

Table 5.1. Composition dependence of thermal diffusion factors α_T of inert gas at $\bar{T}$ = 340 K in a column of L = geometrical length = 149 cm. r_c = the cold wall radius = 1.37cm and r_h = the hot wall radius = 0.6 cm.

System	T_h in K	T_c in K	$\bar{T}$ in K	% of lighter component.	a' x 10^3 (atm)^2	b' x 10^3 (atm)^4	$\ln q_{max}$	F_s	Expt α_T x 10^3 present method	Expt α_T x 10^3 based on models			Theo. α_T (elastic)
										Maxwell	*L - J*	Slieker	
				8.76	5.64	17.47	0.0213		5.40	4.20	1.60	3.80	0.226
				21.63	15.00	127.87	0.0210		5.30	3.00	1.20	2.40	0.253
He - Ar	380	300	340	30.14	23.98	412.46	0.0187	3.946	4.70	2.70	1.00	2.10	0.273
				49.30	59.57	1170.72	0.0275		7.10	3.60	1.40	2.90	0.327
				64.46	77.39	1295.62	0.0340		8.60	7.20	2.50	5.80	0.340
				15.00	0.32	0.19	0.0115		2.90	4.20	4.50	3.40	0.247
Ne - Xe	380	300	340	66.00	3.06	7.32	0.0178	3.946	4.50	7.30	7.50	5.40	0.218
				90.00	7.50	22.76	0.0249		6.30	13.70	15.50	11.00	0.236
Ne^{20} - Ne^{22}	380	300	340	10.00	11.23	148.87	0.0146	3.946	3.70	5.40	1.70	4.40	0.0248

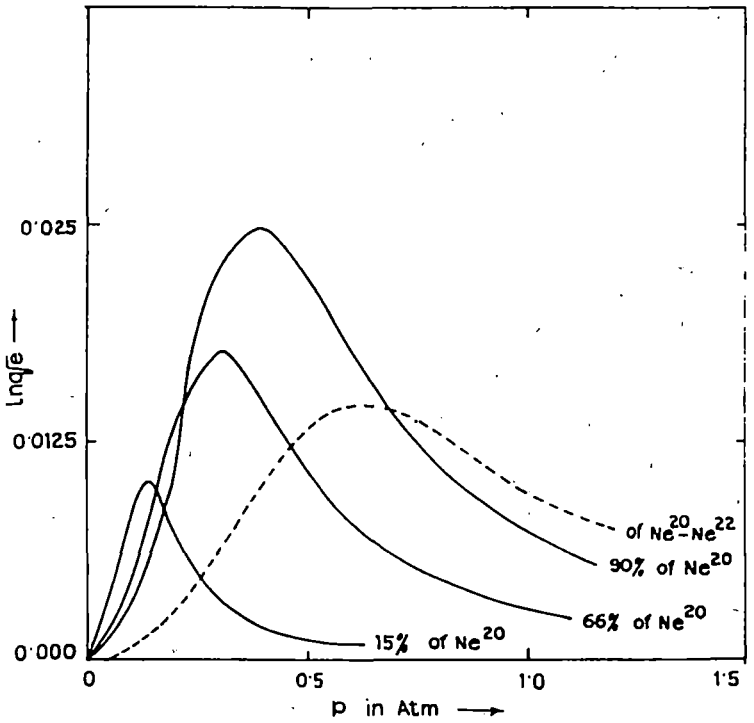

Fig. 5.3. Plot of Inq_e of Ne^{20}–Xe^{132} (binary inert gas mixture) against pressure p in atm at different concentrations of Ne^{20} at temperature $\overline{T}$=340 K. The dotted curve represents that of Ne^{20}–Ne^{22}.

for the Ne^{20} - Ne^{22} mixture. These establish that the graph of $p^2/\ln q_e$ against p^4 is always a straight line as predicted by the FJO theory[9]. Rutherford and Kaminski[10] have recently shown that the FJO theory[9] is applicable mainly in the case of an isotopic binary gas mixture and also in the case of a mixture in which one of the components is in trace concentration.

In the thermal diffusion phenomenon of isotopic gas mixtures, the elastic collisions are supposed to play a prominent role between the interacting molecules. Again, the thermal diffusion phenomenon is very sensitive to intermolecular interactions of the binary gas molecules, therefore, the study of the composition dependence of the TD factors α_T of any gas mixture is necessary to throw much light on the interactions between like molecules and those between unlike molecules of a gas mixture. The temperature dependence of α_T is, however, entirely governed by the factor $(6C_{ij}^* - 5)$, where C_{ij}^* is the ratio of the collision integrals. Moreover, the effect of inelastic collisions on the thermal diffusion, if any, is practically negligible in gas mixtures containing inert gases. All the facts mentioned above inspired us to study He^4 - Ar^{40} and Ne^{20} - Xe^{132} mixtures at different compositions of the lighter components at a given experimental mean temperature $\bar{T}$ = 340 K and also the isotopic mixture Ne^{20} - Ne^{22} with its natural isotopic abundances. The purpose of this work is to observe how far the TD factors α_T as estimated by our column calibration factor method agree with those obtained by the existing methods using the column shape factors involved in the molecular models, and by Slieker's model independent method[3]. The comparison is presented in Table 5.1 and shown graphically in Figs 5.4 and 5.5 for He^4 - Ar^{40} and Ne^{20} - Xe^{132} mixtures, respectively. The molecular parameters as well as the column shape factors used to calculate the experimental α_T by the existing method are shown in Table 5.2. The theoretical α_T's as functions of molefractions of the lighter components are also calculated from the formula derived from the Chapman-Enskog kinetic theory[11] based upon the elastic collisions between the interacting molecules. These are also shown in Table 5.1 and in Figs 5.4 and 5.5 for comparison.

5.2. Mathematical Formulations to Estimate the Experimental α_T's of the Mixtures.

For a TD column with both ends closed, the hydrodynamical part of the column theory related with the transport of the lighter component up the tube, so far developed by Furry, Jones and Onsager[9] yields that the net transport of the ith component of a binary gas mixture up the column tube is zero, i.e.

$$\tau = Hc_i c_j - (K_c + K_d)\frac{\delta c_i}{\delta z} = 0. \qquad \text{..... (5.3)}$$

where z is the coordinate along the column, and H, K_c and K_d are called the transport coefficient, the convective remixing coefficient and the diffusive remixing coefficient respectively; they are complicated functions of the wall temperatures, the geometry of the column and also the transport properties of the binary gas mixture and are given by

$$H = \frac{2\pi}{Q^3}\int_{T_c}^{T_h} \frac{\rho D_{ij}}{\lambda}\,\alpha_T\,\frac{G(T)}{T}\,dT \qquad \text{.....(5.4)}$$

$$K_c = \frac{2\pi}{Q^7}\int_{T_c}^{T_h} \frac{\rho D_{ij}}{\lambda}\,G^2(T)\,dT, \qquad \text{.....(5.5)}$$

$$K_d = \frac{2\pi}{Q}\int_{T_c}^{T_h} r^2\lambda\rho D_{ij}\,dT \qquad \text{.....(5.6)}$$

where ρ is the density, r is the radial coordinate, λ and D_{ij} are the thermal conductivity and diffusion coefficient of the gas mixtures respectively, T_h and T_c are the hot and cold wall temperatures, and $2\pi Q$ denotes the radial heat flow per unit length of the column. The function *G(T)* is the solution of the fourth-order differential equation

$$\frac{d}{dT}\left(\frac{1}{\lambda r^2}\right)\frac{d}{dT}\left(\frac{\eta}{\lambda}\right)\frac{d}{dT}\left(\frac{1}{\lambda\rho r^2}\right)\frac{d}{dT}\left\{\frac{\rho D_{ij}}{\lambda}\,G(T)\right\} = g\frac{d\rho}{dT} \qquad \text{..... (5.7)}$$

with the boundary conditions

$$G(T_c) = G(T_h) = G'(T_c) = G'(T_h) = 0. \qquad \text{..... (5.8)}$$

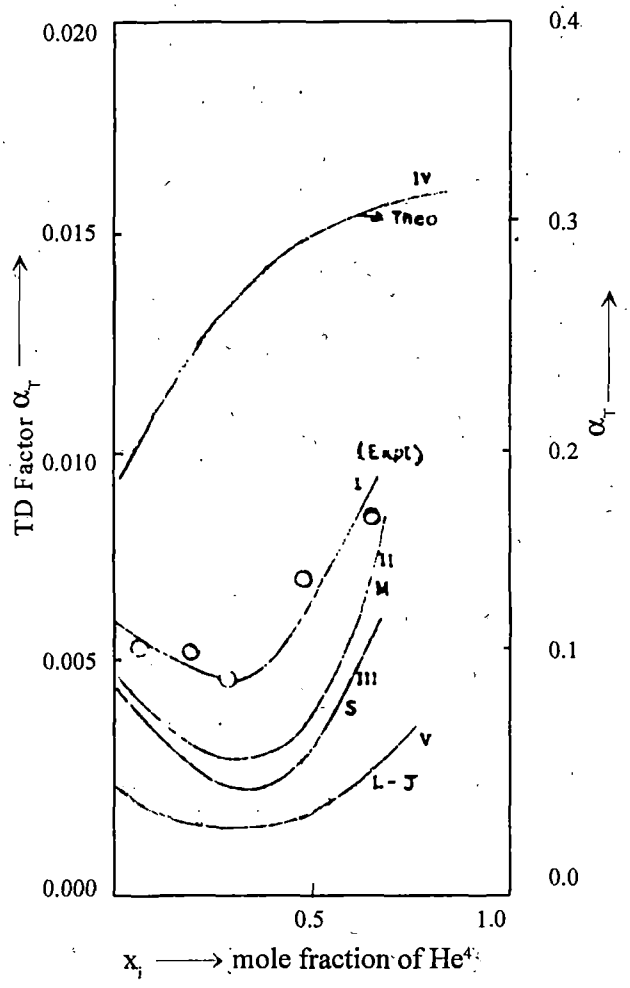

Fig. 5.4. Experimental α_T against mole fraction of He^4 of He^4–Ar^{40} mixture at mean temperature $\overline{T}$=340K. I. Expt α_T (our calibration factor method), II. Expt α_T (Maxwell's model), III. Expt α_T (Slieker), IV. Expt α_T (L-J model).

Here η and g denote the coefficient of viscosity of the gas mixture and the acceleration due to gravity respectively.

Integrating eq (5.3) between the column ends z=0 and z=*L where L* is the geometrical length of the column one gets

$$\ln q_e = \frac{HL}{K_c + K_d} \qquad \text{..... (5.9)}$$

The coefficients *H*, K_c and K_d for an ideal column are proportional to the 2nd, the 4th and the 0th powers of the pressure *p* in atmosphere respectively for a binary gas mixture and hence eq (5.9) reduces to

$$\ln q_e = \frac{ap^2}{b+p^2} \qquad \text{..... (5.10)}$$

However, in a practically constructed column, parasitic remixing of the components of the mixture always occurs. This can be taken into consideration by adding a term K_p, propertional to p^4, in the denominator of eq (5.9), so that eq (5.9) becomes

$$\ln q_e = \frac{a'p^2}{b'+p^4},$$

or

$$p^2/\ln q_e = \frac{b'}{a'} + \frac{1}{a'} p^4 \qquad \text{..... (5.11)}$$

The *a'* and *b'* in eq (5.11) are related to a and b in eq (5.10) by $a=a'(1 + K_p/K_c)$ and $b = b'(1 + K_p/K_c)$ respectively. The a and b in eq (5.10) again are expressed in terms of the column coefficients and the pressure of the binary gas mixture as

$$a = (HL/K_c)p^2 \text{ and } b=(K_d/K_c)p^4.$$

Further, since $(1 + K_p/K_c)=K_d/(b'K_c)$ we have

$$H=(a'K_d)/(b'L)=K_d/(LC), \qquad \text{.....(5.12)}$$

where C=b'/a' and is given by the intercept of the straight line expressing eq (5.11) for $p^2/\ln q_e$ against p^4, demanded by the FJO column theory[9].

The possible values of H, K_c and K_d can be obtained by the following equations :

Table 5.2 : Column Shape factors and other molecular parameters used to calculate α_T of He^3 - Ar^{40}, Ne^{20} - Xe^{132} and Ne^{20} - Ne^{22} mixtures at $\overline{T}$ = 340 and the L - J potential r_{12} in erg

Systems	(r_{12}/k) in K	σ_{12} in A	Shape factors due to Maxwell's model h'	k_d'	Slieker's shape factors $[S.F.]_1$	$(1 - a^2)$
He - Ar^{40}	34.95	3.191				
Ne^{20} - Xe^{132}	79.36	3.457	0.99425	0.97734	0.7041	1.764
Ne^{20} - Ne^{22}	27.50	2.858			6!	

			Lennard-Jones shape factors h	k_c	k_d
He^4 - Ar^{40}	34.95	3.191	0.00750	0.00224	0.41875
Ne^{20} - Xe^{132}	79.36	3.457	0.00250	0.00180	0.40700
Ne^{20} - Ne^{22}	27.50	2.858	0.00975	0.00240	0.42340

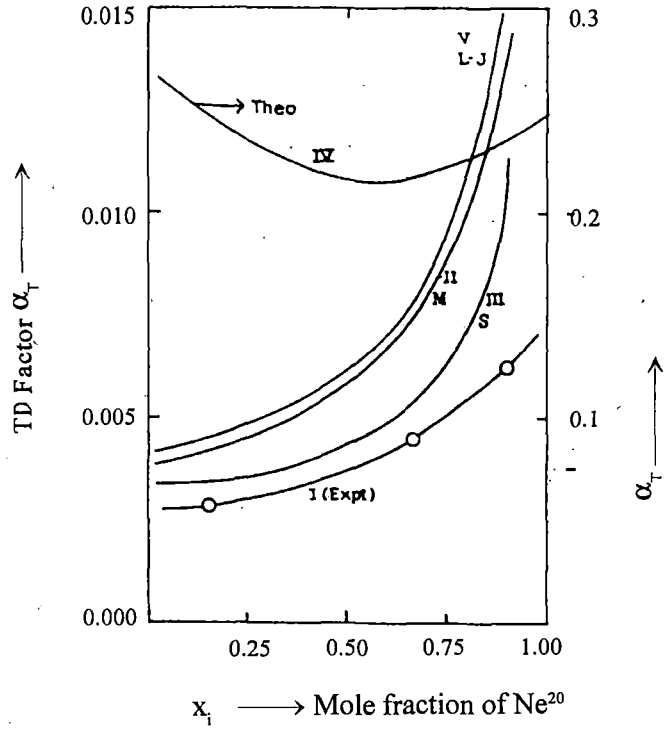

Fig. 5.5. Experimental α_T against mole fraction of Ne^{20} of Ne^{20}–Xe^{132} mixture at mean temperature $\bar{T}$=340K. I. Expt α_T (our calibration factor method), II. Expt α_T (Maxwell's model), III. Expt α_T (Slieker), IV. Theoretical α_T (elastic), V Expt α_T (L-J model).

i) Maxwell's[8] model of binary interaction (α_T being assumed to be temperature independent and n=1, for Maxwellian molecules).

$$H = \frac{2\pi}{6!}\left(\frac{\alpha_T \rho^2 g}{\eta}\right)\frac{1}{2}(r_c+r_h)\,(r_c-r_h)^3\,(2u)^2 h'$$

$$K_c = \frac{2\pi}{9!}(\rho^3 g^2/\eta^2 D)_1 \frac{1}{2}(r_c+r_h)\,(r_c-r_h)^7\,(2u)^2 k'_c$$

$$K_d = 2\pi(\rho D)_1 \frac{1}{2}(r_c+r_h)\,(r_c-r_h)\,k'_d.$$

ii) Slieker's[3] model-independent method.

$$C_1 = H = [S.F]_1\, r_c^4 \left(\frac{\rho^2 g \alpha_T}{\eta}\right)\left(\frac{\Delta T}{\bar{T}}\right)^2$$

$$C_2 = K_d = \pi(1-a^2) r_c^2\,(\rho D)_1,$$

$$C_3 = K_c = [SF]_3\, r_c^8\,(\rho^3 g^2/\eta^2 D)_1 \left(\frac{\Delta T}{\bar{T}}\right)^2$$

iii) Lennard-Jones' molecular model of binary interaction,

$$H = \frac{2\pi}{6!}\left(\frac{\alpha_T \rho^2 g}{\eta}\right) r_c^4 h,$$

$$K_c = \frac{2\pi}{9!}(\rho^3 g^2/\eta^2 D)_1\, r_c^8 k_c,$$

$$K_d = 2\pi(\rho D)_1 r_c^2 k_d.$$

The dimensionless quantities h', k_c' and k'_d, $[S.F]_1$, $[S.F]_3$ and $\pi(1 - a^2)$ and h, k_c, and k_d called the column shape factors due to Maxwell, Slieker and Lennard-Jones respectively are presented in Table 5.2, the factors in (ii) are free from a molecular interaction model, $u=(T_h - T_c)/(T_h + T_c)$, $a=r_h/r_c$ and $\Delta T = T_h - T_c$. The experimental α_T's of He^4 - Ar^{40}, Ne^{20} - Xe^{132} and Ne^{20}-Ne^{22} can thus be evaluated by three methods, the former two at the mean temperature $\bar{T} = (T_h + T_c)/2$ and the last one using L - J model at the cold wall temperature T_c of the column. Equation (5.12) is usually employed to calculate the experimental α_T's in terms of *H*, K_d, *L* and the experimentally observed intercept C(=*b'la'*) for a given experimental temperature by the existing three methods. The experimental values, thus obtained, are presented in Table 5.1 and shown

graphically in Figs. 5.4 and 5.5 for comparison with the experimental α_T's due to our method and the theoretical α_T's also.

Now, the parameters a' and b' in eq. (5.10) influence the manner of variation of $\ln q_e$ for any binary gas mixture with the pressure at any experimental temperature. The graph of $\ln q_e$ against the pressure for He^4-Ar^{40} and Ne^{20}-Xe^{132} mixtures are shown in Figs 5.2 and 5.3 respectively, at different compositions of the lighter components, along with that for Ne^{20}-Ne^{22} isotopic mixture. As in most cases of experimental observation, Fig. 5.2 and 5.3 show that, as the pressure increase $\ln q_e$ increases for a given composition of the binary mixtures mentioned above and becomes maximum at the pressure $p=(b')^{1/4}$, where $\delta \ln q_e/\delta p = 0$. From eq.(5.11) the value $\ln q_e$ at the point of maximum is

$$\ln q_{max} = a'/2\sqrt{b'} \qquad \text{..... (5.13)}$$

The reliable value of $\ln q_{max}$ of the inert gas mixture of a certain composition and at a given temperature can thus be measured from eq (5.13), in terms of the experimental parameters a' and b' which are obtained by fitting the experimental data of $\ln q_e$ and pressure p in atmosphere. Using eqs (5.2) and (5.13) with the knowledge of the value of the column calibration factor, the TD factors α_T of the inert gas mixtures at different concentrations of the lighter components are then estimated, and shown in Table 5.1 and in Figs. 5.4 and 5.5.

5.3. Theoretical Formulations

The theoretical α_T's can be calculated form

$$\alpha_T = \frac{1}{6[\lambda_i]_1} \frac{S^{(i)}x_i - S^{(j)}x_j}{[x_\lambda + y_\lambda]_1} (6C^*_{ij} - 5) \qquad \text{..... (5.14)}$$

where the symbols are defined by Chapman and Enskog[11]. Here, $(6C^*_{ij}-5)$ depends strongly on the temperature alone, and the other factor in eq. (5.14) is not only a function of the temperature but also a complicated function of the compositions and the thermal conductivities of gases and gas mixtures. The α_T's thus computed from eq (5.14) are presented in the last column of Table

5.1 and shown graphically in Figs 5.4 and 5.5 respectively, for the gas mixtures He^4-Ar^{40} and Ne^{20}- Xe^{132}. A sample calculation was also made from

$$\alpha_{ij} = \frac{(6C_{ij}^{*}-5)\mu_{ij}}{5nk\,[D_{ij}]} \left(\frac{\lambda^{\alpha}_{j\,trans}}{x_j m_j} - \frac{\lambda^{\alpha}_{i\,trans}}{x_i m_i}\right) \qquad \text{..... (5.15)}$$

as deduced by Monchick, Munn and Mason[12] by assuming elastic collisions between the molecules and the results obtained are found to be much higher than those computed from eq (5.14).

5.4. Results and Discussions

The Chapman-Enskog kinetic theory of gases[11] is strictly applicable only to spherically symmetric molecules like noble gases, and give a good account of the viscosity, diffusion and heat conductivity of gases so excellently that it has often been used with fair success to interprete the experimental thermal diffusion factors of isotopic mixtures of noble gases[14]. But it has been found that for binary mixtures of spherically symmetric molecules the theory is quite unable to explain the composition dependence and probably the temperature dependence of the experimental thermal diffusion factors α_T for mixtures of different noble gases. We computed the theoretical α_T's from eq (5.14) with the available force parameters as presented in Table 5.2 for the mixtures He^4 - Ar^{40} and Ne^{20}-Xe^{132}, the data thus obtained are shown in Table 5.1 and in Figs 5.4 and 5.5 only to see that they do not tally with the experimental ones computed by the present as well as the existing methods. The theoretical α_T's are found to be two order higher in magnitude than the expermental α_T's estimated while in the case of Ne^{20}-Ne^{22} isotopic mixture the theoretical α_T's agree fairly well with the experimental ones as shown in Table 5.1. This is the reason why most of the authors in this field of research conclude that the FJO column theory is successful in predicting both the temperature and the composition dependence of the experimental α_T's for isotopic mixtures as they are reproduced by the theoretical α_T's as computed by the Chapman-Enskog theory of monatomic gases.

In the column theory, to estimate the experimental α_T's for binary mixtures, molecular models such as Maxwells inverse fifth power and Lennard-Jones

12:6 potential model are commonly used. The method based on Lennard-Jones potential model is applicable to evaluate α_T at the cold wall temperature T_c of the column. The column shape factors and other molecular transport parameters also are required to be determined at the cold wall temperature. As evident from Table 5.1 the α_T's values for He^4-Ar^{40} mixture due to the L-J molecular model shape factor as shown in Table 5.2 are very low compared with our α_T's from the column calibration factor (F_s) method as well as with those due to Maxwell's moelcular model and Slieker's model independent method. For He^4-Ar^{40} mixture, as the percentage of the lighter component, say He^4, increases, the experimental α_T's decrease gradually, attain the minimum values and then increase again as shown in Fig. 5.4. This sort of behaviour of the composition dependence of α_T's for He^4-Ar^{40} could not be at all explained by the elastic theoretical α_T's obtained from the Chapman-Enskog kinetic theory of monatomic gases. The magnitudes of the values are found to be two order higher than all the experimental α_T's as observed in Table 5.1. The similar situation occurs in the case of Ne^{20}-Xe^{132} mixture; the theoretical α_T's here also could not explain the composition dependence of the experimental α_T's, which are also two-order less in magnitude than the theoretical ones, as observed from Table 5.1 and Fig. 5.5.

It is interesting to note that our experimental α_T's due to the column calibration factor method, which is simple, straightforward and free from any binary molecular interaction model, is very close to those due to Slieker's method as well as the method using Maxwell's model, so far as the trends of variation of the α_T's with mole fraction and their magnitudes are concerned. The existing method using *L-J* model yields α_T's of less magnitude for He^4-Ar^{40} mixture, but in the case of Ne^{20}-Xe^{132} these α_T's are of about the same magnitudes as the α_T's due to Slieker's and our mehod.

Thus it is concluded that the present method, with the use of the column calibration factor F_s and the experimental $\ln q_{max}$ as obtained from the experimental parameters a' and b', is not only applicable to isotopic gas mixtures, like the existing methods based on molecular models and Slieker's method, but is also a universal method to estimate the experimental α_T's of

polyatomic gas mixtures. The temperature as well as the composition dependence of the actual and relatively small α_T's of any binary gas mixture can thus be estimated by our present method. This study finally establishes that the column calibration factor F_s plays a significant role in column measurements. Thus it is wise to study a large number of columns of different r_c, r_h and L and $\bar{T}$ to explore the functional relationship of F_s to r_c, r_h, L and $\bar{T}$, by choosing the interesting gas pairs forming binary mixtures, so that we can arrive at the unique formulation of the column calibration factor for a given column.

References

[1] K. Clusius and G. Dickel; Naturwiss. **26**(1938) 546.

[2] J. O. Hirschfelder, C.F. Curtiss and R. B. Bird, Molecular Theory of Gases and Liquids (John Wiley and Sons, N.Y., 1964)

[3] C. J. G. Slieker : Z Naturforsch. **20a** (1965) 52

[4] S. Acharyya, A. K. Das, P. Acharyya, S.K. Datta and I. L. Saha, J. Phys. Soc. Jpn. **50** (1981) 1603

[5] S. Acharyya, I. L. Saha, P.. Acharyya, A.K. Das and S. K. Datta, J. Phys Soc. Jpn . **51**(1982) 1469

[6] S. Acharyya, I.L. Saha, A. K Datta and A.K. Chaterjee : J.Phys. Soc. Jpn. **56**(1987) 105

[7] J.M. Saviron, C.M. Santamaria, J.A. Carrion and J. C. Yarza, J. Chem. Phys, **63**(1975)5318

[8] R.C. Jones and W. H. Furry, Rev. Mod. Phys. **18** (1946) 151

[9] W. H. Furry, R.C. Jones and L Onsager, Phys. Rev. **55**(1939)1083

[10] W.M. Rutherford and K.J. Kaminski, J. Chem. Phys. **47**(1967)5427

[11] S. Chapman and T. G. Cowling : *The Mathematical Theory of Nonuniform Gases* (Cambridge University Press. N. Y.. 1952).

[12] L. Monchick, R. J. Munn and E. A. Mason, J. Chem. Phys **45**(1966) 3051

[13] G. Vasaru : Separation of Isotopes by Thermal Diffusion. ERDA.- tr-32 (1975). National Technical Information Service, U.S, Dept of Commerce, Springfield Virginia 22161.

[14] A.K. Datta and S. Acharyya, J. Phys. soc. Japan **62** (1993) 1527.

CHAPTER 6

Thermal Diffusion Factors of Hydrogenic Trace Mixtures with Helium by Column Calibration Factor

Thermal diffusion factors of hydrogenic trace mixtures with helium by column calibration factor

6.1. Introduction

In the existing column theory as developed by Furry and others [1-3] the column geometry plays an important role in determining the exact value of thermal difusion factor α_T of binary gas mixture. The column as such cannot yield the actual α_T values both in trend and in magnitude with respect to temperature and composition as the binary molecular interactions are often called into play. Thermal diffusion column is still far superior to any other α_T measuring instruments as the equilibrium separation factor q_e defined by

$$q_e = (x_i/x_j)_{top} \Big/ (x_i/x_j)_{bottom}$$

is very large even in the case of small mass difference between the components of a mixture. Here, x_i and x_j are the mass fractions of the lighter and the heavier components respectively. Hence for a binary mixture of almost identical masses, shapes and sizes a calibrated TD column can safely be used to measure a reliable relative and small α_T values. For this reason we have calibrated the given column of Slieker and de Vries[4] with known reliable α_T of He - T_2 mixture to arrive at the column calibration factor (CCF) F_s from the relation :

$$\ln q_{max} = \alpha_T F_s(r_c, r_h, L, \bar{T}) \qquad \ldots\ldots\ldots\ldots\ldots\ldots (6.1)$$

where $\bar{T}$ is the mean temperature of T_h and T_c, T_h and T_c being the hot and cold wall temperatures in *K*. r_c and r_h are the radii of cold and hot wall of a column of geometrical lenght *L*. F_s is supposed to be an independent molecular model solely dependent on the column geometry at any mean temperature $\bar{T}$ in *K*.

A number of studies by Acharyya et al[5-7] and Navarro et al[8] on F_s enabled us to study the temperature dependence of α_T of DT and HT in helium only to explore the fact that the TD column is a reliable relative α_T measuring instrument and to observe the inelastic collision effects in them. In this study, we estimate the experimental parameters a' and b' governing the very nature of variation

of the available experimental lnq_e against pressure p of He-DT and He-HT gas mixtures[4] the hydrogenic components were never becoming larger than 5% in helium at three experimental temperatures.

The computed data of lnq_e of He-DT and He-HT against pressure in atmosphere are shown in Fig. 6.1 and 6.2 respectively to ensure that the least square fitted curves agree excellently with the experimental ones. For He-HT an interesting feature is that unlike the usual behaviour, lnq_e becomes smaller with temperatures, not noticed earlier[7].

The hydrodynamical part of the column theory is excellently obeyed by He-DT and for some selected experimental points of He-HT as their p^2/lnq_e against p^4 were found out to be

$$p^2/lnq_e = 0.7758 + 0.8161\ p^4 \text{ at } 338\ K,$$
$$= 0.4938 + 0.7294\ p^4 \text{ at } 378\ K,$$
$$= 0.3964 + 0.6034\ p^4 \text{ at } 423\ K \text{ and}$$

$$p^2/lnq_e = 9.0749 + 14.8368\ p^4 \text{ at } 338\ K$$
$$= 13.5999 + 64.6412\ p^4 \text{ at } 378\ K$$
$$= 14.6461 + 411.5226\ p^4 \text{ at } 423\ K \text{ respectively.}$$

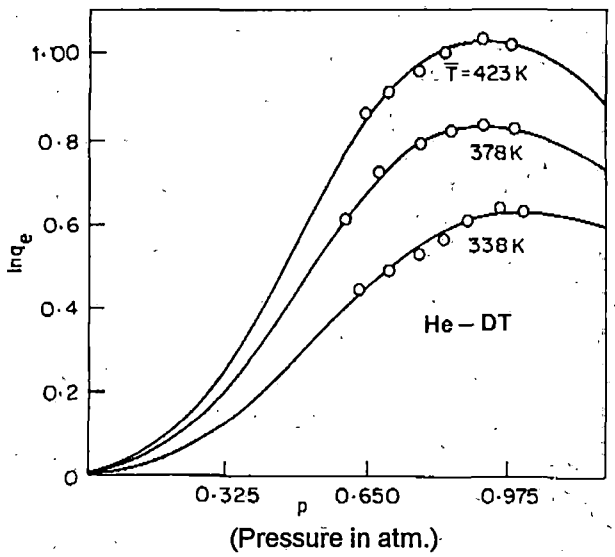

Fig. 6.1. lnq_e against pressure p in atmosphere for He-DT trace mixture at $\bar{T}$ = 338, 378 and 423 K, 'O' experimental points.

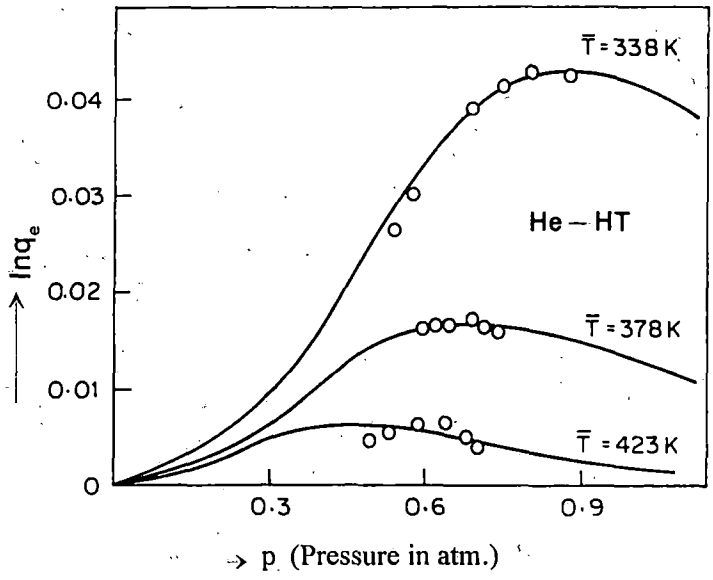

Fig. 6.2. Inq_e against pressure p in atmosphere for He-HT trace mixture, at $\bar{T}$= 338 and 423 K, 'O' experimental points.

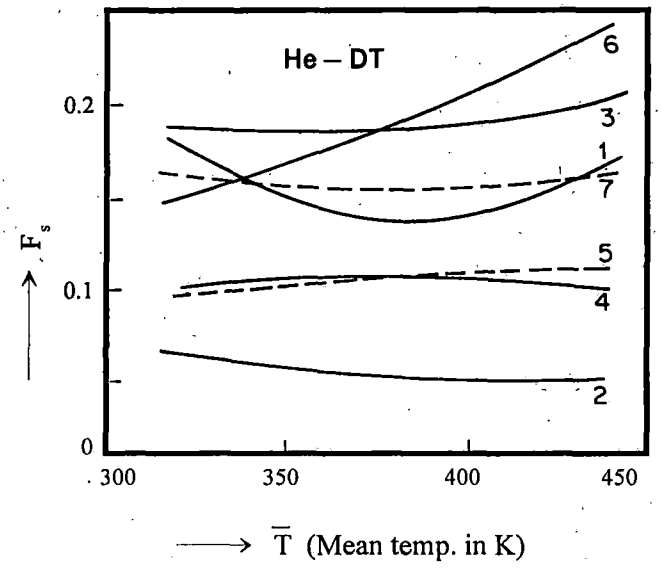

Fig. 6.3. Variation of α_T with $\bar{T}$ of He-DT trace mixture, 1. Our expt α_T from Inq_{max} and F_s; 2. Expt α_T (Maxwell case); 3. Expt α_T(Slieker case); 4. Theor α_T(elastic) from eq (6.7); 5. Theor α_T (inelastic) with Z_{rot}= 300 from eq (6.7); 6. Theor α_T (inelastic) with Z_{rot} calculated from Barua et al (1970) from eq (6.8); 7. Theor α_T (inelastic) with Z_{root} calculated from Parkers[12] formula with adjustable Z^{α}_{rot} = 7.08[13].

In the absence of any reliable possibility to estimate the actual experimental α_T of a mixture through the use of molecular model we used the values of F_s already obtained for the column[7];

$$F_s = -66.52202 + 0.3502286\,\bar{T} - 4.1879 \times 10^{-4}\,\bar{T}^2 .$$

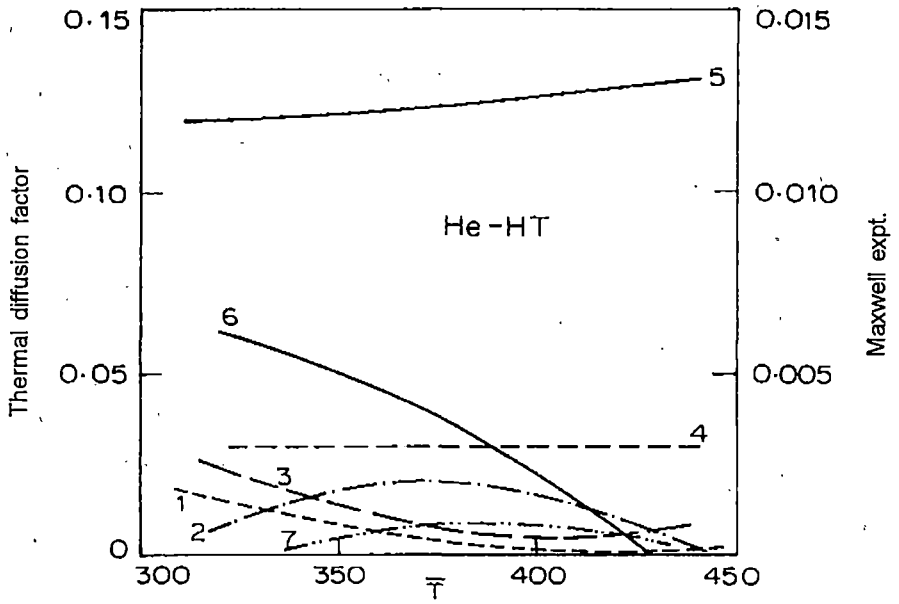

Fig. 6.4. Variation of α_T with $\bar{T}$ of He-HT trace mixture, 1. Our expt α_T from $\ln q_{max}$ and F_s; 2. Expt α_T(Maxwell); 3. Expt α_T(Slieker); 4. Theor α_T(elastic) from Eq (6.7); 5. Theor α_T (inelastic) with $Z_{rot} = 300$ from Eq(6.8) 6. Theor α_T (inelastic) with Z_{rot} calculated from Baura et al[12] from Eq(6.8) 7. Theor α_T(inelastic) with Z_{rot} calculated from Parker[13] formula with adjustable $Z_{rot} = 12.15$.

Now α_T's of He-DT and He-HT were obtained from eq(6.1) and compared with those by the existing methods using column theory as well as the theoretical α_T based on elastic and inelastic[9] collisions in Fig 6.3 and 6.4 respectively in order to reveal the existence of inelastic collisions in these mixtures.

6.2. Theoretical Formulation to Estimate Experimental α_T.

Both ends being closed for the ideal column of length L, $\ln q_e$ of a gas mixture at any mean temperature $\bar{T}$ is given by

$$\ln q_e = HL/(K_c + K_d) \quad \text{..... (6.2)}$$

where H, K_c and K_d are the functions of transport coefficients of a gas mixture and proportional to p^2, p^4 and p^0 respectively, p being pressure in atmosphere.

In order to remove parasitic remixing effect, Furry and Jones[2] simply added a term K_p proportional to p^4 to the denominator when eq.(6.2) becomes

$$\ln q_e = a' p^2/(b' + p^4) \quad \text{..... (6.3)}$$

which is also written as

$$p^2/\ln q_e = b'/a' + (1/a')p^4 \quad \text{..... (6.4)}$$

a' and b' are however related by

$$(HL/K_c)p^2 = a'(1 + K_p/K_c) \text{ and } (K_d/K_c)p^4 = b'(1 + K_p/K_c)$$

H, K_c, K_d are the functions of the transport coefficient of a mixture and K_p is the remixing coefficient.

Again if C represents the intercept of the straight line of eq. (6.4) we have

$$H = (K_d/LC) \quad \text{..... (6.5)}$$

the exact expressions for H, K_c and K_d are given in our previous publications[5-7]

The estimation of the experimental α_T through the existing formulations involved the shape factors taking account of the inherent asymmetry of the column geometry. The mass density ρ, the viscosity coefficient η and the diffusion coefficient D were calculated from MTGL of Hirschfelder et al[10], the column shape factors and the force parameters required had already been reported earlier[7].

It is observed in Fig.6.1 - 6.2, that as the pressure increases $\ln q_e$ increases and becomes maximum when $p = (b')^{1/4}$ for which $\frac{\delta}{\delta p}(\ln q_e) = 0$.

We then have from eq (6.3)

$$\ln q_{max} = (a'/2\sqrt{b'}) \qquad \text{.....(6.6)}$$

It is also observed in He-HT, unlike He-DT, that some experimental data of $\ln q_e$ are not in fit with the hydrodynamical part of the column theory as they have tendency to yield the negative intercept of $p^2/\ln q_e$ against p^4 which is absurd unless inversion of α_T would take place. Hence we are bound to select some six or seven data from the reported graph to fix the values of $\ln q_{max}$ from the eq (6.6).

Table 6.1 and the graphs of Figs 6.1and 6.2 revealed that $\ln q_{max}$ from eq (6.6) in terms of a' and b' are in good agreement with the graphically determined values earlier[7]. This establishes the fact that our choice of the $\ln q_e$ data with pressure particularly for the He-HT mixture where the mass difference between the components is practically nil, is almost right.

6.3. Theoretical Formulations to Calculate α_T

Theoretical α_T can, however, be estimated from

$$\alpha_T = \frac{1}{6[\lambda_{ij}]_1} \frac{S^{(i)} x_i - S^{(j)} x_j}{[X_\lambda + Y_\lambda]} (6C^*_{ij} - 5) \qquad \text{..... (6.7)}$$

where $(6C^*_{ij} - 5)$ depends mainly on the temperature while the other factors involved in eq (6.7) are the complicated functions of composition, masses and thermal conductivities of gases and gas mixtures. The α_T calculated from eq (6.7) is presented in the 12th column of Table 6.1, and shown graphically in Figs 6.3 and 6.4 for He-DT and He-HT respectively.

The inelastic thermal diffusion factor α_{ij} is given by Monchick et al[11]

$$\alpha_{ij} = \frac{(6C^*_{ij} - 5)\mu_{ij}}{5nk[D_{ij}]_1} \left(\frac{\lambda^{\alpha}_{j\ trans}}{x_j m_j} - \frac{\lambda^{\alpha}_{i\ trans}}{x_j m_j} \right) +$$

$$\frac{1}{5nk\,[D_{ij}]_1} \left[\frac{(6\tilde{C}_{ij} - 5)\lambda^{\alpha}_{j\ int}}{x_j} - \frac{(6\tilde{C}_{ij} - 5)\lambda^{\alpha}_{i\ int}}{x_i} \right]. \qquad \text{..... (6.8)}$$

where the symbols have their usual meanings only the collision integral ratio

Table 6.1. Experimental and Theoretical α_T values of binary gas mixtures with temperature.

System	Hot wall temp T_h in K	Cold wall T_c in K	Mean Temp $\bar{T}$ in K	a' in $(atm)^2$	b' in $(atm)^4$	In q_{max} computed from eq(6.5)	Expt F_s Ref (6)	Expt α_T with: Our calibration factor method eq(6.1)	Maxwell shape factor	Slieker shape factor	Theor. α_T from eq(6.6) elastic theor. method	Theoretical α_T from eq(6.7) with Z_{rot}: 300	Barua *et al*	Parker
He–HT	393	283	338	0·0674	0·6116	0·0431	4·001	0·0107	0·0014	0·0017	0·030	0·121	0·055	0·002
	473	283	378	0·0155	0·2104	0·0169	6·026	0·0020	0·0028	0·0007	0·030	0·124	0·037	0·009
	563	283	423	0·0024	0·3559	0·0064	6·691	0·0009	0·0010	0·0006	0·030	0·129	0·005	0·005
He–DT	393	283	338	1·289	1·0519	0·6284	4·001	0·1567	0·060	0·186	0·105	0·100	0·158	0·158
	473	283	378	1·371	0·6670	0·8331	6·026	0·1382	0·054	0·187	0·104	0·105	0·188	0·154
	563	283	423	1·660	0·6580	1·0232	6·691	0·1529	0·050	0·194	0·103	0·109	0·226	0·159

$\tilde{C}_{ij}$ differs from C^*_{ij}. In fact $\tilde{C}_{ij}$ is not symmetric with respect to the interchange of the indices i and j and is very sensitive to inelastic collision.

For a pure gas the exact values of $\lambda^{\alpha}_{j\,trans}$ and $\lambda^{\alpha}_{i\,trans}$ is given by

$$\lambda^{\alpha}_{i\,trans} = \frac{\eta}{M}\left[\left(\frac{5}{2} C_{v\,trams} + \frac{\rho D_{int}}{\eta} C_{int}\right) - \left(\frac{2C_{i\,int}}{\pi Z_{rot}}\right)\left(\frac{5}{2} - \frac{\rho D_{int}}{\eta}\right)^2 \right.$$

$$\left. \left\{1 + \frac{2}{\pi Z_{rot}}\left(\frac{5}{3}\frac{C_{int}}{R} + \frac{\rho D_{int}}{\eta}\right)\right\}^{-1}\right] \quad \text{..... (6.9)}$$

Here $C_{v\,trans} = 3R/2$, the constant value of translational heat capacity, Z_{rot} is the rotational translational collision number for inelastic collision.

The nonspherical terms of eq (6.8), we used Hirschfelder-Euken expression[10] to calculate the thermal conductivity $\lambda^{\alpha}_{i\,int}$ from

$$\lambda^{\alpha}_{i\,int} = \frac{n[D_{ii}]_1 C_{int}}{1 + (x_j / x_i)(D_{ii}/D_{ij})_1} \quad \text{.....(6.10)}$$

Theoretical inelastic α_T's for He-DT and He-HT thus calculated from eq (6.8) with the help of eq (6.9) and eq (6.10) are shown in Table 6.1 and also in Figs 6.3 and 6.4 respectively for comparison with other experimental α_T values.

6.4. Results and Discussion

The inherent asymmetry in the column geometry is however, taken into account by Maxwell, Sileker and Lennard - Jones dimensionless shape factors[7]. We calculated the experimental α_T's of He-HT and He-DT trace mixtures at $\bar{T}$=338, 378 and 423K respectively for eq (6.5) using those shape factors. Slieker's case does not involve any molecular model and it gives rather a rough estimation of the experimental α_T due to L-J case cannot be applicable here. The α_T thus obtained due to Maxwell and Slieker cases is presented in table 6.1 and shown graphically by the curves 2 and 3 respectively of Figs 6.3 and 6.4.

The experimental α_T from eq (6.1) as obtained in terms of $\ln q_{max}$ of eq(6.8) and F_s is shown by curve 1 in Fig. 6.3 and 6.4. When they are compared with those due to Maxwell (curve 2) and Slieker (curve 3) it is found that so far as the trend is concerned the data due to Slieker agree better than those due to Maxwell's shape factors. This is perhaps due to the fact that both Slieker and our method are free from any binary molecular model. As the mass difference between the components of a binary mixture decreases as in the case of He-HT the agreement is more close.

The theoretical α_T based on elastic collision theory of eq (6.7), as shown by curve 4 in Figs 6.3 and 6.4 appears to be temperature independent. Unlike He-HT, He-DT however show slightly lower value at higher temperature. The inelastic α_T as calculated from eq (6.8) with Z_{rot} = 300, show its positive temperature dependence as represented by curve 5 in Figs 6.3 and 6.4.

When α_{ij} were calculated with the available rotational translational collision number of Barua *et. al*[12] an interesting feature is that the curve 6 of Figs 6.3 and 6.4 coincide with α_T's of our CCF method. This fact prompted us to adjust Z_{rot} from Parker's formula[12]. Using Z_{rot}= 2.78, 2.91 and 3.05 for HT and Z_{rot}= 4.78, 5.01 and 5.23 for DT at 338, 378 and 423K respectively inelastic α_{ij}'s are then estimated for both He-DT and He-HT trace mixtures and were shown by curve 7 in Figs 6.3 and 6.4 respectively for comparison with other α_T's.

With Z_{rot} determined by us inelastic theoretical α_T's curve 7 (15th column of table 6.1) so far as the magnitude and trend are concerned in the case of He-DT, support our α_T's curve 1 (9th column of Table 6.1) and only in trend with α_T's due to Slieker (11th column of Table 6.1). In the case of He-HT these theoretical α_T's almost coincide with our α_T's, but in trend with the experimental α_T's due to Maxwell.

All these comparison of α_T's so far obtained thus reveal that inelastic collisions play an important role in such mixtures. Again the variation of $\ln q_{max}$ against $\bar{T}$ for He-HT is given by

$$\ln q_{max} = 0.89879 - 4.2097 \times 10^{-3} \bar{T} + 4.9647 \times 10^{-6} \bar{T}^2$$

showing that at $\bar{T} \simeq 429K$, ln q_{max} may be zero as shown in Fig. 6.5. The isobaric He-HT mixture may yield an interesting phenomenon of inversion of both $\ln q_{max}$ and α_T with respect to temperature like isobaric system N_2-CO as studied in our recent publication of Saha *et.al*[14]. The system He-HT deserves a detailed study of measurements of $\ln q_e$ against pressure for its different composition and temperatures.

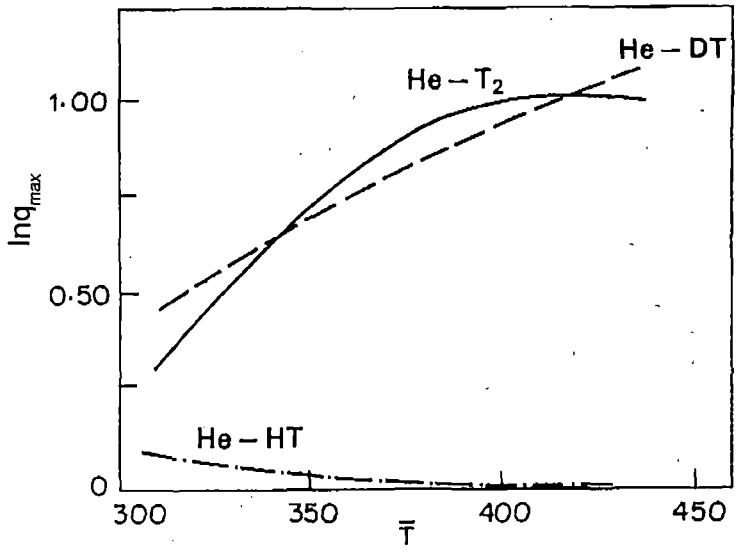

Fig. 6.5. Variation of $\ln q_{max}$ with temperature $\bar{T}$ in K for He-DT, He-T_2 and He-HT mixtures.

We are, therefore, now in a position to conclude that CCF is an accurate α_T determining factor of isotopic, nonisotopic and isobaric α_T for binary gas mixtures. The functional relationship of F_s with r_c, r_h, L and $\bar{T}$ should be studied both from the theoretical and experimental viewpoints.

References

[1] W. H. Furry, R. C. Jones and L. Onsager, *Phys. Rev.* **55**, (1939) 1083.

[2] W. H. Furry and R. C. Jones, *Phys. Rev.* **60**, (1946) 459.

[3] R. C. Jones and W. H. Furry, *Rev. Mod. Phys.* **18**, (1946) 151.

[4] C. J. G. Slieker and A. E. de Vries, *J. Chim. Phys.* **60**, (1967) 172.

[5] S. Acharyya, A. K. Das, P. Acharyya, S. K. Datta and I. L. Saha, *J. Phys. Soc. Jpn.***50,** (1981) 1603.

[6] S. Acharyya, I. L. Saha, P. Acharyya, A. K. Das and S. K. Datta, *J. Phys. Soc. Jpn.***51,** (1982) 1469.

[7] S. Acharyya, I. L. Saha, A. K. Datta and A. K. Chatterjee, *J. Phys. Soc. Jpn.***56,** (1987) 105.

[8] J. L. Navarro, J. A. Madariage and J. M. Saviron, *J. Phys. Soc. Jpn.***52,** (1983) 478.

[9] T. K. Chatterjee and S. Acharyya, J. Phys. **B7,** (1974) 2272.

[10] J. O. Hirschfelder, C. F. Curtiss and R. B. Bird, *Molecular theory of gases and liquids,* (John Wiley, New York, 1964).

[11] L. Monchick, S. I. Sandler and E. A. Mason, J. Chem. Phys. **49**, (1968) 1178.

[12] A. K. Barua, A. Manna, P. Mukhopadhyay and A. Dasgupta, *J. Phys.* **B3,** (1970) 619.

[13] J. G. Parker, *Phys. Fluids.* **2,** (1959) 449.

[14] I. L.Saha, A. K .Datta, A.K.Chatterjee and S. Acharyya,*J. Phys.Soc.Jpn.* **56,**(1987) 2381.

CHAPTER 7

Estimation of Column Calibration Factor and Force Parameters to Predict Temperature Dependence of Thermal Diffusion Factor of Some Simple Molecules

Estimation of Column Calibration Factor and Force Parameters to Predict Temperature Dependence of Thermal Diffusion Factor of Some Simple Molecules

7.1. Introduction

The theoretical thermal diffusion factor as derived from Chapman-Enskog gas kinetic theory[1], based on spherical molecule with spherically symmetric potential field is generally not in good agreement with the experimental α_T's of a binary nonisotopic or even isotopic gas mixture. It is still of special interest from the technical point of view to enrich rare as well as ordinary isotopes. The close correlation between the theoretical α_T's with the intermolecular forces may conveniently be used as an effective tool to investigate the molecular force parameters ε_{ij}/k and σ_{ij} where ε_{ij} is the depth of the potential well, k is the Boltzmann constant and σ_{ij} is the molecular diameter as the process of thermal diffusion unlike viscosity is a second order effect.

Although, TD column was supposed not to yield the actual α_T values both in trend and in magnitude with respect to temperature and composition of the mixture, still it is far superior to any other α_T measuring instruments like two bulbs and trennschaukel as the equilibrium separation factor q_e defined by $q_e=(x_i/x_j)_{top}/(x_i/x_j)_{bottom}$ is very large even in the case of isotopic gas mixture where the mass difference between the components *i* and *j* is practically very small. x_i and x_j are the mass or mole fractions of the lighter (i) and the heavier (j) molecules respectively. The equilibrium separation factor q_e of any binary gas mixture is usually determined for different compositions of a gas mixture at a fixed temperature $\overline{T}$ or for mixture of fixed composition at different experimental temperatures. With the help of q_e thus measured at different pressures well below and around one atmosphere, α_T of a gas mixture could be ascertained. The existing method to evaluate the experimental α_T from $\ln q_e$ measured in a column at different pressures is usually involved with Maxwell and Lennard-Jones model dependent as well as model independent Slieker column shape factors.

In order to obtain the actual α_T of a binary gas mixture, a large number of

workers[2-5] has, however, introduced a scaling factor F_s called the column calibration factor (CCF) for a TD column in the relation:

$$\ln q_{max} = \alpha_T F_s (r_{cold}, r_{hot}, L, \bar{T}) \quad \ldots\ldots\ldots\ldots (7.1)$$

where r_{cold} and r_{hot} are the cold and hot wall radii of a column of geometrical length L. $\bar{T}$ is the mean temperature of the gas mixture defined by $\bar{T}=(T_{hot}+T_{cold})/2$, T_{hot} and T_{cold} are the hot and cold wall temperatures in K respectively. F_s is supposed to be a molecular model independent parameter and entirely depends on the geometry of a TD column.

Roos and Rutherford[6] had measured the pressure dependence of $\ln q_e$ of Kr^{80}-Kr^{86}, Xe^{129}-Xe^{136}, CO^{28}-CO^{29}, $CH_4{}^{16}$-$CH_4{}^{17}$ and $N_2{}^{28}$-$N_2{}^{29}$ with their natural isotopic abundances at two experimental temperatures in K in a hot wire TD column of L=487.7 cm, r_{cold}=0.9525cm and r_{hot} = 0.0795 cm respectively. The measured $\ln q_e$ at different pressures in atmosphere by Roos and Rutherford[6] were plotted in Figs. 7.2 and 7.3 by least square fitted curves with the estimated *a'* and *b'* values at two available temperatures. The *a'* and *b'* for the third temperature were also obtained and the variation of $\ln q_e$ at that temperature is, however, selected for each of them and shown in Figs. 7.2 and 7.3 by dotted curves.

From the known and reliable α_T values[7] as well as experimentally determined $\ln q_{max}$ of Ar^{36}-Ar^{40}, F_s for a column as was derived by Datta and Acharyya[4] was first carried out to yield the temperature dependence of α_T of Kr^{80}-Kr^{86} as

$$\alpha_T = 0.0453\text{-}11.0479 \times 1/\bar{T} \quad \ldots\ldots\ldots\ldots (7.2)$$

The corresponding α_T's at the required experimental temperatures $\bar{T}$ = 455.5, 530.5 and 680.5K in the column of Roos and Rutherford[6] were then obtained. They are shown in Table 7.1. These values together with the experimentally estimated $\ln q_{max}$ of Kr^{80} - Kr^{86} from the curves of $\ln q_e$ vs p as shown elsewhere[8] at those temperatures were then utilised to arrive at the probable temperature dependence of F_s for a column[6] :

$$F_s = 67.1066 - 0.15809\,\bar{T} + 3.29153 \times 10^{-4}\,\bar{T}^2 \quad \ldots\ldots\ldots\ldots (7.3)$$

which is shown graphically in Fig 7.1. The values of F_s together with the corresponding experimental lnq_{max} at any temperature gives us α_T's of the different systems from eq. (7.1). The force parameters ε_{ij}/k and σ_{ij} were estimated from the comparative study of the probable temperature dependence of α_T and C^*_{ij} (12-6 Lennard-Jones potential) with respect to $1/\bar{T}$ and $1/\bar{T}^*$ respectively where $\bar{T}^* = \bar{T}/(\varepsilon_{ij}/k)$. The temperature dependence of α_T could not be predicted with α_T's measured at only two experimental temperatures. Nevertheless, an approximate middle temperature is, however, essential to be selected to reveal the actual variation of α_T's of those systems under consideration with respect to temperature in consistent with the estimation of the actual force parameters among the molecules.

The experimental α_T's for these systems by the existing methods, involved with column shape factors due to Maxwell model[9] and Slieker,[10] as presented in Table 7.2, were obtained and shown graphically in Figs. 7.4-7.8. The theoretical α_T's based on elastic and inelastic collisions were also computed with the estimated force parameters ε_{ij}/k and σ (Table 7.2) and are shown in Figs. 7.4-7.8 for comparison with experimental α_T's. The data thus obtained are, however, shown in Table 7.1 together with the other essential data. The

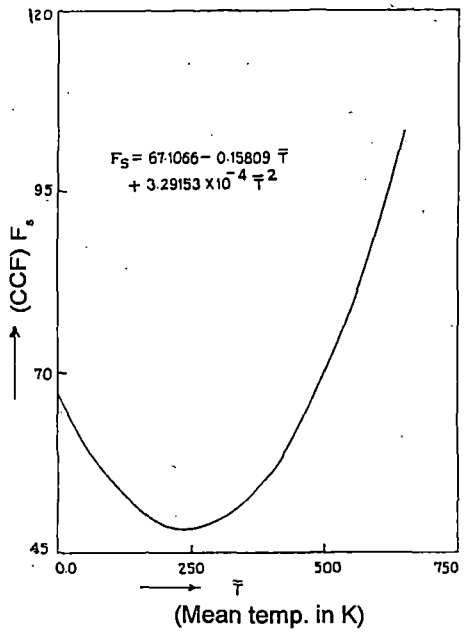

Fig. 7.1. Variation of column calibration factor F_s (CCF) against temperature in K.

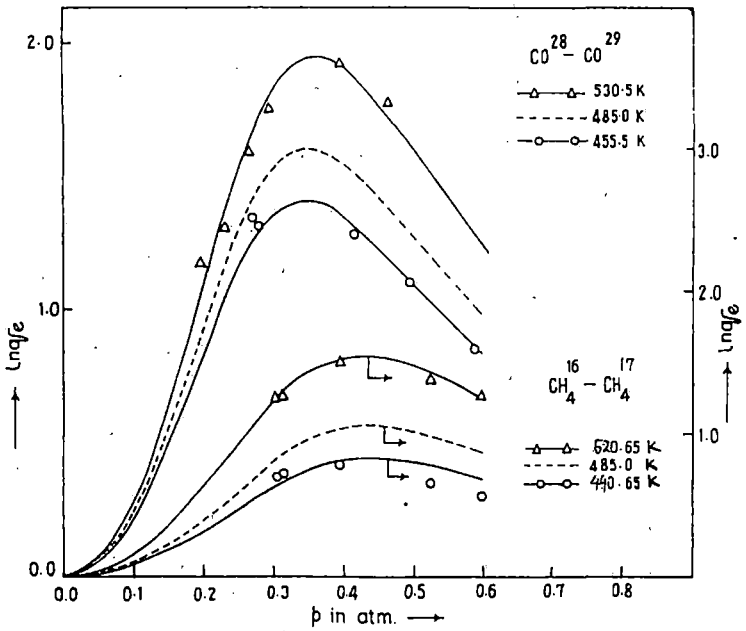

Fig. 7.2. Variation of Inq_e against pressure p in atmosphere: -Δ-Δ- Experimental Inq_e at $\overline{T}$= 530.5K for CO^{28}–CO^{29}, ----- Predicted Inq_e at $\overline{T}$=485K for CO^{28}–CO^{29},–o–o– Experimental Inq_e at $\overline{T}$=455.5K for CO^{28}-CO^{29}, -Δ-Δ- Experimental Inq_e at $\overline{T}$=520.65K for CH_4^{16}–CH_4^{17}, ---- Predicted Inq_e at $\overline{T}$=485 K for CH_4^{16}– CH_4^{17}, –o–o– Experimental Inq_e at $\overline{T}$= 440.65 K for CH_4^{16}– CH_4^{17}.

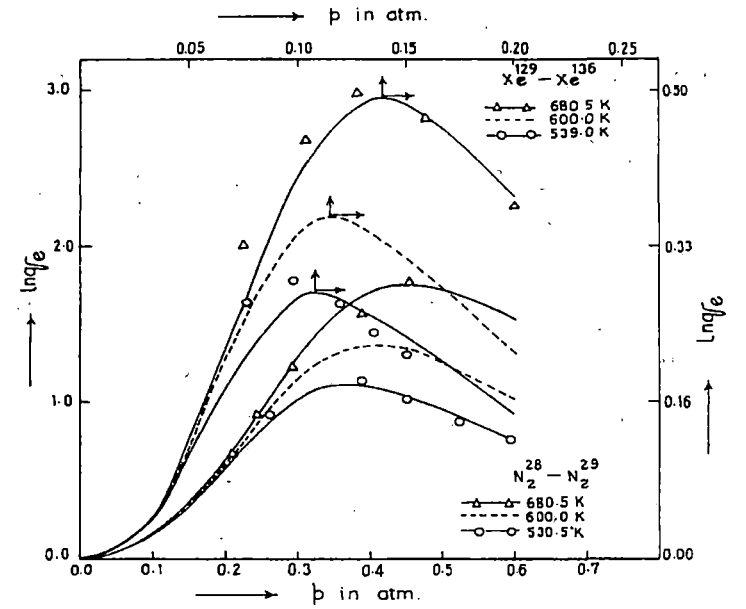

Fig. 7.3. Variation of Inq_e against pressure p in atmosphere: -Δ-Δ- Experimental Inq_e at $\overline{T}$= 680.5K for Xe^{129}–Xe^{136}, ----- Predicted Inq_e at $\overline{T}$= 600.0K for Xe^{129}–Xe^{136},-o-o- Experimental Inq_e at $\overline{T}$= 539.0K for Xe^{129}– Xe^{136}. -Δ-Δ- Experimental Inq_e at 680.5K for N_2^{28}–N_2^{29}. --- Predicted Inq_e at $\overline{T}$=600.0K for N_2^{28}– N_2^{29}. –o–o– Experimental Inq_e at $\overline{T}$= 530.5 K for N_2^{28}– N_2^{29}.

CCF method together with the technique of simultaneous determination of force parameter is thus found to be successful in predicting the exact, reliable and correct temperature variation of α_T of a binary isotopic mixture.

The curves of α_T's against $\bar{T}$ in Figs 7.4-7.8, however, support the possibility of estimation of binary interactions among the molecules as one obtains those from the viscosity of gases and gas mixtures. The estimation of α_T's by the present CCF method are found to be in close agreement so far trends are concerned, as observed in Figs 7.4-7.8, with the theoretical ones in terms of the estimated force parameters (Table 7.2). Thus the methodology so far extended is really a simple, straightforward and unique one.

7.2. Mathematical Formulation to Estimate the Experimental α_T

Both ends being closed for an ideal column of length L, $\ln q_e$ of a gas mixture at any temperature $\bar{T}$ is given by[11]

$$\ln q_e = HL/(K_c + K_d) \qquad \text{..... (7.4)}$$

where H, K_c and K_d are the functions of transport coefficients of a gas mixture. They are proportional to p^2, p^4 and p^0 respectively, p being pressure in atmosphere. In order to remove parasitic remixing effect, Furry and Jones[11] simply added a term K_p called remixing coefficient, being proportional to p^4 to the denominator of eq (7.4). Hence eq (7.4) finally becomes

$$\ln q_e = \frac{a'p^2}{b' + p^4} \qquad \text{..... (7.5)}$$

or, $$p^2/\ln q_e = b'/a' + (1/a')\, p^4 \qquad \text{..... (7.6)}$$

a' and b' are, however, related by

$$(HL/KC)\, p^2 = a' (1 + K_p/K_c)$$

and $$(K_d/K_c)\, p^4 = b' (1 + K_p/K_c)$$

The constants a' and b' were, however, estimated by fitting eq. (7.6) with the

Table 7.1. Experimental and theoretical thermal diffusion factors α_T of binary isotopic mixtures of simple gases with temperatures in K.

Column used	System	Hot wall Temp. (T_{hot}) in K	Cold wall Temp. (T_{cold}) in K	Mean Temp. in K $\bar{T}=\frac{T_{hot}+T_{cold}}{2}$	a' $(atm)^2$	b' $(atm)^4$	Computed $\ln q_{max}$ from eq(7.15)	Column Calibration factor F_ϕ (CCF)
L=Length of the column =487.7 cm	Kr	623	288	455.5	0.0622	0.00055	1.333	63.586
		773	288	530.5	0.1007	0.00074	1.855	75.869
		1073	288	680.5	0.2464	0.00143	3.252	111.94
	Xe	790	288	539	0.0066	0.00014	0.280	77.562
		912	288	600	0.0099	0.00019	0.362	90.748
		1073	288	680.5	0.0187	0.00036	0.492	111.94
Hot wall radius r_{hot} = 0.0795 cm	CO	623	288	455.5	0.3336	0.0142	1.398	63.586
		682	288	485	0.3919	0.0149	1.603	67.858
		773	288	530.5	0.5028	0.0166	1.951	75.869
Cold wall radius r_{cold} = 0.9525 cm	CH_4	593.15	288.15	440.65	0.3414	0.0376	0.886	61.357
		682.00	288.00	485.00	0.4768	0.0361	1.255	65.858
		753.15	288.15	520.65	0.6059	0.0340	1.643	74.023
	N_2	773	288	530.5	0.3156	0.0201	1.115	75.869
		912	288	600	0.4423	0.0265	1.360	90.748
		1073	288	680.5	0.7311	0.0437	1.707	111.94

Column used	System	Estimated α_T using			Computed theoretical α_T	
		Present method	Maxwell shape factor	Slieker shape factor	Elastic	Inelastic
L=Length of the column =487.7 cm	Kr	0.0210	0.0134	0.0146	0.0107	
		0.0245	0.0165	0.0184	0.0127	
		0.0291	0.0252	0.0290	0.0150	
	Xe	0.0036	0.0010	0.0018	0.0087	
		0.0040	0.0018	0.0021	0.0096	
		0.0044	0.0022	0.0025	0.0102	
Hot wall radius r_{hot} = 0.0795 cm	CO	0.0221	0.0100	0.0113	0.0052	0.2861
		0.0236	0.0107	0.0117	0.0057	0.3104
		0.0257	0.0114	0.0127	0.0061	0.3334
Cold wall radius r_{cold} = 0.9525 cm	CH_4	0.0144	0.0070	0.0076	0.0036	0.0230
		0.0191	0.0086	0.0095	0.0046	0.0296
		0.0222	0.0099	0.0110	0.0054	0.0342
	N_2	0.0147	0.0065	0.0073	0.0090	0.4010
		0.0150	0.0069	0.0078	0.0094	0.4081
		0.0153	0.0077	0.0088	0.0102	0.4148

experimentally observed $\ln q_e$ at different pressures in atmosphere. Both a' and b' are now the experimental parameters to govern the variation of $\ln q_e$ against pressure as shown graphically in Figs. 7.2 and 7.3 for CO^{28} - CO^{29}, CH_4^{16} - CH_4^{17} and Xe^{129}- Xe^{136}, N_2^{28}-N_2^{29} respectively with the experimental data[6,8] placed on them at two available temperature. The third temperature would then be selected from the plot of $\alpha_T = A + B/\bar{T}$ with the measured α_T's at two temperatures.

In each case as observed in Figs. 7.2 and 7.3, $\ln q_e$ increases gradually with pressure and assumes maximum value $\ln q_{max}$ at a pressure $p=(b')^{1/4}$ for which $\frac{\delta}{\delta p}(\ln q_e)= 0$. Hence from eq. (7.5) we have

$$\ln q_{max} = \frac{a'}{2\sqrt{b'}} \qquad \text{.....(7.7)}$$

Now a' and b', in Table 7.1, help us fix the values of $\ln q_{max}$ from eq (7.7) and hence the experimental α_T's for the above mentioned systems could, however, be determined from eq.(7.1) with F_s. To use the existing method with Maxwell and Slieker column shape factors eq (7.4) also becomes

$$\ln q_{max} = \frac{HL}{2\sqrt{K_c K_d}} \qquad \text{.....(7.8)}$$

when $\frac{\delta}{\delta p}(\ln q_e) = 0$. The final expression of the experimental α_T's in terms of the column shape factors are finally given by :

$$\alpha_T = 2.39 \times \frac{r_{cold} - r_{hot}}{L} \times \frac{\bar{T}}{\Delta T} \ln q_{max} \cdot \frac{\sqrt{k'_c k'_d}}{h'} \qquad \text{.....(7.9)}$$

and

$$\alpha_T = 2.00 \times \frac{r_{cold}}{L} \cdot \frac{\bar{T}}{\Delta T} \ln q_{max} \frac{\{\pi(1-a^2)[S.F]_3\}^{1/2}}{[S.F]_1} \qquad \text{.....(7.10)}$$

respectively, where the symbols used are of usual significance as mentioned elsewhere[9,10]. The column shape factors which are supposed to take into

account the inherent asymmetry of the column geometry are presented in Table 7.2. The computed α_T's with Maxwell and Slieker column shape factors (Table 7.2) are placed in Table 7.I and shown graphically in Figs 7.4-7.8 by curve No. 2 and 3 respectively in order to compare with those by the present CCF and theoretical ones.

7.3. Derivation of Force Parameters

The principal contribution[12] to the temperature dependence of $\alpha_{T\ theor}$ comes from the factor $(6C^*_{ij} - 5)$ of Chapman-Enskog expression[1] where

$$\alpha_{T\ theor} = g(6C^*_{ij} - 5). \qquad \text{..... (7.11)}$$

The term $(6C^*_{ij} - 5)$ contains only unlike interactions among the molecules. The other part i.e., *'g'* depends on the composition of the gas mixture. Althogh, *'g'* depends slowly on temperature it can be taken fairly constant for a short range of temperature and for a fixed composition of the gas mixture as in the case of the present investigation. It is seen that[13]

$$\alpha_{T\ expt} = A + B/\bar{T} \qquad \text{..... (7.12)}$$

where A and B are two arbitrary constants. C^*_{ij} of eq. (7.11) can also be written as a function of reduced temperature $\bar{T}^*$

$$C^*_{ij} = C + D/\bar{T}^* \qquad \text{..... (7.13)}$$

C and D are two new constants. Now from eqs. (7.11) and (7.13) we have

$$\alpha_{T\ theor} = \left[(6C - 5) + \frac{6D}{\bar{T}^*}\right] g. \qquad \text{..... (7.14)}$$

When $\alpha_{T\ theor} = \alpha_{T\ expt}$ we may write from eqs. (7.12) and (7.14)

$$(6C - 5)g = A. \qquad \text{..... (7.15)}$$

The experimental α_T's at two available temperatures by the CCF method are now used to get the values of A and B. Similarly with the reported C^*_{ij} vs $\bar{T}^*$ curve[14] for 12- 6 Lennard-Jones potential within a short range of reduced temperature $\bar{T}^*$, C and D of eq. (7.13) were easily evaluated. (6C–5) and A could yield *'g'* which enable one to locate the value of C^*_{ij} and T^*; and hence ε_{ij}/k.

This sort of evaluation was further improved by taking into account the small variation of *'g'* with temperature. This was done by repeating the entire procedure as mentioned earlier to get the exact value of *'g'* with the initially estimated ε_{ij}/k and hence the exact value of ε_{ij}/k is finally located. The ε_{ij}/k thus estimated agrees well with the literature values as shown in Table 7.2 for molecules Ar, Kr, Xe, CO, CH_4 and N_2 respectively. With these ε_{ij}/k, the respective σ_{ij}'s were also determined from available viscosity data and are placed in Table 7.2 together with the literature values.

7.4. Theoretical Formula to Estimate $\alpha_{T\,theor}$

(i) **Elastic :** The $\alpha_{T\,theor}$ due to Chapman-Enskog is already given by eq (7.11) which consists of two factors :

$$g = \frac{1}{6[\lambda_{ij}]_1} \cdot \frac{s^{(i)}x_i - s^{(i)}x_j}{X_\lambda + Y_\lambda} \text{ and } (6C^*_{ij} - 5).$$

The first factor is the complicated functions of composition, thermal conductivities of gas and gas mixture while the second one is strongly a temperature dependent term. The symbols used are described in detail in MTGL[1]. The $\alpha_{T\,theor}$ thus computed with ε_{ij}/k and σ_{ij} (Table 7.2) are presented in the 13th column of Table 7.1 and shown graphically in Figs 7.4-7.8 for comparison with $\alpha_{T\,expt}$ by existing and the present CCF method.

(ii) **Inelastic :** According to Monchick *et. al*[15] the $\alpha_{T\,theor}$ due to inelastic collisions is given by :

$$\alpha_{T\,theor} = \frac{(6C^*_{ij} - 5)\mu_{ij}}{5nk[D_{ij}]_1}\left[\frac{\lambda^{\alpha}_{j\,trans}}{x_j M_j} - \frac{\lambda^{\alpha}_{i\,trans}}{x_i M_i}\right] +$$

$$\frac{1}{5nk[D_{ij}]_1}\left[\frac{(6\widetilde{C}^*_{ij} - 5)\lambda^{\alpha}_{j\,int}}{x_j} - \frac{(6\widetilde{C}_{ij} - 5)\lambda^{\alpha}_{i\,int}}{x_i}\right] \qquad \text{..... (7.16)}$$

where the symbols used have their usual meanings[15]. The collision integral ratio $\widetilde{C}_{ij}$ which differs from C^*_{ij}, is very sensitive to inelastic collision and not

symmetric with respect to the interchange of the indices *i* and *j*. The exact value of $\lambda^{\alpha}_{j\,trans}$ or $\lambda^{\alpha}_{i\,trans}$ for a pure gas is given by[15]

$$\lambda^{\alpha}_{j\,trans} = \frac{\eta}{M}\left[\left(\frac{5}{2} C_{v\,trans} + \frac{\rho D_{int}}{\eta} C_{int}\right)\right.$$

$$-\left(\frac{2}{\pi}\cdot\frac{C_{int}}{Z_{rot}}\right)\left(\frac{5}{3}-\frac{\rho D_{int}}{\eta}\right)^{2}$$

$$\left.\left\{1+\frac{2}{\pi Z_{rot}}\left(\frac{5}{3}\frac{C_{int}}{R}+\frac{\rho D_{int}}{\eta}\right)\right\}^{-1}\right] \qquad \text{..... (7.17)}$$

Hence, C_v = 3R/2 = the constant value of translational heat capacity, Z_{rot} = rotational translational collision number for inelastic collision. To evaluate the nonspherical part of eq (7.16) we used Hirschfelder-Euken expression[15] to calculate the internal thermal conductivity λ^{α}_{int} from :

$$\lambda^{\alpha}_{i\,int} = \frac{n[D_{ij}]_1 C_{int}}{1+(x_j / x_i)(D_{ii} / D_{ij})} \qquad \text{..... (7.18)}$$

The inelastic $\alpha_{T\,theor}$ for CO^{28}-CO^{29}, $CH_4{}^{16}$-$CH_4{}^{17}$ and $N_2{}^{28}$-$N_2{}^{29}$ were calculated from eq (7.16) with the help of eqs (7.17) and (7.18). The mass density ρ_{ij}, the coefficient of viscosity η_{ij} and the diffusion coefficient D_{ij} of the gas mixtures were calculated from MTGL[1], in terms of the evaluated ε_{ij}/k and σ_{ij} (Table 7.2). The $\alpha_{T\,theor}$ (inelastic) thus calculated for CO, CH_4 and N_2 isotopic mixtures are placed in Table 7.1 and shown graphically in Figs 7.6-7.8 for comparison.

7.5. Results and Discussions

The least square fitted equations of $p^2/\ln q_e$ against p^4 were worked out from the pressure dependence of experimental $\ln q_e$[6] for Kr^{80}-Kr^{86}, Xe^{129}-Xe^{136}, CO^{28}-CO^{29}, $CH_4{}^{16}$-$CH_4{}^{17}$ and $N_2{}^{28}$-$N_2{}^{29}$ with their natural isotopic abundances. In case of later four systems $\ln q_{max}$ were estimated in terms of a' and b' at two available experimental temperatures. The pressure dependence of $\ln q_e$ at any

intermediate temperature could, however be obtained from the temperature dependence of both α_T and F_s of eqs(7.12) and (7.3). The linearity of b' with a short range of temperature fixes b' and hence a' from eq (7.7) at the intermediate temperature. The pressure dependence of $\ln q_e$ in the selected intermediate

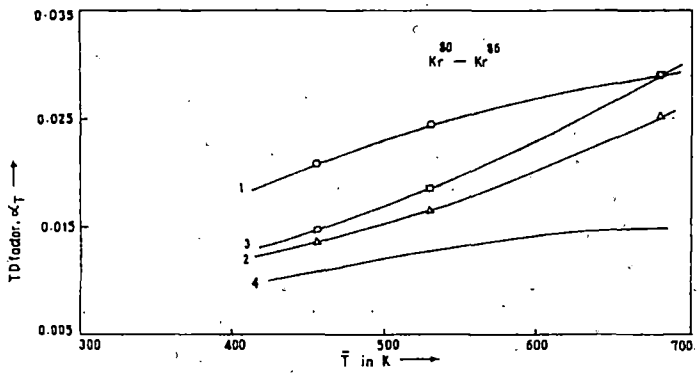

Fig.7.4 Plot of α_T's against $\bar{T}$ in K for Kr^{80}–Kr^{86}. –o–o– Curve 1: Experimental α_T from F_s and $\ln q_{max}$. –△–△– Curve 2: Experimental α_T using Maxwell shape factors. –□–□– Curve 3: Experimental α_T using Slieker shape factors. Curve 4: Theoretical α_T based on elastic collision.

temperature for all the systems except Kr^{80}-Kr^{86} are shown in Figs. 7.2 and 7.3 by dotted lines. The least square fitted equations of $p^2/\ln q_e$ against p^4 at all the temperatures for the aforesaid binary mixtures are given by :

i) Kr^{80}-Kr^{86};

$p^2/\ln q_e = 0.0088 + 16.0771 p^4$ at 455.5 K

$= 0.0074 + 9.9602\ p^4$ at 530.5 K

$= 0.0058 + 4.0584\ p^4$ at 680.5 K

ii) Xe^{129}-Xe^{136};

$p^2/\ln q_e = 0.0212 + 151.515\ p^4$ at 539.0 K

$= 0.0192 + 101.0101\ p^4$ at 600.0 K*

$= 0.0192 + 53.4759\ p^4$ at 680.5 K

iii) CO^{28}-CO^{29};

p^2/lnq_e= 0.0426 + 2.9976 p^4 at 455.5 K

= 0.0382 + 2.5517p^4 at 485.0 K*

= 0.0330 + 1.9888 p^4 at 530.5 K

iv) CH_4^{16}-CH_4^{17};

p^2/lnq_e= 0.1101 + 2.9291p^4 at 440.65 K

= 0.0757 + 2.0973 p^4 at 485.0 K*

= 0.0561 + 1.6504 p^4 at 520.65K

v) N_2^{28}-N_2^{29};

p^2/lnq_e= 0.0637 + 3.1686 p^4 at 520.5 K

= 0.0599 + 2.2609 p^4 at 600.0 K*

= 0.0598 + 1.3678 p^4 at 680.5 K

*Intermediate temperature.

The experimental α_T's due to Maxwell and Slieker column shape factors were placed in the 10th and 11th columns of Table 7.1 and are shown graphically by curve Nos. 2 and 3 respectively in Figs. 7.4-7.8 as a function of temperature. They are almost of the same trends with those of CCF method as evident in Table 7.1 and Figs 7.4-7.8, although, the Slieker column shape factors are very crude in comparison with those of Maxwell inverse fifth power potential model.

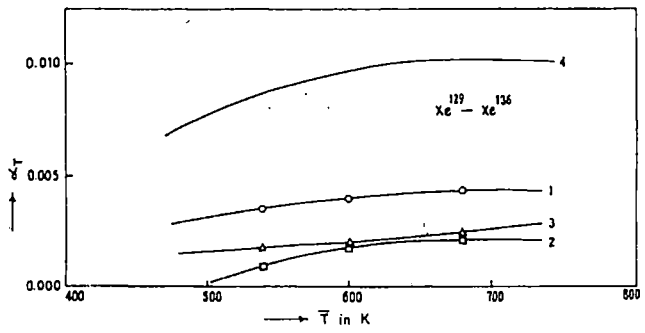

Fig.7.5. Plot of α_T's against $\bar{T}$ in K for Xe^{129}–Xe^{136}. -o-o- Curve 1: Experimental α_T from F_s and lnq_{max}. -□-□- Curve 2: Experimental α_T using Maxwell shape factors. -Δ-Δ- Curve 3: Experimental α_T using Slieker shape factors. Curve 4: Theoretical α_T based on elastic collision.

Table 7.2. Maxwell's model dependent and Slieker's model independent column shape factors, coefficient of viscosity η_{ij} and Diffusion coefficient D_{ij} together with estimated force parameters ϵ_{ij}/k and molecular diameters σ_{ij} used in the calculation of α_T of simple isotopic gas mixtures

System	Model Potential	Estimated		Reported		Mean Temp. ($\bar{T}$) in K
		ϵ_{ij}/k in K	σ_{ij} in Å	ϵ_{ij}/k in K	σ_{ij} in Å	
Ar^{36}–Ar^{40}	LJ 12-6	125.03	3.516	125.2* 119.5**	3.405*	371.0 378.0 387.5
Kr^{80}–Kr^{86}	LJ 12-6	199.55	3.712	199.2* 166.7**	4.020*	455.5 530.5 680.5
Xe^{129}–Xe^{136}	LJ 12-6	228.20	4.253	222.2* 229.0**	4.362*	539 600 680.5
CO^{28}–CO^{29}	LJ 12-6	200.56	3.620	110.0†	3.590†	455.5 485.0 530.5
CH_4^{16}–CH_4^{17}	LJ 12-6	323.28	3.360	148.9* 310.0*	3.630*	440.65 485.00 520.65
N_2^{28}–N_2^{29}	LJ 12-6	80.963	3.914	95.2* 91.5*	3.341*	530.5 600.0 680.5

System	Model Potential	Column shape factors						$\eta_{ij} \times 10^5$ gm cm^{-1} sec^{-1}	D_{ij} cm^{-1} sec^{-1}
		Maxwell			Slieker				
		h'	k_c'	k_d'	$[S \cdot F]_1 \times 6.1$	$\pi(1-a^2)$	$[S \cdot F]_3 \times 9.1$		
Ar^{36}–Ar^{40}	LJ 12-6								
Kr^{80}–Kr^{86}	LJ 12-6	1.015	2.05	0.8143	1.2165	3.121	0.7702	28.53	
		1.225	3.00	0.7829				32.25	
		1.580	4.81	0.7571				39.01	
Xe^{129}–Xe^{136}	LJ 12-6	1.251	3.105	0.7804				33.61	
		1.405	3.85	0.7679				36.62	
		1.579	4.81	0.7571				40.39	
CO^{28}–CO^{29}	LJ 12-6	1.015	2.05	0.8143				24.17	0.4157
		1.095	2.40	0.8000				25.45	0.4629
		1.225	3.00	0.7829				27.33	0.5499
CH_4^{16}–CH_4^{17}	LJ 12-6	0.965	1.84	0.8229				12.58	0.3639
		1.095	2.40	0.8000				13.77	0.4379
		1.195	2.85	0.7857				14.68	0.5009
N_2^{28}–N_2^{29}	LJ 12-6	1.225	3.00	0.7829				33.31	0.6742
		1.405	3.85	0.7679				35.85	0.8293
		1.580	0.81	0.7571				38.97	1.0141

* Maitland *et al.* (1981).
** Hirchfelder *et al.* (1964).
† G. Vasaru (1975).

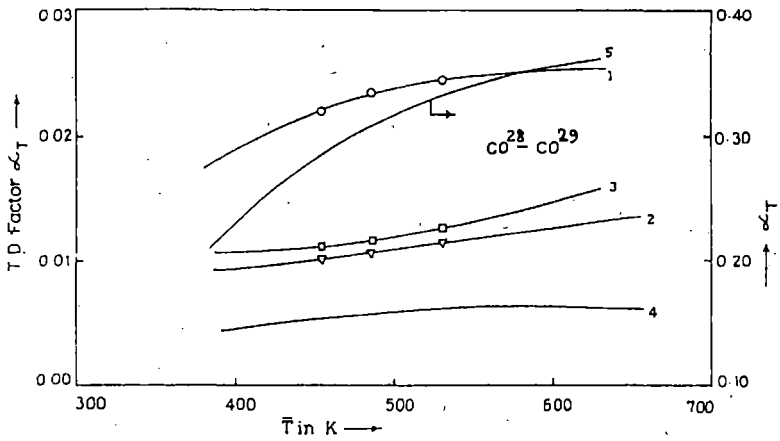

Fig.7.6. Plot of α_T's against $\bar{T}$ in K for CO^{28}–CO^{29}. –o–o– Curve 1: Experimental α_T from F_s and $\ln q_{max}$. –△–△– Curve 2: Experimental α_T using Maxwell shape factors. –□–□– Curve 3 Experimental α_T using Slieker shape factors. Curve 4: Theoretical α_T based on elastic collision. Curve 5: Theoretical α_T based on inelastic collision.

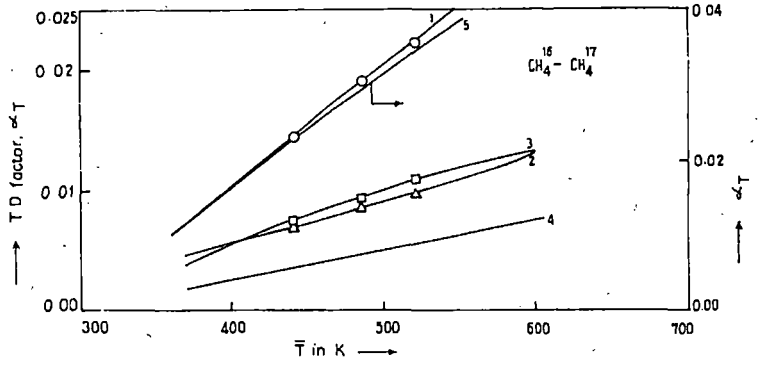

Fig.7.7. Plot of α_T's against $\bar{T}$ in K for CH_4^{16}–CH_4^{17}. –o–o– Curve 1: Experimental α_T from F_s and $\ln q_{max}$ –△–△– Curve 2: Experimental α_T using Maxwell shape factors. –□–□– Curve 3: Experimental α_T using Slieker shape factors. Curve 4: Theoretical α_T based on elastic collision. Curve 5: Theoretical α_T based on inelastic collision.

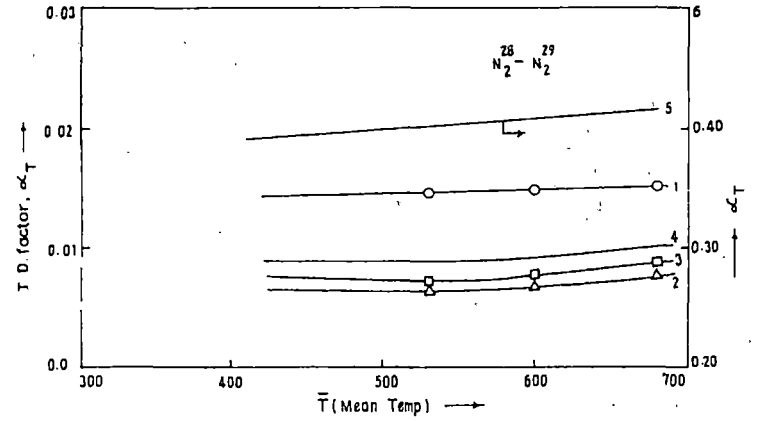

Fig.7.8. Plot of α_T's against $\bar{T}$ in K for N_2^{28}–N_2^{29}. –o–o– Curve 1: Experimental α_T from F_s and $\ln q_{max}$. –△–△– Curve 2: Experimental α_T using Maxwell shape factors. –□–□– Curve 3: Experimental α_T using Slieker shape factors. Curve 4: Theoretical α_T based on elastic collision. Curve 5: Theoretical α_T based on inelastic collision.

The experimental α_T's as obtained in terms of lnq_{max} and F_s from eqs (7.1) and (7.3) are placed in the 9th column of Table 7.1 and shown graphically by the curve No. 1 in all the Figs 7.4-7.8. These are slightly higher than those due to Maxwell (curve 2) and Slieker (curve 3), but exhibit the similar trends as mentioned earlier.

The reliability of the temperature dependence of the experimental α_T's by the CCF method of the aforesaid binary mixtures is, however, ensured with the determination of the respective molecular force parameter ε_{ij}/k's and σ_{ij}'s for the molecules. The estimated force parameters seem to be sensitive to intermolecular interactions and agree excellently well for Ar, Kr, and Xe while for CO, CH_4 and N_2 they deviate remarkably. Both ε_{ij}/k's and σ_{ij}'s are all presented in columns 3 and 4 to compare with the literature values placed in columns 5 and 6 respectively of Table 7.2. This fact at once suggests the existence of inelastic collisions in the later three isotopic mixtures. It was, however, pointed out by some workers[16, 17] that the theory of inelastic collision effect in thermal diffusion is not widely applicable except for eccentrically loaded sphere molecule as one of the component in binary mixtures. The simple theory so far adopted here to estimate the force parameters is based on the elastic collision amongst the molecules. The inelastic collision in molecules like CO, CH_4 and N_2 may be the reason of such deviations (Table 7.2.).

The α_T's due to elastic collision theory from eq. (7.11) in terms of ε_{ij}/k and σ_{ij} are also shown graphically by the curve no 4 of Figs. 7.4-7.8 for comparison with α_T's by CCF method. They are placed in the 12th column of Table 7.1. The graphs in Figs, 7.4-7.8 and Table 7.1, clearly show that in case of Kr and Xe elastic α_T's almost coincide with α_T's by CCF method so far the magnitudes and trends are concerned. But in case of CO, CH_4 and N_2 elastic α_T's are of one order smaller in magnitudes and not with the same trends with α_T's from CCF method.

The fact as mentioned above indicates that Chapman Enskog gas kinetic theory[1] could not interprete the variation of α_T's of CO, CH_4 and N_2 isotopic mixtures with temperature probably due to the presence of inelastic collision among such molecules as shown in Tables 7.1 and 7.2. But the theory appears

to be successful to explain the temperature dependence of α_T's of spherically symmetric molecules like Ar, Kr, and Xe as evident from Tables 7.1 and 7.2 and Figs 7.4 and 7.5.

The α_T based on inelastic collisions as derived by Monchick *et al*[15] from eq (7.16) for CO^{28}-CO^{29}, CH_4^{16}-CH_4^{17} and N_2^{28}-N_2^{29} are presented in column 13 of Table 7.1. They are plotted graphically by the curve No. 5 in Figs 7.6-7.8 for comparison.

From all the discussions we may conclude that α_T's as obtained by CCF method is a simple, straightforward and unique one. This study further indicates that the nature of variation of F_s is the same as observed earlier,[2-4, 17] but differing in the magnitudes of coefficients A, B and C in $F_s = A + B\bar{T} + C\bar{T}^2$. Thus the nature of variation of F_s with temperature $\bar{T}$(Fig 7.1) confirms that the CCF method to locate the magnitude and trend of α_T in Figs 7.4-7.8 is correct.

7.6. Conclusions

Although, F_s is supposed to be an essential tool in determining the experimental α_T in a column measurement, still the functional relationship of F_s with r_{cold}, r_{hot}, L and $\bar{T}$ remains unexplored. Simultaneous determination of F_s and the force parameters seems to be an important step forward to observe α_T of both isotopic and nonisotopic binary mixtures of simple molecules as a function of temperature. A rigorous study of experimental F_s through experimentally determined $\ln q_{max}$ of binary mixture having accurate α_T is needed with different column geometries to serve this purpose.

The very existence of inelastic collision effects in thermal diffusion of suitable molecules forming binary mixture have to be studied in detail through $\ln q_{max}$ and F_s to improve the theory of inelastic collision effects in thermal diffusion.

References

[1] J. O. Hirchfelder, C. F. Curtiss and R. B. Bird: *Molecular Theory of Gases and Liquids* (John Willey and Sons, New York, 1964) p. 541.

[2] S. Acharyya, A.K. Das, P.Acharyya, S.K. Datta and I. L. Saha : J. Phys. Soc. Jpn. **50** (1981) 1603.

[3] S. Acharyya, I.L. Saha, P. Acharyya, A. K. Das and S. K. Datta : J. Phys. Soc. Jpn. **51** (1982) 1469.

[4] A. K. Datta and S. Acharyya : J. Phys. Soc. Jpn. **62** (1993) 1527.

[5] J. L. Navarro, J. A. Madariage and J M. Saviron : J. Phys. Soc. Jpn. **50** (1983) 1603.

[6] W. J. Roos and W. M. Rutherford : J. Chem. Phys. **50** (1969) 3936

[7] F. Vandervolk : Ph. D. Dissertation (1963).

[8] I. Yamamoto, H. Makino and A. Kanagawa : J. Nucl. Sci. Technol. **27** (1990) 156.

[9] G. Vasaru : *Thermal Diffusion Column, supplied by S. Raman* (B.A.R.C., Bombay).

[10] C. J. G. Slieker : Z. Naturforsch. **20** (1965) 591.

[11] W. H. Furry and R. C. Jones, Phys. Rev. **69** (1946)459.

[12] B. N. Srivastava and K. P. Srivastava : Physica, **23** (1957) 103.

[13] R. Paul, A. J. Howard and W. W. Watson : J. Chem, Phys. **39** (1963) 3053.

[14] M. Klein and F. J. Smith : Tables of collision integral for the (m,6) potential for the values of m, Arnold Engineering Development Centre, Tennessee, 1968.

[15] L. Monchick, S. I. Sandlar and E. A. Mason : J. Chem. Phys. **49** (1968) 1178.

[16] T. K. Chattopadhyay and S. Acharyya : J. Phys. B **7** (1974) 2277.

[17] G. Dasgupta, A. K. Datta and S. Acharyya : Pramana **43** (1994) 81..

CHAPTER 8

Molecular Force Parameters through Thermal Diffusion to Ensure the Model Independency of Column Calibration Factor

Molecular Force Parameters through Thermal Diffusion to Ensure the Model Independency of Column Calibration Factor

8.1. Introduction

The theoretical formulation of thermal diffusion factor α_T as derived from Chapman-Enskog gas kinetic theory[1] is based on the assumption that the molecules are elastic spheres with spherically symmetric potential field. The theory can, however, hardly explain the experimental α_T of binary nonisotopic or even isotopic gas mixtures. Thermal diffusion is still interesting for its close correlation with the intermolecular forces. Moreover, unlike viscosity, thermal diffusion is a second order effect. Thus it is generally used to investigate the elastic or inelastic collisions among the molecules. The phenomenon is also responsible to enrich rare as well as ordinary isotopes in thermal diffusion column.

The temperature dependence of experimental α_T's of a binary gas mixture may offer a convenient method to estimate the molecular force parameters like ε_{ij}/k and σ_{ij} where ε_{ij} is the depth of potential well, k is the Boltzmann constant and σ_{ij} is the molecular diameter. ε_{ij}/k and σ_{ij} become ε_{ii}/k or ε_{jj}/k and σ_{ii} or σ_{jj} for isotopic components in a binary mixture of gases. They are, therefore, expected to play an important role to yield the exact theoretical α_T's based on elastic or inelastic collisions.

To estimate experimental α_T the theory of TD column which was already developed by a large number of workers[2-4] is still insufficient. TD column, on the other hand, is a very sensitive instrument to investigate the temperature and composition dependence of α_T particularly for a binary isotopic gas mixture of molecules having practically no mass difference.

The equilibrium separation factor of a gas mixture in a TD column is defined by :

$$q_e = (x_i/x_j)_{top} / (x_i/x_j)_{bottom}$$

where x_i and x_j are the mass or mole fractions of the lighter (i) and heavier (j) components respectively. In a TD column q_e is usually measured at different pressure in atmosphere, for a fixed composition of a binary gas mixture at different temperatures or at a fixed temperature for different compositions. The existing method of evaluating the experimental α_T is involved with Maxwell, Lennard-Jones model dependent as well as Slieker model independent column shape factors (CSF). The method is, however, complicated and the resulting α_T's usually not in agreement with the theoretical α_T's so far its temperature and composition dependences are concerned.

We [5-7] therefore, introduce a scaling factor F_s called CCF for a TD column to get the actual α_T of a binary gas mixture from column measurements by the following relation:

$$\ln q_{max} = \alpha_T F_s (r_c, r_h, L, \bar{T}). \quad \text{..... (8.1)}$$

Here $\ln q_{max}$ is the logarithmic maximum equilibrium separation factor, r_c and r_h are the cold and hot wall radii maintained at temperatures T_c and T_h respectively in a TD column of geometrical length L and the mean temperature $\bar{T}$ of the gas mixture is given by $\bar{T} = (T_h+T_c)/2$.

The molecular model independent parameter[7,8] F_s can now be used to evaluate the actual α_T's of binary isotopic or nonisotopic gas mixtures from their $\ln q_{max}$ measurements. Moran and Watson[9] had already measured the pressure dependence of $\ln q_e$ of Ne^{20}-Ne^{22}, Ar^{36}-Ar^{40}, and Kr^{80}-Kr^{86} mixtures at two experimental temperatures in a TD column of L=182.0 cm, r_c=0.635 cm and r_h=0.0254 cm respectively. The measurements[9], however, inspired us to observe the probable temperature dependence of α_T of those isotopic mixtures in terms of CCF together with the estimation of ε_{ij}/k and σ_{ij} of the respective molecules. The purpose of such study is to establish the molecular model independency of F_s too.

The experimental[9] $\ln q_{max}$ of Ar^{36}-Ar^{40} at 432K and 537K and the reliable[10] α_T's of Ar were, however, used to give two values of F_s. As F_s is a molecular model independent parameter, the experimental[9] $\ln q_{max}$ and reliable[10] α_T of

Ne^{20}-Ne^{22} were used again to get F_s at the intermediate temperature 447K. The probable temperature dependence of F_s for the column[9] is then obtained

$$F_s = 54.3777 - 0.1152\bar{T} + 1.4350 \times 10^{-4}\bar{T}^2 \quad \text{..... (8.2)}$$

which is shown graphically in Fig. 8.1. This F_s and the experimental $\ln q_{max}$ for any gas mixture yield α_T at the experimental temperature $\bar{T}$ from eq. (8.1).

A large number of workers[11,12] had expressed α_T in the form :

$$\alpha_T = A + B / \bar{T} \quad \text{..... (8.3)}$$

where A and B are two arbitrary constants. The experimental α_T's for Ne^{20}-Ne^{22}, Ar^{36}-Ar^{40} and Kr^{80}-Kr^{86} as a function of $\bar{T}$ are, however given by

$$\alpha_T = 0.03019 - 0.80013 / \bar{T},$$

$$\alpha_T = 0.03476 - 5.08155 / \bar{T} \text{ and} \quad \text{..... (8.4)}$$

$$\alpha_T = 0.27993 - 69.3446 / \bar{T}$$

which are shown in Figs. 8.3-8.5 respectively. The plot of experimental α_T's against $\bar{T}$ thus enables us to evaluate ε_{ij}/k and σ_{ij} of the respective molecules[13,14]. The results are shown in Table 8.2 for comparison with the literature values. The comparison finally indicates that curves as shown in Figs. 8.3-8.5 in terms of F_s and $\ln q_{max}$ from eq (8.1) for Ne, Ar and Kr gas mixtures are claimed to be perfect. The theoretical as well as the experimental α_T's by the CCF method as a function of $\bar{T}$ were however, used to estimate a' and b' and hence $\ln q_e$ at any intermediate temperature between 432K to 537K for each system. They are also shown in Fig. 8.2 by the dotted lines together with actual $\ln q_e$ at two available $\bar{T}$K.

The experimental α_T's by the existing method involved with CSF due to Maxwell and Slieker were also evaluated and shown in Figs. 8.3-8.5. The CSF due to L-J model can not be applied here as the cold wall temperature of the column was held fixed. The theoretical α_T's based on elastic collisions were also found out with the estimated ε_{ij}/k and σ_{ij} placed in Table 8.2 and shown in Figs. 8.3-8.5 only to see how far the elastic theory is now successful to

explain the experimental α_T's (Table 8.1) by the CCF and the existing method. The theoretical α_T's are placed in the last column of Table 8.1. Both the Tables 8.1 and 8.2, however, indicate the adequacy or otherwise of the CCF method to predict the actual and reliable α_T of such isotopic mixtures together with their correct force parameters from thermal diffusion.

8.2. Mathematical Formulations to Estimate Experimental α_T

In case of an ideal column of length *L*, both ends being closed, $\ln q_e$ of a gas mixture at any temperature $\bar{T}$ is given by[7,8]

$$\ln q_e = \frac{HL}{K_c + K_d} \qquad \text{..... (8.5)}$$

H, K_c and K_d are the functions of the transport coefficients of a gas mixture and are proportional to p^2,p^4 and p^0 respectively, *p* being the pressure in atmosphere. The above eq (8.5) thus becomes

$$\ln q_e = ap^2 / (b+p^4) \qquad \text{.....(8.6)}$$

But in case of actual column, parasitic remixing generally occurs. This can be taken into consideration by adding a term K_p, proportional to p^4 in the denominator of eq (8.5), $\ln q_e$ then becomes

$$\ln q_e = a'p^2/(b'+p^4) \qquad \text{..... (8.7)}$$

where *a'* and *b'* are related to *a* and *b* by :

$$a=a'(1+K_p/K_c) \text{ and } b=b'(1+K_p/K_c)$$

The above eq (8.7) can then be written as

$$p^2 / \ln q_e = b'/a' + (1/a')\, p^4 \qquad \text{.....(8.8)}$$

where a' and *b'* are two arbitrary constants which can be obtained from experimental $\ln q_e$ at different pressures *p* in atmosphere at a given temperature $\bar{T}$K.

Again, it has been found in Fig 8.2 that the experimental $\ln q_e$ increases with *p* and eventually becomes maximum at $p = (b')^{1/4}$ for which $\frac{\delta}{\delta p}(\ln q_e)=0$. The eq (8.7) then becomes

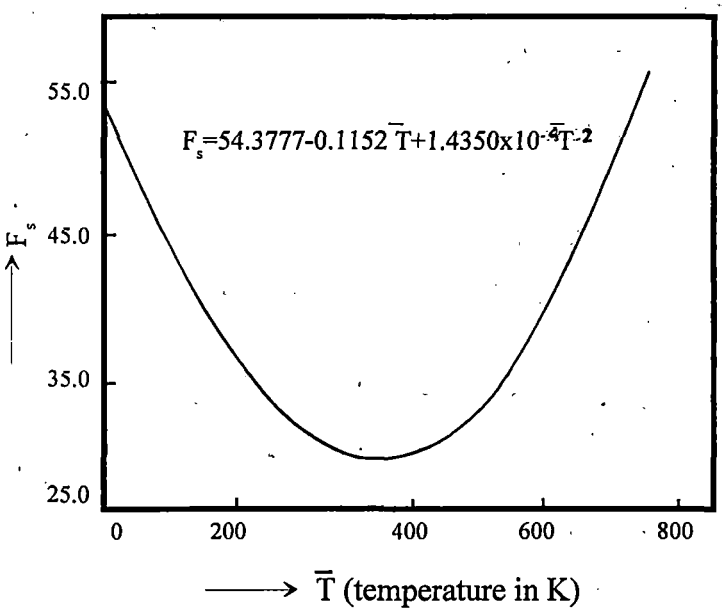

Fig. 8.1. Variation of column calibration factor F_s (CCF) against temperature in K

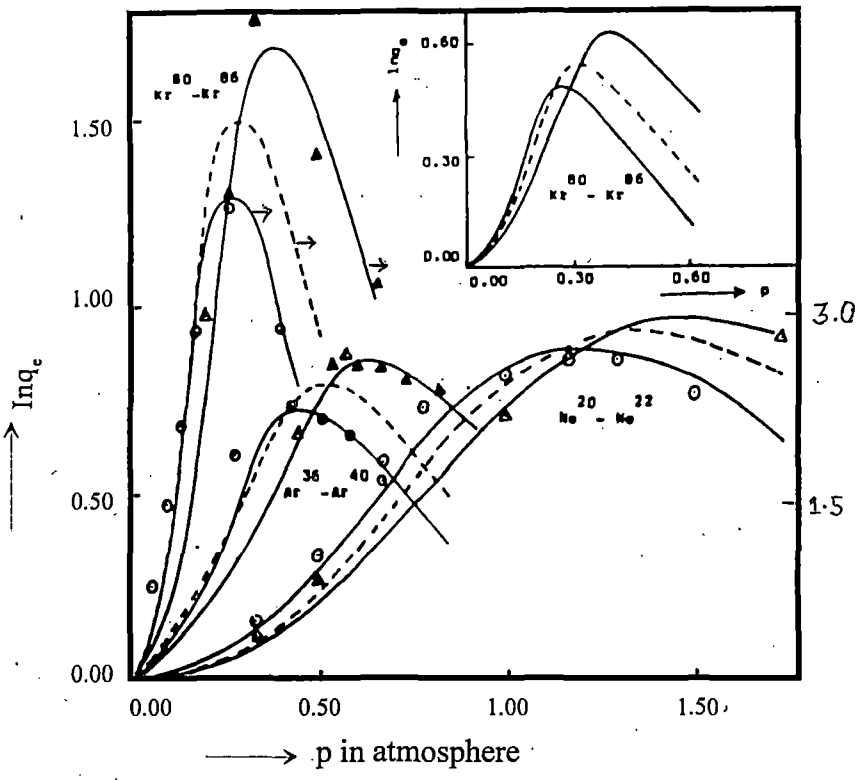

Fig. 8.2. i) Variation of Inq_e against p in atmosphere for Ne^{20}–Ne^{22}. -o-o- Experimental Inq_e at 447K, ----- Predicted In q_e at 492 K,-Δ-Δ- Experimental Inq_e at 537 K. (ii) Variation of Inq_e against p in atmosphere for Ar^{36}–Ar^{40}: -o-o- Experimental Inq_e at 432K, ----- Predicted Inq_e at 484.5 K, -Δ-Δ- Experimental Inq_e at 537 K. iii) Variation of Inq_e against p in atmosphere for Kr^{80}–Kr^{86}: -o-o- Experimental Inq_e at 447K, ----- Predicted Inq_e at 492K, -Δ-Δ- Experimental Inq_e at 537K. iv) Kr^{80}–Kr^{86} (Adjacent graph): ——— Adjusted Inq_e against p in atmosphere at 447K, ----- Predicted Inq_e against p in atmosphere at 492 K. —— Adjusted Inq_e against p in atmosphere at 537K.

$$\ln q_{max} = \frac{a'}{2\sqrt{b'}} \qquad \text{.....(8.9)}$$

With the known $\ln q_{max}$ in terms of a' and b' (Table 8.1) and F_s (Fig 8.1) of a given column[9], α_T of binary isotopic gas mixtures of Ne, Ar, Kr were found out from eq (8.1). They are placed in Table 8.1 and shown graphically in Figs 8.3-8.5.

One may obtain the experimental $\ln q_{max}$ from eq (8.5) which is also given by :

$$\ln q_{max} = \frac{HL}{2\sqrt{K_c K_d}} \qquad \text{..... (8.10)}$$

The exact expressions for H, K_c and K_d are given by:

$$\text{(i)} \quad H = \frac{2\pi}{6!}\left(\frac{\alpha_T \rho^2_{ij} g}{\eta_{ij}}\right) \cdot \frac{1}{2}(r_c + r_h)(r_c - r_h)^3 (2u)^2 h'$$

$$K_c = \frac{2\pi}{9!}(\rho^3_{ij} g^2 / \eta^2_{ij} D_{ij})_1 \frac{1}{2}(r_c + r_h)(r_c - r_h)^7 (2u)^2 k'_c$$

$$K_d = 2\pi(\rho_{ij} D_{ij})_1 \frac{1}{2}(r_c + r_h)(r_c - r_h) k'_d \qquad \text{.....(8.11)}$$

and

$$\text{(ii)} \quad H = C_1 = [S.F]_1 r_c^4 \left(\frac{\alpha_T \rho^2_{ij} g}{\eta_{ij}}\right)_1 \left(\frac{\Delta T}{\bar{T}}\right)^2$$

$$K_c = C_3 = [S.F]_3 r_c^8 (\rho^3_{ij} g^2 / n^2_{ij} D_{ij})_1 \left(\frac{\Delta T}{\bar{T}}\right)^2$$

$$K_d = C_2 = \pi(1-a^2) r_c^2 (\rho_{ij} D_{ij})_1 \qquad \text{..... (8.12)}$$

for Maxwell model and Slieker's model independent methods. The α_T in Maxwell model dependent and Slieker's model independent methods[15,16] could, however, be obtained by using eqs (8.10) to (8.12) in the following forms:

$$\alpha_T = (\text{Maxwell model}) = 2.39\,\frac{r_c - r_h}{L}\cdot\frac{\bar{T}}{\Delta T}\,\frac{\sqrt{k'_c k'_d}}{h'}\,\ln q_{max} \quad \ldots\ldots\ldots (8.13)$$

and

$$\alpha_T\,(\text{Slieker}) = 2.00\,\frac{r_c}{L}\,\frac{T}{\Delta T}\,\frac{\sqrt{\pi(1-a^2)[S.F]_3}}{[S.F]_1}\,\ln q_{max} \quad \ldots\ldots\ldots (8.14)$$

The symbols h', k_c', k'_d and $[S.F]_1$, $\pi(1-a^2)$, $[S.F]_3$ are dimensionless CSF due to Maxwell and Slieker respectively ρ_{ij} is the mass density of the gas mixture of coefficient of viscosity η_{ij} and diffusion coefficient D_{ij}, $u = \frac{T_h - T_c}{T_h + T_c}$, $\Delta T = T_h - T_c$ and g is the acceleration due to gravity.

The α_T's thus evaluated from eqs. (8.13) and (8.14) due to Maxwell model and Slieker's CSF respectively are placed in Table 8.1. They are also shown in Figs. 8.3-8.5 for Ne^{20}-Ne^{22}, Ar^{36}-Ar^{40} and Kr^{80}-Kr^{86} mixtures in order to compare them with the theoretical α_T computed with their respective ε_{ij}/k and σ_{ij}.

8.3. Theoretical Elastic α_T together with Force Parameters ε_{ij}/k and σ_{ij}.

According to gas kinetic theory the theoretical α_T based on elastic collisions[1] is

$$\alpha_T = g(6C^*_{ij} - 5) \quad \ldots\ldots\ldots (8.15)$$

where

$$g = \frac{1}{6[\lambda_{ij}]_1}\,\frac{S^{(i)}x_i - S^{(j)}x_i}{X_\lambda + Y_\lambda}$$

is a complicated function of composition and thermal conductivities of a gas mixture. The temperature dependence of α_T is mainly governed by $(6C^*_{ij}-5)$ which involves with like or unlike interactions. The experimental α_T as a function of $\bar{T}$ is[17]

$$(\alpha_T)_{expt} = A + B / \bar{T}. \quad \ldots\ldots\ldots (8.16)$$

Although g is a slowly varying function of $\bar{T}$, we may assume to be a temperature

Table 8.1. Experimental and theoretical thermal diffusionfactor α_T of binary isotopic mixtures of Neon, Argon and Krypton with temperatures in K.

Column used	System	Hot Wall Temp. (T_h) in K.	Cold Wall Temp. (T_c) in K.	Mean Temp. in K $T=\frac{T_h+T_c}{2}$	a' $(atm)^2$	b' $(atm)^4$	Computed $\ln q_{max}$ from eq (8.9)	Column calibration factor (F_c)
L=Length of the column. =182.0 cm.	Ne^{20}–Ne^{22}	596	298	447	2.5470	2.0188	0.8963	31.5599
		656	328	492	3.3670	3.3025	0.9264	32.4355
		716	358	537	4.3365	4.9660	0.9730	33.9012
Hot Wall radius r_h = 0.0254 cm.	Ar^{36}–Ar^{40}	576	288	432	0.2942	0.0415	0.7221	31.3957
		646	323	484.5	0.4149	0.0701	0.7836	32.2485
		716	358	537	0.7037	0.1683	0.8577	33.9012
Cold Wall radius r_c = 0.635 cm.	Kr^{80}–Kr^{86}	596	298	447	0.5342	0.0046	3.9382	31.5599
					0.0653	0.0046	0.4814	
		656	328	492	0.7963	0.0078	4.5082	32.4355
					0.0973	0.0078	0.5511	
		716	358	537	1.5540	0.0231	5.1123	33.9012
					0.1900	0.0231	0.6250	

Column used	System	Estimated α_T using			Computed theoritical α_T
		Present method	Maxwell's shape factor	Slieker's shape factor	
L=Length of the column =182.0 cm.	Ne^{20}–Ne^{22}	0.0284	0.0156	0.0179	0.0294
		0.0286	0.0161	0.0185	0.0298
		0.0287	0.0169	0.0195	0.0297
Hot Wall radius r_h = 0.0254 cm.	Ar^{36}–Ar^{40}	0.0230	0.0126	0.0144	0.0259
		0.0243	0.0136	0.0156	0.0268
		0.0253	0.0149	0.0171	0.0277
Cold Wall radius r_c = 0.635 cm.	Kr^{80}–Kr^{86}	0.1248	0.0684	0.0785	0.0135
		0.0153			
		0.1390	0.0783	0.0899	0.0157
		0.0170			
		0.1508	0.0888	0.1019	0.0170
		0.0184			

independent one. C^*_{ij} may be expressed as a function of reduced temperature $\bar{T}^*$ like

$$C^*_{ij} = C + D/\bar{T}^* \qquad \text{.....(8.17)}$$

where

$$\bar{T}^* = \bar{T}/(\varepsilon_{ij}/k).$$

The above eq (8.15) thus becomes

$$(\alpha_T)_{theor.} = (6C - 5)g + 6gD/T^* \qquad \text{.....(8.18)}$$

where C and D are new constants. Comparing eqs. (8.16) and (8.18) one may get

$$g=A/(6C-5)$$

From the fitted equations of $(\alpha_T)_{expt}$ against $1/\bar{T}$, A and B were first evaluated. Similarly C^*_{ij} reported elsewhere[18] for (12-6) L-J potential was plotted against $1/\bar{T}^*$ to get C and D of eq (8.17)

Thus 'g' along with $(\alpha_T)_{expt.} = (6C^*_{ij} - 5)g$ fixes C^*_{ij} and hence $\bar{T}^*$ to estimate ε_{ij}/k of the respective molecule.

With the value of ε_{ij}/k first estimated, one may repeat the total procedure as mentioned above, to get more correct ε_{ij}/k in order to present them in Table 8.2. They are found in good agreement with the available literature values. Reported viscosity data are then used with the estimated ε_{ij}/k to get the molecular diameter σ_{ij} as shown in Table 8.2. The theoretical α_T's for Ne^{20}- Ne^{22}, Ar^{36}-Ar^{40} and Kr^{80}-Kr^{86} were then evaluated with those ε_{ii}/k, ε_{jj}/k and ε_{ij}/k (Table 8.2) and shown in Figs. 8.3-8.5 respectively.

8.4. Results and Discussions

The least square fitted euqations of $p^2/\ln q_e$ against p^4 from the available $\ln q_e$ vs p in atmosphere[9] as illustrated graphically in Fig. 8.2, were worked out for 9.7% of Ar^{36} in Ar^{40}, Ne^{20}-Ne^{22} and Kr^{80}-Kr^{86}, the latter two with their natural isotopic abundances, at two experimental temperatures. The pressure

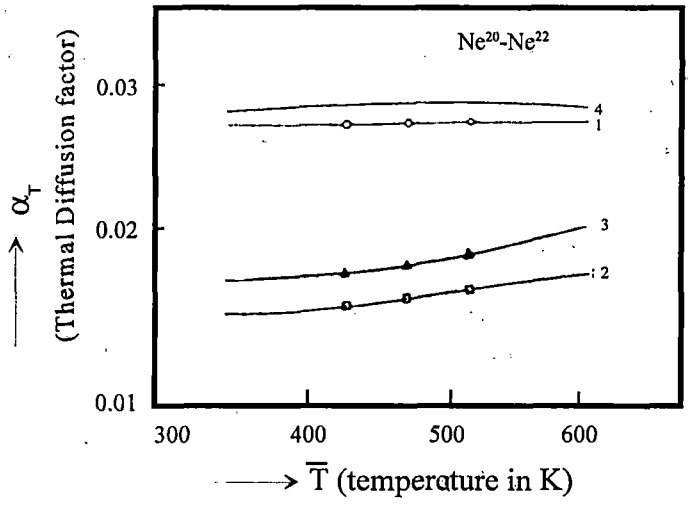

Fig. 8.3. Plot of α_T's against $\overline{T}$ in K for Ne^{20}–Ne^{22}. -o-o- Curve 1:Experimental α_T from F_s and Inq_{max}. -□-□- Curve 2: Experimental α_T from Maxwell's shape factors. -Δ-Δ- Curve 3: Experimental α_T using Slieker's shape factors. —— Curve 4: Theoretical α_T based on elastic collision.

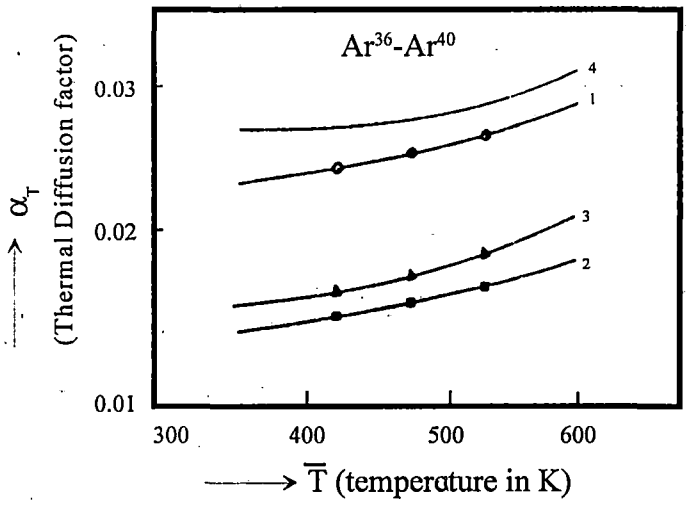

Fig. 8.4. Plot of α_T's against $\overline{T}$ for Ar^{36}–Ar^{40}. -O-O- Curve 1:Experimental α_T from F_s and Inq_{max}. -□-□- Curve 2: Experimental α_T from Maxwell's shape factors. -Δ-Δ- Curve 3: Experimental α_T using Slieker's shape factors. —— Curve 4: Theoretical α_T based on elastic collision.

dependence of $\ln q_e$ at any intermediate temperature for them, as shown by dotted lines in Fig. 8.2, were also inferred from $\ln q_{max}$ in terms of known F_s and α_T assuming the linear relationship of (b'/a') with $\bar{T}$ for the three aforesaid mixtures. $p^2/\ln q_e$ as a linear function of p^4 are, however, expressed by the following equations for;

i) Ar^{36}-Ar^{40} (with 9.7% of Ar^{36} in Ar^{40})

$p^2/\ln q_e = 0.1411 + 3.3990p^4$ at 432 K

$p^2/\ln q_e = 0.1690 + 2.4102p^4$ at 484 K

$p^2/\ln q_e = 0.2392 + 1.4210p^4$ at 537 K

ii) Ne^{20}-Ne^{22} (with natural isotopic abundances)

$p^2/\ln q_e = 0.7926 + 0.3926p^4$ at 447 K

$p^2/\ln q_e = 0.9808 + 0.2970p^4$ at 492 K

$p^2/\ln q_e = 1.1452 + 0.2306p^4$ at 537 K

and for Kr^{80}- Kr^{86} (with natural isotopic abundances)

$p^2/\ln q_e = 0.0086 + 1.8720p^4$ at 447 K

$p^2/\ln q_e = 0.0098 + 1.2558p^4$ at 492 K

$p^2/\ln q_e = 0.0149 + 0.6435p^4$ at 537 K.

But $\ln q_{max}$ of Krypton, estimated from the measured values of $\ln q_e$ as a function of pressure (Fig. 8.2) in terms of a' and b' (Table 8.1) is found to be 8.18 times larger than the widely reported data elsewhere.[7] Adjustment of $\ln q_e$ is, therefore, necessary to get actual α_T's of Kr^{80}-Kr^{86}, as shown by curve 5 in Fig. 8.5, from the follwoing $p^2/\ln q_e$ against p^4 relations :

$p^2/\ln q_e = 0.0704 + 15.3139p^4$ at 447 K

$p^2/\ln q_e = 0.0802 + 10.2775p^4$ at 492 K

$p^2/\ln q_e = 0.1216 + 5.2632p^4$ at 537 K.

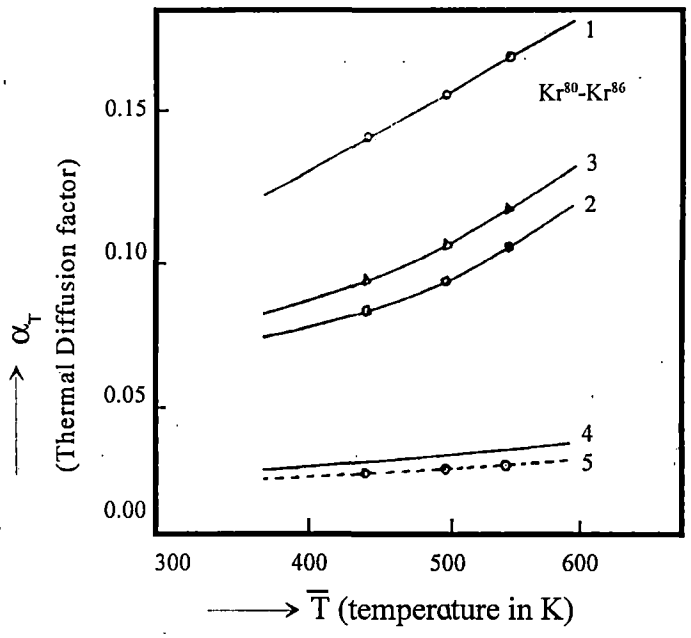

Fig. 8.5. Plot of α_T's against $\overline{T}$ for Kr^{80}–Kr^{86}: -O-O- Curve 1:Experimental α_T from F_s and Inq_{max}, -□-□- Curve 2: Experimental α_T from Maxwell's shape factors, -Δ-Δ- Curve 3: Experimental α_T using Slieker's shape factors, —— Curve 4: Theoretical α_T based on elastic collision, –o–o– Curve 5: Experimental α_T from F_s and adjusted Inq_{max}

Table8.2. Maxwell's model dependent and slicker's model independent column shape factors, (CSF) coefficient of viscosity together with estimated force parameters ϵ_{ij}/k and molecular diameter σ_{ij} used in the calculation of α_T of simple isotopic gas mixtures.

System	Model potential	Estimated		Reported		Mean Temp. (T) in K
		ϵ_{ij}/k in K	σ_{ij}/k in Å	ϵ_{ij}/k in K	σ_{ij} in Å	
Ne^{20}-Ne^{22}	LJ 12-6	40.77	3.1840	41.19*	3.074*	417
						492
				27.50**	2.858**	537
Ar^{36}-Ar^{40}	LJ 12-6	118.41	3.9543	125.20*	3.405*	432
						484.5
				119.50**	3.826**	537
Kr^{80}-Kr^{86}	LJ 12-6	202.41	4.1689	199.20*	4.020*	417
						492
				166.70**	4.130**	537

System	Model potential	Column shape factors (CSF)						$\eta_{ij} \times 10^5$ gm × cm^{-1} × sec^{-1}
		Maxwell			Slicker			
		k'	k'_c	k'_d	$[S \cdot F]_1 \times 6!$	$\pi(1-a^2)$	$[S \cdot F]_3 \times 9!$	
Ne^{20}-Ne^{22}	LJ 12-6	0.815	1.760	0.790	0.937	3.137	0.711	31.40
								33.35
								35.17
Ar^{36}-Ar^{40}	LJ 12-6	0.815	1.760	0.790	0.937	3.137	0.711	21.80
								23.95
								26.10
Kr^{80}-Kr^{86}	LJ 12-6	0.815	1.760	0.790	0.937	3.137	0.711	25.50
								28.15
								30.80

*Maitland *et al.* (1981)
**Hirchfelder *et al.* (1964)

The new $\ln q_e$ against p in atmosphere is shown by the adjacent curves in Fig. 8.2. The corresponding $\ln q_{max}$'s are placed in Table 8.1 together with those obtained from $\ln q_e$ vs p measured by Moran and Watson[9]. The $\ln q_{max}$'s for all the isotopic molecular mixtures were, however, determined from eq. (8.9) with a' and b' governing their pressure variation of $\ln q_e$ as shown in Fig. 8.2. They are placed in the 8th column of Table 8.1.

Since F_s is supposed not to depend on molecular model we therefore, estimated three values of F_s from eq. (8.1.) for this column[9] through the measured $\ln q_{max}$ and reliable α_T's from the other sources[10] for Ar^{36}-Ar^{40} at 432 K, 537K and Ne^{20}-Ne^{22} at 447K respectively. It is interesting to note in Fig. 8.1, that the temperature varition of F_s is the same as observed earlier[5-6] only the coefficients of $\bar{T}$ and $\bar{T}^2$ are slightly different. Although r_c/r_h (=25) for the present column is too large, the temperatue variation of F_s is found to be concave in nature.

The magnitudes and trends of α_T with respect to temperature $\bar{T}$ could, now be obtained for Ne^{20}-Ne^{22}, Ar^{36}-Ar^{40} and Kr^{80}-Kr^{86} from eq. (8.1) in terms of $\ln q_{max}$ and F_s. The expected close agreement of α_T's from the CCF method with theoretical ones might express the reliability of F_s and the model independency of CCF method may once again be confirmed. The α_T's by the CCF method are placed in the 10th column of Table 8.1. The variation of these α_T's with $\bar{T}$ are shown graphically in Figs. 8.3.-8.5 for Ne^{20}-Ne^{22}, Ar^{36}-Ar^{40} and Kr^{80}-Kr^{86} respectively by the curve No.1.

In order to ensure the reliability of the temperature dependence of α_T the molecular force parameters ε_{ij}/k and σ_{ij} were also detemined by using eq (8.18) and the available coefficients of viscosity respectively. The estimated ε_{ii}/k or ε_{jj}/k and σ_{ii} or σ_{jj} of the isotopic gases are placed in the 3rd and the 4th columns of Table 8.2. The close agreement of them with the literature values at once suggests the technique to estimate α_T is really accurate and reliable. The experimental α_T's were also computed from eqs (8.13) and (8.14) by using Maxwell's inverse fifth power potential and Slieker's model independent column shape factors (CSF) which are placed in Table 8.2. These α_T's are placed in

the 11th and the 12th columns of Tables 8.1 respectively. The variation of these α_T's with $\bar{T}$ are also shown graphically by curves 2 and 3 respectively in Figs 8.3-8.5. The α_T's as shown in Figs 8.3-8.5, due to Maxwell and Slieker's methods agree excellently with α_T's by the CCF method so far their trends with $\bar{T}$ are concerned, although the magnitude of α_T by the present method is higher.

The existing frame work of derivation of eqs. (8.13) and (8.14) are really very interesting. The formulations so derived show that the molecular model appears in them through CSF which seems to be an important stepforward in the existing method based on Furry[2] and Jones[4] column theory.

With the estimatd force parameters ε_{ij}/k and σ_{ij}, presented in Table 8.2, theoretical α_T's based on the elastic collisions were also evaluated and placed in the 13th column of Table 8.1 The variation of theoretical α_T's with $\bar{T}$ are shown graphically by curve 4 in each of the Figs. 8.3-8.5 for Ne^{20}-Ne^{22}, Ar^{36}-Ar^{40} and Kr^{80}-Kr^{86} respectively. The α_T's due to elastic collision theory are found to be almost of the same magnitude with those by the CCF method. Besides all these, it is seen that the trends of α_T's with respect to temperature by the present CCF method agree excellently well with the theoretical one in all the systems.

From the discussions made above, it is confirmed that F_s is a molecular model independent parameter. F_s is further, claimed to be a perfect, simple and straightforward one to locate the magnitude and trend of α_T with respect to $\bar{T}$. Moreover, α_T against $1/\bar{T}$ may be considered as a simple and useful technique in determining the exact force parameter of molecules too, to observe the temperature dependence of α_T of any binary isotopic and nonisotopic gas mixture.

8.5. Conclusion

Model independency of CCF, F_s is now once again established in determining the reliable α_T's of any binary gas mixture in column measurements. It is, therefore, desirable to study more TD columns of different column

geometries to arrive at the functional relationship of F_s with r_c, r_h L and $\bar{T}$ with the experimentally determined lnq_{max} and α_T of interesting pair of molecules. The simultaneous estimation of α_T's and F_s with the corresponding force parameters from α_T vs $1/\bar{T}$ seems to be an important stepforward to test the applicability of F_s. Furthermore, the very existence of inelastic collisions among the molecules in the process of thermal diffusion might be detected and improved with certainty through such rigorous study.

References

[1] S. Chapman and T.G. Cowling : *The Mathematical Theory of Non Uniform Gases (*Cambridge University Press, NY, 1952).

[2] W. H. Furry and R.C. Jones : Phys. Rev. **69** (1946) 459.

[3] J. L. Navarro, J. A. Madariage and J.M. Saviron : J. Phys. Soc. Jpn. **50** (1983) 1603.

[4] R. C. Jones and W.H. Furry. : Mod. Phys. **18** (1946) 151.

[5] S. Acharyya, I. L. Saha, A. K. Datta and A. K. Chatterjee : J. Phys. Soc. Jpn. **56** (1990) 3602.

[6] A. K. Datta, G.Dasgupta and S. Acharyya : J. Phys. Soc. Jpn. **59** (1990) 3602.

[7] A. K. Datta and S. Acharyya : J. Phys. Soc. Jpn. **62** (1993) 1527.

[8] G. Dasgupta, A. K. Datta and S. Acharyya : Pramana J. Phys., India, **43** (1994) 81.

[9] T. I. Moran and W.W. Watson : Phys. Rev. **111** (1957) 103.

[10] F. Vandervolk : Ph. D. Dissertation, 1963.

[11] R. Paul, A. J. Howard and W.W. Watson : J. Chem. Phys. **39** (1963) 3053.

[12] H. Brown : Phys. Rev. **58** (1940) 661.

[13] B. N.Srivastava and K. P. Srivastava : Physica **23** (1957) 103.

[14] B. N. Srivastava and M.P. Madan : Proc. Phys. Soc. London **66** (1953) 277.

[15] G. Vasaru : *Thermal Diffusion Column,* supplied by S. Raman (B.A.R.C., Bombay).

[16] C. J. G. Slieker : Z. Naturforsch. **20** (1965) 591.

[17] G. Dasgupta, N. Ghosh, N. Nandi, A.K. Chatterjee and S. Acharyya: J. Phys. Soc. Jpn. **65** (1996) 2506.

[18] M. Klein and F.J. Smith : Tables of collision integral for the (m, 6) potential for the values of m, Arnold Engineering Development Centre, Tennessee, 1968.

CHAPTER 9

The Functional Relationship of the column Calibration Factor in Thermal Diffusion Column Measurement

The functional relationship of the column calibration factor in thermal diffusion column measurement

9.1. Introduction

The thermal diffusion column (TDC) is a very useful device for concentrating impurities of a gas. The enrichment of impurities becomes squared when the length of the column is doubled. The TDC is also used to determine the thermal diffusion factor α_T of any isotopic or nonisotopic gas mixture. The column theory, on the other hand, may be improved by the accurate experimental determination of α_T of the binary gas mixture in a column. Again, the close correlation of α_T with the molecular force parameters allows one to locate the exact force parameters of the interacting molecules. Thus both from experimental and from theoretical points of view, an accurate estimation of α_T is necessary.

In the absnce of a theoretical possibility of estimating the actual experimental α_T from the existing column theory, Acharyya *et. al* [1] and Datta *et. al* [2], however, introduced a scaling factor F_s called the column calibration factor (CCF) into the relation :

$$\ln q_{max} = \alpha_T F_s (r_c, r_h, L, \bar{T}) \qquad \text{..... (9.1)}$$

r_c and r_h are the cold and hot wall radii of a given column of geometrical length L and $\bar{T} = (T_h + T_c)/2$, T_h and T_c being the hot and cold wall temperatures in kelvin respectively. Here $\ln q_{max}$ is the maximum value of $\ln q_e$ at the optimum pressure and q_e is the equilibrium separation factor. Although, the model independency of F_s is well established[3] for its important role in the estimation of reliable α_T[1-4], the functional relationship of F_s with r_c, r_h, L and $\bar{T}$ remains unknown.

Rutherford and Kaminsky[5] had measured the column coefficients H', K'_c and K'_d using Ne^{20}-Ne^{22} gas mixtures with their natural isotopic abundances at various experimental temperatures in four different columns; see Table 9.1. The hot Nichrome V wire of their[5] I, II and III TD columns had radius r_h = 8×10^{-4}m. Their column IV was a thin-walled Nichrome V tube of radius r_h=3.2x

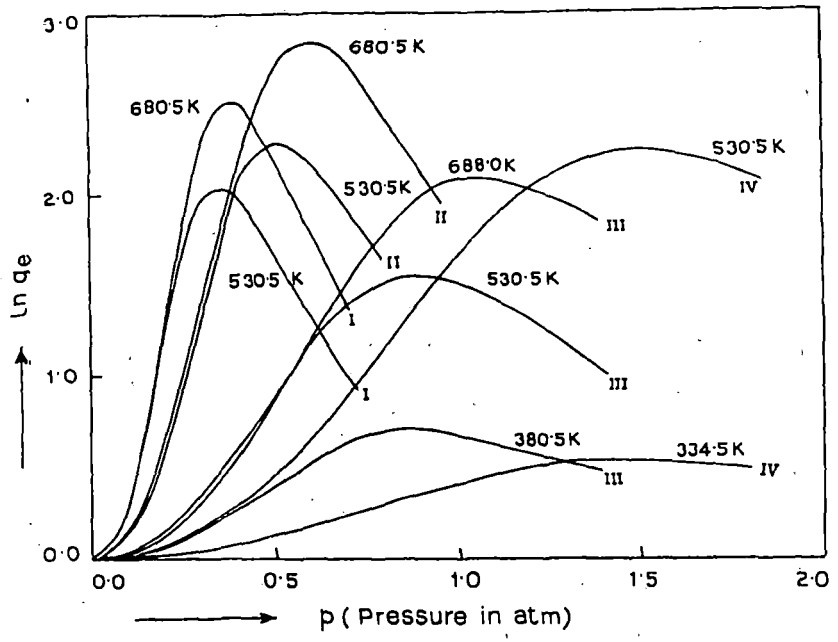

Fig. 9.1. A plot of the $\ln q_e$ against the pressure p in atmospheres of Ne^{20}–Ne^{22} mixtures : curve I, for column I at 530.5 K and 680.5K; curve II, for column II at 530.5 K and 680.5K; curve III, for column III at 380.5 K, 530.5 K and 688.5 K; and curve IV, for column IV at 334.5 K and 530.5 K.

10^{-3}m. The radii of water-cooled metal tubes of all these columns were r_c=1.6 x 10^{-2} m, 1.27 x 10^{-2} m, 9.43 x 10^{-3} m and 9.43 x 10^{-3} m respectively. The geometrical length of columns I and II was L = 3.05 m whereas columns III and IV had L=1.534 m. This inspired us to observe α_T values from the pressure dependences of $\ln q_e$ values of Ne^{20}- Ne^{22} mixtures at the experimental temperatures. The $\ln q_e$ of Ne^{20}-Ne^{22} gas mixtures as a function of the atmospheric pressure are shown in Fig. 9.1 by the least square fitted curves for these columns. The H', K'_c and K'_d[5] are used to study the temperature dependence of α_T and hence the molecular force parameters of neon. The experimetnal α_T values due to Maxwell's model-dependent and Slieker's model-independent column shape factors (CSF) together with the theoretical α_T values based on Chapman-Enskog gas kinetic theory[6] were also estimated. They are plotted against $\bar{T}$ in Fig. 9.2 for comparison. The experimental and theoretical F_s as well as the estimated experimental and theoretical α_T values are presented in Tables 9.1 and 9.2 respectively. The theoretical formulation of F_s is, however, derived in section 9.3 and is compared with the experimental F_s as seen in Fig. 9.3.

The plots of α_T against $\bar{T}$ obtained by the CCF method and of the collision integral C^*_{ij} against the reduced temperature $\bar{T}^*$ were simultaneously used to calculate the force parameters ε_{ii}/k or ε_{jj}/k of the isotopic components of neon. ε_{ii}/k or ε_{jj}/k are the depths of the potential well (see section 9.4). The molecular diameters σ_{ii} or σ_{jj} were then obtained from the coefficients of viscosity with the estimated force parameters (see Table 9.3). The excellent agreement of the force parameters with the literature values (Table 9.2) and the close agreement of α_T obtained by the CCF method with the theoretical ones as seen in Table 9.2 and Fig. 9.2 establish the fact that the derived relationship of F_s is reliable.

9.2. Formulations of the Experimental Thermal Diffusion Factor

Both ends being closed in an ideal TD column of length L, $\ln q_e$ is given by

$$\ln q_e = HL/(K_c + K_d) \qquad \text{..... (9.2)}$$

where q_e is defined by

$$q_e = (x_i / x_j)_{top} / (x_i / x_j)_{botom}$$

$(x_i / x_j)_{top}$ and $(x_i / x_j)_{bottom}$ represent the ratio of mole or mass fractions of lighter (i) and heavier (j) components of a binary gas mixture at the top and at the bottom of a TD column of geometrical length L. The column coefficients H, K_c and K_d are proportional to the second, fourth and zeroth powers of the pressure p in atmospheres respectively. On writing $H = H' p^2$, $K_c = K'_c p^4$ and $K_d = K'_d$ eq (9.2) can be put into the form

$$\ln q_e = \frac{(H' L / K'_c)p^2}{(K'_d / K'_c) + p^4}$$

or

$$p^2 / \ln q_e = b' / a' + (1/a')p^4 \qquad \text{..... (9.3)}$$

where $a' = (H'L / K'_c)$ and $b' = (K'_d / K'_c)$. The experimental parameters a' and b' of Table 9.1 govern the variation of the experimental $\ln q_e$ as a function of the pressure p in atmosphere at a given temperature. They were obtained from the measured values of H', K'_c and K'_d by Rutherford and Kaminsky[5]. The pressure dependences of $\ln q_e$ thus estimated are illustrated graphically in Fig. 9.1 by the fitted curves for four columns I, II, III and IV at various experimental temperatures. It is evident from eq (9.3) that , in each case seen in Fig. 9.1, as p increases $\ln q_e$ of the gas mixture increases and eventually reaches a maximum value of $\ln q_{max}$ given by

$$\ln q_{max} = \frac{a'}{2\sqrt{b'}} , \qquad \text{..... (9.4)}$$

at the optimum pressure P_{opt} given by $P_{opt} = (b')^{1/4}$ for which $(\delta/\delta p) \ln q_e = 0$. The experimental α_T or often the experimental F_s is obtained by using eqs. (9.1) and (9.4) in terms of F_s and $\ln q_{max}$ or α_T and $\ln q_{max}$.

Again, (9.2) on maximization becomes

$$\ln q_{max} = \frac{HL}{2(K_c K_d)^{1/2}} \qquad \text{..... (9.5)}$$

Table 9.1 The geometry of the columns with length L, cold wall radius r_c and hot wall radius r_h together with column constants G_1 and G_2, column calibration factor F_s, a', b' and $\ln q_{max}$.

Geometry of the column in m	Hot wall temp. T_h (K)	Cold wall temp. T_c (K)	Mean temp. $\overline{T}$ (K)	a' (atm^2)	b' (atm^4)	$\ln q_{max}$	Column constant $G_1(10^3)$	Column constant $G_2(10^5)$	Theoretical F_s from eq(9.14)	Experimental F_s
Column I										
$L = 3.05$										
$r_c = 1.6 \times 10^{-2}$								5.9120		
$r_h = 8.0 \times 10^{-4}$	1073	288	680.5	0.7367	0.0211	2.5358	4.3580		76.4942	91.8768
Column II										
$L = 3.05$	773	288	530.5	1.1982	0.0684	2.2907	3.2700	5.2986	76.4391	84.8407
$r_c = 1.27 \times 10^{-2}$										
$r_h = 8.0 \times 10^{-4}$	1073	288	680.5	2.0376	0.1282	2.8460	4.1831		97.7822	103.1159
Column III										
$L = 1.524$	473	288	380.5	1.0358	0.5498	0.6985	1.7285	4.4228	281091	27.0736
$r_c = 9.43 \times 10^{-3}$	773	288	530.5	2.3547	0.5902	1.5327	3.0576		49.7242	56.7667
$r_h = 8.0 \times 10^{-4}$	1088	288	688.0	4.7567	1.2955	2.0896	3.9524		64.2766	75.7101
Column IV										
$L = 1.524$	381	288	334.5	2.3265	4.6460	0.5397	0.7025	2.1957	18.2122	21.5880
$r_c = 9.43 \times 10^{-3}$										
$r_h = 3.2 \times 10^{-3}$	773	288	530.5	10.2385	5.2510	2.2340	2.9767		77.1747	82.7407

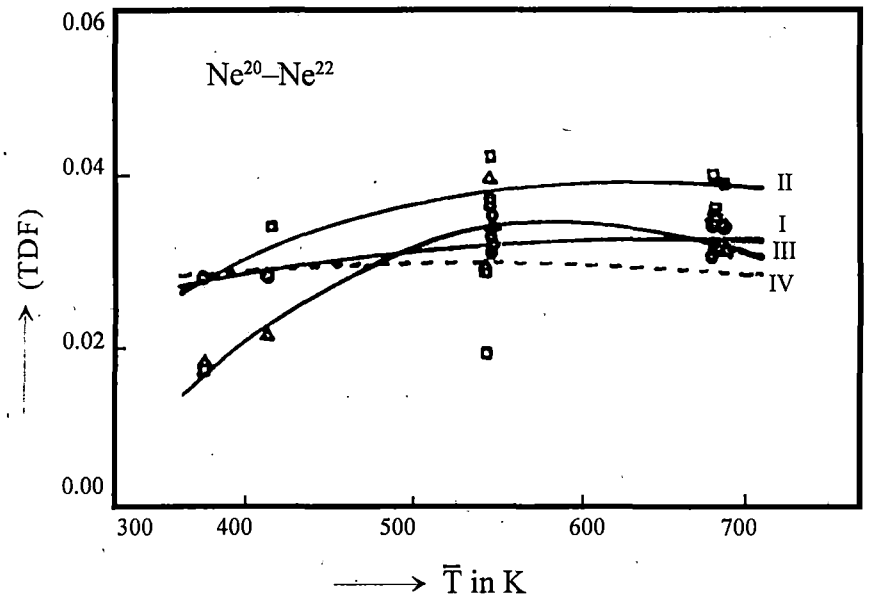

Fig. 9.2. A plot of TD factor α_T of Ne^{20}–Ne^{22} against $\bar{T}$ in kelvins : curve I, (O), by the CCF method; curve II, (Δ), due to the Slieker CSF; curve III, (□), due to the Maxwell CSF; and curve IV, (---), due to the elastic collision theory.

The column coefficients H, K_c and K_d based on Maxwell model dependent CSF h', k'_c and k'_d are[7]

$$H = \frac{2\pi}{6!}\left(\frac{\alpha_T \rho^2_{ij} g}{\eta_{ij}}\right)\frac{1}{2}(r_c + r_h)(r_c - r_h)^3\left(\frac{\Delta T}{\bar{T}}\right)^2 h'$$

$$K_c = \frac{2\pi}{9!}\left(\frac{\rho^3_{ij} g^2}{\eta^2_{ij} D_{ij}}\right)_1 \frac{1}{2}(r_c + r_h)(r_c - r_h)^7\left(\frac{\Delta T}{\bar{T}}\right)^2 k_c'$$

$$K_d = 2\pi(\rho_{ij} D_{ij})\frac{1}{2}(r_c + r_h)(r_c - r_h)k'_d.$$

The experimental α_T due to the Maxwell model dependent CSF is thus

$$\alpha_T \text{ (Maxwell model)} = 2.39\frac{r_c - r_h}{L}\frac{\bar{T}}{\Delta T}\frac{(k'_c k'_d)^{1/2}}{h'}\ln q_{max} \quad \ldots\ldots\ldots\ldots (9.6)$$

where $\Delta T = T_h - T_c$. Similarly the column coefficients due to the model-independent Slieker's[8] CSF $(SF)_1$, $\pi(1-a^2)$ and $(SF)_3$ are

$$H = (SF)_1 r_c^4 \frac{\alpha_T \rho^2_{ij} g}{\eta_{ij}}\left(\frac{\Delta T}{\bar{T}}\right)^2$$

$$K_d = \pi(1-a^2) r_c^2 p_{ij} D_{ij}$$

$$K_c = (SF)_3 r_c^8\left(\frac{\rho^3_{ij} g^2}{\eta^2_{ij} D_{ij}}\right)\left(\frac{\Delta T}{\bar{T}}\right)^2$$

where $a = r_h / r_c$. Using Slieker's CSF, α_T is given by

$$\alpha_T \text{ (Slieker)} = 2.0\frac{r_c}{L}\frac{\bar{T}}{\Delta T}\frac{[\pi(1-a^2)(SF)_3]^{1/2}}{(SF)_1}\ln q_{max}. \quad \ldots\ldots (9.7)$$

The experimental α_T values using the CSF were obtained from eqs. (9.6) and (9.7) together with those by CCF method from eq (9.1) in terms of measured $\ln q_{max}$ and F_s. All these α_T values are placed in Table 9.2 for comparison with the theoretical ones. They are also shown graphically in Fig 9.2 with respect to $\bar{T}$ for Ne^{20}-Ne^{22} gas mixtures. The corresponding CSF's based on Maxwell model dependent and Slieker model independent methods are entered in Table 9.3.

Table 9.2. Experimental and theoretical α_T at various experimental temperatures together with estimated force parameters ϵ_{ij}/k and molecular diameters σ_{ij}.

		Experimental α_T using				Estimated		Reported	
Column	Mean temp. $\overline{T}$ (K)	F_s of equation (9.14)	Slieker's shape factor	Maxwell's shape factor	Theoretical α_T using equation (9.15)	ϵ_{ij}/k (K)	σ_{ij} (10^{10} m)	ϵ_{ij}/k (K)	σ_{ij} (10^{10} m)
Column I	530.5	0.034	0.043	0.040	0.028				
	680.5	0.033	0.042	0.035	0.028				
Column II	530.5	0.030	0.037	0.033	0.028				
	680.5	0.029	0.036	0.029	0.028			47.0[a]	2.72[a]
						48.58	2.69		
								41.186[b]	3.07[b]
Column III	380.5	0.025	0.032	0.017	0.027				
	530.5	0.031	0.037	0.030	0.028				
	688.0	0.033	0.040	0.030	0.028				
Column IV	334.5	0.030	0.012	0.013	0.026				
	530.5	0.029	0.015	0.027	0.028				

a Clifford et al (1977)[13]
b Aziz (1976)[13]

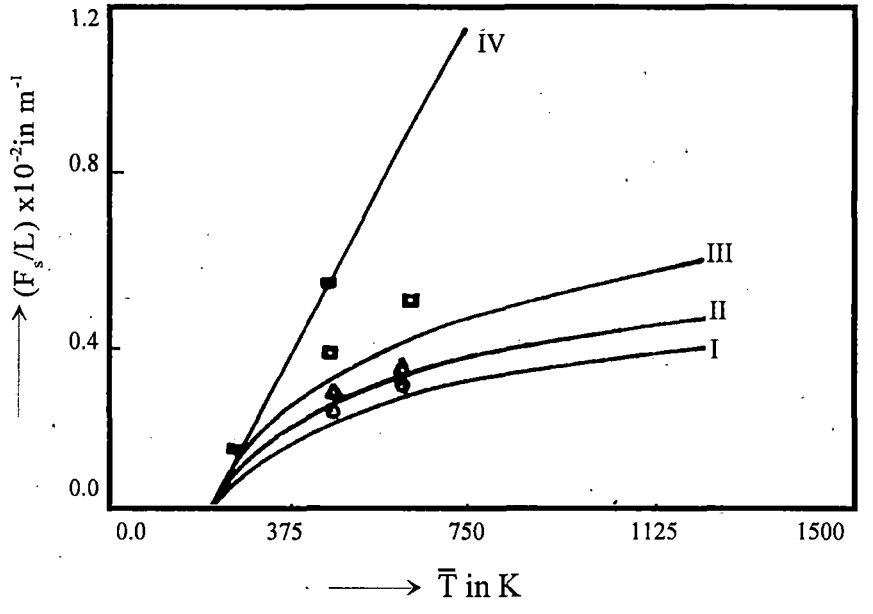

Fig. 9.3. A plot of the theoretical F_s (equation (9.14) with the experimental F_s on it against $\bar{T}$ in kelvins : curve I, for column I, (O) experimental points; curve II, for column II, (Δ), experimental points; curve III, for column III, (□), experimental points; and curve IV, for column IV, (■), experimental points.

9.3. The Theoretical Formation of the Column Calibration Factor

The column parameters in cylindrical coordinates derived from the most elementary theory of the thermal diffusion column by Cohen[9] are

$$H = 2\pi \int_{r_h}^{r_c} \alpha_T \frac{\delta}{\delta r}(\ln T)\, dr \left(\int_{r_h}^{r} \rho_{ij} \upsilon r\, dr\right),$$

$$K_c = 2\pi \int_{r_h}^{r_c} \frac{dr}{\rho_{ij} D_{ij} r} \left(\int_{r_h}^{r} \rho_{ij} \upsilon r\, dr\right)^2$$

and $$K_d = 2\pi \int_{r_h}^{r_c} \rho_{ij} D_{ij} r\, dr$$

which can, however, be approximated almost in the same manner as was done earlier by Slieker[8]. Here ρ_{ij} and D_{ij} are the density and diffusion coefficients of the gas mixture, r is the radial coordinate and T is the absolute temperature in kelvin.

Under the influence of the temperature gradient along the horizontal plane of the column, the convective velocity υ of the molecule in the vertical direction is obtained from the Navier-Stokes equation in cylindrical coordinates:

$$\frac{\delta^3 \upsilon}{\delta r^3} + \frac{1}{r}\frac{\delta^2 \upsilon}{\delta r^2} - \frac{1}{r^2}\frac{\delta \upsilon}{\delta r} = \frac{\rho_{ij} g}{\eta_{ij} \bar{T}} \frac{dT}{dr}.$$

If we consider the rectilinear flow of heat from the hot wire or wall of temperature T_h to the cold wall of temperature T_c of a TDC, the temperature T is given by

$$T = T_h - \frac{\Delta T}{r_c - r_h}(r - r_h)$$

Puting $r = e^x$ and solving the above equation, we get

$$v = C_1 + C_2 \ln r + C_3 r^2 - \frac{\rho_{ij} g}{\eta_{ij} \bar{T}} \frac{\Delta T}{(r_c - r_h)} \frac{r^3}{9}$$

Table 9.3. Maxwell model dependent and Slieker-model-independent column shape factors, coefficient of viscosity η_{ij} and thermal conductivity λ_{ij} of Ne^{20}–Ne^{22} gas mixture.

Column	Mean temp $\overline{T}$ (K)	Column shape factor: Maxwell h'	Maxwell k'_c	Maxwell k'_d	Slieker $(SF)_1(10^3)$	Slieker $(SF)_3(10^6)$	η_{ij} (10^5 kg m^{-1} s^{-1})	λ_{ij} (10^2 cal m^{-1} s^{-1} K^{-1})
	530.5	1.035	3.300	0.700			5.0333	1.7900
Column I					1.3639	1.9717		
	680.5	1.585	6.075	0.725			6.2543	2.2236
	530.5	1.060	3.100	0.715			5.0333	1.7900
Column II					1.3914	1.9140		
	680.5	1.600	5.525	0.740			6.2543	2.2236
	380.5	0.800	1.050	0.745			3.8123	1.3558
Column III	530.5	1.120	2.975	0.750	1.2838	1.6646	5.0333	1.7900
	688.0	1.590	4.975	0.770			6.3153	2.2459
	334.5	0.970	0.500	0.912			3.4378	1.2226
Column IV					239.23	4662.2		
	530.5	1.185	1.775	0.925			5.0333	1.7900

$$= Gr_c^2 (K_1 + K_2 \ln\phi + K_3\phi^2 + \phi^3) \quad \text{..... (9.8)}$$

where $K_1 = \frac{C_1}{Gr_c^2} + \frac{C_2}{Gr_c^2} \ln r_c$,

$$K_2 = \frac{C_2}{Gr_c^2}, \quad K_3 = C_3 / G$$

and $$G = \frac{\rho_{ij} g}{\eta_{ij} \bar{T}} \frac{\Delta T}{(a-1)} \frac{1}{9}.$$

C_1, C_2 and C_3 being the integration constant, $\phi = r/r_c$ is the new veriable and $a = r_h/r_c$. The boundary conditions are

i) $v = 0$ *at* $r=r_c$ for which $\phi = 1$

ii) $v = 0$ at $r=r_h$ for which $\phi = a$ and since there is no transport of components of the gas mixture at equilibrium in the vertical direction up and down the column, we have

(iii) $$r_c^2 \int_a^1 \rho v \phi d\phi = 0.$$

Here, K_1, K_2 and K_3 are dimensionless constants which are, however, given explicitly in terms of $a(= r_h/r_c)$ of a TDC by applying the boundary conditions mentioned above :

$$K_1 = \frac{5a^2(1-a)(1+2a^2 \ln a - a^2) + \ln a}{5(a^2-1)^2 + 5(1-2a^4)\ln a},$$

$$K_2 = \frac{5a^2(1-a)(1-2a^2) - (1-a^2)}{5(a^2-1)^2 + 5(1-2a^4)\ln a} \quad \text{and}$$

$$K_3 = -(K_1 + 1).$$

The column coefficients H, K_c and K_d are now derived as follows :

$$H = -2\pi r_c^2 \int_a^1 \alpha_T \frac{\delta}{\delta\phi}(\ln T)d\phi \int_a^{\phi} \rho_{ij} v\phi d\phi$$

$$= 2\pi\alpha_T \frac{\Delta T}{1\text{-}a} \rho_{ij} Gr_c^4$$

$$x \int_a^1 \frac{1}{T}\left[\left(\frac{K_1\phi^2}{2} + \frac{K_2\phi^2}{2}\left(\ln\phi - \frac{1}{2}\right) + \frac{K_3\phi^4}{4} + \frac{\phi^5}{5} + K_4\right]d\phi\right.$$

where $K_4 = -\frac{a^2}{2}\left[K_1 + K_2\left(\ln a - 1/2\right) + K_3 a^2/2 + 2a^3/5\right]$

Here, the temperature and composition dependences of n_{ij}, ρ_{ij}, D_{ij} and α_T are not taken into account[7-9] and the above equation for H becomes

$$H = 2\pi\alpha_T r_c^4 \frac{\rho_{ij}^2 g}{\eta_{ij}\bar{T}} \frac{\Delta T}{(a-1)9} G_1 \qquad \text{..... (9.9)}$$

where $G_1 = \frac{\Delta T}{\bar{T}(1\text{-}a)}\left(\frac{2K_1 - K_2}{12}(1 - a^3) - \frac{K_2}{18}(1\text{-}a^3)\right.$

$$\left. - \frac{K_2 a^3}{6}\ln a + \frac{K_3}{20} + K_4(1-a) + \frac{1}{30}\right)$$

$$- \left(\frac{\Delta T}{\bar{T}(1\text{-}a)}\right)^2 \left[\frac{2K_1 - K_2}{48} - \frac{K_2}{24}\left(7/12 + a^4 \ln a\right)\right.$$

$$\left. + \frac{K_3}{120} + \frac{K_4}{2}(1 - a^2) + 1/210\right]$$

$$+ \left(\frac{\Delta T}{T(1\text{-}a)}\right)^3 \left[\frac{2K_1 - K_2}{120} - \frac{47K_2}{3600} + \frac{K_3}{420} + \frac{K_4}{3}(1 - a^3) + 1/840\right]$$

..... (9.10)

rataining the term containing up to the third power of $\Delta T/[\bar{T}(1\text{-}a)]$ because the contributions of higher terms are negligibly small. Again, a^n is very small compared with unity for $n \geq 4$.

The coefficient K_c of a TDC is given by

$$K_c = 2\pi\int_a^{\phi} \frac{d\phi}{\rho_{ij} D_{ij} \phi}\left(\int_a^{\phi} \rho_{ij} v \phi d\phi\right)^2.$$

$$= \frac{2\pi\rho_{ij} G^2 r_c^8}{D_{ij}}\int_a^1 \frac{1}{\phi}\left[\frac{K_1\phi^2}{2} + \frac{K_2\phi^2}{2}\left(\ln\phi - \frac{1}{2}\right)\right.$$

$$\left. + \frac{K_3\phi^4}{4} + \frac{\phi^5}{5} + K_4\right]^2 d\phi$$

$$= \frac{2\pi\rho^3_{ij} g^2}{\eta^2_{ij} D_{ij}}\left(\frac{\Delta T}{\bar{T}}\right)\frac{r_c^8}{81(1\text{-}a)^2} G_2 \qquad \text{.....(9.11)}$$

Where $$G_2 = \frac{K_1^2}{16} + \frac{5K_2^2}{128} - K_4^2 \ln a + \frac{K_3^2}{128} - \frac{3K_1K_2}{32} + \frac{K_1K_3}{24}$$

$$+ \frac{K_1K_4}{2}(1-a^2) - \frac{K_2K_3}{36} + \frac{K_3K_4}{8} - \frac{K_2K_4}{4}(2+2a^2\ln a - a^2)$$

$$+ \frac{K_1}{35} - \frac{9K_2}{490} + \frac{K_3}{90} + \frac{2K_4}{25} + \frac{1}{250}. \qquad \text{..... (9.12)}$$

For column IV where a=0.34, the higher power of 'a' in G_2 i.e., $\frac{a^4}{32}[2K_1K_2 + K_2^2(\ln a - 1) - 4k_3k_4]$ is taken.

The coefficient K_d of a TDC is obtained as

$$K_d = 2\pi r_c^2 \int_a^1 \rho_{ij} D_{ij} \phi d\phi$$

$$= \pi r_c^2 \rho_{ij} D_{ij}(1-a^2). \qquad \text{..... (9.13)}$$

Thus the CCF per unit length , F_s/L, is finally obtained from eq. (9.5) with the help of eqs (9.9)-(9.13). It is given by

$$F_s / L = \frac{G_1}{r_c[2(1-a^2)\, G_2]^{1/2}}. \qquad \text{..... (9.14)}$$

The theoretical CCF per unit length of any TD column can thus be approximated in terms of G_1, G_2, a and r_c of the column. The values of formulated F_s are placed in Table 9.1 for columns I, II, III and IV. They are shown in Fig.9.3 together with the experimental F_s/L obtained from $\ln q_{max}$ and known α_T values of Ne^{20}-Ne^{22} gas mixtures. F_s / L of eq. (9.14) plays an important role in determining α_T of any binary gas mixture[1-4]. Because its model independency is well established[3], F_s/L can safely be used to concentrate impurities of any gas to any desired level in TDC experiments.

9.4. Force Parameters from the TD Factor

The theoretical α_T based on Chapman -Enskog gas kinetic theory[6] is given by

$$\alpha_T = g(6C_{ij}^* - 5) \qquad \text{..... (9.15)}$$

where $$g = \frac{1}{6\lambda_{ij}} \frac{S^{(i)} x_i - S^{(j)} x_j}{X_\lambda + Y_\lambda}$$

is a complicated function of the composition of the gas mixture and of the thermal conductivity λ_{ij} where as $(6C_{ij}^* - 5)$ strongly depends on the temperature. The λ_{ij}'s are, however, obtained from the η_{ij}'s by using the relation

$$\lambda_{ij} = (15R / 4M)\eta_{ij}$$

The experimental values of η_{ij} of the Ne^{20}-Ne^{22} gas mixture are taken from Yamamoto *et. al.*[10]. The estimated theoretical α_T values for Ne^{20}-Ne^{22} are shown by curve IV of Fig. 9.2 in which they are compared with α_T obtained by the existing method, curve II and curve III, due to the Maxwell and Slieker CSF's as well as with α_T values of curve I obtained by the CCF method.

Now, the slowly varying function of temperature g is given by[3,11]

$$g = A/(6C - 5)$$

A and C are two arbitrary constants. A is determined from α_T of the CCF method at two available temperatures $\bar{T}$ in kelvins and C from the reported data[12] of C_{ij}^* versus $\bar{T}^*$. Using the relation

$$(6C^*_{ij} - 5) = [(\alpha_T)_{expt}] / g \qquad (9.16)$$

the collision integral[12] C^*_{ij} fixes $\bar{T}^*$ where $\bar{T}^* = \bar{T} /(\varepsilon_{ij}/k)$ and hence ε_{ij}/k of the molecule is located. Because the variation of g with the temperature is very slow, the entire procedure with the initially estimated ε_{ij}/k is repeated to get the exact value of ε_{ij}/k. The molecular diameter σ_{ij} is then determined from the viscosity data[10] with the estimated ε_{ij}/k. It is worthy to mention that, in the case of isotopic components, the force parameters due to binary interactions ε_{ij}/k and σ_{ij} become ε_{ii}/k or ε_{jj}/k and σ_{ii} or σ_{jj} respectively.

9.5. Results and Discussion

The equations of $p^2 / \ln q_e$ against p^4 of Ne^{20}-Ne^{22} gas mixtures were, however, worked out in terms of the measured values of H', K'_c and K'_d[5] from the pressure dependences of $\ln q_e$ in four columns of different column geometries and at various experimental temperatures. They are for column I:

$p^2/\ln q_e$ = $0.0305 + 1.9290p^4$ at $\bar{T}$ = 530.5 K

$0.0286 + 1.3574p^4$ at $\bar{T}$ = 680.5 K

for column II :

$p^2/\ln q_e$ = $0.0571 + 0.8346p^4$ at $\bar{T}$ = 530.5 K

$0.0629 + 0.4908p^4$ at $\bar{T}$ = 680.5 K

for column III :

$0.5309 + 0.9654p^4$ at $\bar{T}$ = 380.5 K

$p^2/\ln q_e$ = $0.2506 + 0.4247p^4$ at $\bar{T}$ = 530.5 K

$0.2703 + 0.2102p^4$ at $\bar{T}$ = 688.0 K

for column IV :

$p^2/\ln q_e$ = $1.9970 + 0.4298p^4$ at $\bar{T}$ = 334.5 K

$0.5129 + 0.0977p^4$ at $\bar{T}$ = 530.5 K.

The variation of $\ln q_e$ with p in atmospheres is found to increase with increasing length L and r_h / r_c of the TD columns as shown in Fig. 9.1. p_{opt}, the optimum pressure at which $\ln q_e$ becomes maximum as observed in Fig. 9.1, also increases on going from column I to column IV for increasing r_h / r_c. The variation of

$p^2 / \ln q_e$ against p^4 is governed by a' and b' of eq (9.3). a' and b' were, however, obtained by applying a least square fitting technique to eq (9.3) with the experimental data[5] of H', K'_c and K'_d. They are placed in the fifth and sixth columns of Table 9.1. $\ln q_{max}$ in terms of a' and b' of eq (9.4) are also placed in the seventh column of Table 9.1.

An approximate formulation of theoretical F_s with the column geometry has been derived by considering the convective velocity of the molecules in a TD column from the Navier-Stokes equation in cylindrical coordinates. Rectilinear flow of heat from a hot wire or wall to a cold wall seems to be a better choice, unlike Slieker's derivation. Although the temperature and composition dependences of the transport parameters like p_{ij}, n_{ij}, D_{ij}, λ_{ij} and α_T were not taken into account, the derived relationship of F_s with the column geometry and the temperature is reliable, simple and straightforward. This is strictly valid in the case of a hot wire or cryogenic wall or even for a hot wall column.

The column constants G_1 and G_2 depending on the column geometry and wall temperatures were worked out for four columns and are placed in the eight and ninth columns of Table 9.1. F_s / L of each column at experimental temperatures were then determined using eq. (9.14) and are placed in the tenth column of Table 9.1. G_1 and G_2 of eqs (9.10) and (9.12) are dimensionless column constants, suggesting the fact that these parameters are indenpendent of the molecular model. G_1 depends on $\Delta T / \overline{T}$ and r_h/r_c of a TDC where as G_2 is expressed in terms of r_h/r_c alone. The physical meanings of G_1 and G_2 can be realized from eqs (9.9) and (9.11). G_1 is related to the column transport coefficient H which is involved in the process of thermal diffusion, whereas G_2 is related to K_c, occurring in a TD process. However, K_c and K_d are the longitudinal and back diffusion coefficients in a TDC. Nevertheless, G_1 and G_2 are of much importance for locating the exact values of F_s, α_T and p_{opt} at which $\ln q_e$ becomes maximum. The available α_T values of $Ne^{20} - Ne^{22}$ gas mixtures, which are 0.0250, 0.0258, 0.0270, 0.0276 and 0.0276 at 334.5 K, 380.5K, 530.5K, 680.5K and 688K respectively [5], help one to get experimental F_s at various values of $\overline{T}$ from estimated $\ln q_{max}$ of eq (9.4) of the TD columns. The experimental F_s when plotted against $\overline{T}$ in Fig. 9.3 are in close agreement with

theoretical F_s derived from eq (9.14) at various $\bar{T}$.

Using eq (9.1) the α_T values of Ne^{20}–Ne^{22} gas mixtures are estimated through theoretical F_s by the CCF method. These α_T values are presented in the third columns of Table 9.2 and plotted against $\bar{T}$ in Fig. 9.2. The experimental α_T values obtained by the CCF method from $\ln q_{max}$ and F_s are found to fall almost on the same curve I and increase slowly with $\bar{T}$.

The slight disagreement between the experimental and theoretical F_s seen in Fig 9.3. and Table 9.1 results in a slight difference between the theoretical α_T values and the experimental ones obtained by the CCF method. This may, perhaps, arise due to the effect of parasitic remixing in the thermal diffusion process.

The molecular force parameters of Ne^{20}-Ne^{22} were estimated from the slope and the intercept of the α_T against $1/\bar{T}$ equation. The α_T at 500.0 K and 600.0 K from curve 1 of Fig. 9.2 were found to obey an equation of the form $\alpha_T = 0.02913 - 1.12501(1/\bar{T})$. The molecular force parameters, ε_{ij}/k of Ne^{20}-Ne^{22} were thus determined as explained elsewhere [3,11]. The η_{ij} [10] of Ne^{20}–Ne^{22} were then used to obtain the molecular diameter σ_{ii} or σ_{jj}. The close agreement of the estimated force parameters, placed in Table 9.2 with the reported ones[13] establishes the reliability of α_T as obtained by CCF method.

The α_T due to Slieker's CSF, as seen in Table 9.3, are calculated from eq (9.7) and are placed in the fourth column of Table 9.2. These α_T values, although slightly higher in magnitude than the α_T values obtained by the CCF method, are plotted with $\bar{T}$ in Fig 9.2 on curve II. The α_T values from $\ln q_{max}$ of column IV are scattered (Fig. 9.2), but still maintain the same trend as that of the CCF method. The magnitudes of the Maxwell model dependent CSF are really very difficult to locate exactly. They were, however, obtained by interpolation and extrapolation from the data of Vasaru[7] and placed in Table 9.3. The probable temperature dependence of α_T using the Maxwell model dependent CSF was then obtained from eq (9.6) and shown in the fifth column of Table 9.2. They are plotted with $\bar{T}$ in Fig 9.2 on curve III, showing both the trend and the magnitude of α_T against $\bar{T}$. It fails to accord with α_T obtained by the other methods. The theoretical α_T values based on elastic collision among molecules were also calculated from eq (9.15) at 334.5 K, 380.5 K, 530.5K, 680.5K and

688.0K for Ne^{20}-Ne^{22} and placed in the sixth column of Table 9.2. These are plotted against $\overline{T}$ on curve IV of Fig. 9.2. Both the magnitudes and the trends of these α_T values are more or less the same as those of the α_T values obtaind from the CCF. It is also interesting to note that the theoretical α_T values of curve IV exhibit the same trend of increasing with temperature as do the α_T values obtained by the CCF method.

In fact, asymmetry in column geometry is an inherent property and as such it invites remixing. Thus in the TD column theory Furry and Jones[14] added a term K_p called the remixing coefficient, proportional to p^4 in the denominator of eq (9.2). Obviously in an ideal column K_p is supposed to be zero. Leyarovski et at[15] had shown that K_p never exceeds 20% of K_c. Thus, owing to remixing effects, the maximum error that creeps into F_s and hence into α_T is 9.54%. In spite of that the excellent agreement of the experimental α_T (curve I) and the theoretical α_T (curve IV) in Fig. 9.2 it is evident that eq (9.14) is reliable for F_s/L. Moreover, it indicates that K_p increases with $\overline{T}$ particularly after $\overline{T} = 2T_c$,; that is, remixing starts from $\overline{T} = 2T_c$ in a TD column.

The discussion above makes it clear that the theoretical formulation of the CCF, which is the central point of study in this paper, is a model independent parameter, as observed earlier[1,4, 8,16]. Furthermore, the α_T values obtained from the CCF with $\overline{T}$ of a binary gas mixture are convenient means of estimating the molecular force parameters like ε_{ij}/k and σ_{ij} of the molecules. The subject in this paper is thus related to the efficiency of the gas separation using thermal diffusion column to throw some light on the basic physical properties of a gas mixture through the CCF and α_T.

9.6. Conclusions

In fact, the theoretical background of the process of thermal diffusion simultaneously involved with longitudinal and back diffusion in a TDC is much too complicated. The presented mathematical formulation of eq (9.14), achieved so far, seems to be a significant improvement over the existing theories. Determination of F_s/L appears to be an important means of estimating the experimental α_T through $\ln q_{max}$, particularly when $\Delta T/\overline{T}$ is close to unity or

$\bar{T} = 2T_c$. When $\Delta T / \bar{T}$ is well above unity the experimental α_T obtained by the CCF method differs from the theoretical α_T. Again, experimental α_T values obtained by using Slieker model independent and Maxwell model dependent CSF's are low compared with theoretical α_T values in the lower temperature region. Asymmetry in column geometry through K_p may be a reason for such a deviation. The theoretical α_T derived from the elastic collision theory is not in good agrement with experimental α_T for the non-spherical molecules. Even in the case of spherical molecules, the agreement is no better. The model independent parameter F_s/L of eq (9.14) thus ought to be used to estimate α_T for the pair of molecules concerned through experimental lnq_{max} in the TDC. The procedure of determining α_T by the CCF method is, therefore, necessary in order to improve the theory for obtaining α_T for elastic or inelastic collisions among the molecules[17]. The simultaneous use of reliable α_T by the CCF method and C^*_{ij} against $1/\bar{T}$ and $1/\bar{T}^*$ respectively appears to be a unique method of locating the exact force parameters of the molecules too.

References

[1] S. Acharyya, I. L. Saha, A. K. Dutta and A.K. Chatterjee, J. Phys. Soc. Japan **56** (1987) 105.

[2] A.K Datta, G. Dasgupta and S. Acharyya, J. Phys. Soc. Japan **59** (1990) 3602.

[3] G. Dasgupta, N. Ghosh, N. Nandi and S. Acharyya, J. Phys. Soc. Japan, **66** (1997) 108.

[4] A. K. Datta and S. Acharyya, J. Phys. Soc. Japan, **62** (1993) 1527.

[5] W.M. Rutherford and K. J. Kaminsky, J. Chem. Phys. **47** (1967) 5427.

[6] S. Chapman and T.G. Cowling, The mathametical theory of non-uniform gases (1952) (London's Cambridge University Press).

[7] G. Vasaru, Tharmal Diffussion Column, Supplied by S. Raman (Bombay; BARC).

[8] C.J.G. Slieker, Ph.D thesis, (1964) Amsterdam University.

[9] K. Cohen, The theory of isotope separation, (1951) (New York ; McGraw Hill).

[10] I. Yamamoto, H Makino and A. Kanagawa, J. Nucl. Sci.Technol. **27**(1990) 156.

[11] G. Dasgupta, N. Ghosh, N. Nandi, A. K. Chatterjee and S. Acharyya, J. Phys. Soc. Japan, **65** (1996) 2506.

[12] M. Klein and F.J. Smith, Tables of Collision Integral for the (m,6) potential for the value of m, Arnold Engineering Development Centre, Air Force Systems Command, Arnold Air Force Station, Tennessee.

[13] G. C. Maitland, M. Rigby E.B. Smith and W.A. Wakeham, Intermolecular Forces; Their origin and determinaiton, (1981) (Oxford, Clarendon).

[14] W.H. Furry and R. C. Jones, Phys. Rev. **69** (1946) 459.

[15] E.I. Leyarovski, J.K. Georgiev and A.L. Zahariev, Int. J. Thermophys. **9** (1988) 391.

[16] J.A. Madariaga, J.L. Navarro, J.M. Saviron and J.L. Brun, J. Phys. A; Math. Gen. **16** (1983) 1947.

[17] T. K. Chattopadhya and S. Acharyya, J. Phys. B; At. Mol. Phys. **7** (1974) 2277.

CHAPTER 10

Formulation of column Calibration Factor and Optimum Pressure of the Thermal Diffusion Column

Formulation of column Calibration Factor and Optimum Pressure of the Thermal Diffusion Column

10.1. Introduction

The thermal diffusion column (TDC) is of much importance to enrich rare or even ordinary isotopes as well as to obtain thermal diffusion factor α_T of the binary isotopic or nonisotopic mixture of gas molecules. Accurate experimental results of $\ln q_e$ are, therefore, necessary to improve the column theory and to estimate experimental α_T of the binary or ternary mixture of the gas molecules. Further the close correlation of α_T with the molecular force parameter ε_{ij}/k and σ_{ij} inspired us to estimate α_T of pair of molecules by column experiments.

The TD column theory as developed by Jones and Furry[1] gives radially integrated concentration distribution along the column. The theory can explain only the column behavior roughly[2]. Moreover, the analysis is not so simple and it requres numerical calculations with high speedy computer.

In order to make the methodology simpler, Acharyya et al[3-4] has, however, introduced a scaling factor called the column calibration factor CCF, in the relation

$$\ln q_{max} = \alpha_T F_s (r_c, r_h, L \& \bar{T}) \quad \text{.....(10.1)}$$

to estimate the experimental α_T of isotopic or nonisotopic binary gas mixture in a TD column. Here $\ln q_{max}$ is the maximum value of the equlibrium separation factor q_e. The cold and hot wall radii of a TD column of geometrical length L are r_c and r_h. $\bar{T}$ is the experimental mean temperatuer given by $\bar{T} = (T_h+T_c)/2$, T_h and T_c being the hot and cold wall temperature in K. Using the coefficients of Cohen[5] the approximate formulation of the TD column coefficients in terms of the column geometry are derived explicitly to give the CCF, F_s of the column. The columns I,II,III and IV used by Rutherford[6] had the cold wall radii $r_c = 1.27 \times 10^{-2}$, 1.6×10^{-2}m, 1.9×10^{-2}m and 2.05×10^{-2}m respectively and geometrical length L=3.05m each. Experimental F_s values for these columns at different experimental temperatures

were obtained in terms of experimental $\ln q_{max}$ and reliable α_T values of He^3-He^4 gas mixture. Graphical illustrations of the derived F_s against $\bar{T}$ in Fig. 10.2 are found to be close to the experimental F_s. Least square fitting technique is , however, applied on the experimental values[6] of $p^2/\ln q_e$ against p^4 for He^3 and He^4 gas mixture in all the columns to obtain a' and b'. the $\ln q_e$ against the pressure p in pascal at different temperatures in terms of the estimated a' and b' were then found out and are shown graphically in Fig. 10.1. The optimum pressure, p_{opt}, at which $\ln q_e$ becomes maximum i.e., $\ln q_{max}$, is further evaluated from a' and b' of Table 10.1.

$\ln q_{max}$ as determined from a' and b' is used to obtain the α_T values of He^3-He^4 gas mixture at their experimental temperatures from eq (10.1). These α_T's are plotted against $\bar{T}$ in Fig. 10.3 by curve No I.Expremental α_T's by the existing methods using Maxwell and Slieker CCF were also worked out in order to compare with those by the CSF method. Theoretical α_T's assuming the molecules are perfectly elastic spheres are measured for both (12-6) L-J and exp-6 potentials. All these α_T's as a function of $\bar{T}$ are graphically shown in Fig. 10.3. The experimental α_T's from the present CCF method and the theoretical α_T's due to elastic collision theory are finally placed in Table 10.3. for comparison.

Approximate formulations of the column coefficients were used again to predict the optimum operating pressure, P_{opt} of the TD column. The derivation is expressed in terms of the column geometries and the transport coefficients of the gas mixture. The predicted pressure is compared with the experimental data as seen in Table 10.3. They are also shown by the down headed arrow (↓) in Fig. 10.1. of $\ln q_e$ against pressure p is pascal at each experimental temperature in K.

10.2. Theoretical Formulations

In an ideal TD column both ends being closed the logarithmic separation factor $\ln q_e$ is

$$\ln q_e = HL/(K_c+K_d) \qquad \text{..... (10.2)}$$

where H, K_c and K_d are proportional to p^2, p^4 and p^0 respectively, p being the pressure in pascal. Due to asymmetry in the column geometry the remixing of the

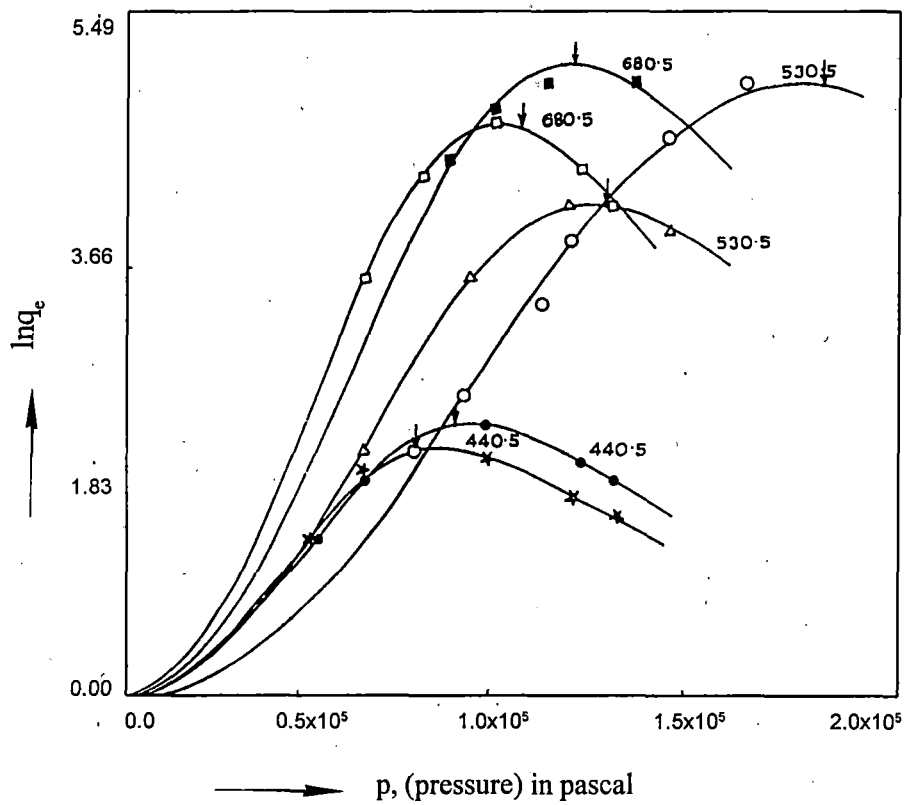

Fig. 10.1. $\ln q_e$ against pressure p in pascal of He^3–He^4 gas mixture : -○-○- experimental points at 530.5K for column I, -Δ-Δ- experimental points at 530.5K for column II, -■-■- experimental points at 680.5 for column III, -●-●- experimental points at 440.5K for column III, -□-□- experimental points at 680.5 K for column IV and -*-* experimental points at 440.5 K for column IV.

gas mixture always occurs. This is taken into consideration by adding a term K_p called the remixing coefficient being proportional to p^4 in the denominator of eq (10.2). Now assuming $(K_c + K_p)/HL = p^2/a'$ and $(K_c + K_p)/K_d = p^4/b'$ where a' and b' are independent of pressure we have

$$\ln q_e = a'p^2/(b' + p^4) \quad \text{..... (10.3)}$$

Least square fitting technique with the available experimental data[6] of He^3-He^4 gas mixture were made to get the experimental parameter a' and b'. This is to obtain the nature of variation of $\ln q_e$ against pressure p in pascal as illustrated graphically in Fig 10.1 for columns I to IV at different experimental temperatures in K. It is seen from Fig 10.1 that as p increases $\ln q_e$ increases and eventually reaches a maximum value of $\ln q_e$ i.e. $\ln q_{max}$ at an optimum pressure p_{opt} for which $\frac{\delta}{\delta p}(\ln q_e) = 0$, at each experimental temperature in K. Thus $p_{opt} = (b')^{1/4}$ and $\ln q_{max}$ becomes

$$\ln q_{max} = \frac{a'}{2\sqrt{b'}} \quad \text{..... (10.4)}$$

The experimental α_T by the CCF method with available F_s could, however, be obtained from eqs (10.1) and (10.4).

Further eq (10.2) on maximisation becomes

$$\ln q_{max} = \frac{HL}{2\sqrt{K_c\ K_d}} \quad \text{..... (10.5)}$$

The column coefficients, H, K_c and K_d based on Maxwell model dependent CSF[4], h', k_c' and k_d' are

$$H = \frac{2\pi}{6!}\left(\frac{\alpha_T \rho^2_{ij} g}{\eta_{ij}}\right)\frac{1}{2}(r_c + r_h)(r_c - r_h)^3 (2u)^2 h'$$

$$K_c = \frac{2\pi}{9!}\left(\frac{\rho^3_{ij} g^2}{\eta^2_{ij} D_{ij}}\right)_1 \frac{1}{2}(r_c + r_h)(r_c - r_h)^7 (2u)^2 k_c'$$

$$K_d = 2\pi(\rho_{ij} D_{ij})\frac{1}{2}(r_c + r_h)(r_c - r_h)k'_d.$$

where $\Delta T = T_h - T_c$ and $u=(T_h-T_c)/(T_h+T_c)$

Hence experimental α_T due to Maxwell model dependent CSF is

$$\alpha_T \text{ (Maxwell model)} = 2.39 \frac{r_c - r_h}{L} \frac{\bar{T}}{\Delta T} \frac{(k'_c k'_d)^{1/2}}{h'} \ln q_{max} \quad \ldots\ldots (10.6)$$

The column coefficients due to model independent CSF of Slieker[4] are :

$$H = C_1 = (S.F)_1 r_c^4 \frac{\alpha_T \rho_{ij}^2 g}{\eta_{ij}} \left(\frac{\Delta T}{\bar{T}}\right)^2$$

$$K_d = C_2 = \pi(1-a^2) r_c^2 \rho_{ij} D_{ij} \qquad \text{and}$$

$$K_c = C_3 = (S.F)_3 r_c^8 \left(\frac{\rho^3_{ij} g^2}{\eta^2_{ij} D_{ij}}\right) \left(\frac{\Delta T}{\bar{T}}\right)^2$$

where $a = r_h/r_c$ of the column. The experimental α_T due to Slieker model independent CSF is

$$\alpha_T \text{ (Slieker)} = 2.0 \frac{r_c}{L} \frac{\bar{T}}{\Delta T} \frac{[\pi(1-a^2)(SF)_3]^{1/2}}{(SF)_1} \ln q_{max}. \quad \ldots\ldots (10.7)$$

The experimental α_T by Maxwell model dependent and Slieker model independent CSF methods were obtained from eqs (10.6) and (10.7) respectively. They are placed in Table 10.3 and plotted graphically against $\bar{T}$ in Fig 10.3 for comparison.

10.3. Theoretical Formulations of Column Calibration Factor

The thermal diffusion column parameter in cylindrical coordinates as given by Cohen[5] are :

$$H = -2\pi \int_{r_h}^{r_c} \alpha_T \frac{\delta}{\delta r}(\ln T)\, dr \left(\int_{r_h}^{r} \rho_{ij} \upsilon r\, dr \right),$$

$$K_c = 2\pi \int_{r_h}^{r_c} \frac{dr}{\rho_{ij} D_{ij} r} \left(\int_{r_h}^{r} \rho_{ij} \upsilon r \, dr \right)^2$$

and $$K_d = 2\pi \int_{r_h}^{r_c} \rho_{ij} D_{ij} r \, dr$$

where r is the radial coordinate. The convective velocity υ of the of the molecule in vertical or downward direction under the influence of temperature gradient along the horizontal planes of the column can be derived from the Navier-Stokes hydrodynamical equation :

$$\frac{\delta^3 \upsilon}{\delta r^3} + \frac{1}{r} \frac{\delta^2 \upsilon}{\delta r^2} - \frac{1}{r^2} \frac{\delta \upsilon}{\delta r} = \frac{\rho_{ij} g}{\eta_{ij} \bar{T}} \frac{dT}{dr} \quad \text{..... (10.8)}$$

If we consider the rectilinear flow of heat from hot wire or wall to the cold wall of the column, the temperature T is given by :

$$T = T_h - \Delta T (r - r_h) / (r_c - r_h)$$

or, $$\frac{\delta T}{\delta r} = - \frac{\Delta T}{r_c - r_h}$$

Now, putting $r = e^x$ and solving eq. (10.8) we get the convective velocity υ up and down the TD column :

$$\upsilon = G r_c^2 [K_1 + K_2 \ln\phi + K_3 \phi^2 + \phi^3] \quad \text{..... (10.9)}$$

in which $G = -(\rho_{ij} g / \eta_{ij} \bar{T}) \{\Delta T / 9(r_c - r_h)\}$ and $\phi = (r/r_c)$ is another variable. The three arbitrary constants K_1, K_2 and K_3 of the column in eq. (10.9) are, however, derived in terms of column geometries satisfying the boundary conditions given below

i) $\upsilon = 0$ at $r = r_c$ for which $\phi = 1$

ii) $\upsilon = 0$ at $r = r_h$ for which $\phi = a (= r_h / r_c)$ and

there is no transport of components of a gas mixture at equilibrium in vertical direction up and down the column, we have,

iii) $r_c^2 \int_a^1 \rho \upsilon \phi d\phi = 0.$

The dimensionless constants K_1, K_2 and K_3 are, therefore, given explicitly in terms of a TDC without any approximation,

$$K_1 = \frac{5a^5 - (6a^5 - 5a^4 - 1)\ln a - 5a^2(a^2 + a - 1)}{5\,[a^4 + (1 - a^4)\ln a + (1 - 2a^2)]}$$

$$K_2 = \frac{a^7 - 6a^2(a^3 + 1) - 5a^3(a + 1) - 1}{5\,[a^4 + (1 - a^4)\ln a + (1 - 2a^2)]} \qquad \text{and}$$

$$K_3 = -(K_1 + 1).$$

The column coefficient H in terms of K_1, K_2 and K_3 is derived as follows :

$$H = 2\pi r_c^2 \int_a^1 \alpha_T \frac{\delta}{\delta \phi}(\ln T) d\phi \int_a^{\phi} \rho_{ij} \upsilon \phi d\phi$$

$$= 2\pi \alpha_T \frac{\Delta T}{1 - a} \rho_{ij} G r_c^4$$

$$x \int_a^1 \frac{1}{T} \left[\left(\frac{K_1 \phi^2}{2} + \frac{K_2 \phi^2}{2} \left(\ln \phi - \frac{1}{2} \right) + \frac{K_3 \phi^4}{4} + \frac{\phi^5}{5} + K_4 \right] d\phi$$

where $K_4 = (-a^2/2)\{K_1 + K_2(\ln a - 1/2) + K_3 a^2/2 + 2a^3/5\}$ is another constant.

or $$H = 2\pi \alpha_T r_c^4 \frac{\rho_{ij}^2 g}{\eta_{ij} \bar{T}} \frac{\Delta T}{(a - 1)9} G_1 \qquad \text{..... (10.10)}$$

where $$G_1 = \frac{\Delta T}{\bar{T}(1 - a)} \left(\frac{2K_1 - K_2}{12}(1 - a^3) - \frac{K_2}{18}(1 - a^3) \right.$$

$$-\frac{K_2 a^3}{6}\ln a+\frac{K_3}{20}+K_4(1-a)+\frac{1}{30}\Big)$$

$$-\Big(\frac{\Delta T}{\bar{T}(1-a)}\Big)^2\Big[\frac{2K_1-K_2}{48}-\frac{K_2}{24}\Big(7/12+a^4\ln a\Big)$$

$$+\frac{K_3}{120}+\frac{K_4}{2}(1-a^2)+1/210\Big]$$

$$+\Big(\frac{\Delta T}{\bar{T}(1-a)}\Big)^3\Big[\frac{2K_1-K_2}{120}-\frac{47K_2}{3600}+\frac{K_3}{420}+\frac{K_4}{3}(1-a^3)+1/840\Big].$$

The coefficient K_c of a TDC is given by :

$$K_c=2\pi\int_a^1\frac{d\phi}{\rho_{ij}D_{ij}\phi}\Big(\int_a^\phi\rho_{ij}\upsilon\phi d\phi\Big)^2.$$

$$=\frac{2\pi\rho_{ij}G^2r_c^{\,8}}{D_{ij}}\int_a^1\frac{1}{\phi}\Big[\frac{K_1\phi^2}{2}+\frac{K_2\phi^2}{2}\Big(\ln\phi-\frac{1}{2}\Big)$$

$$+\frac{K_3\phi^4}{4}+\frac{\phi^5}{5}+K_4\Big]^2d\phi$$

$$=\frac{2\pi\rho^3_{ij}g^2}{\eta^2_{ij}D_{ij}}\Big(\frac{\Delta T}{\bar{T}}\Big)^2\frac{r_c^{\,8}}{81(1-a)^2}G_2 \qquad \text{.....(10.11)}$$

where G_2 is a constant being given by :

$$G_2=\frac{K_1^2}{16}+\frac{5K_2^2}{128}-K_4^2\ln a+\frac{K_3^2}{128}-\frac{3K_1K_2}{32}+\frac{K_1K_3}{24}$$

$$+\frac{K_1K_4}{2}(1-a^2)-\frac{K_2K_3}{36}+\frac{K_3K_4}{8}-\frac{K_2K_4}{4}(2+2a^2\ln a-a^2)$$

$$+\frac{K_1}{35}-\frac{9K_2}{490}+\frac{K_3}{90}+\frac{2K_4}{25}+\frac{1}{250}.$$

For $n \geq 4$, 'a' is very small compared to unity and hence is neglected in the derivations.

The coefficient K_d is derived as :

$$K_d = 2\pi r_c^2 \int_a^1 \rho_{ij} D_{ij} \phi d\phi$$

$$= \pi r_c^2 \rho_{ij} D_{ij} (1-a^2). \qquad \text{..... (10.12)}$$

The column calibration factor per unit length F_s/L, is obtained from eqs (10.5) and (10.10)-(10.12)

$$F_s/L = \frac{G_1}{r_c[2(1-a^2)\, G_2]^{1/2}}. \qquad \text{..... (10.13)}$$

Thus the CCF per unit length of the column can easily be approximated in terms of G_1, G_2, a and r_c of the column. Theoretical values of F_s for columns I to IV at different experimental temperatures are placed in Table 10.1. The CCF per unit length, F_s/L against $\bar{T}$ for column I to IV are plotted in Fig 10.2 along with experimental values of F_s/L on them. F_s/L plays an important role in determining the thermal diffusion factor α_T of any gas mixture[3-4]. Its model independency was earlier established[7]. It can be further used to concentrate the impurity of any gas to any desired level in a TDC experiment. The α_T obtained from F_s and $\ln q_{max}$ helps one to get the force parameters of binary interactions of the molecules in order to conceive elastic or inelastic collisions occuring among molecules.

10.4. Optimum Pressure in a Thermal Diffusion Column

The optimum pressure of a gas mixture in an operating column is derived from eq (10.2) as a solution of $\frac{\delta}{\delta p}(\ln q_e) = 0$

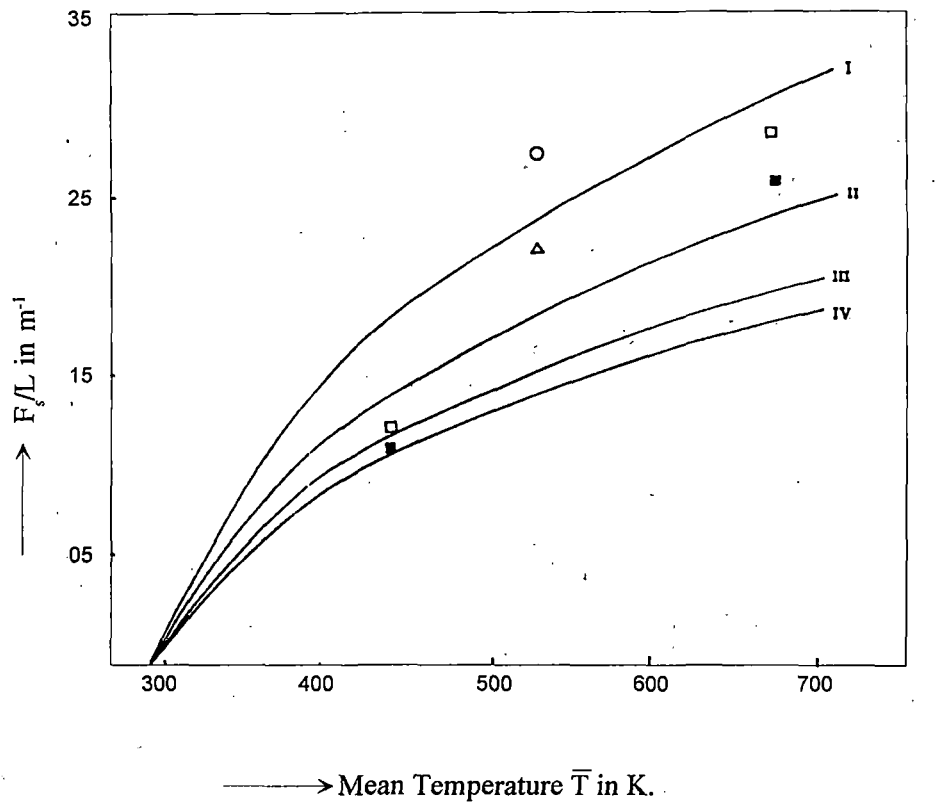

Fig. 10.2. Theoretical F_s/L against $\bar{T}$ with experimental F_s/L on it : Curve I, for column I, -○-○- experimental points; Curve II, for column II, -Δ-Δ-experimental points; Curve III, for column III, -□-□- experimental points; Curve IV, for Column IV, -■-■- experimental points.

from which the condition for optimum pressure is found out to be

$$K_c = K_d \qquad \text{..... (10.14)}$$

Now, from eqs (10.11), (10.12) and (10.14) we have

$$\frac{\rho_{ij} g}{\eta_{ij} D_{ij}} \frac{1}{9(1-a)} \frac{\Delta T}{\bar{T}} r_c^3 (2G_2)^{1/2} = (1-a^2)^{1/2}$$

the density ρ_{ij} at a given temperature $\bar{T}$ is given by

$$\rho_{ij} = p_{opt} M/(R\bar{T})$$

where M is the molecular weight and R the gram molecular gas constant. The diffusion coefficient is inversely proportional to pressure p. Writting $D_{ij} = D'/p_{opt}$ we have,

$$p^2_{opt} = p_0 \frac{R\eta_{ij} D_0}{gM} \frac{9(1-a)^{3/2}(1+a)^{1/2}}{r_c^3 (2G_2)^{1/2}} \left(\frac{\bar{T}}{\Delta T}\right) \qquad \text{..... (10.15)}$$

where $D_0 = D'/p_0$ is to be determined at any reference pressure p_o. p_{opt} thus obtained in terms of the column parameters and the transport coefficients of the gas mixture are placed in Table 10.3. These are shown by the down headed arrows in Fig 10.1. of $\ln q_e$ against p at all the temperatures. The transport coefficients which strongly depends on the composition of the He^3-He^4 gas mixture is, however, obtained from Yamamoto et al[2] at the experimental temperatures.

10.5. Theoretical Formulations for TD Factor

The theoretical formulation for α_T is obtained from the Chapman - Enskog gas Kinetic theory[8] which is based on elastic collisions among molecules. For monatomic gases like He^3-He^4 gas mixture the theory is assumed to be suitable and the experession for α_T is given by :

$$\alpha_T = \frac{1}{6\lambda_{ij}} \frac{S^{(i)} x_i - S^{(j)} x_j}{X_\lambda + Y_\lambda} (6C^*_{ij} - 5) \qquad \text{..... (10.16)}$$

The term $(6C^*_{ij} - 5)$ depends mainly on the temperature of the mixture. The other

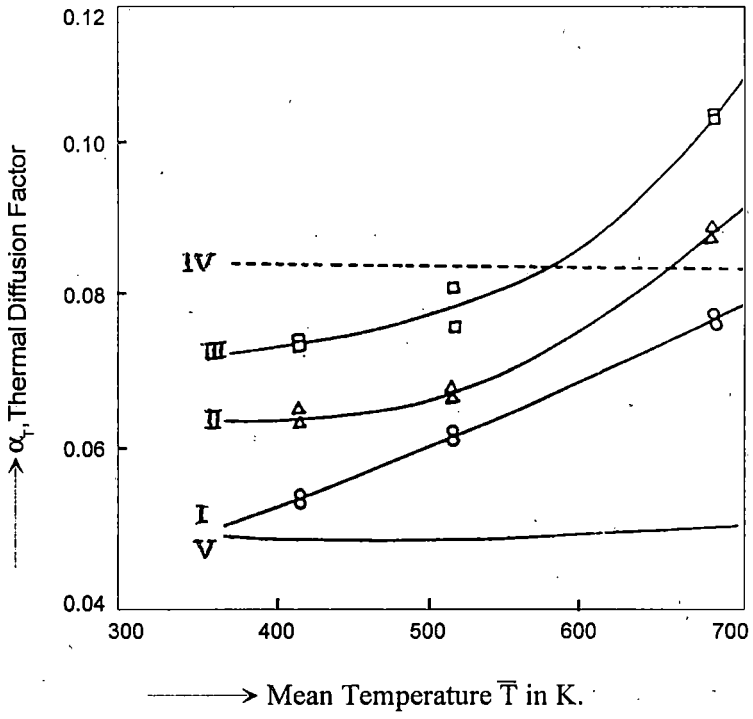

Fig. 10.3. TD factor α_T of He^3–He^4 against $\bar{T}$ in K : Curve I, α_T's by the CCF method, -o-o- experimental points; Curve II, α_T's due to Maxwell CSF,-Δ-Δ- experimental points; Curve III, α_T's due to Slieker CSF, -□-□- experimental points; Curve IV, α_T's due to elastic collision theory using 12-6 potential and Curve V, α_T's due to elastic collision theory using exp-6 potential.

terms involved in eq (10.16) are complicated functions of composition, masses and thermal conductivities of the mixture. The theoretical α_T for He^3-He^4 gas mixture are calculated from eq (10.16) and are entered in Table 10.3. They are also shown graphically in Fig 10.3 by curve no IV.

In accordence with our findings it is claimed by other workers[9] that α_T using Chapman Enskog formula could not interprete the experimental α_T for He^3-He^4 mixture. α_T for exp-6 potential are, however, cited from the dissertation of Vandervolk[10]. These α_T are displayed both in Table 10.3 and Fig 10.3 by curve no V for comparison.

10.6. Results and Discussions

The equations of $p^2/\ln q_e$ against p^4 of He^3-He^4 gas mixture were arrived at to get a' and b' of eq (10.3) in four columns with different column geometries at different experimental temperatures. They are :

$p^2/\ln q_e = 3.0934\times10^9 + 3.0429\times10^{-12}\, p^4$ at $\bar{T} = 530.5K$ for column I,

$p^2/\ln q_e = 1.8850\times10^9 + 7.6073\times10^{-12}\, p^4$ at $\bar{T} = 530.5K$ for column II,

$p^2/\ln q_e = 1.8834\times10^9 + 2.3667\times10^{-11}\, p^4$ at $\bar{T} = 440.5K$ for column III,

$p^2/\ln q_e = 1.3383\times10^9 + 6.5473\times10^{-12}\, p^4$ at $\bar{T} = 680.5K$ for column III,

$p^2/\ln q_e = 1.7568\times10^9 + 3.0142\times10^{-11}\, p^4$ at $\bar{T} = 440.5K$ for column IV and

$p^2/\ln q_e = 1.0239\times10^9 + 1.0307\times10^{-11}\, p^4$ at $\bar{T} = 680.5K$ for column IV.

In Fig 10.1 for all the columns the $\ln q_e$'s of He^3-He^4 gas mixture are found to increase gradually as the pressure increases and reaches the maximum value of $\ln q_{max}$ at optimum pressure at all the experimental temperatures $\bar{T}$ in K and then decreases in accordance with eq (10.3). The optimum pressure p_{opt} as seen by down headed arrow in Fig 10.1 at which $\ln q_e$ becomes maximum is of decreasing nature with increasing r_c/r_h of the columns. The values of the estimated a' and b' in case of He^3-He^4 gas mixture in different columns at their experimental temperatures are placed in the 5th and 6th columns of Table 10.1. $\ln q_{max}$'s in terms of a' and b' of eq (10.4) are shown in the 7th column of Table

Table 10.1 : Geometry of the columns, experimental a', b' and $\ln q_{max}$ and the column constants G_1 and G_2 together with column calibration factor (CCF) F_s of the columns.

Geometry column in m	Hot wall temp T_h in K	Cold wall temp T_c in K	Mean Temp $\bar{T}$ in K	a'x10^{-10} pascal^2	b'x10^{-20} pascal^4	$\ln q_{max}$	Column constant G_1x10^3	Column constant G_2x10^5	CCF(theo) F_s From eq(10.13)	Expt F_s using α_T of Nier[10]
Column I										
L = 3.05	773	288	530.5	32.8631	10.1660	5.1535	3.2741	5.4802	75.2540	87.3475
$r_c = 1.27 \times 10^{-2}$										
$r_h = 7.95 \times 10^{-4}$										
Column II										
L = 3.05	773	288	530.5	13.1452	2.4779	4.1754	3.4089	5.9196	59.7963	70.7995
$r_c = 1.6 \times 10^{-2}$										
$r_h = 7.95 \times 10^{-4}$										
Column III										
L = 3.05	593	288	440.5	4.2258	0.7958	2.3685	2.7000	6.3365	38.5345	40.1441
$r_c = 1.9 \times 10^{-2}$										
	1073	288	680.5	15.2735	2.0441	5.3414	4.4637	6.3367	63.7050	90.5322
$r_h = 7.95 \times 10^{-4}$										
Column IV										
L = 3.05	593	288	440.5	3.3176	0.5828	2.1728	2.7272	6.4985	35.6179	36.8271
$r_c = 2.05 \times 10^{-2}$										
	1073	288	680.5	9.7024	0.9934	4.8673	4.5143	6.1985	58.9577	82.4966
$r_h = 7.95 \times 10^{-4}$										

Table 10.2 : Maxwell model dependent and Slieker model independent column shape factors (CSF), coefficient of viscosity and diffusion coefficient of He^3 - He^4 isotopic gas mixture.

Column	Mean temp $\bar{T}$ in K	Column Shape Factors					Coefficient of viscosity $\eta_{ij} \times 10^5$ kg. m^{-1} sec^{-1} of He^3 - He^4 mixture	Diffusion coefficient $D_{ij} \times 10^4$ m^2 sec^{-1} of He^3 - He^4 mixture
		Maxwell			Slieker			
		h'	k_c'	k_d'	$[S.F.]_1 \times 6!$	$[S.F.]_3 \times 9!$		
Column I	530.5	1.060	3.10	0.715	1.0018	0.6946	2.7443	4.6770
Column II	530.5	1.035	3.30	0.700	0.9820	0.7155	2.7443	4.6770
Column III	440.5	0.86	2.05	0.795	0.9469	0.7121	2.3777	3.4040
	680.5	1.42	5.70	0.790	0.9469	0.7121	3.3553	7.2344
Column IV	440.5	0.84	2.10	0.710	0.9298	0.7086	2.3777	3.4040
	680.5	1.32	5.85	0.705	0.9298	0.7086	3.3553	7.2344

10.1. The F_s as functions of the column constants G_1 and G_2 of the four TD columns were obtained. G_1 and G_2 are placed in the 8th and 9th columns of Table 10.1. The experimental F_s of each column at each working temperature was also determined in order to place them in the 11th column of Table 10.1.The close agreement of theoretical and experimental F_s suggest that the derivation of F_s from Navier Stokes equation is more than accurate. The derived values of F_s are then used to obtain α_T of light isotopic He^3-He^4 gas mixture. The α_T's of He^3-He^4 as obtained through F_s are shown in the 3rd column of Table 10.3. They are plotted against $\bar{T}$ in Fig10.3. The data are found to fall on curve 1 which increase with temperature $\bar{T}$ in K like those of the existing methods using CSF.

Slieker's molecular model independent CSF and Maxwell's model dependent CSF as presented in the 3rd, 4th, 5th, and 6th ,7th columns of Table 10.2 respectively were used to get experimental α_T's from eqs (10.6) and (10.7). They are placed in the 4th and 5th columns of Table 10.3 and shown by curve No II and III in Fig 10.3. They are found to be higher in magnitudes in comparison with α_T's due to CCF method, maintaing the same trend with temperature $\bar{T}$ in K.

Theoretical α_T's using L - J (12-6) molecular potential are calculated at 440.5, 530.5, and 680.5 K in order to place them in the 6th column of Table 10.3. The α_T's thus obtained are seen by curve No IV of Fig 10.3. They are found not in agreement with the experimental α_T's by all the experimental methods cited above.

The theoretical α_T's by using exp-6 potential were found[10] to be of the same order of magnitudes with α_T's obtained by the CCF method. The α_T's with $\bar{T}$ for exp-6 model are plotted in Fig (10.3) by curve V and entered in the 7th column of Table 10.3 for comparison. These α_T's, however, failed to accord with the temperature dependence of experimental α_T's of He^3-He^4 gas mixtures by the existing experimental methods. The experimental α_T's strongly depends on $\bar{T}$ and is in good agreement with the finding of others.[9,10]

To check how far the column coefficient of eqs (10.10)-(10.12) are reliable the optimum pressure p_{opt}'s of the gas mixture in all the operating columns at their respective temperature are obtained. Taking $p_0 = 10^5$ pascal as the reference pressure, p_{opt}'s are obtained from eq (10.15) in terms of G_2 and other transport

Table 10.3 : Experimental and theoretical α_T of He^3 - He^4 isotopic mixture together with optimum pressure in the operating columns at different temperatures.

Column	Mean temp $\bar{T}$ in K.	Experimental α_T using			Theoretical α_T using		P_{opt} experimental in M. Pa	P_{opt} using eq(10.15) in M.Pa
		F_s of eq(10.13)	Slieker's shape factor (CSF)	Maxwell shape factor (CSF)	12 - 6 potential	exp - 6 potential		
Column I	530.5	0.0685	0.082	0.074	0.0902	0.057	0.1786	0.1862
Column II	530.5	0.0698	0.087	0.080	0.0902	0.057	0.1255	0.1297
Column III	440.5	0.0615	0.084	0.072	0.0903	0.057	0.0944	0.0901
	680.5	0.0838	0.109	0099	0.0899	0.058	0.1196	0.1209
Column IV	440.5	0.0610	0.081	0.070	0.0903	0.057	0.0874	0.0800
	680.5	0.0826	0.109	0.100	0.0899	0.058	0.0998	0.1073

coefficients. They are compared with the experimental p_{opt}'s ($p_{opt} = b'^{1/4}$) of the mixture. These are seen in the 9th and 8th columns of Table 10.2 respectively for comparison. The p_{opt} as derived from eq (10.15) are seen to be almost in close agreement with the experimental results. These are shown by down headed arrows in all the curves of $\ln q_e$ against pressure p in pascal.

The established methodology [7,11] to estimate ε_{ij}/k from the temperature dependence of α_T by the CCF method yields 185.78 which is larger than the reported one for He^3-He^4 isotopic mixture. The assumed quantum diffraction effect in He molecule was applied in terms of Λ^*. The quantum parameter Λ^* is defined[12] as the ratio of the de Broglie wave length λ of the relative molecular kinetic energy E to the molecular diameter σ by : $\Lambda^* = \lambda/\sigma = h/\{\sigma(mkT)^{1/2}\}$ where h is the plancks constant and m is the reduced mass. The modified L - J (12-6) potential in terms of ε/k (=183.67) is finally obtained to calculate α_T of He^3-He^4 mixture at varius $\bar{T}$ in K. These α_T's of 0.0503, 0.059 and 0.0682 at 440.5K, 530.5K and 680.5K respectively were found to show the same magnitudes maintaining the similar trend with respect to $\bar{T}$.

Due to usual asymmetric nature of TD column remixing coefficient had already been taken into consideration by adding a term K_p in the denominator of eq (10.2). Leyarovski[13] had shown that this $K_p \leq 20\%$ of K_c. Thus remixing effect may creep an error of 9.54% and 4.46% in experimental α_T and in p_{opt} respectively. However, the close agreement in magnitudes between the experimental and theoretical α_T's (curve I and curve V), experimental and theoretical p_{opt}'s suggests that the derived relationship of F_s/L are more than adequate.

It is thus clear once again that the theoretical formulations of the model independent CCF is a simple, straightforward and reliable one as observed elsewhere[7].

10.7. Conclusions

The formulations of F_s in terms of the coefficients appears to be an importent tool in obtaining both the experimental α_T of any binary gas mixture as well as p_{opt} of the working column at their respective temperatures. However, the non-

agreement between the theoretical and the experimental α_T's is perhaps due to quantum effect in He^3-He^4 gas mixture[10]. The CCF, F_s should further be used to determine the experimental α_T of the interesting pair of molecules only to improve the elastic or inelastic collision theories of thermal diffusion among the pair of molecules[14].

Reference

[1] W. H. Furry and R.C. Jones, Phy. Rev. **69** (1946) 459.

[2] I. Yamamoto, H. Makino and A. Kanagawa, J. Nuel. Sci. Technol, **27** (1990)156

[3] S. Acharyya, I. L. Saha, A. K. Datta and A. K. Chattarjee, J. Phys. Soc. Japan, **56** (1987) 105

[4] A. K. Datta and S. Acharyya J. Phys. Soc. Japan, **62** (1993) 1527

[5] K. Cohen: The Theory of isotope seperation, McGrew-Hill Book Cy Inc. NY (1951).

[6] W. M. Rutherford, J. Chem. Phys. **23** (1970) 4319.

[7] G. Dasgupta and S. Acharyya J. Phys. D: Appl. Phys. (London) **31** (1998)1092.

[8] S. Chapman and T. G. Cowling, The Mathematical Theory of Non Uniform gases (Cambridge Univ. Press, NY,1952)

[9] S.C. Saxena, J.G. Kelley and W. W. Watson: Phy. Fluids, **4** (1961) 1216

[10] F. Vander Volk : Ph.D Dissertation (1963)

[11] G. Dasgupta, N. Ghosh, N. Nandy and S. Acharyya, J. Phys. Soc. Japan, **66** (1997) 108.

[12] B. K. Singh and S. K. Sinha, Ind. J. Phys. **71A** (1997) 285.

[13] E. I. Leyarovski, J. K. Georgiev and A. L. Zahariev, Sep. Sci. and Technol, **25** (1990) 557.

[14] T. K. Chattopadhyay and S.Acharyya, J. Phys. B. (At. Mol. Phys) **7** (1974) 2277.

CHAPTER 11

Summary and Conclusion

SUMMARY AND CONCLUSION

The thesis entitled "Column Calibration Factor and Force Parameters to Predict Temperature and Composition Dependence of Thermal Diffusion Factor of Some Simple Molecules" deals with several theoretical and experimental aspects of thermal diffusion column (TDC). Role of the column calibration factor to determine the temperature or composition dependence of thermal diffusion factor α_T is examined in the earlier part of the thesis. The thesis presents a new theory to determine the molecular force parameters of the gas molecules by thermal diffusion. Occurrence of elastic or inelastic collisions among molecules are examined carefully. Furthermore, a simple, adequate and straightforward column constants are given explicitly to explain the thermal diffusion column behaviour.

The phenomenon of thermal diffusion is well known for its wide applicability in different fields of science and technology. Two bulbs, Swing separator and Thermal diffusion column are the commonly used apparatus in which separation by thermal diffusion can be made. The general theories of separation by the above instruments are well discussed in the 1st chapter of this thesis.

Several authors have engaged themselves deeply in thermal diffusion to improve the column theory while a qualitative agreement is only observed. A brief review of the previous theoretical and experimental works are thus presented in chapter 2 of the thesis.

The scope and objective of the thesis work is presented in chapter 3. It involves with the measurements of α_T by the column calibration factor in thermal diffusion column. The α_T's as measured could be shown as a function of composition or temperature of the binary or ternary gas mixture.

Chapter 4 of the thesis deals with theoretical formulation of TD factor α_T based on elastic or inelastic collisions among molecules. Furthermore, determination of experimental α_T by the existing method of Maxwell model dependent and Slieker molecular model independent column shape factor (CSF) has been discussed to compare them with the experimental α_T by the CCF method.

Composition dependences of experimental α_T of He^4- Ar^{40}, Ne^{20} - Xe^{132} and Ne^{20} - Ne^{22} gas mixture through F_s of the column are estimated in the 5th chapter of the thesis. So far their magnitude and trends of variation with the molefraction of the lighter component are concerned these α_T's agree excellently with those α_T's by the existing methods. This suggests that the evaluation of α_T's by the CCF method is a unique one and can safely be used to study the composition dependences of α_T in both isotopic or nonisotopic molecules.

Chapter 6 of the thesis describes the temperature dependence of experimental α_T of hydrogenic trace mixtures in Helium through CCF of a given column. Experimental α_T's by the CCF method are compared with those by the existing methods as well as with the theoretical α_T's based on either elastic or inelastic collisions among molecules. Besides the role of the CCF in determining the experimental α_T this study observes the inelastic collision effect among these experimental simple molecules.

The thermal diffusion column of Roos and Rutherford has been accurately calibrated in chapter 7. Thermal diffusion factors α_T's against $\bar{T}$ of Kr, Xe, CO, CH_4 and N_2 binary isotopic mixtures have been obtained in terms of the CCF of the column. These α_T's are used to estimate the molecular force parameters of all the aforesaid molecules. Theoretical α_T's based on elastic or inelastic collisions among molecules as well as experimental α_T's by the existing method are evaluated. Comparison of the obtained results finally suggests that the technique of predicting α_T as a function of temperature is extremely useful.

In the 8th chapter of the thesis simultaneous determination of α_T as well as prediction of pressure dependence of lnq_e are made possible in terms of the CCF of a given column. Experimental α_T due to Maxwell and Slieker CSF as well as theoretical α_T based on elastic collisions among molecules are evaluated for comparison. α_T's against $\bar{T}$ as obtained by the CCF method are used to estimate the molecular force parameters of the experimental molecules. Evaluated force parameters agree excellently with the reported data. It may thus be concluded that α_T plays an important role in determining the molecular force parameters. Further, F_s is a sensitive α_T measuring parameter and its model independency is established.

From Navier - Stoke's hydrodynamical equation in cylindrical coordinates

an approximate formulation of F_s at any given temperature is derived in the 9th chapter. Derived formulation is used to determine F_s of four different experimental columns and thereby to determine α_T of Ne^{20} - Ne^{22} isotopic gas mixture by the CCF method. Furthermore, molecular force parameters of Ne are evaluated from the temperature dependence of experimental α_T. The excellent agreement of the estimated force parameters with the available literature values and the comparison of the temperature variation of α_T by the CCF method with the existing experimental and theoretical α_T establish the fact that the derived relationship of F_s is more than adequate.

Relationship of F_s derived in chapter 9 is extended further in chapter 10 of the thesis. From the available $\ln q_{max}$ of four different TD column α_T of He^3 - He^4 gas molecules is obtained by the CCF method. Column parameters as obtained are used to determine the optimum pressure of the working column. Excellent agreement of the estimated optimum pressure with the experimental results and the comparison of the temperature variation of α_T by the CCF method with the existing experimental and theoretical α_T clearly signify that the column parameters acheived so far is a significant improvement over the existing theories.

APPENDIX

Journal of The Physical Society of Japan
Vol. 59, No. 10, October, 1990, pp. 3602–3609

Column Calibration Factor to Study the Composition Dependence of the Thermal Diffusion Factors of Inert Gas Mixtures

A. K. DATTA, G. DASGUPTA and S. ACHARYYA

Department of Physics, University College,
P. O. Raiganj, Dist. West Dinajpur, PIN 733134, India

(Received March 19, 1990)

The experimental thermal diffusion factors α_T of He^4–Ar^{40} and Ne^{20}–Xe^{132} gas mixtures at different compositions of the lighter components and an isotopic natural mixture of Ne^{20}–Ne^{22} are estimated at the mean temperature $\bar{T}=340$ K by the column calibration factor method from the available values of $\ln q_e$ (q_e being the equilibrium separation factor) for those mixtures at different pressures in atmosphere for each composition, measured by J. M. Saviron *et al.* in a thermal diffusion column with the column calibration factor $F_s=3.946$, the value (at $\bar{T}=340$ K) derived from the formula $F_s=68.94796-0.3174514\ \bar{T}+3.71383\times10^{-4}\bar{T}^2$ as obtained by S. Acharyya *et al.* It is shown that the experimental α_T's, thus estimated with the help of F_s and $\ln q_{max}$, agree excellently with those due to the existing methods using molecular models as well as with those due to Slieher's model-independent method, so far as their magnitudes and the trends of their variation with the mole fraction of the lighter components are concerned. This suggests that the present method is a unique one which can safely be used to study the composition dependence of α_T in both the isotopic and nonisotopic cases.

§1. Introduction

Nowadays the study of thermal diffusion is mostly directed to measuring the equilibrium separation factor q_e, defined by

$$q_e=(c_i/c_j)_{top}/(c_i/c_j)_{bottom}, \tag{1}$$

for isotopic and nonisotopic binary gas mixtures of different compositions at a fixed temperature, or for a binary gas mixture of fixed composition at different temperatures, in a thermal diffusion (TD) column first introduced by Clusius and Dickel.[1] Here c_i and c_j are the mass fractions of the lighter and heavier components of a gas mixture, respectively, and the subscripts top and bottom denote the values at the top and bottom of a TD column. The experimental values of q_e are measured usually at different pressures below and around one atmosphere with the help of a precision type mass spectrometer, and hence the TD factor α_T of a binary gas mixture as a function of the composition or the temperature is estimated by using various molecular models such as those of Maxwell and Lennard-Jones[2] and sometimes by using Slieker's model-independent method,[3] which is, however, a crude one. In an attempt to get the actual α_T, we,[4–6] however, introduced a factor F_s, called the column calibration factor of a TD column, by the relation

$$\ln q_{max}=\alpha_T F_s(r_c, r_h, L, \bar{T}), \tag{2}$$

where q_{max} is the maximum value of q_e measured experimentally in a TD column, r_c and r_h are the cold wall and hot wall radii of the column of geometrical length L, and $\bar{T}$ is the mean temperature in K of the gas mixture in the column, defined by $\bar{T}=(T_h+T_c)/2$, T_h and T_c being the temperatures of the hot and cold walls of the column, respectively. The column calibration factor F_s, which is purely an apparatus quantity, is supposed to be independent of a molecular interaction model and depends only on the geometry of the column at any mean temperature $\bar{T}$.

The column calibration factor F_s of a column with $L=149$ cm, $r_c=1.37$ cm and $r_h=0.6$ cm has already been studied elsewhere,[5] and the empirical relation of F_s to $\bar{T}$ has been

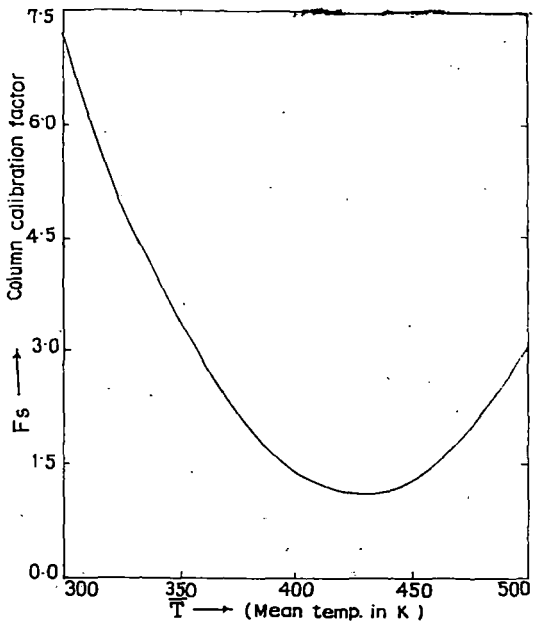

Fig. 1. Plot of the column calibration factor against $\bar{T}$, the mean temperature in K.

found to be

$$F_s=68.94796-0.3174514\,\bar{T}+3.71383\times10^{-4}\,\bar{T}^2,$$

yielding the value of $F_s=3.946$ at $\bar{T}=340$ K. The F_s for this column is plotted against $\bar{T}$ in Fig. 1. Fortunately J. M. Saviron *et al.*[7] have recently studied the pressure dependence of the reduced logarithmic separation factors, $\ln \bar{Q}_{exp}$, for two binary inert gas mixtures of He^4-Ar^{40} and Ne^{20}-Xe^{132} and also an isotopic natural mixture of Ne^{20}-Ne^{22} for different compositions of the lighter components in the respective mixtures, in this column, at the experimental mean temperature $\bar{T}=340$ K, the hot wall and cold wall temperatures being $T_h=380$ K and $T_c=300$ K, respectively. From these results we estimate $\ln q_c$ of the mixtures for different concentrations of the lighter components at different pressures in atmosphere, and the data thus obtained are found to satisfy the hydrodynamical part of the column theory, as developed by Furry and Jones[8] and Furry, Jones and Onsager,[9] so excellently as shown in Figs. 2 and 3 that we have at once the following relations of $p^2/\ln q_c$ to p^4 for these mixtures at different concentrations:

$$p^2/\ln q_c=3.09752+177.30496\,p^4,$$
$$p^2/\ln q_c=8.52467+66.65334\,p^4,$$
$$p^2/\ln q_c=17.20000+41.70213\,p^4,$$
$$p^2/\ln q_c=19.65238+16.78669\,p^4,$$
$$p^2/\ln q_c=18.74249+12.92235\,p^4,$$

for the He^4-Ar^{40} mixture for the concentrations 8.76, 21.63, 30.14, 49.30 and 64.46% of He^4, respectively;

$$p^2/\ln q_c=0.59848+3156.6\,p^4,$$
$$p^2/\ln q_c=2.39745+327.3\,p^4,$$
$$p^2/\ln q_c=3.03368+133.3\,p^4,$$

for the Ne^{20}-Xe^{132} mixture for 15, 66 and 90% of Ne^{20}; and finally

$$p^2/\ln q_c=13.3+89.06\,p^4,$$

for the Ne^{20}-Ne^{22} mixture. These establish that the graph of $p^2/\ln q_c$ against p^4 is always a straight line as predicted by the FJO theory.[9] Rutherford and Kaminski[10] have recently shown that the FJO theory[9] is applicable mainly in the case of an isotopic binary gas mixture and also in the case of a mixture in which one of the components is in trace concentrations.

In the thermal diffusion phenomena of isotopic gas mixtures, the elastic collisions are supposed to play a prominent role between the interacting molecules. Again, the thermal diffusion phenomenon is very sensitive to intermolecular interactions of the binary gas molecules; therefore, the study of the composition dependence of the TD factors α_T of any gas mixture is necessary to throw much light on the interactions between like molecules and those between unlike molecules of a gas mixture. The temperature dependence of α_T is, however, entirely governed by the factor $(6C_{ij}^*-5)$, where C_{ij}^* is the ratio of the collision integrals. Moreover, the effect of inelastic collisions on the thermal diffusion, if any, is practically negligible in gas mixtures containing inert gases. All the facts mentioned above inspired us to study He^4-Ar^{40} and Ne^{20}-Xe^{132} mixtures at different compositions of the lighter components at a given experimental mean temperature $\bar{T}=340$ K and also the isotopic mixture Ne^{20}-Ne^{22} with its natural isotopic abun-

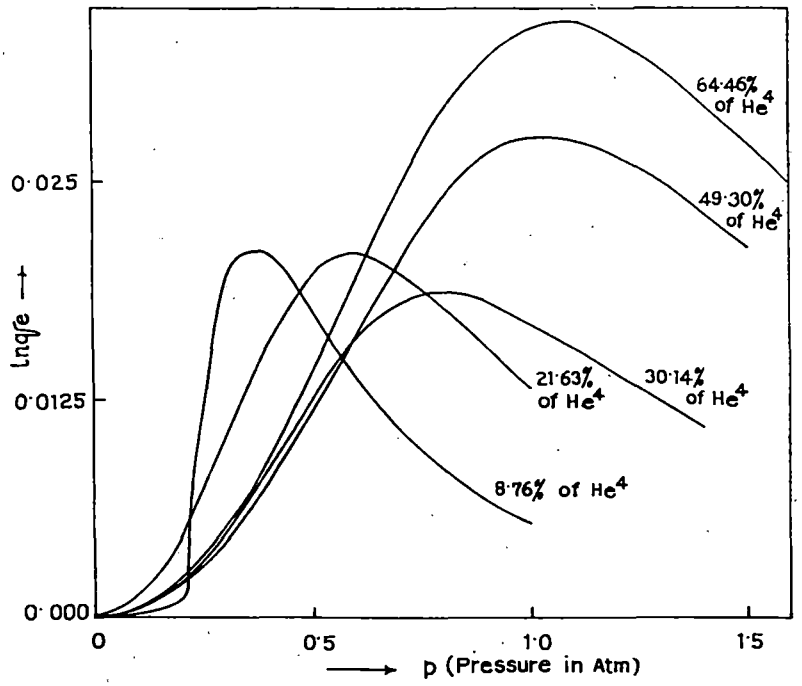

Fig. 2. Plot of ln q_e of He^4-Ar^{40} (binary inert gas mixture) against pressure p in atm. at different concentrations of He^4 at temperature $\bar{T}=340$ K.

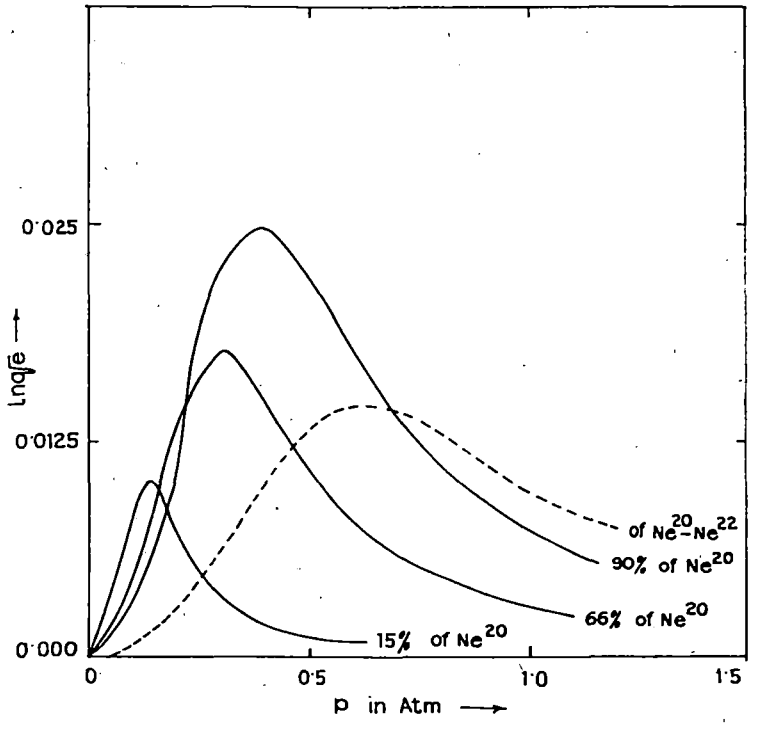

Fig. 3. Plot of ln q_e of Ne^{20}-Xe^{132} (binary inert gas mixture) against pressure p in atm. at different concentrations of Ne^{20} at temperature $\bar{T}=340$ K. The dotted curve represents that of Ne^{20}-Ne^{22}.

Table I. Composition dependence of thermal diffusion factors α_T of inert gas mixture at $\bar{T}=340$ K in a column of L=geometrical length=149 cm, r_c=the cold wall radius=1.37 cm and r_h=the hot wall radius=0.6 cm.

System	T_hK	T_cK	$\bar{T}$K	% of lighter component.	$a'\times10^3$ (atm)^2	$b'\times10^3$ (atm)^4	ln q_{max}	F_s	Expt. $\alpha_T\times10^3$ present method	Expt. $\alpha_T\times10^3$ based on models			Theo. α_T (elastic)
										Maxwell	$L-J$	Slieker	
				8.76	5.64	17.47	0.0213		5.40	4.20	1.60	3.80	0.226
				21.63	15.00	127.87	0.0210		5.30	3.00	1.20	2.40	0.253
He–Ar	380	300	340	30.14	23.98	412.46	0.0187	3.946	4.70	2.70	1.00	2.10	0.273
				49.30	59.57	1170.72	0.0275		7.10	3.60	1.40	2.90	0.327
				64.46	77.39	1295.62	0.0340		8.60	7.20	2.50	5.80	0.340
				15.00	0.32	0.19	0.0115		2.90	4.20	4.50	3.40	0.247
Ne–Xe	380	300	340	66.00	3.06	7.32	0.0178	3.946	4.50	7.30	7.50	5.40	0.218
				90.00	7.50	22.76	0.0249		6.30	13.70	15.50	11.00	0.236
Ne^{20}–Ne^{22}	380	300	340	10.00	11.23	148.87	0.0146	3.946	3.70	5.40	1.70	4.40	0.0248

dances. The purpose of this work is to observe how far the TD factors α_T as estimated by our column calibration factor method agree with those obtained by the existing methods, using the column shape factors involved in the molecular models, and by Slieker's model-independent method.[3] The comparison is presented in Table I, and shown graphically in Figs. 4 and 5 for He^4–Ar^{40} and Ne^{20}–Xe^{132} mixtures, respectively. The molecular parameters as well as the column shape factors used to calculate the experimental α_T's by the existing method are shown in Table II. The theoretical α_T's as functions of the mole fractions of the lighter components are also calculated from the formula derived from the Chapman-Enskog kinetic theory[11] based upon the elastic collisions between the interacting molecules. These α_T's are also shown in Table I and in Figs. 4 and 5 for comparison.

§2. Mathematical Formulations to Estimate the Experimental α_T's of the Mixtures

For a TD column with both ends closed, the hydrodynamical part of the column theory related with the transport of the lighter component up the tube, so far developed by Furry, Jones and Onsager,[9] yields that the net transport of the ith component of a binary gas mixture up the column tube is zero, i.e.

$$\tau_i = Hc_ic_j - (K_c+K_d)\frac{\partial c_i}{\partial z}=0, \qquad (3)$$

where z is the coordinate along the column, and H, K_c and K_d are called the transport coefficient, the convective remixing coefficient and the diffusive remixing coefficient, respec-

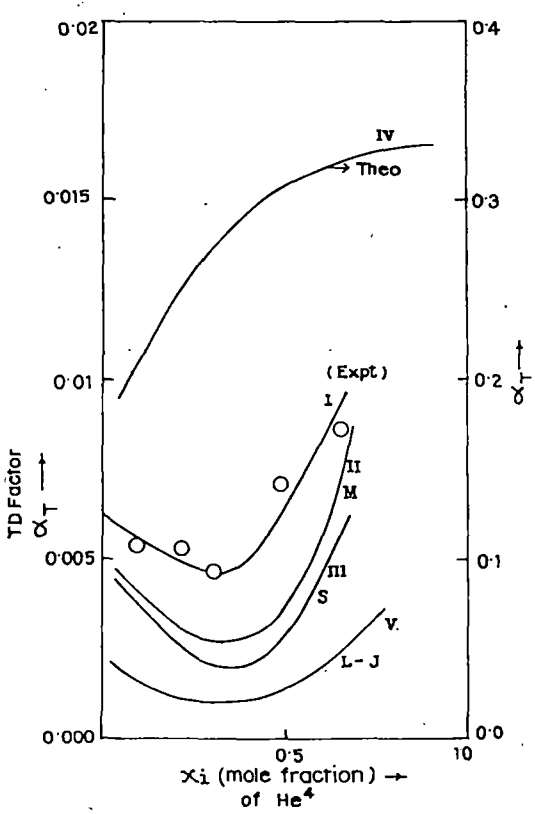

Fig. 4. Experimental α_T against mole fraction of He^4 of He^4–Ar^{40} mixture at mean temperature $\bar{T}=340$ K. I Expt. α_T (our calibration factor method), II Expt. α_T (Maxwell's model), III Expt. α_T (Slieker), IV Theoretical α_T (elastic), V Expt. α_T ($L-J$ model).

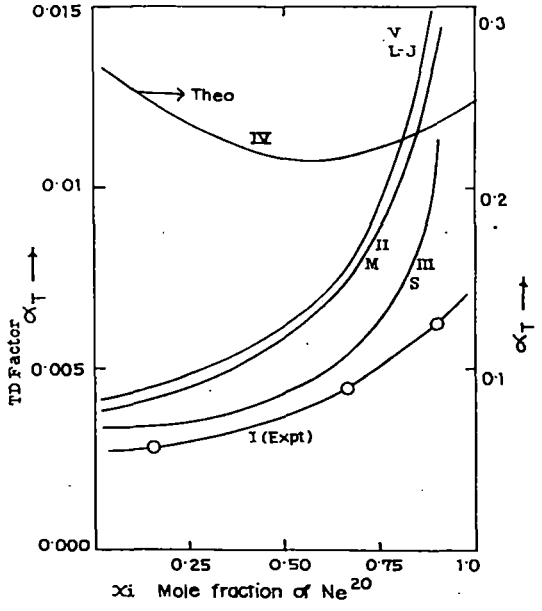

Fig. 5. Experimental α_T against mole fraction of Ne^{20} of Ne^{20}–Xe^{132} mixture at mean temperature $\bar{T}=340$ K. I Expt. α_T (our calibration factor method), II Expt. α_T (Maxwell's model), III Expt. α_T (Slieker), IV Theoretical α_T (elastic), V Expt. α_T ($L-J$ model).

tively; they are complicated functions of the wall temperatures, the geometry of the column and also the transport properties of the binary gas mixture, and are given by

$$H=\frac{2\pi}{Q^3}\int_{T_c}^{T_h}\frac{\rho D_{ij}}{\lambda}\alpha_T\frac{G(T)}{T}\,dT, \tag{4}$$

$$K_c=\frac{2\pi}{Q^2}\int_{T_c}^{T_h}\frac{\rho D_{ij}}{\lambda}G^2(T)\,dT, \tag{5}$$

$$K_d=\frac{2\pi}{Q}\int_{T_c}^{T_h}r^2\lambda\rho D_{ij}\,dT, \tag{6}$$

where ρ is the density, r is the radial coordinate, λ and D_{ij} are the thermal conductivity and diffusion coefficient of the gas mixtures, respectively, T_h and T_c are the hot and cold wall temperatures, and $2\pi Q$ denotes the radial heat flow per unit length of the column. The function $G(T)$ is the solution of the fourth-order differential equation

$$\frac{d}{dT}\left(\frac{1}{\lambda r^2}\right)\frac{d}{dT}\left(\frac{\eta}{\lambda}\right)\frac{d}{dT}\left(\frac{1}{\lambda\rho r^2}\right)\frac{d}{dT}\left(\frac{\rho D_{ij}}{\lambda}G(T)\right)=-g\frac{d\rho}{dT}, \tag{7}$$

with the boundary conditions

$$G(T_c)=G(T_h)=G'(T_c)=G'(T_h)=0. \tag{8}$$

Here η and g denote the coefficient viscosity of the gas mixture and the acceleration of gravity, respectively.

Integrating eq. (3) between the column ends $z=0$ and $z=L$, where L is the geometrical length of the column, one gets

$$\ln q_e=\frac{HL}{K_c+K_d}. \tag{9}$$

The coefficients H, K_c and K_d for an ideal column are proportional to the 2nd, the 4th and the 0th powers of the pressure p in at-

Table II. Column shape factors and other molecular parameters used to calculate α_T of He^4–Ar^{40}, Ne^{20}–Xe^{132} and Ne^{20}–Ne^{22} mixtures at $\bar{T}=340$ K and the $L-J$ potential ε_{12} in erg.

Systems	ε_{12}/k K	σ_{12} Å	Shape factors due to Maxwell's model		Slieker's shape factors	
			h'	k_d'	$[SF]_1$	$\pi(1-a^2)$
He^4–Ar^{40}	34.95	3.191				
Ne^{20}–Xe^{132}	79.36	3.457	0.99425	0.97734	$\frac{0.7041}{6!}$	1.7647
Ne^{20}–Ne^{22}	27.50	2.858				
			Lennard-Jones' shape factors			
			h	k_c	k_d	
He^4–Ar^{40}	34.95	3.191	0.00750	0.00224	0.41875	
Ne^{20}–Xe^{132}	79.36	3.457	0.00250	0.00180	0.40700	
Ne^{20}–Ne^{22}	27.50	2.858	0.00975	0.00240	0.42310	

mosphere, respectively, for a binary gas mixture, and hence eq. (9) reduces to

$$\ln q_c = \frac{ap^2}{b+p^4}. \tag{10}$$

However, in a practically constructed column, parasitic remixing of the components of the mixture always occurs. This can be taken into consideration by adding a term K_p, proportional to p^4, in the denominator of eq. (9), so that eq. (9) becomes

$$\ln q_c = \frac{a'p^2}{b'+p^4},$$

or

$$p^2/\ln q_c = \frac{b'}{a'} + \frac{1}{a'}p^4. \tag{11}$$

The a' and b' in eq. (11) are related to a and b in eq. (10) by a $a=a'(1+K_p/K_c)$ and $b=b'(1+K_p/K_c)$, respectively. The a and b in eq. (10) again are expressed in terms of the column coefficients and the pressure of the binary gas mixture as

$$a=(HL/K_c)p^2 \quad \text{and} \quad b=(K_d/K_c)p^4.$$

Further, since $(1+K_p/K_c)=K_d/b'K_c$, we have

$$H=a'K_d/b'L=K_d/LC, \tag{12}$$

where $C=b'/a'$ is given by the straight line expressing eq. (11) for $p^2/\ln q_c$ against p^4, demanded by the FJO column theory.[9]

The possible values of H, K_c and K_d can be obtained by the following equations:

i) Maxwell's[8] model of binary interaction (α_T being assumed to be temperature-independent and $n=1$, for Maxwellian molecules),

$$H=\frac{2\pi}{6!}\left(\frac{\alpha_T\rho^2 g}{\eta}\right)_1 \frac{1}{2}(r_c+r_h)(r_c-r_h)^3(2u)^2h',$$

$$K_c=\frac{2\pi}{9!}(\rho^3g^2/\eta^2D)_1 \frac{1}{2}(r_c+r_h)(r_c-r_h)^7(2u)^2k_c',$$

$$K_d=2\pi(\rho D)_1 \frac{1}{2}(r_c+r_h)(r_c-r_h)k_d',$$

ii) Slieker's[3] model-independent method,

$$C_1=H=[SF]_1 r_c^4\left(\frac{\rho^2 g\alpha_T}{\eta}\right)_1\left(\frac{\Delta T}{\bar{T}}\right)^2,$$

$$C_2=K_d=\pi(1-a^2)r_c^2(\rho D)_1,$$

$$C_3=K_c=[SF]_3 r_c^8(\rho^3g^2/\eta^2D)_1\left(\frac{\Delta T}{\bar{T}}\right)^2,$$

iii) Lennard-Jones' molecular model of binary interaction,

$$H=\frac{2\pi}{6!}\left(\frac{\alpha_T\rho^2 g}{\eta}\right)_1 r_c^4 h,$$

$$K_c=\frac{2\pi}{9!}(\rho^3g^2/\eta^2D)_1 r_c^8 k_c,$$

$$K_d=2\pi(\rho D)_1 r_c^2 k_d.$$

The dimensionless quantities h', k_c' and k_d', $[SF]_1$, $[SF]_3$ and $\pi(1-a^2)$ and h, k_c, and k_d, called the column shape factors due to Maxwell, Slieker and Lennard-Jones, respectively, are presented in Table II; the factors in (ii) are free from a molecular interaction model; $u=(T_h-T_c)/(T_h+T_c)$, $a=r_h/r_c$ and $\Delta T=T_h-T_c$. The experimental α_T's of He^4–Ar^{40}, Ne^{20}–Xe^{132} and Ne^{20}–Ne^{22} can thus be evaluated by three methods, the former two at the mean temperature $\bar{T}=(T_h+T_c)/2$ and the last one using $L-J$ model at the cold wall temperature T_c of the column. Equation (12) is usually employed to calculate the experimental α_T's, in terms of H, K_d, L and the experimentally observed intercept $C(=b'/a')$ for a given experimental temperature by the existing three methods. The experimental values, thus obtained, are presented in Table I and shown graphically in Figs. 4 and 5 for comparison with the experimental α_T's due to our method and the theoretical α_T's also.

Now, the parameters a' and b' in eq. (11) influence the manner of variation of $\ln q_c$ for any binary gas mixture with the pressure at any experimental temperature. The graph of $\ln q_c$ against the pressure for He^4–Ar^{40} and Ne^{20}–Xe^{132} mixtures are shown in Figs. 2 and 3, respectively, at different compositions of the lighter components, along with that for Ne^{20}–Ne^{22} isotopic mixture. As in most cases of experimental observation, Figs. 2 and 3 show that, as the pressure increases, $\ln q_c$ increases for a given composition of the binary mixtures mentioned above and becomes maximum at the pressure $p=(b')^{1/4}$, where $\partial \ln q_c/\partial p=0$. From eq. (11) the value of $\ln q_c$ at the point of maximum is

$$\ln q_{max} = a'/2 \cdot b'. \quad (13)$$

The reliable value of $\ln q_{max}$ of the inert gas mixture of a certain composition and at a given temperature can thus be measured from eq. (13), in terms of the experimental parameters a' and b' which are obtained by fitting the experimental data of $\ln q_e$ and pressure p in atmosphere. Using eqs. (2) and (13) with the knowledge of the value of the column calibration factor, the TD factors α_T of the inert gas mixtures at different concentrations of the lighter components are then estimated, and shown in Table I and in Figs. 4 and 5.

§3. Theoretical Formulations

The theoretical α_T's can be calculated from

$$\alpha_T = \frac{1}{6[\lambda_{ij}]_1} \frac{S^{(i)}x_i - S^{(j)}x_j}{[X_\lambda + Y_\lambda]} (6C^*_{ij} - 5), \quad (14)$$

where the symbols are defined by Chapman and Enskog.[11,2] Here, $(6C^*_{ij}-5)$ depends strongly on the temperature alone, and the other factor in eq. (14) is not only a function of the temperature but also a complicated function of the compositions and the thermal conductivities of gases and gas mixtures. The α_T's thus computed from eq. (14) are presented in the last column of Table I, and shown graphically in Figs. 4 and 5, respectively, for the gas mixtures He^4–Ar^{40} and Ne^{20}–Xe^{132}. A sample calculation was also made from

$$\alpha_{ij} = \frac{(6C^*_{ij}-5)\mu_{ij}}{5nk[D_{ij}]_1} \left(\frac{\lambda^\infty_{j\,trans}}{x_j m_j} - \frac{\lambda^\infty_{i\,trans}}{x_i m_i} \right), \quad (15)$$

as deduced by Monchik, Munn and Mason[12] by assuming elastic collisions between the molecules; and the results obtained are found to be much higher than those computed from eq. (14).

§4. Results and Discussions

The Chapman-Enskog kinetic theory of gases[11] is strictly applicable only to spherically symmetric molecules like noble gases, and give a good account of the viscosity, diffusion and heat conductivity of gases so excellently that it has often been used with fair success to interprete the experimental thermal diffusion factors of isotopic mixtures of noble gases.[10] But it has been found that for binary mixtures of spherically symmetric molecules the theory is quite unable to explain the composition dependence and probably the temperature dependence of the experimental thermal diffusion factors α_T for mixtures of different noble gases. We computed the theoretical α_T's from eq. (14) with the available force parameters as presented in Table II, for the mixtures He^4–Ar^{40} and Ne^{20}–Xe^{132}; the data thus obtained are shown in Table I and in Figs. 4 and 5, only to see that they do not tally with the experimental ones computed by the present as well as the existing methods. The theoretical α_T's are found to be two-order higher in magnitude than the experimental α_T's estimated, while in the case of Ne^{20}–Ne^{22} isotopic mixture the theoretical α_T's agree fairly well with the experimental ones as shown in Table I. This is the reason why most of the authors, in this field of research, conclude that the FJO column theory is successful in predicting both the temperature and the composition dependence of the experimental α_T's for isotopic mixtures as they are reproduced by the theoretical α_T's as computed by the Chapman-Enskog theory of monatomic gases.

In the column theory, to estimate the experimental α_T's for binary mistures, molecular models such as Maxwell's inverse fifth power and Lennard-Jones' 12:6 potential model are commonly used. The method based on Lennard-Jones' potential model is applicable to evaluating α_T at the cold wall temperature T_c of the column. The column shape factors and other molecular transport parameters also are required to be determined at the cold wall temperature. As evident from Table I, the α_T values for He^4–Ar^{40} mixture due to the $L-J$ molecular model shape factor as shown in Table II, are very low compared with our α_T's from the column calibration factor (F_s) method as well as with those due to Maxwell's moelcular model and Slieker's model-independent method. For He^4–Ar^{40} mixture, as the percentage of the lighter component, say He^4, increases, the experimental α_T's decrease gradually, attain the minimum values, and then increase again as shown in Fig. 4. This sort of behaviour of the composition de-

pendence of α_T for He^4–Ar^{40} could not be at all explained by the elastic theoretical α_T's obtained from the Chapman-Enskog kinetic theory of monatomic gases. The magnitudes of the values are found to be two-order higher than all the experimental α_T's as observed in Table I. The similar situation occurs in the case of Ne^{20}–Xe^{132} mixture; the theoretical α_T's here also could not explain the composition dependence of the experimental α_T's , which are also two-order less in magnitude than the theoretical ones, as observed from Table I and Fig. 5.

It is interesting to note that our experimental α_T's due to the column calibration factor method, which is simple, straightforward and free from any binary molecular interaction model, is very close to those due to Slieker's method as well as the method using Maxwell's model, so far as the trends of variation of the α_T's with mole fraction and their magnitudes are concerned. The existing method using $L-J$ model yields α_T's of less magnitude for He^4–Ar^{40} mixture but, in the case of Ne^{20}–Xe^{132}, gives α_T's of about the same magnitudes as the α_T's due to Slieker's and our method.

Thus it is concluded that the present method, with the use of the column calibration factor F_s and the experimental ln q_{max} as obtained from the experimental parameters a' and b', is not only applicable to isotopic gas mixtures, like the existing methods based on molecular models and Slieker's method, but is also a universal method to estimate the experimental α_T's of polyatomic gas mixtures. The temperature as well as the composition dependence of the actual and relatively small α_T of any binary gas mixture can thus be estimated by our present method. This study finally establishes that the column calibration factor F_s plays a significant role in column measurements. Thus it is wise to study a large number of columns of different r_c, r_h and L and to explore the functional relationship of F_s to r_c, r_h, L and $\bar{T}$, by choosing the interesting gas pairs forming binary mixtures, so that we can arrive at the unique formulation of the column calibration factor for a given column.

Acknowledgement

The authors convey their thanks to Sri Arindam Mukherjee for his help in this work.

References

1) K. Clusius and G. Dickel: Naturwiss. **26** (1938) 546.
2) J. O. Hirschfelder, C. F. Curtiss and R. B. Bird: *Molecular Theory of Gases and Liquids* (John Wiley and Sons, N. Y., 1964)
3) C. J. G. Slieker: Z. Naturforsch. **20 a** (1965) 521.
4) S. Acharyya, A. K. Das, P. Acharyya, S. K. Datta and I. L. Saha: J. Phys. Soc. Jpn. **50** (1981) 1603.
5) S. Acharyya, I. L. Saha, P. Acharyya, A. K. Das and S. K. Datta: J. Phys. Soc. Jpn. **51** (1982) 1469.
6) S. Acharyya, I. L. Saha, A. K. Datta and A. K. Chaterjee: J. Phys. Soc. Jpn. **56** (1987) 105.
7) J. M. Saviron, C. M. Santamaria, J. A. Carrion and J. C. Yarza: J. Chem. Phys. **63** (1975) 5318.
8) R. C. Jones and W. H. Furry: Rev. Mod. Phys. **18** (1946) 151.
9) W. H. Furry, R. C. Jones and L. Onsager: Phys. Rev. **55** (1939) 1083.
10) W. M. Rutherford and K. J. Kaminski: J. Chem. Phys. **47** (1967) 5427.
11) S. Chapman and T. G. Cowling: *The Mathematical Theory of Nonuniform Gases* (Cambridge University Press, N. Y., 1952).
12) L. Monchick, R. J. Munn and E. A. Mason: J. Chem. Phys. **45** (1966) 3051.
13) G. Vâsaru: Separation of Isotopes by Thermal Diffusion, ERDA-tr-32 (1975), National Technical Information Service, U. S., Dept. of Commerce, Springfield Virginia 22161.
14) A. K. Datta and S. Acharyya: Communicated for publication to J. Phys. B (Atomic and Molec. Phys.) London.

PRAMANA
— journal of
physics

© Printed in India

Vol. 43, No. 1,
July 1994
pp. 81–89

Thermal diffusion factors of hydrogenic trace mixtures with helium by column calibration factor

G DASGUPTA, A K DATTA and S ACHARYYA
Department of Physics, University College, Raiganj 733 134, India

MS received 20 July 1993; revised 11 March 1994

Abstract. Using column calibration factor (CCF) F_s for a given column, the temperature dependence of experimental thermal diffusion factors α_T of hydrogenic trace mixtures in helium are accurately determined. This study, however, observes the inelastic collision effect in these trace mixtures when α_T by our CCF method are compared with those by the existing methods and theoretical ones respectively.

Keywords. Column calibration factor; thermal diffusion factor; thermal diffusion column; inelastic and elastic collisions.

PACS No. 44·90

1. Introduction

In the existing column theory as developed by Furry and others [1–3] the column geometry plays an important role in determining the exact value of thermal diffusion factor α_T of a binary gas mixture. The column as such cannot yield the actual α_T values both in trend and in magnitude with respect to temperature and composition as the binary molecular interactions are often called into play. Thermal diffusion column is still far superior to any other α_T measuring instruments as the equilibrium separation factor q_e defined by

$$q_e = \frac{(\chi_i/\chi_j)_{\text{top}}}{(\chi_i/\chi_j)_{\text{bot}}}$$

is very large even in the case of small mass difference between the components of a mixture. Here, χ_i and χ_j are the mass fractions of the lighter and the heavier components respectively. Hence for a binary mixture of almost identical masses, shapes and sizes a calibrated TD column can safely be used to measure a reliable relative and small α_T values. For this reason we have calibrated the given column of Slieker and de Vries [4] with known and reliable α_T of He – T_2 mixture to arrive at the column calibration factor (CCF) F_s from the relation:

$$\ln q_{\max} = \alpha_T F_s(r_c, r_h, L, \bar{T}) \tag{1}$$

where $\bar{T}$ is the mean temperature of T_h and T_c, T_h and T_c being the hot and cold wall temperatures in K. r_c and r_h are the radii of cold and hot wall of a column of geometrical length L. F_s is supposed to be an independent molecular model solely dependent on the column geometry at any mean temperature $\bar{T}$ in K.

A number of studies by Acharyya *et al* [5–7] and Navarro *et al* [8] on F_s enabled us to study the temperature dependence of α_T of DT and HT in helium only to explore the fact that the TD column is a reliable relative α_T measuring instrument and to observe the inelastic collision effects in them. In this study, we estimate the experimental parameters a' and b' governing the very nature of variation of the available experimental $\ln q_e$ against pressure p of He–DT and He–HT gas mixtures [4], the hydrogenic components were never becoming larger than 5% in helium at three experimental temperatures.

The computed data of $\ln q_e$ of He–DT and He–HT against pressure in atmosphere are shown in figures 1 and 2 respectively to ensure that the least square fitted curves agree excellently with the experimental ones. For He–HT an interesting feature is that unlike the usual behaviour, $\ln q_e$ becomes smaller with temperatures, not noticed earlier [7].

The hydrodynamical part of the column theory is excellently obeyed by He–DT and for some selected experimental points of He–HT as their $p^2/\ln q_e$ against p^4 were found out to be

$$p^2/\ln q_e = 0{\cdot}7758 + 0{\cdot}8161\ p^4 \text{ at } 338\text{ K.}$$
$$= 0{\cdot}4938 + 0{\cdot}7294\ p^4 \text{ at } 378\text{ K}$$
$$= 0{\cdot}3964 + 0{\cdot}6024\ p^4 \text{ at } 423\text{ K}$$

and

$$p^2/\ln q_e = 9{\cdot}0749 + 14{\cdot}8368\ p^4 \text{ at } 338\text{ K}$$
$$= 13{\cdot}5999 + 64{\cdot}6412\ p^4 \text{ at } 378\text{ K}$$
$$= 14{\cdot}6461 + 411{\cdot}5226\ p^4 \text{ at } 423\text{ K respectively.}$$

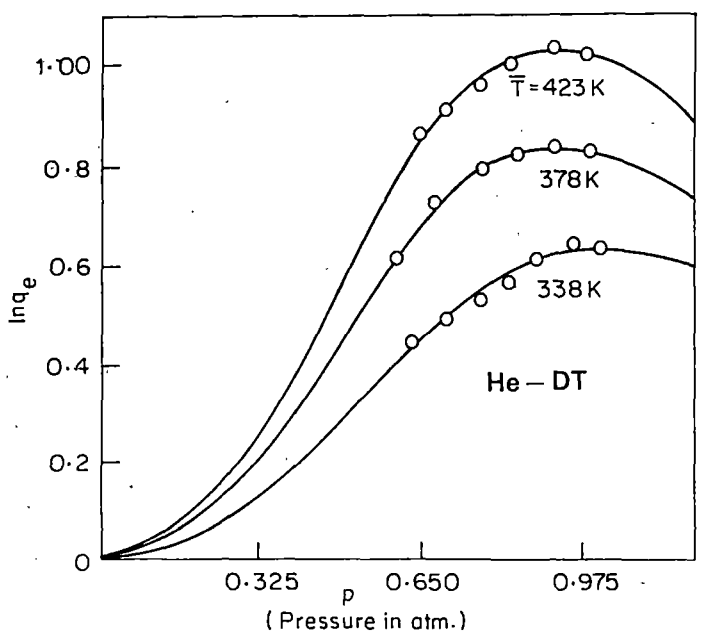

Figure 1. $\ln q_e$ against pressure p in atmosphere for He–DT trace mixture, at $\bar{T}$= 338, 378 and 423 K, 'O' experimental points.

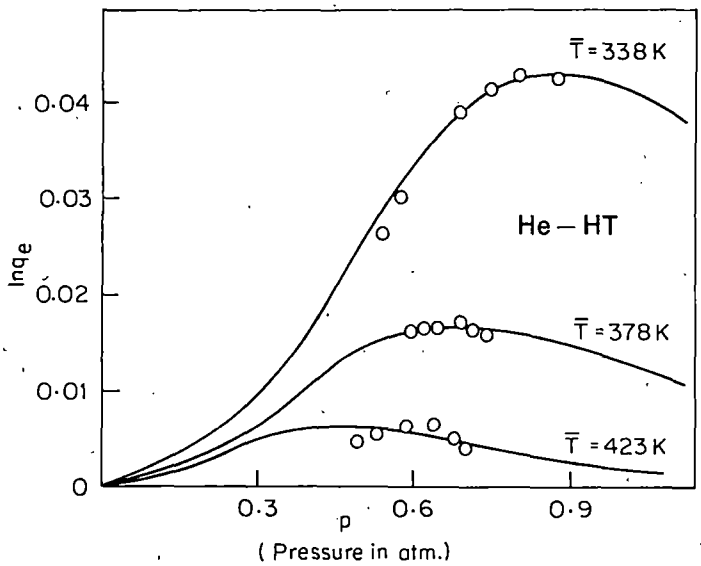

Figure 2. $\ln q_e$ against pressure p in atmosphere for He–HT trace mixture at $\bar{T} = 338$, 378 and 423 K, 'O' experimental points.

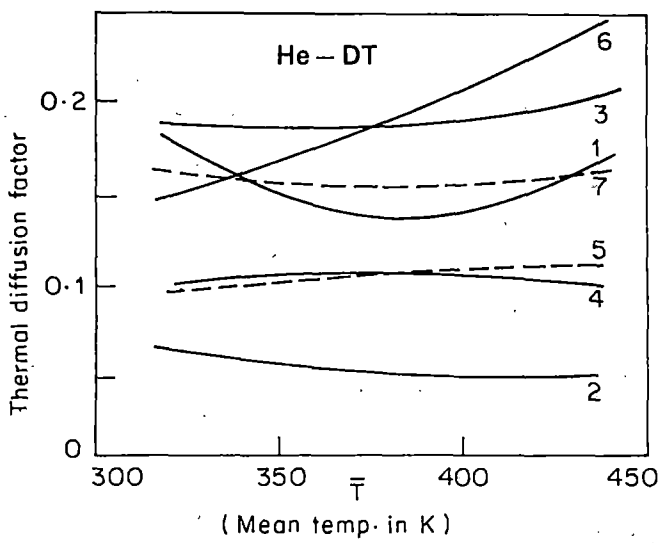

Figure 3. Variation of α_T with $\bar{T}$ of He–DT trace mixture, 1. Our expt α_T from $\ln q_{max}$ and F_s; 2. Expt α_T(Maxwell case); 3. Expt α_T(Slieker case); 4. Theor α_T(elastic) from Eq (7); 5. Theor α_T(inelastic) with $Z_{rot} = 300$ from Eq (7); 6. Theor α_T(inelastic) with Z_{rot} calculated from Barua *et al* (1970) from Eq (8); 7. Theor α_T(inelastic) with Z_{rot} calculated from Parkers [12] formula with adjustable $Z^a_{rot} = 7{\cdot}08$ [13].

In the absence of any reliable possibility to estimate the actual experimental α_T of a mixture through the use of molecular model we used the values of F_s already obtained for the column [7]:

$$F_s = -66{\cdot}52202 + 0{\cdot}3502286\,\bar{T} - 4{\cdot}1879 \times 10^{-4}\,\bar{T}^2.$$

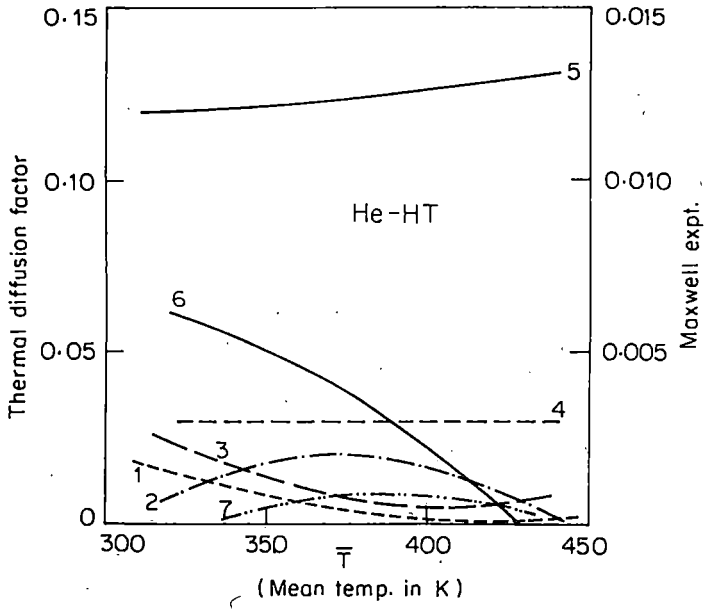

Figure 4. Variation of α_T with $\bar{T}$ of He–HT trace mixture
1. Our expt α_T from $\ln q_{max}$ and F_s; 2. Expt α_T(Maxwell); 3. Expt α_T(Slieker); 4. Theor α_T(elastic) from Eq (7); 5. Theor α_T(inelastic) with $Z_{rot} = 300$ from Eq (8); 6. Theor α_T(inelastic) with Z_{rot} calculated from Barua *et al* [12] from Eq (8); 7. Theor α_T(inelastic) with Z_{rot} calculated from Parker [13] formula with adjustable $Z^{\alpha}_{rot} = 12{\cdot}15$.

Now α_T's of He–DT and He–HT were obtained from (1) and compared with those by the existing methods using column theory as well as the theoretical α_T's based on elastic and inelastic [9] collisions in figures 3 and 4 respectively in order to reveal the existence of inelastic collisions in these mixtures.

2. Theoretical formulation to estimate experimental α_T

Both ends being closed for the ideal column of length L, $\ln q_e$ of a gas mixture at any mean temperature $\bar{T}$ is given by

$$\ln q_e = \frac{HL}{K_c + K_d} \tag{2}$$

where H, K_c and K_d are the functions of transport coefficients of a gas mixture and proportional to p^2, p^4 and p^0 respectively, p being pressure in atmosphere.

In order to remove parasitic remixing effect, Furry and Jones [2] simply added a term K_p proportional to p^4 to the denominator when (2) becomes

$$\ln q_e = \frac{a' p^2}{b' + p^4} \tag{3}$$

which is also written as

$$p^2/\ln q_e = b'/a' + (1/a')p^4 \tag{4}$$

a' and b' are however related by

$$(HL/K_c)p^2 = a'(1 + K_p/K_c) \text{ and } (K_d/K_c)p^4 = b'(1 + K_p/K_c)$$

H, K_c, K_d are the functions of the transport coefficient of a mixture and K_p is the remixing coefficient.

Again if c represents the intercept of the straight line of (4) we have

$$H = (K_d/Lc) \tag{5}$$

the exact expressions for H, K_c and K_d are given in our previous publications [5–7].

The estimation of the experimental α_T through the existing formulations involved the shape factors taking account of the inherent asymmetry of the column geometry. The mass density ρ, the viscosity coefficient η and the diffusion coefficient D were calculated from MTGL of Hirschfelder *et al* [10], the column shape factors and the force parameters required had already been reported earlier [7].

It is observed in figures 1–2 that as the pressure increases $\ln q_e$ increases and becomes maximum when $p = (b')^{1/4}$ for which $(\delta \ln q_e/\delta p) = 0$.

We then have from (3)

$$\ln q_{max} = (a'/2\sqrt{b'}) \tag{6}$$

It is also observed in He–HT, unlike He–DT, that some experimental data of $\ln q_e$ are not in fit with the hydrodynamical part of the column theory as they have tendency to yield the negative intercept of $p^2/\ln q_e$ against p^4 which is absurd unless inversion of α_T would take place. Hence we are bound to select some six or seven data from the reported graph to fix the values of $\ln q_{max}$ from the (6).

Table 1 and the graphs of figures 1–2, revealed that $\ln q_{max}$ from (6) in terms of a' and b' are in good agreement with the graphically determined values earlier [7]. This establishes the fact that our choice of the $\ln q_e$ data with pressure particularly for the He–HT mixture where the mass difference between the components is practically nil, is almost right.

3. Theoretical formulations to calculate α_T

Theoretical α_T can, however, be estimated from

$$\alpha_T = \frac{1}{6[\lambda_{ij}]_1} \frac{S^{(i)}\chi_i - S^{(j)}\chi_j}{[X_\lambda + Y_\lambda]} (6C^*_{ij} - 5) \tag{7}$$

where $(6C^*_{ij} - 5)$ depends mainly on the temperature while the other factors involved in (7) are the complicated functions of composition, masses and thermal conductivities of gases and gas mixtures. The α_T, calculated from (7), is presented in the 12th column of table 1, and shown graphically in figures 3–4 for He–DT and He–HT respectively.

Table 1. Experimental and Theoretical α_T values of binary gas mixtures with temperature.

System	Hot wall temp T_h in K	Cold wall T_c in K	Mean Temp $\bar{T}$ in K	a' in $(atm)^2$	b' in $(atm)^4$	In q_{max} computed from Eq (5)	Expt F_s Ref (6)	Expt α_T with: Our calibration factor method Eq. (1)	Maxwell shape factor	Slieker shape factor	Theor. α_T from Eq (6) elastic theor. method	Theoretical α_T from Eq (7) with Z_{rot}: 300	Barua *et al*	Parker
He–HT	393	283	338	0·0674	0·6116	0·0431	4·001	0·0107	0·0014	0·0017	0·030	0·121	0·055	0·002
	473	283	378	0·0155	0·2104	0·0169	6·026	0·0020	0·0028	0·0007	0·030	0·124	0·037	0·009
	563	283	423	0·0024	0·3559	0·0064	6·691	0·0009	0·0010	0·0006	0·030	0·129	0·005	0·005
He–DT	393	283	338	1·289	1·0519	0·6284	4·001	0·1567	0·060	0·186	0·105	0·100	0·158	0·158
	473	283	378	1·371	0·6670	0·8331	6·026	0·1382	0·054	0·187	0·104	0·105	0·188	0·154
	563	283	423	1·660	0·6580	1·0232	6·691	0·1529	0·050	0·194	0·103	0·109	0·226	0·159

Thermal diffusion factors

The inelastic thermal diffusion factor α_{ij} is given by according to Monchick *et al* [11]

$$\alpha_T = \frac{(6C_{ij}^* - 5)\mu_{ij}}{5nk[D_{ij}]_1}\left(\frac{\lambda^a_{j\,\text{trans}}}{\chi_j m_j} - \frac{\lambda^a_{i\,\text{trans}}}{\chi_i m_i}\right) + \frac{1}{5nk[D_{ij}]_1}$$
$$\left[\frac{(6\tilde{C}_{ji} - 5)\lambda^a_{j\,\text{int}}}{\chi_j} - \frac{(6\tilde{C}_{ij} - 5)\lambda^a_{i\,\text{int}}}{\chi_i}\right] \tag{8}$$

where the symbols have their usual meanings only the collision integral ratio $\tilde{C}_{ij}$ differs from C^*_{ij}. In fact $\tilde{C}_{ij}$ is not symmetric with respect to the interchange of the indices i and j and is very sensitive to inelastic collision.

For a pure gas the exact values of $\lambda^a_{j\,\text{trans}}$ and $\lambda^a_{i\,\text{trans}}$ is given by

$$\lambda_{i\,\text{trans}} = \frac{\eta}{M}\left[\left(\frac{5}{2}C_{v\,\text{trans}} + \frac{\rho D_{\text{int}}}{\eta}C_{\text{int}}\right) - \left(\frac{2}{\pi}\frac{C_{i\,\text{int}}}{Z_{\text{rot}}}\right)\left(\frac{5}{2} - \frac{\rho D_{\text{int}}}{\eta}\right)^2\right.$$
$$\left.\left\{1 + \frac{2}{\pi Z_{\text{rot}}}\left(\frac{5}{3}\frac{C_{\text{int}}}{R} + \frac{\rho D_{\text{int}}}{\eta}\right)\right\}^{-1}\right]. \tag{9}$$

Here $C_{v\,\text{trans}} = 3R/2$, the constant value of translational heat capacity, Z_{rot} is the rotational translational collision number for inelastic collision.

The nonspherical terms of (8) we used Hirchfelder–Euken expression [10] to calculate the thermal conductivity $\lambda^a_{i\,\text{int}}$ from

$$\lambda^a_{i\,\text{int}} = \frac{n[D_{ii}]_1 C_{\text{int}}}{1 + (\chi_j/\chi_i)(D_{ii}/D_{ij})_1} \tag{10}$$

Theoretical inelastic α_T's for He–DT and He–HT thus calculated from (8) with the help of (9) and (10) are shown in table 1 and also in figures 3–4 respectively for comparison with other experimental α_T values.

4. Results and discussion

The inherent asymmetry in the column geometry is however, taken into account by Maxwell, Slieker and Lennard–Jones dimensionless shape factors [7]. We calculated the experimental α_T's of He–HT and He–DT trace mixtures at $T = 338$, 378 and 423 K respectively from (5) using those shape factors. Slieker's case does not involve any molecular model and it gives rather a rough estimation of the experimental α_T while the former includes inverse fifth power potential. As the cold wall temperature T_c was held fixed experimental α_T due to L–J case cannot be applicable here. The α_T thus obtained due to Maxwell and Slieker cases is presented in table 1 and shown graphically by the curves 2 and 3 respectively of figures 3 and 4.

The experimental α_T from (1) as obtained in terms of $\ln q_{\max}$ of (6) and F_s is shown by curve 1 in figures 3 and 4. When they are compared with those due to Maxwell (curve 2) and Slieker (curve 3) it is found that so far as the trend is concerned the data due to Slieker agree better than those due to Maxwell's shape factors. This is perhaps due to the fact that both Slieker and our method are free from any binary molecular model. As the mass difference between the components of a binary mixture decreases as in the case of He–HT the agreement is more close.

The theoretical α_T based on elastic collision theory, (7), as shown by curve 4 in

figures 3–4 appears to be temperature independent. Unlike He–HT, He–DT however show slightly lower value at higher temperature. The inelastic α_T as calculated from (8) with $Z_{rot} = 300$, show its positive temperature dependence as represented by curve 5 in figures 3–4.

When α_{ij} were calculated with the available rotational translational collision number of Barua *et al* [12] an interesting feature is that the curve 6 of figures 3–4 coincide with α_T's of our CCF method. This fact prompted us to adjust Z_{rot} from Parker's formula [13]. Using $Z_{rot} = 2{\cdot}78$, 2·91 and 3·05 for HT and $Z_{rot} = 4{\cdot}78$, 5·01 and 5·23 for DT at 338, 378 and 423 K respectively inelastic α_{ij}'s are then estimated for both He–DT and He–HT trace mixtures and were shown by curve 7 in figures 3–4 respectively for comparison with other α_T's.

With Z_{rot} determined by us inelastic theoretical α_T's curve 7 (15th column of table 1) so far as the magnitude and trend are concerned in the case of He–DT, support our α_T's curve 1 (9th column of table 1) and only in trend with α_T's due to Slieker (11th column of table 1). In the case of He–HT these theoretical α_T's almost coincide with our α_T's, but in trend with the experimental α_T's due to Maxwell.

All these comparison of α_T's so far obtained thus reveal that inelastic collisions play an important role in such trace mixtures. Again the variation of $\ln q_{max}$ against $\bar{T}$ for He–HT is given by

$$\ln q_{max} = 0{\cdot}89879 - 4{\cdot}2097 \times 10^{-3}\,\bar{T} + 4{\cdot}9647 \times 10^{-6}\,\bar{T}^2$$

showing that at $\bar{T} \simeq 429$ K, $\ln q_{max}$ may be zero as shown in figure 5. The isobaric He–HT mixture may yield an interesting phenomenon of inversion of both $\ln q_{max}$ and α_T with respect to temperature like isobaric system N_2–CO as studied in our recent publication of Saha *et al* [14]. The system He–HT deserves a detailed study of measurements of $\ln q_e$ against pressure for its different composition and temperatures.

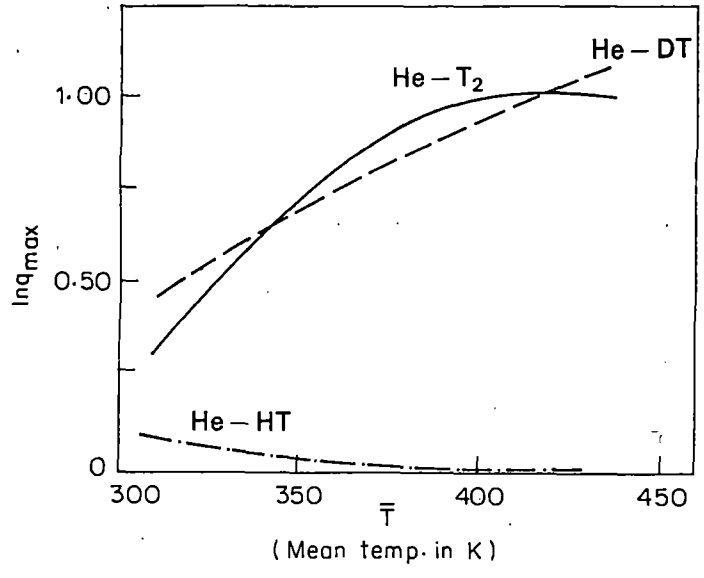

Figure 5. Variation of $\ln q_{max}$ with temperature $\bar{T}$ in K for He–DT He–T_2 and He–HT mixtures.

We are, therefore, now in a position to conclude that CCF is an accurate α_T determining factor of isotopic, nonisotopic and isobaric α_T's of binary gas mixtures. The functional relationship of F_s with r_c, r_h, L and $\bar{T}$ should be studied both from the theoretical and experimental viewpoints.

References

[1] W H Furry, R C Jones and L Onsager, *Phys. Rev.* **55**, 1083 (1939)
[2] W H Furry and R C Jones, *Phys. Rev.* **60**, 459 (1946)
[3] R C Jones and W H Furry, *Rev. Mod. Phys.* **18**, 151 (1946)
[4] C J G Slieker and A E deVries, *J. Chim. Phys.* **60**, 172 (1967)
[5] S Acharyya, A K Das, P Acharyya, S K Datta and I L Saha, *J. Phys. Soc. Jpn.* **50**, 1603 (1981)
[6] S Acharyya, I L Saha, P Acharyya, A K Das and S K Datta, *J. Phys. Soc. Jpn.* **51**, 1469 (1982)
[7] S Acharyya, I L Saha, A K Datta and A K Chatterjee, *J. Phys. Soc. Jpn.* **56**, 105 (1987)
[8] J L Navarro, J A Madariage and J M Saviron, *J. Phys. Soc. Jpn.* **52**, 478 (1983)
[9] T K Chatterjee and S Acharyya, *J. Phys.* **B7**, 2277 (1974)
[10] J O Hirschfelder, C F Curtiss and R B Bird, *Molecular theory of gases and liquids*, (John Wiley, New York, 1964)
[11] L Monchick, S I Sandler and E A Mason, *J. Chem. Phys.* **49**, 1178 (1968)
[12] A K Barua, A Manna, P Mukhopadhyay and A Dasgupta, *J. Phys.* **B3**, 619 (1970)
[13] J G Parker, *Phys. Fluids* **2**, 449 (1959)
[14] I L Saha, A K Datta, A K Chatterjee and S Acharyya, *J. Phys. Soc. Jpn.* **56**, 2381 (1987)

Journal of the Physical Society of Japan
Vol. 65, No. 8, August, 1996, pp. 2506-2513

Estimation of Column Calibration Factor and Force Parameters to Predict Temperature Dependence of Thermal Diffusion Factor of Some Simple Molecules

G. DASGUPTA, N. GHOSH, N. NANDI, A. K. CHATTERJEE and S. ACHARYYA

Department of Physics, Sudarsanpur D.P.U. Vidyachakra, Sudarsanpur, P.O. Raiganj, Dist. Uttar Dinajpur, Pin-733134, India

(Received October 30, 1995)

The column calibration factor (CCF) F_s of a column (Roos and Rutherford 1969) has been accurately estimated to yield the thermal diffusion factor α_T's of Kr^{80}–Kr^{86}, Xe^{129}–Xe^{136}, CO^{28}–CO^{29}, CH_4^{16}–CH_4^{17} and N_2^{28}–N_2^{29} respectively at two different experimental temperatures. The probable temperature dependence of α_T's are used to obtain the force parameters ε_{ij}/k and σ_{ij} of the respective molecules. Again, the α_T's as obtained from $\ln q_{max}$ and F_s are compared with the experimental α_T's by the existing method involved with column shape factors as well as theoretical α_T's based on elastic and inelastic collisions among the molecules. The comparison of the estimated force parameters with the reported ones finally suggests the technique of predicting α_T's as a function of temperature is extremely useful.

KEYWORDS: thermal diffusion factor, elastic and inelastic collisions, column calibration factor

§1. Introduction

The theoretical thermal diffusion factor as derived from Chapman-Enskog gas kinetic theory,[1] based on spherical molecule with spherically symmetric potential field is generally not in good agreement with the experimental α_T's of a binary nonisotopic or even isotopic gas mixture. It is still of special interest, from the technical point of view to enrich rare as well as ordinary isotopes. The close correlation between the theoretical α_T's with the intermolecular forces may conveniently be used as an effective tool to investigate the molecular force parameters ε_{ij}/k and σ_{ij} where ε_{ij} is the depth of the potential well, k is the Boltzmann constant and σ_{ij} is the molecular diameter as the process of thermal diffusion unlike viscosity is a second order effect.

Although, TD column was supposed not to yield the actual α_T values both in trend and in magnitude with respect to temperature and composition of the mixture, still it is far superior to any other α_T measuring instruments like two bulbs and trennschaukel as the equilibrium separation factor q_e defined by; $q_e = (x_i/x_j)_{top}/(x_i/x_j)_{bottom}$ is very large even in the case of isotopic gas mixture where the mass difference between the components i and j is practically very small. x_i and x_j are the mass or mole fractions of the lighter (i) and the heavier (j) molecules respectively. The equilibrium separation factor q_e of any binary gas mixture is usually determined for different compositions of a gas mixture at a fixed temperature $\bar{T}$ or for mixture of fixed composition at different experimental temperatures. With the help of q_e thus measured at different pressures well below and around one atmosphere, α_T of a gas mixture could be ascertained. The existing method to evaluate the experimental α_T from $\ln q_e$ measured in a column at different pressures is usually involved with Maxwell and Lennard-Jones model dependent as well as model independent Slieker column shape factors.

In order to obtain the actual α_T of a binary gas mixture, a large number of workers[2-5] has, however, introduced a scaling factor F_s called the column calibration factor (CCF) for a TD column in the relation:

$$\ln q_{max} = \alpha_T F_s(r_{cold}, r_{hot}, L, \bar{T}) \qquad (1)$$

where r_{cold} and r_{hot} are the cold and hot wall radii of a column of geometrical length L. $\bar{T}$ is the mean temperature of the gas mixture defined by $\bar{T} = \frac{T_{hot}+T_{cold}}{2}$ where T_{hot} and T_{cold} are the hot and cold wall temperatures in K respectively. F_s is supposed to be a molecular model independent parameter and entirely depends on the geometry of a TD column.

Roos and Rutherford[6] had measured the pressure dependence of $\ln q_e$ of Kr^{80}–Kr^{86}, Xe^{129}–Xe^{136}, CO^{28}–CO^{29}, CH_4^{16}–CH_4^{17} and N_2^{28}–N_2^{29} with their natural isotopic abundances at two experimental temperatures in K in a hot wire TD column of L = 487.7 cm, r_{cold} = 0.9525 cm and r_{hot} = 0.0795 cm respectively. The measured $\ln q_e$ at different pressures in atmosphere by Roos and Rutherford[6] were plotted in Figs. 2 and 3 respectively by least square fitted curves with the estimated a' and b' values at two available temperatures. The a' & b' for the third temperature were also obtained and the variation of $\ln q_e$ at that temperature is, however, selected for each of them and shown in Figs. 2 and 3 by dotted curves.

From the known and reliable α_T values[7] as well as experimentally determined $\ln q_{max}$ of Ar^{36}–Ar^{40}, F_s for a column as was derived by Datta and Acharyya[4] was first carried out to yield the temperature dependence of α_T of Kr^{80}–Kr^{86} as

$$\alpha_T = 0.0453 - 11.0479\frac{1}{\bar{T}}. \quad (2)$$

The corresponding α_T's at the required experimental temperatures $\bar{T} = 455.5, 530.5$ and 680.5 K in the column of Roos and Rutherford[6] were then obtained. They are shown in Table I. These values together with the experimentally estimated $\ln q_{max}$ of Kr^{80}–Kr^{86} from the curves of $\ln q_e$ vs p as shown elsewhere[8] at those temperatures were then utilised to arrive at the probable temperature dependence of F_s for a column:[6]

$$F_s = 67.1066 - 0.15809\bar{T} + 3.29153 \times 10^{-4}\bar{T}^2 \quad (3)$$

which is shown graphically in Fig. 1. The values of F_s together with the corresponding experimental $\ln q_{max}$ at any temperature give us α_T's of the different systems from eq. (1). The force parameters ε_{ij}/k and σ_{ij} were estimated from the comparative study of the probable temperature dependence of α_T and C^*_{ij} (12-6 Lennard-Jones potential) with respect to $\frac{1}{\bar{T}}$ and $\frac{1}{\bar{T}^*}$ respectively where $\bar{T}^* = \bar{T}/(\varepsilon_{ij}/k)$. The temperature dependence of α_T could not be predicted with α_T's measured at only two experimental temperatures. Nevertheless, an approximate middle temperature is, however, essential to be selected to reveal the actual variation of α_T's of those systems under consideration with respect to temperature in consistent with the estimation of the actual force parameters among the molecules.

The experimental α_T's for these systems by the existing method, involved with column shape factors due to Maxwell model[9] and Slieker,[10] as presented in Table II, were obtained and shown graphically in Figs. 4–8. The theoretical α_T's based on elastic and inelastic collisions were also computed with the estimated force parameters ε_{ij}/k and σ_{ij} (Table II) and are shown in Figs. 4–8, for comparison with experimental α_T's. The data thus obtained are, however, shown in Table I together with the other essential data. The CCF method together with the technique of simultaneous determination of force parameter is thus found to be successful in predicting the exact, reliable and correct temperature variation of α_T of a binary isotopic mixture.

The curves of α_T's against $\bar{T}$ in Figs. 4–8, however, support the possibility of estimation of binary interactions among the molecules as one obtains those from the viscosity of gases and gas mixtures. The estimation of α_T's by the present CCF method are found to be in close agreement so far trends are concerned, as observed

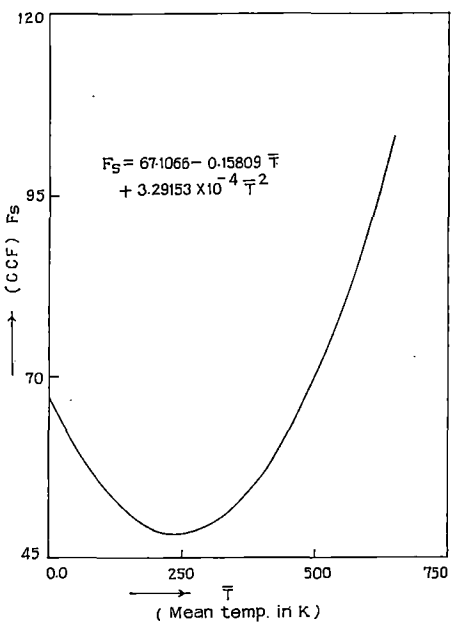

Fig. 1. Variation of column calibration factor F_s (CCF) against temperature in K.

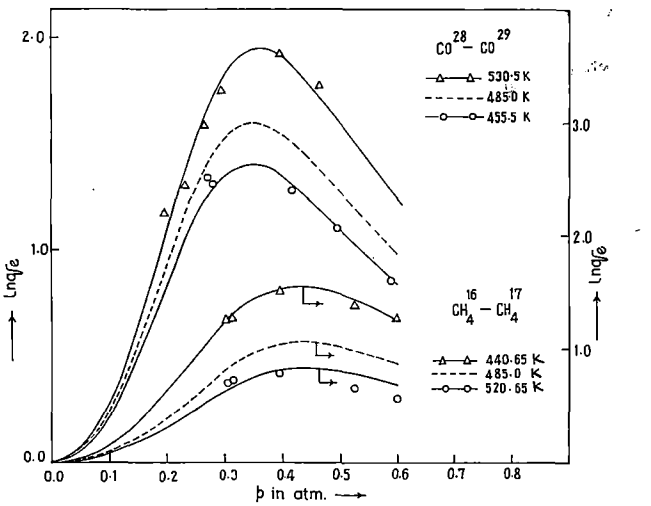

Fig. 2. Variation of $\ln q_e$ against pressure p in atmosphere. -△-△- Experimental $\ln q_e$ at $\bar{T}$=530.5 K for CO^{28}–CO^{29}. ----- Predicted $\ln q_e$ at $\bar{T}$=485 K for CO^{28}–CO^{29}. -o-o- Experimental $\ln q_e$ at $\bar{T}$=455.5 K for CO^{28}–CO^{29}. -△-△- Experimental $\ln q_e$ at $\bar{T}$=520.65 K for CH_4^{16}–CH_4^{17}. ----- Predicted $\ln q_e$ at $\bar{T}$=485 K for CH_4^{16}–CH_4^{17}. -o-o- Experimental $\ln q_e$ at $\bar{T}$=440.65 K for CH_4^{16}–CH_4^{17}.

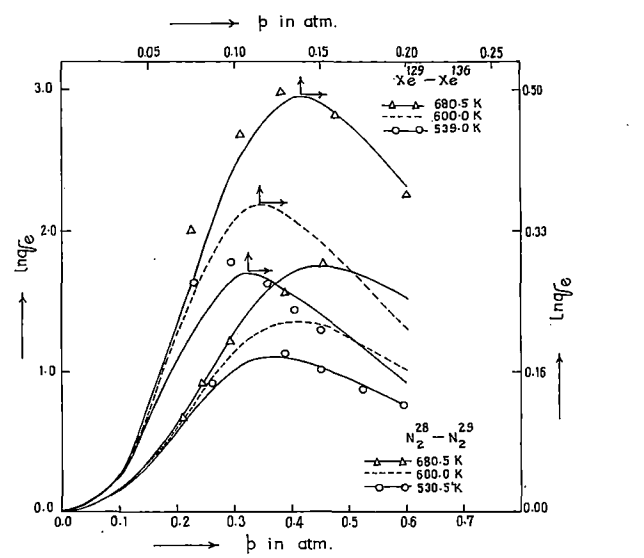

Fig. 3. Variation of $\ln q_e$ against pressure p in atmosphere. -△-△- Experimental $\ln q_e$ at $\bar{T}$=680.5 K for Xe^{129}–Xe^{136}. ----- Predicted $\ln q_e$ at $\bar{T}$=600.0 K for Xe^{129}–Xe^{136}. -o-o- Experimental $\ln q_e$ at $\bar{T}$=539.0 K for Xe^{129}–Xe^{136}. -△-△- Experimental $\ln q_e$ at $\bar{T}$=680.5 K for N_2^{28}–N_2^{29} ----- Predected $\ln q_e$ at $\bar{T}$=600.0 K for N_2^{28}–N_2^{29} -o-o- Experimental $\ln q_e$ at $\bar{T}$=530.5 K for N_2^{28}–N_2^{29}.

in Figs. 4–8, with the theoretical ones in terms of the estimated force parameters (Table II). Thus the methodology so far extended is really a simple, straightforward and unique one.

§2. Mathematical Formulation to Estimate the Experimental α_T

Both ends being closed for an ideal column of length L of a gas mixture at any temperature $\bar{T}$ is given by[11]

$$\ln q_e = \frac{HL}{K_c + K_d} \tag{4}$$

where H, K_c and K_d are the functions of transport coefficients of a gas mixture. They are proportional to p^2, p^4 and p^0 respectively, p being pressure in atmosphere. In order to remove parasitic remixing effect, Furry and Jones[11] simply added a term K_p called remixing coefficient, being proportional to p^4 to the denominator of eq. (4). Hence eq. (4) finally becomes

$$\ln q_e = \frac{a'p^2}{b' + p^4} \tag{5}$$

or,

$$p^2/\ln q_e = \frac{b'}{a'} + \frac{1}{a'}p^4 \tag{6}$$

a' and b' are, however, related by

$$\frac{HL}{K_c} \cdot p^2 = a'\left(1 + \frac{K_p}{K_c}\right)$$

and

$$\frac{K_d}{K_c} \cdot p^4 = b'\left(1 + \frac{K_p}{K_c}\right).$$

Table I. Experimental and theoretical thermal diffusion factors α_T of binary isotopic mixtures of simple gases with temperatures in K.

Column used	System	Hot wall Temp. (T_{hot}) in K	Cold wall Temp. (T_{cold}) in K	Mean Temp. in K $\bar{T}=\frac{T_{hot}+T_{cold}}{2}$	a' $(atm)^2$	b' $(atm)^4$	Computed $\ln q_{max}$ from eq. (15)	Column Calibration factor F_s (CCF)
L=Length of the column =487.7 cm	Kr	623	288	455.5	0.0622	0.00055	1.333	63.586
		773	288	530.5	0.1007	0.00074	1.855	75.869
		1073	288	680.5	0.2464	0.00143	3.252	111.94
	Xe	790	288	539	0.0066	0.00014	0.280	77.562
		912	288	600	0.0099	0.00019	0.362	90.748
		1073	288	680.5	0.0187	0.00036	0.492	111.94
Hot wall radius $r_{hot} = 0.0795$ cm	CO	623	288	455.5	0.3336	0.0142	1.398	63.586
		682	288	485	0.3919	0.0149	1.603	67.858
		773	288	530.5	0.5028	0.0166	1.951	75.869
Cold wall radius $r_{cold} = 0.9525$ cm	CH_4	593.15	288.15	440.65	0.3414	0.0376	0.886	61.357
		682.00	288.00	485.00	0.4768	0.0361	1.255	65.858
		753.15	288.15	520.65	0.6059	0.0340	1.643	74.023
	N_2	773	288	530.5	0.3156	0.0201	1.115	75.869
		912	288	600	0.4423	0.0265	1.360	90.748
		1073	288	680.5	0.7311	0.0437	1.707	111.94

Column used	System	Estimated α_T using			Computed theoretical α_T	
		Present method	Maxwell shape factor	Slieker shape factor	Elastic	Inelastic
L=Length of the column =487.7 cm	Kr	0.0210	0.0134	0.0146	0.0107	
		0.0245	0.0165	0.0184	0.0127	
		0.0291	0.0252	0.0290	0.0150	
	Xe	0.0036	0.0010	0.0018	0.0087	
		0.0040	0.0018	0.0021	0.0096	
		0.0044	0.0022	0.0025	0.0102	
Hot wall radius $r_{hot} = 0.0795$ cm	CO	0.0221	0.0100	0.0113	0.0052	0.2861
		0.0236	0.0107	0.0117	0.0057	0.3104
		0.0257	0.0114	0.0127	0.0061	0.3334
Cold wall radius $r_{cold} = 0.9525$ cm	CH_4	0.0144	0.0070	0.0076	0.0036	0.0230
		0.0191	0.0086	0.0095	0.0046	0.0296
		0.0222	0.0099	0.0110	0.0054	0.0342
	N_2	0.0147	0.0065	0.0073	0.0090	0.4010
		0.0150	0.0069	0.0078	0.0094	0.4081
		0.0153	0.0077	0.0088	0.0102	0.4148

The constants a' and b' were, however, estimated by fitting eq. (6) with the experimentally observed $\ln q_e$ at different pressures in atmosphere. Both a' and b' are now the experimental parameters to govern the variation of $\ln q_e$ against pressure as shown graphically in Figs. 2 and 3 for CO^{28}–CO^{29}, CH_4^{16}–CH_4^{17}, Xe^{129}–Xe^{136} and N_2^{28}–N_2^{29} respectively with the experimental data[6,8] placed on them at two available temperatures. The third temperature would then be selected from the plot of $\alpha_T = A + B/\bar{T}$ with the measured α_T's at two temperatures.

In each case as observed in Figs. 2 and 3, $\ln q_e$ increases gradually with pressure and assumes maximum value $\ln q_{max}$ at a pressure $p = (b')^{\frac{1}{4}}$ for which $\frac{\partial}{\partial p}(\ln q_e) = 0$. Hence from eq. (5) we have

$$\ln q_{max} = \frac{a'}{2\sqrt{b'}}. \tag{7}$$

Now a' and b', in Table I, help us fix the values of $\ln q_{max}$ from eq. (7) and hence the experimental α_T's for the above mentioned systems could, however, be determined from eq. (1) with F_s. To use the existing method with Maxwell and Slieker column shape factors eq. (4) also becomes.

$$\ln q_{max} = \frac{HL}{2\sqrt{k_c k_d}} \tag{8}$$

when $\frac{\partial}{\partial p}(\ln q_e) = 0$. The final expressions of the experimental α_T's in terms of the column shape factors are finally given by:

$$\alpha_T = 2.39 \times \frac{r_{cold} - r_{hot}}{L} \times \frac{\bar{T}}{\Delta T} \ln q_{max} \cdot \frac{\sqrt{k_c' k_d'}}{h'} \tag{9}$$

and

$$\alpha_T = 2.00 \times \frac{r_{cold}}{L} \cdot \frac{\bar{T}}{\Delta T} \ln q_{max} \frac{\{\pi(1-a^2)[S \cdot F]_3\}^{\frac{1}{2}}}{[S \cdot F]_1} \tag{10}$$

respectively, where the symbols used are of usual significance as mentioned elsewhere.[9,10] The column shape factors which are supposed to take into account the inherent asymmetry of the column geometry are presented in Table II. The computed α_T's with Maxwell and Slieker column shape factors (Table II) are placed in Table I and shown graphically in Figs. 4–8 by curve No. 2 and 3 respectively in order to compare with those by the present CCF and theoretical ones.

§3. Derivation of Force Parameters

The principal contribution[12] to the temperature dependence of $\alpha_{T\ theor}$ comes from the factor $(6C_{ij}^* - 5)$ of Chapman-Enskog expression[1] where

$$\alpha_{T\ theor} = g(6C_{ij}^* - 5). \tag{11}$$

The term $(6C_{ij}^* - 5)$ contains only unlike interactions among the molecules. The other part i.e., 'g' depends on the composition of the gas mixture. Although, 'g' depends slowly on temperature it can be taken fairly constant for a short range of temperature and for a fixed composition of the gas mixture as in the case of the present investigation. It is also seen that[13]

$$\alpha_{T\ expt} = A + \frac{B}{\bar{T}} \tag{12}$$

where A and B are two arbitrary constants. C_{ij}^* of eq. (11) can also be written as a function of reduced temperature $\bar{T}^*$

$$C_{ij}^* = C + \frac{D}{\bar{T}^*} \tag{13}$$

C and D are two new constants. Now from eqs. (11) and (13) we have

$$\alpha_{T\ theor} = \left[(6C - 5) + \frac{6D}{\bar{T}^*}\right] g. \tag{14}$$

When $\alpha_{T\ theor} = \alpha_{T\ expt}$ we may write from eqs. (12) and (14)

$$(6C - 5)g = A. \tag{15}$$

The experimental α_T's at two available temperatures by the CCF method are now used to get values of A and B. Similarly with the reported C_{ij}^* vs $\bar{T}^*$ curve[14] for 12-6 Lennard-Jones potential within a short range of temperature $\bar{T}^*$, C and D of eq. (13) were easily evaluated. $(6C-5)$ and A could yield 'g' which enables one to locate the value of C_{ij}^* and $\bar{T}^*$; and hence ε_{ij}/k.

This sort of evaluation was further improved by taking into account the small variation of 'g' with temperature. This was done by repeating the entire procedure as mentioned earlier to get the exact value of 'g' with the initially estimated ε_{ij}/k and hence the exact value of ε_{ij}/k is finally located. The ε_{ij}/k thus estimated agrees well with the literature values as shown in Table II, for molecules Ar, Kr, Xe, CO, CH_4 and N_2 respectively. With these ε_{ij}/k, the respective σ_{ij}'s were also determined from available viscosity data and are placed in Table II, together with the literature values.

§4. Theoretical Formula to Estimate $\alpha_{T\ theor}$

(i) **Elastic**: The $\alpha_{T\ theor}$ due to Chapman-Enskog[1] is already given by eq. (11) which consists of two factors:

$$g = \frac{1}{6[\lambda_{ij}]_1} \cdot \frac{s^{(i)}x_i - s^{(j)}x_j}{x_\lambda + y_\lambda} \quad \text{and} \quad (6C_{ij} - 5).$$

The first factor is the complicated functions of composition, thermal conductivities of gas and gas mixture while the second one is strongly a temperature dependent term. The symbols used are described in detail in MTGL.[1] The $\alpha_{T\ theor}$ thus computed with ε_{ij}/k and σ_{ij} (Table II) are presented in the 13th column of Table I and shown graphically in Figs. 4–8 for comparison with $\alpha_{T\ expt}$ by existing and the present CCF method.

(ii) **Inelastic**: According to Monchick *et al.*[15] the $\alpha_{T\ theor}$ due to inelastic collisions is given by:

$$\alpha_{T\ theor} = \frac{(6C_{ij}^* - 5)}{5nk[D_{ij}]_1}\left[\frac{\lambda_{j\ trans}^{\propto}}{x_j M_j} - \frac{\lambda_{i\ trans}^{\propto}}{x_i M_i}\right] + \frac{1}{5nk[D_{ij}]_1} \times \left[\frac{(6\tilde{C}_{ji} - 5)\lambda_{j\ int}^{\propto}}{x_j} - \frac{(6\tilde{C}_{ij} - 5)\lambda_{i\ int}^{\propto}}{x_i}\right] \tag{16}$$

where the symbols used have their usual meanings.[15] The collision integral ratio $\tilde{C}_{ij}$ which differs from C_{ij}^*,

is very sensitive to inelastic collision and not symmetric with respect to the interchange of the indices i and j. The excact value of $\lambda_{j\,\text{trans}}^{\propto}$ or $\lambda_{i\,\text{trans}}^{\propto}$ for a pure gas is given by[15]

$$\lambda_{j\,\text{trans}}^{\propto} = \frac{\eta}{M}\left[\left(\frac{5}{2}C_{v\ \text{trans}} + \frac{\rho D_{\text{int}}}{\eta}C_{\text{int}}\right) - \left(\frac{2}{\pi}\cdot\frac{C_{\text{int}}}{Z_{\text{rot}}}\right)\left(\frac{5}{2} - \frac{\rho D_{\text{int}}}{\eta}\right)^2 \times \left\{1 + \frac{2}{\pi Z_{\text{rot}}}\left(\frac{5}{3}\frac{C_{\text{int}}}{R} + \frac{\rho D_{\text{int}}}{\eta}\right)\right\}^{-1}\right]. \quad (17)$$

Here, $C_v = \frac{3}{2}R$ = the constant value of translational heat capacity, Z_{rot} = rotational translational collision number for inelastic collision. To evaluate the nonspherical part of eq. (16) we used Hirschfelder-Euken expression[15] to calculate the internal thermal conductivity $\lambda_{i\,\text{int}}^{\propto}$ from:

$$\lambda_{i\,\text{int}}^{\propto} = \frac{n[D_{ij}]_1 C_{\text{int}}}{1 + (x_j/x_i)(D_{ii}/D_{ij})}. \quad (18)$$

The inelastic $\alpha_{T\ \text{theor}}$ for CO^{28}–CO^{29}, CH_4^{16}–CH_4^{17} and N_2^{28}–N_2^{29} were calculated from eq. (16) with the help of eqs. (17) and (18). The mass density ρ_{ij}, the coefficient of viscosity η_{ij} and the diffusion coefficient D_{ij} of the gas mixtures were calculated from MTGL,[1] in terms of the evaluated ε_{ij}/k and σ_{ij} (Table II). The $\alpha_{T\ \text{theor}}$ (inelastic) thus calculated for CO, CH_4 and N_2 isotopic mixtures are placed in Table I and shown graphically in Figs. 6–8 for comparison.

§5. Results and Discussions

The least square fitted equations of $p^2/\ln q_e$ against p^4 were worked out from the pressure dependence of experimental $\ln q_e$[6] for Kr^{80}–Kr^{86}, Xe^{129}–Xe^{136}, CO^{28}–CO^{29}, CH_4^{16}–CH_4^{17} and N_2^{28}–N_2^{29} with their natural isotopic abundances. In case of later four systems $\ln q_{\max}$ were estimated in terms of a' and b' at two available experimental temperatures. The pressure dependence of $\ln q_e$ at any intermediate temperature could, however, be obtained from the temperature dependence of both α_T and F_s of eqs. (12) and (3). The linearity of b' with a short range of temperature fixes b' and hence a' from eq. (7) at the intermediate temperature. The pressure dependence of $\ln q_e$ in the selected intermediate temperature for all the systems except Kr^{80}–Kr^{86} is shown in Figs. 2 and 3 by dotted lines. The least square fitted equations of $p^2/\ln q_e$ against p^4 at all the temperatures for the aforesaid binary mixtures are given by:

i) Kr^{80}–Kr^{86}; $p^2/\ln q_e$
$= 0.0088 + 16.0771p^4$ at 455.5 K
$= 0.0074 + 9.9602p^4$ at 530.5 K
$= 0.0058 + 4.0584p^4$ at 680.5 K

ii) Xe^{129}–Xe^{136}; $p^2/\ln q_e$
$= 0.0212 + 151.515p^4$ at 539.0 K
$= 0.0192 + 101.0101p^4$ at 600.0 K*
$= 0.0192 + 53.4759p^4$ at 680.5 K

iii) CO^{28}–CO^{29}; $p^2/\ln q_e$
$= 0.0426 + 2.9976p^4$ at 455.5 K
$= 0.0382 + 2.5517p^4$ at 485.0 K*
$= 0.0330 + 1.9888p^4$ at 530.5 K

iv) CH_4^{16}–CH_4^{17}; $p^2/\ln q_e$
$= 0.1101 + 2.9291p^4$ at 440.65 K
$= 0.0757 + 2.0973p^4$ at 485.0 K*
$= 0.0561 + 1.6504p^4$ at 520.65 K

and

v) N_2^{28}–N_2^{29}; $p^2/\ln q_e$
$= 0.0637 + 3.1686p^4$ at 520.5 K
$= 0.0599 + 2.2609p^4$ at 600.0 K*
$= 0.0598 + 1.3678p^4$ at 680.5 K

* Intermediate temperature.

The experimental α_T's due to Maxwell and Slieker column shape factors were placed in the 10th and 11th columns of Table I and are shown graphically by curve Nos. 2 and 3 respectively in Figs. 4–8 as a function of temperature. They are almost of the same trends with those of CCF method as evidient in Table I and Figs. 4–8, although, the Slieker column shape factors are very crude in comparison with those of Maxwell inverse fifth power potential model.

The experimental α_T's as obtained in terms of $\ln q_{\max}$ and F_s from eqs. (1) and (3) are placed in the 9th column of Table I and shown graphically by the curve No. 1 in all the Figs. 4–8. These are slightly higher than those due

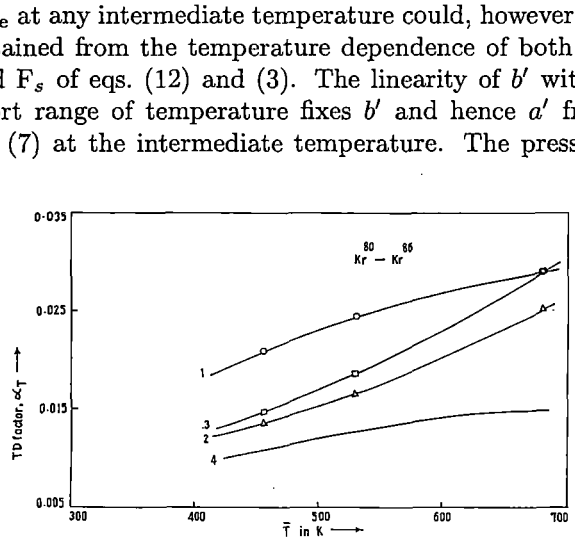

Fig. 4. Plot of α_T's against $\bar{T}$ in K for Kr^{80}–Kr^{86}. –o–o– Curve 1: Experimental α_T from F_s and $\ln q_{\max}$. –△–△– Curve 2: Experimental α_T using Maxwell shape factors. –□–□– Curve 3: Experimental α_T using Slieker shape factors. Curve 4: Theoretical α_T based on elastic collision.

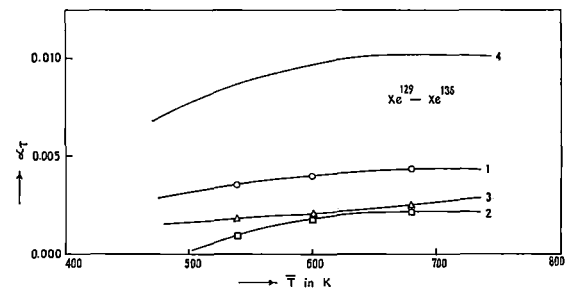

Fig. 5. Plot of α_T's against $\bar{T}$ in K for Xe^{129}–Xe^{136}. –o–o– Curve 1: Experimental α_T from F_s and $\ln q_{\max}$. –△–△– Curve 2: Experimental α_T using Maxwell shape factors. –□–□– Curve 3: Experimental α_T using Slieker shape factors. Curve 4: Theoretical α_T based on elastic collision.

Table II. Maxwell's model dependent and Slieker's model independent column shape factors, coefficient of viscosity η_{ij} and Diffusion coefficient D_{ij} together with estimated force parameters ε_{ij}/k and molecular diameters σ_{ij} used in the calculation of α_T of simple isotopic gas mixtures.

System	Model Potential	Estimated		Reported		Mean Temp. ($\bar{T}$) in K
		ε_{ij}/k in K	σ_{ij} in Å	ε_{ij}/k in K	σ_{ij} in Å	
Ar^{36}–Ar^{40}	LJ 12-6	125.03	3.516	125.2* 119.5**	3.405*	371.0 378.0 387.5
Kr^{80}–Kr^{86}	LJ 12-6	199.55	3.712	199.2* 166.7**	4.020*	455.5 530.5 680.5
Xe^{129}–Xe^{136}	LJ 12-6	228.20	4.253	222.2* 229.0**	4.362*	539 600 680.5
CO^{28}–CO^{29}	LJ 12-6	200.56	3.620	110.0†	3.590†	455.5 485.0 530.5
CH_4^{16}–CH_4^{17}	LJ 12-6	323.28	3.360	148.9* 310.0*	3.630*	440.65 485.00 520.65
N_2^{28}–N_2^{29}	LJ 12-6	80.963	3.914	95.2* 91.5*	3.341*	530.5 600.0 680.5

System	Model Potential	Column shape factors						$\eta_{ij} \times 10^5$ gm cm^{-1} sec^{-1}	D_{ij} cm^{-1} sec^{-1}
		Maxwell			Slieker				
		h'	k'_c	k'_d	$[S \cdot F]_1 \times 6.1$	$\pi(1-a^2)$	$[S \cdot F]_3 \times 9.1$		
Ar^{36}–Ar^{40}	LJ 12-6								
Kr^{80}–Kr^{86}	LJ 12-6	1.015	2.05	0.8143	1.2165	3.121	0.7702	28.53	
		1.225	3.00	0.7829				32.25	
		1.580	4.81	0.7571				39.01	
Xe^{129}–Xe^{136}	LJ 12-6	1.251	3.105	0.7804				33.61	
		1.405	3.85	0.7679				36.62	
		1.579	4.81	0.7571				40.39	
CO^{28}–CO^{29}	LJ 12-6	1.015	2.05	0.8143				24.17	0.4157
		1.095	2.40	0.8000				25.45	0.4629
		1.225	3.00	0.7829				27.33	0.5499
CH_4^{16}–CH_4^{17}	LJ 12-6	0.965	1.84	0.8229				12.58	0.3639
		1.095	2.40	0.8000				13.77	0.4379
		1.195	2.85	0.7857				14.68	0.5009
N_2^{28}–N_2^{29}	LJ 12-6	1.225	3.00	0.7829				33.31	0.6742
		1.405	3.85	0.7679				35.85	0.8293
		1.580	0.81	0.7571				38.97	1.0141

* Maitland *et al.* (1981).
** Hirchfelder *et al.* (1964).
† G. Vasaru (1975).

to Maxwell (curve 2) and Slieker (curve 3), but exhibit the similar trends as mentioned earlier.

The reliability of the temperature dependence of the experimental α_T's by the CCF method of the aforesaid binary mixtures is, however, ensured with the determination of the respective molecular force parameter ε_{ij}/k's and σ_{ij}'s for the molecules. The estimated force parameters seem to be very sensitive to intermolecular interactions and agree excellently well for Ar, Kr and Xe while for CO, CH_4 and N_2 they deviate remarkably. Both ε_{ij}/k's and σ_{ij}'s are all presented in columns 3 and 4 to compare with the literature values placed in columns 5 and 6 respectively of Table II. This fact at once suggests the existence of inelastic collisions in the later three isotopic mixtures. It was, however, pointed out by some workers[16,17] that the theory of inelastic collision effect

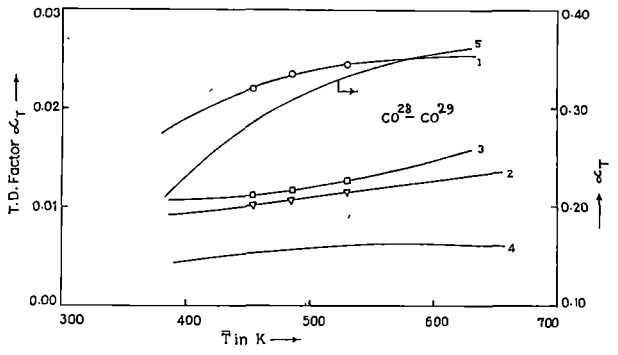

Fig. 6. Plot of α_T's against $\bar{T}$ in K for CO^{28}–CO^{29}. –o–o– Curve 1: Experimental α_T from F_s and $\ln q_{max}$. –△–△– Curve 2: Experimental α_T using Maxwell shape factors. –□–□– Curve 3: Experimental α_T using Slieker shape factors. Curve 4: Theoretical α_T based on elastic collision. Curve 5: Theoretical α_T based on inelastic collision.

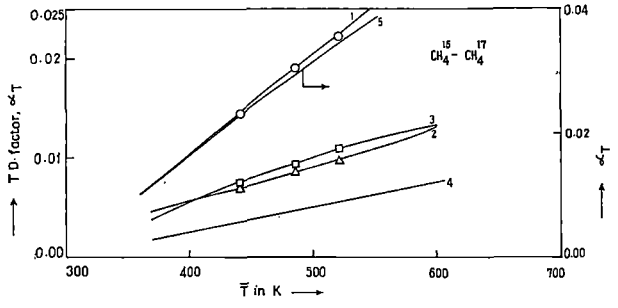

Fig. 7. Plot of α_T's against $\bar{T}$ in K for CH_4^{16}–CH_4^{17}. –o–o– Curve 1: Experimental α_T from F_s and $\ln q_{max}$ –△–△– Curve 2: Experimental α_T using Maxwell shape factors. –□–□– Curve 3: Experimental α_T using Slieker shape factors. Curve 4: Theoretical α_T based on elastic collision. Curve 5: Theoretical α_T based on inelastic collision.

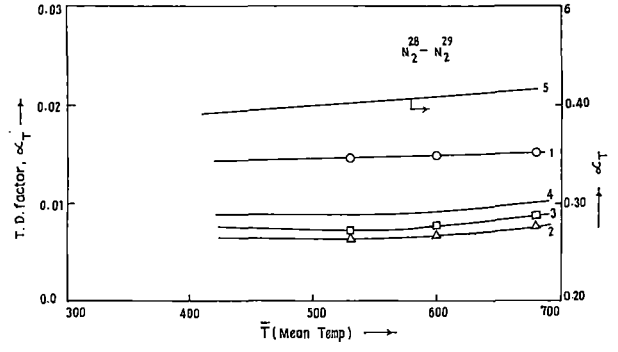

Fig. 8. Plot of α_T's against $\bar{T}$ in K for N_2^{28}–N_2^{29}. –o–o– Curve 1: Experimental α_T from F_s and $\ln q_{max}$. –△–△– Curve 2: Experimental α_T using Maxwell shape factors. –□–□– Curve 3: Experimental α_T using Slieker shape factors. Curve 4: Theoretical α_T based on elastic collision. Curve 5: Theoretical α_T based on inelastic collision.

in thermal diffusion is not widely applicable except for eccentrically loaded sphere molecule as one of the component in binary mixtures. The simple theory so far adopted here to estimate the force parameters is based on the elastic collision amongst the molecules. The inelastic collision in molecules like CO, CH_4 and N_2 may be the reason of such deviations (Table II).

The α_T's due to elestic collision theory from eq. (11) in terms of ε_{ij}/k and σ_{ij} are also shown graphically by the curve no 4 of Figs. 4–8 for comparison with α_T's by CCF method. They are placed in the 12th column of Table I. The graphs in Figs. 4–8 and Table I, clearly show that in case of Kr and Xe elastic α_T's almost coincide with α_T's by CCF method so far the magnitudes and trends are concerned. But in case of CO, CH_4 and N_2 elastic α_T's are of one-order smaller in magnitudes and not with the same trends with α_T's from CCF method.

The fact as mentioned above indicates that Chapman-Enskog gas kinetic theory[1] could not interprete the variation of α_T's of CO, CH_4 and N_2 isotopic mixtures with temperature probably due to the presence of inelastic collision among such molecules as shown in Tables I and II. But the theory appears to be successful to explain the temperature dependence of α_T of spherically symmetric molecules like Ar, Kr and Xe as evident from Tables I and II and Figs. 4 and 5.

The α_T based on inelastic collisions as derived by Monchick *et al.*[15] from eq. (16) for CO^{28}–CO^{29}, CH_4^{16}–CH_4^{17} and N_2^{28}–N_2^{29} are presented in column 13 of Table I. They are plotted graphically by the curve No. 5 in all the Figs. of 6–8 for comparison.

From all the discussions we may conclude that α_T's as obtained by CCF method is a simple, straightforward and unique one. This study further indicates that the nature of variation of F_s is the same as observed earlier,[2-4,17] but differing in the magnitudes of coefficients A, B and C in $F_s = A + B\bar{T} + C\bar{T}^2$. Thus the nature of variation of F_s with temperature $\bar{T}$ (Fig. 1) confirms that the CCF method to locate the magnitude and trend of α_T in Figs. 4–8 is correct.

§6. Conclusions

Although, F_s is supposed to be an essential tool in determining the experimental α_T in a column measurement, still the functional relationship of F_s with r_{cold}, r_{hot}, L and $\bar{T}$ remains unexplored. Simultaneous determination of F_s and the force parameters seems to be an important step forward to observe α_T of both isotopic and nonisotopic binary mixtures of simple molecules as a function of temperature. A rigorous study of experimental F_s through experimentally determined $\ln q_{max}$ of binary mixture having accurate α_T is needed with different column geometries to serve this purpose.

The very existence of inelastic collision effects in thermal diffusion of suitable molecules forming binary mixture have to be studied in detail through $\ln q_{max}$ and F_s to improve the theory of inelastic collision effects in thermal diffusion.

1) J. O. Hirchfelder, C. F. Curtiss and R. B. Bird: *Molecular Theory of Gases and Liquids* (John Willey and Sons, New York, 1964) p. 541.
2) S. Acharyya, A. K. Das, P. Acharyya, S. K. Datta and I. L. Saha: J. Phys. Soc. Jpn. **50** (1981) 1603.
3) S. Acharyya, I. L. Saha, P. Acharyya, A. K. Das and S. K. Datta: J. Phys. Soc. Jpn. **51** (1982) 1469.
4) A. K. Datta and S. Acharyya: J. Phys. Soc. Jpn. **62** (1993) 1527.
5) J. L. Navarro, J. A. Madariage and J. M. Saviron: J. Phys.

Soc. Jpn. **50** (1983) 1603.
6) W. J. Roos and W. M. Rutherford: J. Chem. Phys. **50** (1969) 3936.
7) F. Vandervolk: Ph. D. Dissertation (1963).
8) I. Yamamoto, H. Makino and A. Kanagawa: J. Nucl. Sci. Technol. **27** (1990) 156.
9) G. Vasaru: *Thermal Diffusion Column*, supplied by S. Raman (B.A.R.C., Bombay).
10) C. J. G. Slieker: Z. Naturforsch. **20** (1965) 591.
11) W. H. Furry and R. C. Jones: Phys. Rev. **69** (1946) 459.
12) B. N. Srivastava and K. P. Srivastava: Physica **23** (1957) 103.
13) R. Paul, A. J. Howard and W. W. Watson: J. Chem. Phys. **39** (1963) 3053.
14) Max Klein and F. J. Smith: Tables of Collision Integral for the (m, 6) Potential for the Values of m, Arnold Engineering Development Centre, Tennessee, 1968.
15) L. Monchick, S. I. Sandlar and E. A. Mason: J. Chem. Phys. **49** (1968) 1178.
16) T. K. Chattspadhyay and S. Acharyya: J. Phys. B **7** (1974) 2277.
17) G. Dasgupta, A. K. Datta and S. Acharyya: Pramana **43** (1994) 81.

Journal of the Physical Society of Japan
Vol. 66, No. 1, January, 1997, pp. 108-114

Molecular Force Parameters through Thermal Diffusion to Ensure the Model Independency of Column Calibration Factor

G. DASGUPTA, N. GHOSH, N. NANDI and S. ACHARYYA

Department of Physics, Raiganj College (University College), P.O. Raiganj, Dist. Uttar Dinajpur, West Bengal, 733134, India

(Received July 29, 1996)

Using Ar^{36}–Ar^{40} as calibrating gas, the simultaneous determination of thermal diffusion factors α_T's at two available experimental temperatures as well as the prediction of pressure dependence of $\ln q_e$ at an intermediate temperature is possible for some isotopic inert gas mixtures in terms of column calibration factor F_s (CCF) of a given column. The variation of α_T with $\bar{T}$ is then used to estimate the force parameters of the molecules only to ensure the reliability of the proposed temperature dependence of α_T. The experimental α_T's due to Maxwell and Slieker shape factors are also calculated for comparison with those by the CCF method as well as by theoretical ones based on elastic collisions among the molecules. It seems that α_T's by CCF method play an important role in determining the force parameters of molecules indicating thereby the model independency of F_s as a sensitive α_T measuring parameter.

KEYWORDS: thermal diffusion factor, column calibration factor, elastic and inelastic collisions

§1. Introduction

The theoretical formulation of thermal diffusion factor α_T as derived from Chapman-Enskog gas kinetic theory[1] is based on the assumption that the molecules are elastic spheres with spherically symmetric potential field. The theory can, however, hardly explain the experimental α_T of binary nonisotopic or even isotopic gas mixtures. Thermal diffusion is still interesting for its close correlation with the intermolecular forces. Moreover, unlike viscosity, thermal diffusion is a second order effect. Thus it is generally used to investigate the elastic or inelastic collisions among the molecules. The phenomenon is also responsible to enrich rare as well as ordinary isotopes in thermal diffusion column.

The temperature dependence of experimental α_T's of a binary gas mixture may offer a convenient method to estimate the molecular force parameters like ϵ_{ij}/k and σ_{ij} where ϵ_{ij} is the depth of potential well, k is the Boltzmann constant and σ_{ij} is the molecular diameter. ϵ_{ij}/k and σ_{ij} become ϵ_{ii}/k or ϵ_{jj}/k and σ_{ii} or σ_{jj} for isotopic components in a binary mixture of gases. They are, therefore, expected to play an important role to yield the exact theoretical α_T's based on elastic or inelastic collisions.

To estimate experimental α_T the theory of TD column which was already developed by a large number of workers,[2-4] is still insufficient. TD column, on the other hand, is a very sensitive instrument to investigate the temperature and composition dependence of α_T, particularly for a binary isotopic gas mixture of molecules having practically no mass difference.

The equilibrium separation factor 'q_e' of a gas mixture in a TD column is defined by:

$$q_e = (x_i/x_j)_{\text{top}}/(x_i/x_j)_{\text{bottom}}$$

where x_i and x_j are the mass or mole fractions of the lighter (i) and heavier (j) components respectively. In a TD column q_e is usually measured at different pressures in atmospheres, for a fixed composition of a binary gas mixture at different temperatures or at a fixed temperature for different compositions. The existing method of evaluating the experimental α_T is involved with Maxwell, Lennard-Jones model dependent as well as Slieker model independent column shape factors (CSF). The method is, however, complicated and the resulting α_T's are usually not in agreement with the theoretical α_T so far its temperature and composition dependences are concerned.

We,[5-7] therefore, introduced a scaling factor F_s called CCF for a TD column to get the actual α_T of a binary gas mixture from column measurements by the following relation:

$$\ln q_{\text{max}} = \alpha_T F_s(r_c, r_h, L, \bar{T}). \tag{1}$$

Here $\ln q_{\text{max}}$ is the logarithmic maximum equilibrium separation factor, r_c and r_h are the cold and hot wall radii maintained at temperatures T_c and T_h respectively in a TD column of geometrical length L and the mean temperature $\bar{T}$ of the gas mixture is given by $\bar{T} = \frac{T_h+T_c}{2}$.

The molecular model independent parameter,[7,8] F_s can now be used to evaluate the actual α_T's of binary isotopic or nonisotopic gas mixtures from their $\ln q_{\text{max}}$ measurements. Moran and Watson[9] had already measured the pressure dependence of $\ln q_e$ of Ne^{20}–Ne^{22}, Ar^{36}–Ar^{40}, and Kr^{80}–Kr^{86} mixtures at two experimental temperatures in a TD column of $L = 182.0$ cm, $r_c = 0.635$ cm and $r_h = 0.0254$ cm respectively. The measurements,[9] however, inspired us to observe the probable temperature dependence of α_T of those isotopic mixtures in terms of CCF together with the estimation of ϵ_{ij}/k and σ_{ij} of the respective molecules. The purpose of such study is to establish the molecular model independency

of F_s, too.

The experimental[9] $\ln q_{max}$ of Ar^{36}–Ar^{40} at 432 K and 537 K and the reliable[10] α_T's of Ar were, however, used to give two values of F_s. As F_s is a molecular mass independent parameter, the experimental[9] $\ln q_{max}$ and reliable[10] α_T of Ne^{20}–Ne^{22} were used again to get F_s at the intermediate temperature 447 K. The probable temperature dependence of F_s for the column[9] is then obtained:

$$F_s = 54.3777 - 0.1152\bar{T} + 1.4350 \times 10^{-4}\bar{T}^2 \quad (2)$$

which is shown graphically in Fig. 1. This F_s and the experimental $\ln q_{max}$ for any gas mixture yield α_T at the experimental temperature $\bar{T}$ from eq. (1).

A large number of workers[11,12] had expressed α_T in the form:

$$\alpha_T = A + B/\bar{T} \quad (3)$$

where A and B are two arbitrary constants. The experimental α_T's for Ne^{20}–Ne^{22}, Ar^{36}–Ar^{40} and Kr^{80}–Kr^{86} as a function of $\bar{T}$ are, however given by

$$\alpha_T = 0.03019 - 0.80013 \cdot \frac{1}{\bar{T}},$$

$$\alpha_T = 0.03476 - 5.08155 \cdot \frac{1}{\bar{T}} \quad \text{and}$$

$$\alpha_T = 0.27993 - 69.3446 \cdot \frac{1}{\bar{T}} \quad (4)$$

which are shown in Figs. 3–5 respectively. The plot of experimental α_T's against $\bar{T}$ thus enables us to evaluate ε_{ij}/k and σ_{ij} of the respective molecules.[13,14] The results are shown in Table II for comparison with the literature values. The comparison finally indicates that curves as shown in Figs. 3–5 in terms of F_s and $\ln q_{max}$ from eq. (1) for Ne, Ar and Kr gas mixtures are claimed to be perfect. The theoretical as well as the experimental α_T's by the CCF method as a function of $\bar{T}$ were, however, used to estimate a' and b' and hence $\ln q_e$ at any intermediate temperature between 432 K to 537 K for each system. They are also shown in Fig. 2 by the dotted lines together with actual $\ln q_e$ at two available $\bar{T}$ K.

The experimental α_T's by the existing method involved with CSF due to Maxwell and Slieker were also evaluated and shown in Figs. 3–5. The CSF due to L-J model can not be applied here as the cold wall temperature of the column was held fixed. The theoretical α_T's based on elastic collisions were also found out with the estimated ε_{ij}/k and σ_{ij}, placed in Table II, and shown in Figs. 3–5 only to see how far the elastic theory is now successful to explain the experimental α_T's (Table I) by the CCF and the existing method. The theoretical α_T's are placed in the last column of Table I. Both the Tables I and II however, indicate the adequacy or otherwise of the CCF method to predict the actual and reliable α_T of such isotopic mixtures together with their correct force parameters from thermal diffusion.

§2. Mathematical Formulations to Estimate Experimental α_T

In case of an ideal column of length L, both ends being closed, $\ln q_e$ of a gas mixture at any mean temperature $\bar{T}$ is given by:[7,8]

$$\ln q_e = \frac{HL}{K_c + K_d}. \quad (5)$$

H, K_c and K_d are the functions of the transport coefficients of a gas mixture and are proportional to p^2, p^4 and p^0 respectively, p being the pressure in atmosphere. The above eq. (5) thus becomes

$$\ln q_e = \frac{ap^2}{b + p^4}. \quad (6)$$

But in case of actual column, parasitic remixing generally occurs. This can be taken into consideration by adding a term K_p, proportional to p^4, in the denominator of eq. (5), $\ln q_e$ then becomes

$$\ln q_e = \frac{a'p^2}{b' + p^4} \quad (7)$$

where a' and b' are related to a and b by:

$$a = a'\left(1 + \frac{K_p}{K_c}\right) \quad \text{and} \quad b = b'\left(1 + \frac{K_p}{K_c}\right).$$

The above eq. (7) can then be written as

$$p^2/\ln q_e = \frac{b'}{a'} + \frac{1}{a'}p^4 \quad (8)$$

where a' and b' are two arbitrary constants which can be obtained from experimental $\ln q_e$ at different pressures p in atm. at a given temperature $\bar{T}$ K.

Again, it has been found in Fig. 2 that the experimental $\ln q_e$ increases with p and eventually becomes maximum at $p = (b')^{1/4}$ for which $\frac{\partial}{\partial p}(\ln q_e) = 0$. The eq. (7) then becomes

$$\ln q_{max} = \frac{a'}{2\sqrt{b'}}. \quad (9)$$

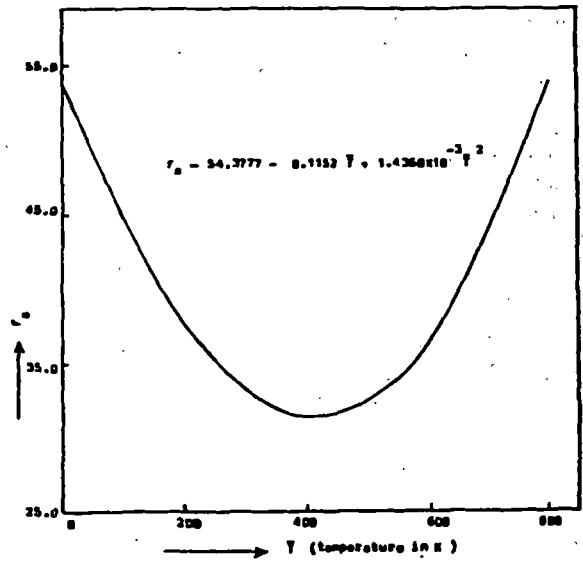

Fig. 1. Variation of column calibration factor F_s (CCF) against temperature in K.

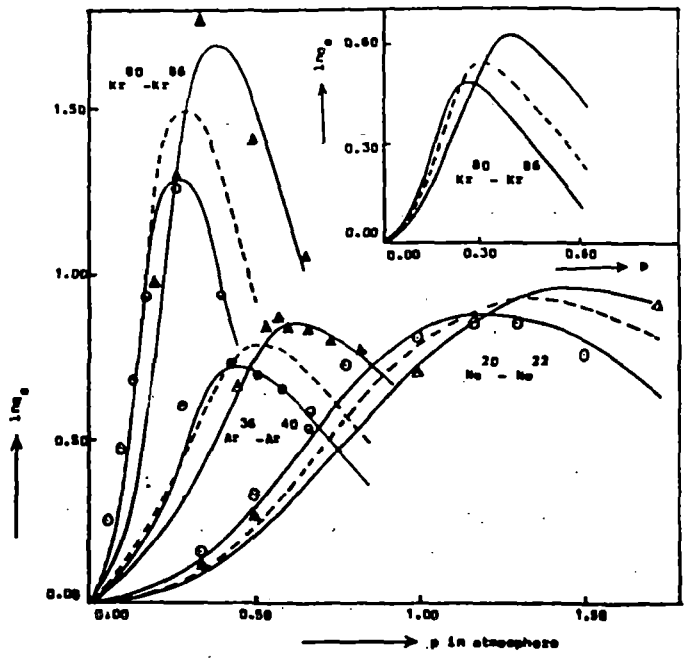

Fig. 2. i) Variation of $\ln q_0$ against p in atmosphere for Ne^{20}–Ne^{22}. –O–O– Experimental $\ln q_0$ at 447 K. ------ Predicted $\ln q_0$ at 492 K. –Δ–Δ– Experimental $\ln q_0$ at 537 K. ii) Variation of $\ln q_0$ against p in atmosphere for Ar^{36}–Ar^{40}. –O–O– Experimental $\ln q_0$ at 432 K. ------ Predicted $\ln q_0$ at 484.5 K. –Δ–Δ– Experimental $\ln q_0$ at 537 K. iii) Variation of $\ln q_0$ against p in atmosphere for Kr^{80}–Kr^{86}. –O–O– Experimental $\ln q_0$ at 447 K. ------ Predicted $\ln q_0$ at 492 K. –Δ–Δ– Experimental $\ln q_0$ at 537 K. iv) Kr^{80}–Kr^{86} (Adjacent graph). ——— Adjusted $\ln q_0$ against p in atmosphere at 447 K. ------ Predicted $\ln q_0$ against p in atmosphere at 492 K. ——— Adjusted $\ln q_0$ against p in atmosphere at 537 K.

With the known $\ln q_{max}$ in terms of a' and b' (Table I) and F_s (Fig. 1) of a given column,[9] α_T of binary isotopic gas mixtures of Ne, Ar, Kr were found out from eq. (1). They are placed in Table I and shown graphically in Figs. 3–5.

One may obtain the experimental $\ln q_{max}$ from eq. (5) which is also given by:

$$\ln q_{max} = \frac{HL}{2\sqrt{K_c K_d}}. \tag{10}$$

The exact expressions for H, K_c and K_d are given by:

$$\text{(i)}\quad H = \frac{2\pi}{6!}\left(\frac{\alpha_T \rho_{ij}^2 g}{\eta_{ij}}\right)_1 \cdot \frac{1}{2}(r_c + r_h)(r_c - r_h)^3 (2u)^2 h'$$

$$K_c = \frac{2\pi}{9!}(\rho_{ij}^3 g^2/\eta_{ij}^2 D_{ij})_1 \frac{1}{2}(r_c + r_h)(r_c - r_h)^7 (2u)^2 k_c'$$

$$K_d = 2\pi(\rho_{ij} D_{ij})_1 \frac{1}{2}(r_c + r_h)(r_c - r_h) k_d' \tag{11}$$

and

$$\text{(ii)}\quad H = C_1 = [S \cdot F]_1 r_c^4 \left(\frac{\alpha_T \rho_{ij}^2 g}{\eta_{ij}}\right)_1 \left(\frac{\Delta T}{\bar{T}}\right)^2$$

$$K_c = C_3 = [S \cdot F]_3 r_c^8 (\rho_{ij}^3 g^2/\eta_{ij}^2 D_{ij})_1 \left(\frac{\Delta T}{\bar{T}}\right)^2$$

$$K_d = C_2 = \pi(1 - a^2) r_c^2 (\rho_{ij} D_{ij})_1 \tag{12}$$

in Maxwell model and Slieker's model independent methods. The α_T in Maxwell model dependent and Slieker's model independent methods[15, 16] could, however, be obtained by using eqs. (10) & (11), and (10) & (12) respectively in the following forms:

$$\alpha_T\left(\begin{matrix}\text{Maxwell}\\ \text{model}\end{matrix}\right) = 2.39\frac{r_c - r_h}{L} \cdot \frac{\bar{T}}{\Delta T}\frac{\sqrt{k_c' k_d'}}{h'} \ln q_{max} \tag{13}$$

and

$$\alpha_T(\text{Slieker}) = 2.00\frac{r_c}{L}\frac{\bar{T}}{\Delta T}\frac{\sqrt{\pi(1 - a^2)[S \cdot F]_3}}{[S \cdot F]_1} \ln q_{max}. \tag{14}$$

The symbols h', k_c' & k_d'; $[S \cdot F]_1$, $\pi(1 - a^2)$ & $[S \cdot F]_3$ are dimensionless CSF due to Maxwell and Slieker respectively. ρ_{ij} is the mass density of the gas mixture of coefficient of viscosity η_{ij} and diffusion coefficient D_{ij}, $u = \frac{T_h - T_c}{T_h + T_c}$, $\Delta T = T_h - T_c$ and g is the acceleration due to gravity.

The α_T's thus evaluated from eqs. (13) and (14) due to Maxwell model and Slieker's CSF respectively are placed in Table I. They are also shown in Figs. 3–5 for Ne^{20}–Ne^{22}, Ar^{36}–Ar^{40} and Kr^{80}–Kr^{86} mixtures in order to compare them with the theoretical α_T computed with their respective ϵ_{ij}/k and σ_{ij}.

§3. Theoretical Elastic α_T together with Force Parameters ϵ_{ij}/k and σ_{ij}

According to gas kinetic theory the theoretical α_T based on elastic collisions[1] is

$$\alpha_T = g(6C_{ij}^* - 5) \tag{15}$$

where

Table I. Experimental and theoretical thermal diffusion factor α_T of binary isotopic mixtures of Neon, Argon and Krypton with temperatures in K.

Column used	System	Hot Wall Temp. (T_h) in K.	Cold Wall Temp. (T_c) in K.	Mean Temp in K $T=\frac{T_h+T_c}{2}$	a' $(atm)^2$	b' $(atm)^4$	Computed $\ln_{e\,max}$ from eq. (9)	Column calibration factor (F_c)
L=Length of the column =182.0 cm.	Ne^{20}–Ne^{22}	596	298	447	2.5470	2.0188	0.8963	31.5599
		656	328	492	3.3670	3.3025	0.9264	32.4355
		716	358	537	4.3365	4.9660	0.9730	33.9012
Hot Wall radius r_h = 0.0254 cm.	Ar^{36}–Ar^{40}	576	288	432	0.2942	0.0415	0.7221	31.3957
		646	323	484.5	0.4149	0.0701	0.7836	32.2485
		716	358	537	0.7037	0.1683	0.8577	33.9012
Cold Wall radius r_c = 0.635 cm.	Kr^{80}–Kr^{86}	596	298	447	0.5342	0.0046	3.9382	31.5599
					0.0653	0.0046	0.4814	
		656	328	492	0.7963	0.0078	4.5082	32.4355
					0.0973	0.0078	0.5511	
		716	358	537	1.5540	0.0231	5.1123	33.9012
					0.1900	0.0231	0.6250	

Column used	System	Estimated α_T using: Present method	Maxwell's shape factor	Slicker's shape factor	Computed theoritical α_T
L=Length of the column =182.0 cm.	Ne^{20}–Ne^{22}	0.0284	0.0156	0.0179	0.0294
		0.0286	0.0161	0.0185	0.0298
		0.0287	0.0169	0.0195	0.0297
Hot Wall radius r_h = 0.0254 cm.	Ar^{36}–Ar^{40}	0.0230	0.0126	0.0144	0.0259
		0.0243	0.0136	0.0156	0.0266
		0.0253	0.0149	0.0171	0.0277
Cold Wall radius r_c = 0.635 cm.	Kr^{80}–Kr^{86}	0.1248	0.0684	0.0785	0.0135
		0.0153			
		0.1390	0.0783	0.0899	0.0157
		0.0170			
		0.1508	0.0888	0.1019	0.0170
		0.0184			

$$g = \frac{1}{6[\lambda_{ij}]_1}\frac{S^{(i)}x_i - S^{(j)}x_j}{X_\lambda + Y_\lambda}$$

is a complicated function of composition and thermal conductivities of a gas mixture. The temperature dependence of α_T is mainly governed by $(6C^*_{ij} - 5)$ which involves with like or unlike interactions. The experimental α_T as a function of $\bar{T}$ is:[17]

$$(\alpha_T)_{expt.} = A + B/\bar{T}. \qquad (16)$$

Although g is a slowly varying function of $\bar{T}$, we may assume it to be a temperature independent one. C^*_{ij} may be expressed as a function of reduced temperature T^* like

$$C^*_{ij} = C + D/\bar{T}^* \qquad (17)$$

where

$$\bar{T}^* = \bar{T}/(\epsilon_{ij}/k).$$

The above eq. (15) thus becomes

$$(\alpha_T)_{theor.} = (6C - 5)g + \frac{6gD}{\bar{T}^*} \qquad (18)$$

where C and D are new constants. Comparing eqs. (16) and (18) one may get

$$g = \frac{A}{(6C - 5)}.$$

From the fitted equations of $(\alpha_T)_{expt.}$ against $1/\bar{T}$, A and B were first evaluated. Similarly C^*_{ij} reported elsewhere[18] for (12–6) L-J potential was plotted against $1/\bar{T}^*$ to get C and D of eq. (17).

Thus 'g' along with $(\alpha_T)_{expt.} = (6C^*_{ij} - 5)g$ fixes

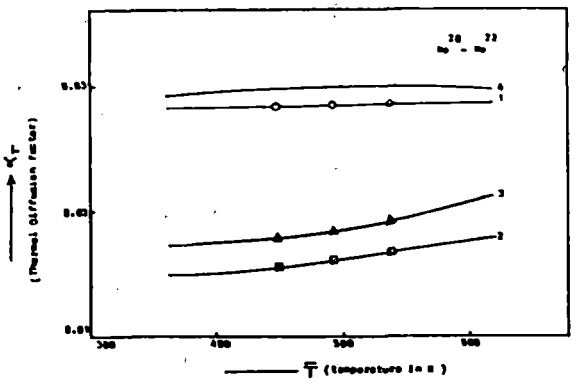

Fig. 3. Plot of α_T's against $\bar{T}$ in K for Ne^{20}–Ne^{22}. –O–O– Curve 1: Experimental α_T from F_s and $\ln q_{max}$. –□–□– Curve 2: Experimental α_T from Maxwell's shape factors. –Δ–Δ– Curve 3: Experimental α_T using Slieker's shape factors. – — – Curve 4: Theoretical α_T based on elastic collision.

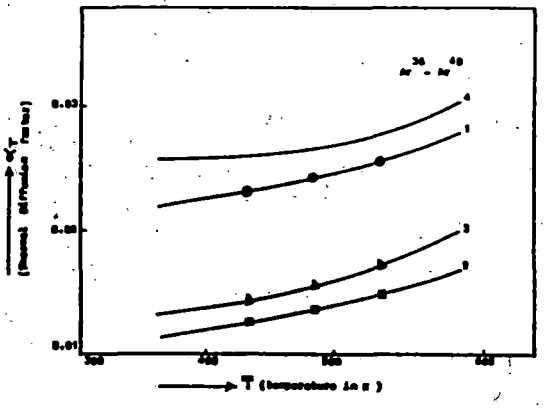

Fig. 4. Plot of α_T against $\bar{T}$ for Ar^{36}–Ar^{40}. –O–O– Curve 1: Experimental α_T from F_s and $\ln q_{max}$. –□–□– Curve 2: Experimental α_T using Maxwell's shape factors. –Δ–Δ– Curve 3: Experimental α_T using Slieker's shape factors. ——— Curve 4: Theoretical α_T based on elastic collision.

C_{ij}^* and hence $\bar{T}^*$ to estimate ϵ_{ij}/k of the respective molecule.

With the value of ϵ_{ij}/k first estimated, one may repeat the total procedure as mentioned above, to get more correct ϵ_{ij}/k in order to present them in Table II. They are found in good agreement with the available literature values. Reported viscosity data are then used with the estimated ϵ_{ij}/k to get the molecular diameter σ_{ij} as shown in Table II. The theoretical α_T's for Ne^{20}–Ne^{22}, Ar^{36}–Ar^{40} and Kr^{80}–Kr^{86} were then evaluated with those ϵ_{ii}/k, ϵ_{jj}/k and ϵ_{ij}/k (Table II) and shown in Figs. 3–5 respectively.

§4. Results and Discussions

The least square fitted equations of $p^2/\ln q_e$ against p^4 from the available $\ln q_e$ vs p in atmosphere[9] as illustrated graphically in Fig. 2, were worked out for 9.7% of Ar^{36} in Ar^{40}, Ne^{20}–Ne^{22} and Kr^{80}–Kr^{86}, the latter two with their natural isotopic abundances, at two experimental temperatures. The pressure dependence of $\ln q_e$ at any

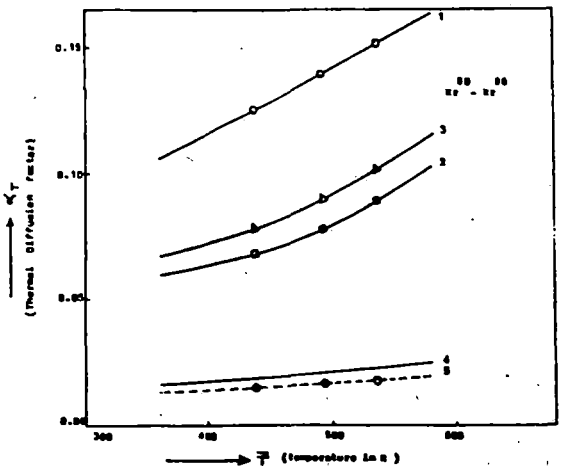

Fig. 5. Plot of α_T against $\bar{T}$ for Kr^{80}–Kr^{86}. –O–O– Curve 1: Experimental α_T from F_s and $\ln q_{max}$. –□–□– Curve 2: Experimental α_T using Maxwell's shape factor. –Δ–Δ– Curve 3: Experimental α_T using Slieker's shape factor. ——— Curve 4: Theoretical α_T based on elastic collision. –⊙–⊙– Curve 5: Experimental α_T from F_s and adjusted $\ln q_{max}$.

intermediate temperature for them, as shown by dotted lines in Fig. 2, were also inferred from $\ln q_{max}$ in terms of known F_s and α_T assuming the linear relationship of (b'/a') with $\bar{T}$ for the three aforesaid mixtures. $p^2/\ln q_e$ as a linear function of p^4 are, however, expressed by the following equations for

i) Ar^{36}–Ar^{40} (with 9.7% of Ar^{36} in Ar^{40})

$$p^2/\ln q_e = 0.1411 + 3.3990p^4 \quad \text{at} \quad 432\,\text{K}$$
$$p^2/\ln q_e = 0.1690 + 2.4102p^4 \quad \text{at} \quad 484\,\text{K}$$
$$p^2/\ln q_e = 0.2392 + 1.4210p^4 \quad \text{at} \quad 537\,\text{K}$$

ii) Ne^{20}–Ne^{22} (with natural isotopic abundances)

$$p^2/\ln q_e = 0.7926 + 0.3926p^4 \quad \text{at} \quad 447\,\text{K}$$
$$p^2/\ln q_e = 0.9808 + 0.2970p^4 \quad \text{at} \quad 492\,\text{K}$$
$$p^2/\ln q_e = 1.1452 + 0.2306p^4 \quad \text{at} \quad 537\,\text{K}$$

and for Kr^{80}–Kr^{86} (with natural isotopic abundances)

$$p^2/\ln q_e = 0.0086 + 1.8720p^4 \quad \text{at} \quad 447\,\text{K}$$
$$p^2/\ln q_e = 0.0098 + 1.2558p^4 \quad \text{at} \quad 492\,\text{K}$$
$$p^2/\ln q_e = 0.0149 + 0.6435p^4 \quad \text{at} \quad 537\,\text{K}$$

respectively. But $\ln q_{max}$ of Krypton, estimated from the measured values of $\ln q_e$ as a function of pressure (Fig. 2) in terms of a' and b' (Table I) is found to be 8.18 times larger than the widely reported data elsewhere.[7] Adjustment of $\ln q_e$ is, therefore, necessary to get actual α_T's of Kr^{80}–Kr^{86}, as shown by curve 5 in Fig. 5, from the following $p^2/\ln q_e$ against p^4 relations:

$$p^2/\ln q_e = 0.0704 + 15.3139p^4 \quad \text{at} \quad 447\,\text{K}$$
$$p^2/\ln q_e = 0.0802 + 10.2775p^4 \quad \text{at} \quad 492\,\text{K}$$
$$p^2/\ln q_e = 0.1216 + 5.2632p^4 \quad \text{at} \quad 537\,\text{K}.$$

Table II. Maxwell's model dependent and Slieker's model independent column shape factors, (CSF coefficient of viscosity together with estimated force parameters ϵ_{ij}/k and molecular diameter σ_{ij} used in the calculation of α_T of simple isotopic gas mixtures.

System	Model potential	Estimated		Reported		Mean Temp. (T) in K
		ϵ_{ij}/k in K	σ_{ij} in Å	ϵ_{ij}/k in K	σ_{ij} in Å	
Ne^{20}–Ne^{22}	LJ 12-6	40.77	3.1840	41.19*	3.074*	447
						492
				27.50**	2.858**	537
Ar^{36}–Ar^{40}	LJ 12-6	118.41	3.9543	125.20*	3.405*	432
						484.5
				119.50**	3.826**	537
Kr^{80}–Kr^{86}	LJ 12-6	202.41	4.1689	199.20*	4.020*	447
						492
				166.70**	4.130**	537

System	Model potential	Column shape factors (CSF)						$\eta_{ij} \times 10^5$ gm × cm^{-1} × sec^{-1}
		Maxwell			Slieker			
		h'	k'_c	k'_d	$[S \cdot F]_1 \times 6!$	$\pi(1-a^2)$	$[S \cdot F]_3 \times 9!$	
Ne^{20}–Ne^{22}	LJ 12-6	0.815	1.760	0.790	0.937	3.137	0.711	31.40
								33.35
								35.17
Ar^{36}–Ar^{40}	LJ 12-6	0.815	1.760	0.790	0.937	3.137	0.711	21.80
								23.95
								26.10
Kr^{80}–Kr^{86}	LJ 12-6	0.815	1.760	0.790	0.937	3.137	0.711	25.50
								28.15
								30.80

*Maitland *et al.* (1981)
**Hirchfelder *et al.* (1964)

The new $\ln q_e$ against p in atmosphere is shown by the adjacent curves in Fig. 2. The corresponding $\ln q_{max}$'s are placed in Table I, together with those obtained from $\ln q_e$ vs p measured by Moran and Watson.[9] The $\ln q_{max}$'s for all the isotopic molecular mixtures were, however, determined from eq. (9) with a' and b' governing their pressure variation of $\ln q_e$ as shown in Fig. 2. They are placed in the 8th column of Table I.

Since F_s is supposed not to depend on molecular model we therefore, estimated three values of F_s from eq. (1) for this column[9] through the measured $\ln q_{max}$ and reliable α_T's from the other sources:[10] for Ar^{36}–Ar^{40} at 432 K, 537 K and Ne^{20}–Ne^{22} at 447 K respectively. It is interesting to note in Fig. 1, that the temperature variation of F_s is the same as observed earlier[5-8] only the coefficients of $\bar{T}$ and $\bar{T}^2$ are slightly different. Although r_c/r_h (=25) for the present column is too large, the temperature variation of F_s is found to be concave in nature.

The magnitudes and trends of α_T with respect to temperature $\bar{T}$ could, now be obtained for Ne^{20}–Ne^{22}, Ar^{36}–Ar^{40} and Kr^{80}–Kr^{86} from eq. (1) in terms of $\ln q_{max}$ and F_s. The expected close agreement of α_T's from the CCF method with theoretical ones might express the reliability of F_s and the model independency of CCF method may once again be confirmed. The α_T's by the CCF method are placed in the 10th column of Table I. The variation of these α_T's with $\bar{T}$ are shown graphically in Figs. 3–5 for Ne^{20}–Ne^{22}, Ar^{36}–Ar^{40} and Kr^{80}–Kr^{86} respectively by the curve No. 1.

In order to ensure the reliability of the temperature dependence of α_T the molecular force parameters ϵ_{ij}/k and σ_{ij} were also determined by using eq. (18) and the available coefficients of viscosity respectively. The estimated ϵ_{ii}/k or ϵ_{jj}/k and σ_{ii} or σ_{jj} of the isotopic gases are placed in the 3rd and the 4th columns of Table II. The close agreement of them with the literature values at once suggests the technique to estimate α_T is really accurate and reliable. The experimental α_T's were also computed from eqs. (13) and (14) by using Maxwell's inverse fifth power potential and Slieker's model independent column shape factors (CSF) which are placed in Table II. These α_T's are placed in the 11th and the 12th columns of Table I respectively. The variation of these α_T's with $\bar{T}$ are also shown graphically by curves 2 and 3 respectively in Figs. 3–5. The α_T's as shown in Figs. 3–5, due to Maxwell and Slieker's methods agree excellently with α_T's by the CCF method, so far their trends with $\bar{T}$ are concerned, although the magnitude of α_T by the present method is higher.

The existing frame work of derivations of eqs. (13) and (14) are really very interesting. The formulations so derived show that the molecular model appears in them through CSF which seems to be an important step-forward in the existing method based on Furry[2] and Jones[4] column theory.

With the estimated force parameters of ϵ_{ij}/k and σ_{ij} presented in Table II theoretical α_T's based on the elastic collisions were also evaluated and placed in the 13th column of Table I. The variation of theoretical α_T's with $\bar{T}$ are shown graphically by curve 4 in each of the Figs. 3

5 for Ne^{20}-Ne^{22}, Ar^{36}-Ar^{40} and Kr^{80}-Kr^{86} respectively. The α_T's due to elastic collision theory are found to be almost of the same magnitude with those by the CCF method. Besides all these, it is seen that the trends of α_T's with respect to temperature by the present CCF method agree excellently well with the theoretical ones in all the systems.

From the discussions made above, it is confirmed that F_s is a molecular model independent parameter. F_s is further, claimed to be a perfect, simple and straightforward one to locate the magnitude and trend of α_T with respect to $\bar{T}$. Moreover, α_T against $1/\bar{T}$ may be considered as a simple and useful technique in determining the exact force parameter of molecules too, to observe the temperature dependence of α_T of any binary isotopic and nonisotopic gas mixture.

§5. Conclusion

Model independency of CCF F_s, is now once again established in determining the reliable α_T's of any binary gas mixture in column measurements. It is, therefore, desirable to study more TD columns of different column geometries to arrive at the functional relationship of F_s with r_c, r_h, L and $\bar{T}$ with the experimentally determined $\ln q_{max}$ and α_T of interesting pair of molecules. The simultaneous estimation of α_T's and F_s with the corresponding force parameters from α_T vs $1/\bar{T}$ seems to be an important stepforward to test the applicability of F_s. Furthermore, the very existence of inelastic collisions among the molecules in the process of thermal diffusion might be detected and improved with certainty through such rigorous study.

Acknowledgement

The authors are thankful to Mr. S. K. Sit MSc. for helpful discussion and Dr. A. K. Chatterjee for the initial participation in this work. At last, the authors are grateful to acknowledge the financial support extended by the Physical Society of Japan towards publication of this paper.

1) S. Chapman and T. G. Cowling: *The Mathematical Theory of Non Uniform Gases* (Cambridge University Press, NY, 1952).
2) W. H. Furry and R. C. Jones: Phys. Rev. **69** (1946) 459.
3) J. L. Navarro, J. A. Madariage and J. M. Saviron: J. Phys. Soc. Jpn. **50** (1983) 1603.
4) R. C. Jones and W. H. Furry: Mod. Phys. **18** (1946) 151.
5) S. Acharyya, I. L. Saha, A. K. Datta and A. K. Chatterjee: J. Phys. Soc. Jpn. **56** (1987) 105.
6) A. K. Datta, G. Dasgupta and S. Acharyya: J. Phys. Soc. Jpn. **59** (1990) 3602.
7) A. K. Datta and S. Acharyya: J. Phys. Soc. Jpn. **62** (1993) 1527.
8) G. Dasgupta, A. K. Datta and S. Acharyya: Pramana **43** (1994) 81.
9) T. I. Moran and W. W. Watson: Phys. Rev. **111** (1957) 380.
10) F. Vandervolk: Ph. D Dissertation, 1963.
11) R. Paul, A. J. Howard and W. W. Watson: J. Chem. Phys. **39** (1963) 3053.
12) H. Brown: Phys. Rev. **58** (1940) 661.
13) B. N. Srivastava and K. P. Srivastava: Physica **23** (1957) 103.
14) B. N. Srivastava and M. P. Madan: Proc. Phys. Soc. London **66** (1953) 277.
15) G. Vasaru: *Thermal Diffusion Column*, supplied by S. Raman (B.A.R.C., Bombay).
16) C. J. G. Slieker: Z. Naturforsch. **20** (1965) 591.
17) G. Dasgupta, N. Ghosh, N. Nandi, A. K. Chatterjee and S. Acharyya: J. Phys. Soc. Jpn. **65** (1996) 2506.
18) Max Klein and F. J. Smith: Tables of collision integral for the $(m, 6)$ potential for the values of m, Arnold Engineering Development Centre, Air Force Systems Command Arnold Air Force Station Tennessee, 1968.

J. Phys. D: Appl. Phys. 31 (1998) 1092–1099. Printed in the UK PII: S0022-3727(98)82549-7

The functional relationship of the column calibration factor in thermal diffusion column measurement

G Dasgupta and S Acharyya

Department of Physics, Raiganj College (University College), PO Raiganj, District Uttar Dinajpur, West Bengal, PIN 733134, India

Received 12 March 1997, in final form 17 December 1997

Abstract. An approximate formulation of the column calibration factor (CCF), F_s, at any given temperature $\overline{T}$ is derived for thermal diffusion columns (TDC) from the Navier–Stokes equation in cylindrical coordinates. The values of F_s are then used to estimate the experimental thermal diffusion factor α_T of a neon gas mixture with its natural isotopic abundances from $\ln q_{max}$ measured in four columns of different column geometries. The molecular force parameters of the molecule are estimated from the intercepts and slopes of the linear variations of α_T and the collision integral C_{ij}^* against $1/\overline{T}$ and $1/\overline{T}^*$ respectively. The excellent agreement of the estimated force parameters with the available literature values and the comparison of the temperature variation of α_T by the CCF method with the existing experimental and theoretical ones establish the fact that the derived relationship of F_s with the column geometries is more than adequate.

Mathematical symbols used in the text and tables

F_s	column calibration factor (CCF)
α_T	thermal diffusion factor (TDF)
$\overline{T}$	mean temperature $\overline{T} = (T_h + T_c)/2$
T_h	temperature of hot wall of radius r_h
T_c	temperature of cold wall of radius r_c
C_{ij}^*	collision integral
q_e	equilibrium separation factor defined by $q_e = (x_i/x_j)_{top}/(x_i/x_j)_{bottom}$
x_i	mass or mole fraction of the ith component
ϵ_{ij}	depth of the potential well
σ_{ij}	molecular diameter
L	length of the column
q_{max}	maximum value of separation factor at optimum pressure p_{opt}
λ_{ij}	coefficient of thermal conductivity of a binary gas mixture
η_{ij}	coefficient of viscosity of a binary gas mixture
H	column transport coefficient
K_c	column remixing coefficient
K_d	back diffusion coefficient
D_{ij}	diffusion coefficient
h', k_c' and k_d'	Maxwell-model-dependent column shape factors (CSF) and
$(SF)_1$, $(SF)_3$ and $\pi(1-a^2)$	Slieker-model-independent CSFs.

1. Introduction

The thermal diffusion column (TDC) is a very useful device for concentrating impurities of a gas. The enrichment of impurities becomes squared when the length of the column is doubled. The TDC is also used to determine the thermal diffusion factor α_T of any isotopic or non-isotopic gas mixture. The column theory, on the other hand, may be improved by the accurate experimental determination of α_T of the binary gas mixture in a column. Again, the close correlation of α_T with the molecular force parameters allows one to locate the exact force parameters of the interacting molecules. Thus, both from experimental and from theoretical points of view, an accurate estimation of α_T is necessary.

In the absence of a theoretical possibility of estimating the actual experimental α_T from the existing column theory, Acharyya *et al* [1] and Datta *et al* [2], however, introduced a scaling factor F_s called the column calibration factor (CCF) into the relation:

$$\ln q_{max} = \alpha_T F_s(r_c, r_h, L, \overline{T}). \tag{1}$$

r_c and r_h are the cold and hot wall radii of a given column of geometrical length L and $\overline{T} = (T_h + T_c)/2$, T_h and T_c being the hot and cold wall temperatures in kelvins respectively. Here $\ln q_{max}$ is the maximum value of $\ln q_e$ at the optimum pressure and q_e is the equilibrium separation factor. Although, the model independency of F_s is well established [3] for its important role in the estimation of reliable α_T [1–4], the functional relationship of F_s with r_c, r_h, L and $\overline{T}$ remains unknown.

0022-3727/98/091092+08$19.50

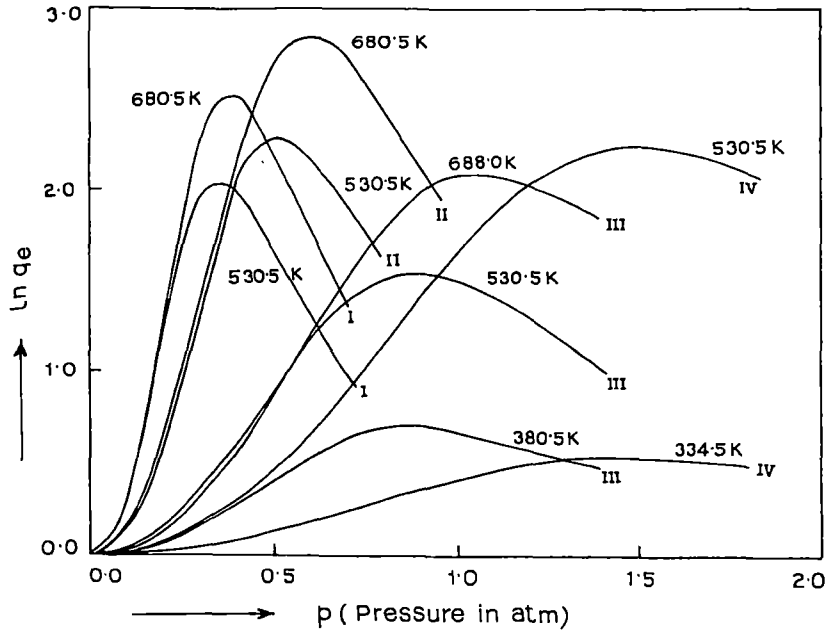

Figure 1. A plot of $\ln q_e$ against the pressure p in atmospheres of Ne^{20}–Ne^{22} mixtures: curve I, for column I at 530.5 K and 680.5 K; curve II, for column II at 530.5 K and 680.5 K; curve III, for column III at 380.5 K, 530.5 K and 688.0 K; and curve IV, for column IV at 334.5 K and 530.5 K.

Rutherford and Kaminsky [5] had measured the column coefficients H', K_c' and K_d' using Ne^{20}–Ne^{22} gas mixtures with their natural isotopic abundances at various experimental temperatures in four different columns; see table 1. The hot Nichrome V wire of their [5] I, II and III TD columns had radius $r_h = 8 \times 10^{-4}$ m. Their column IV was a thin-walled Nichrome V tube of radius $r_h = 3.2 \times 10^{-3}$ m. The radii of water-cooled metal tubes of all these columns were $r_c = 1.6 \times 10^{-2}$ m, 1.27×10^{-2} m, 9.43×10^{-3} m and 9.43×10^{-3} m respectively. The geometrical length of columns I and II was $L = 3.05$ m whereas columns III and IV had $L = 1.524$ m. This inspired us to observe α_T values from the pressure dependences of $\ln q_e$ values of Ne^{20}–Ne^{22} mixtures at the experimental temperatures. The $\ln q_e$ of Ne^{20}–Ne^{22} gas mixtures as a function of the atmospheric pressure are shown in figure 1 by the least square fitted curves for these columns. The H', K_c' and K_d' [5] are used to study the temperature dependence of α_T and hence the molecular force parameters of neon. The experimental α_T values due to Maxwell's model-dependent and Slieker's model-independent column shape factors (CSF) together with the theoretical α_T values based on Chapman–Enskog gas kinetic theory [6] were also estimated. They are plotted against $\overline{T}$ in figure 2 for comparison. The experimental and theoretical F_s as well as the estimated experimental and theoretical α_T values are presented in tables 1 and 2 respectively. The theoretical formulation of F_s is, however, derived in section 3 and is compared with the experimental F_s as seen in figure 3.

The plots of α_T against $\overline{T}$ obtained by the CCF method and of the collision integral C_{ij}^* against the reduced temperature $\overline{T}^*$ were simultaneously used to calculate the force parameters ϵ_{ii}/k or ϵ_{jj}/k of the isotopic components of neon. ϵ_{ii}/k or ϵ_{jj}/k are the depths of the potential well (see section 4). The molecular diameters σ_{ii} or σ_{jj} were then obtained from the coefficients of viscosity with the estimated force parameters (see table 3). The excellent agreement of the force parameters with the literature values (table 2) and the close agreement of α_T obtained by the CCF method with the theoretical ones as seen in table 2 and figure 2 establish the fact that the derived relationship of F_s is reliable.

2. Formulations of the experimental thermal diffusion factor

Both ends being closed in an ideal TD column of length L, $\ln q_e$ is given by

$$\ln q_e = HL/(K_c + K_d) \tag{2}$$

where q_e is defined by

$$q_e = (x_i/x_j)_{top}/(x_i/x_j)_{bottom}.$$

$(x_i/x_j)_{top}$ and $(x_i/x_j)_{bottom}$ represent the ratio of mole or mass fractions of lighter (i) and heavier (j) components of a binary gas mixture at the top and at the bottom of a TD column of geometrical length L. The column coefficients H, K_c and K_d are proportional to the second, fourth and zeroth powers of the pressure p in atmospheres respectively. On writing $H = H'p^2$, $K_c = K_c'p^4$ and $K_d = K_d'$, equation (2) can be put into the form

$$\ln q_e = \frac{(H'L/K_c')p^2}{(K_d'/K_c') + p^4}$$

or

$$p^2/\ln q_e = b'/a' + (1/a')p^4 \tag{3}$$

where $a' = (H'L/K_c')$ and $b' = (K_d'/K_c')$. The experimental parameters a' and b' of table 1 govern

Table 1. The geometry of the columns with length L, cold wall radius r_c and hot wall radius r_h together with column constants G_1 and G_2, column calibration factor F_s, a', b' and $\ln q_{max}$.

Geometry of the column in m	Hot wall temp. T_h (K)	Cold wall temp. T_c (K)	Mean temp. $\overline{T}$ (K)	a' (atm^2)	b' (atm^4)	$\ln q_{max}$	Column constant $G_1(10^3)$	Column constant $G_2(10^4)$	Theoretical F_s from equation (14)	Experimental F_s
Column I										
$L = 3.05$	773	288	530.5	0.5184	0.0158	2.0621	9.4145		67.8322	76.3741
$r_c = 1.6 \times 10^{-2}$								3.4997		
$r_h = 8.0 \times 10^{-4}$	1073	288	680.5	0.7367	0.0211	2.5358	11.6400		83.9669	91.8768
Column II										
$L = 3.05$	773	288	530.5	1.1982	0.0684	2.2907	9.6822		88.7777	84.8407
$r_c = 1.27 \times 10^{-2}$								3.4138		
$r_h = 8.0 \times 10^{-4}$	1073	288	680.5	2.0376	0.1282	2.8460	11.9803		110.3101	103.1159
Column III										
$L = 1.524$	473	288	380.5	1.0358	0.5498	0.6985	5.6300		33.8041	27.0736
$r_c = 9.43 \times 10^{-3}$	773	288	530.5	2.3547	0.5902	1.5327	10.0152	3.6486	60.1340	56.7667
$r_h = 8.0 \times 10^{-4}$	1088	288	688.0	4.7567	1.2955	2.0896	12.4915		75.0028	75.7101
Column IV										
$L = 1.524$	381	288	334.5	2.3265	4.6460	0.5397	3.3865		27.1315	21.5880
$r_c = 9.43 \times 10^{-3}$								2.2993		
$r_h = 3.2 \times 10^{-3}$	773	288	530.5	10.2385	5.2510	2.2340	10.4788		83.9535	82.7407

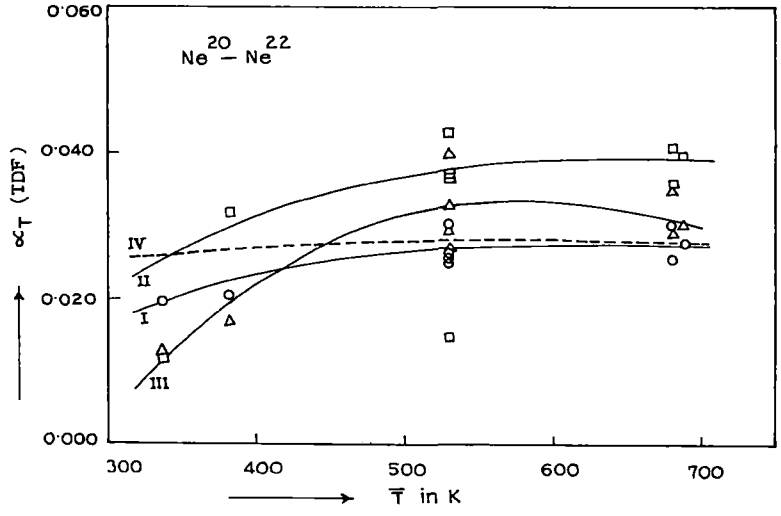

Figure 2. A plot of TD factor α_T of Ne^{20}–Ne^{22} against $\overline{T}$ in kelvins: curve I, (○), by the CCF method; curve II, (□), due to the Slieker CSF; curve III, (△), due to the Maxwell CSF; and curve IV, (···), due to the elastic collision theory.

the variation of the experimental $\ln q_e$ as a function of the pressure p in atmospheres at a given temperature. They were obtained from the measured values of H', K_c' and K_d' by Rutherford and Kaminsky [5]. The pressure dependences of $\ln q_e$ thus estimated are illustrated graphically in figure 1 by the fitted curves for four columns I, II, III and IV at various experimental temperatures. It is evident from equation (3) that, in each case seen in figure 1, as p increases $\ln q_e$ of the gas mixture increases and eventually reaches a maximum value of $\ln q_{max}$ given by

$$\ln q_{max} = \frac{a'}{2\sqrt{b'}} \tag{4}$$

at the optimum pressure p_{opt} given by $p_{opt} = (b')^{1/4}$ for which $(\partial/\partial p) \ln q_e = 0$. The experimental α_T or often the experimental F_s is obtained by using equations (1) and (4) in terms of F_s and $\ln q_{max}$ or α_T and $\ln q_{max}$.

Again, equation (2) on maximization becomes

$$\ln q_{max} = \frac{HL}{2(K_c K_d)^{1/2}}. \tag{5}$$

The column coefficients H, K_c and K_d based on Maxwell-model-dependent CSF h', k_c' and k_d' [7] are

$$H = \frac{2\pi}{6!}\left(\frac{\alpha_T \rho_{ij}^2 g}{\eta_{ij}}\right)\frac{1}{2}(r_c + r_h)(r_c - r_h)^3\left(\frac{\Delta T}{\overline{T}}\right)^2 h'$$

$$K_c = \frac{2\pi}{9!}\left(\frac{\rho_{ij}^3 g^2}{\eta_{ij}^2 D_{ij}}\right)_1\frac{1}{2}(r_c + r_h)(r_c - r_h)^7\left(\frac{\Delta T}{\overline{T}}\right)^2 k_c'$$

$$K_d = 2\pi(\rho_{ij} D_{ij})\frac{1}{2}(r_c + r_h)(r_c - r_h)k_d'.$$

Table 2. Experimental and theoretical α_T at various experimental temperatures together with estimated force parameters ϵ_{ij}/k and molecular diameters σ_{ij}.

Column	Mean temp. $\overline{T}$ (K)	Experimental α_T using F_s of equation (14)	Slieker's shape factor	Maxwell's shape factor	Theoretical α_T using equation (15)	Estimated ϵ_{ij}/k (K)	Estimated σ_{ij} (10^{10} m)	Reported ϵ_{ij}/k (K)	Reported σ_{ij} (10^{10} m)
Column I	530.5	0.030	0.043	0.040	0.028				
	680.5	0.030	0.042	0.035	0.028				
Column II	530.5	0.026	0.037	0.033	0.028				
	680.5	0.026	0.036	0.029	0.028			47.0[a]	2.72[a]
						48.58	2.69		
								41.186[b]	3.07[b]
Column III	380.5	0.021	0.032	0.017	0.027				
	530.5	0.026	0.037	0.030	0.028				
	688.0	0.028	0.040	0.030	0.028				
Column IV	334.5	0.020	0.012	0.013	0.026				
	530.5	0.027	0.015	0.027	0.028				

[a] Clifford *et al* (1977) [13].
[b] Aziz (1976) [13].

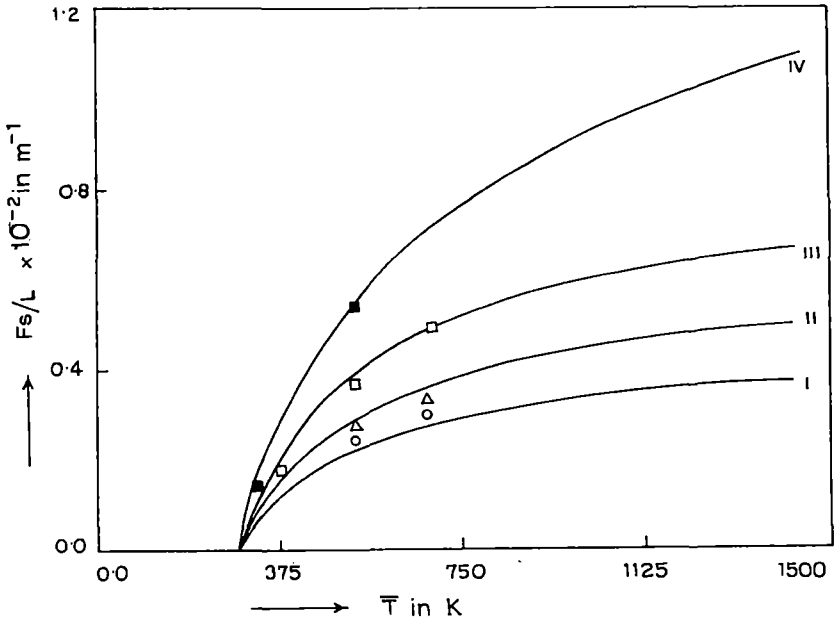

Figure 3. A plot of the theoretical F_s (equation (14)) with the experimental F_s on it against $\overline{T}$ in kelvins: curve I, for column I, (○), experimental points; curve II, for column II, (△), experimental points; curve III, for column III, (□), experimental points; and curve IV, for column IV, (■), experimental points.

The experimental α_T due to the Maxwell-model-dependent CSF is thus

$$\alpha_T(\text{Maxwell model}) = 2.39\frac{r_c - r_h}{L}\frac{\overline{T}}{\Delta T}\frac{(k'_c k'_d)^{1/2}}{h'}\ln q_{max} \tag{6}$$

where $\Delta T = T_h - T_c$. Similarly the column coefficients due to the model-independent Slieker's [8] CSF $(SF)_1$, $\pi(1-a^2)$ and $(SF)_3$ are

$$H = (SF)_1 r_c^4 \frac{\alpha_T \rho_{ij}^2 g}{\eta_{ij}}\left(\frac{\Delta T}{\overline{T}}\right)^2$$

$$K_d = \pi(1-a^2) r_c^2 \rho_{ij} D_{ij}$$

$$K_c = (SF)_3 r_c^8 \left(\frac{\rho_{ij}^3 g^2}{\eta_{ij}^2 D_{ij}}\right)_1 \left(\frac{\Delta T}{\overline{T}}\right)^2$$

where $a = r_h/r_c$. Using Slieker's CSF, α_T is given by

$$\alpha_T(\text{Slieker}) = 2.0\frac{r_c}{L}\frac{\overline{T}}{\Delta T}\frac{[\pi(1-a^2)(SF)_3]^{1/2}}{(SF)_1}\ln q_{max}. \tag{7}$$

The experimental α_T values using the CSF were obtained from equations (6) and (7) together with those by the CCF method from equations (1) and (4) in terms of measured $\ln q_{max}$ and F_s. All these α_T values are placed in table 2 for comparison with the theoretical ones. They are also shown graphically in figure 2 with respect to $\overline{T}$ for Ne^{20}–Ne^{22}

Table 3. Maxwell-model-dependent and Slieker-model-independent column shape factors, coefficient of viscosity η_{ij} and thermal conductivity λ_{ij} of Ne^{20}–Ne^{22} gas mixture.

Column	Mean temp $\overline{T}$ (K)	Column shape factor: Maxwell h'	Maxwell k_c'	Maxwell k_d'	Slieker $(SF)_1(10^3)$	Slieker $(SF)_3(10^6)$	η_{ij} (10^5 kg m^{-1} s^{-1})	η_{ij} (10^2 cal m^{-1} s^{-1} K^{-1})
	530.5	1.035	3.300	0.700			5.0333	1.7900
Column I					1.3639	1.9717		
	680.5	1.585	6.075	0.725			6.2543	2.2236
	530.5	1.060	3.100	0.715			5.0333	1.7900
Column II					1.3914	1.9140		
	680.5	1.600	5.525	0.740			6.2543	2.2236
	380.5	0.800	1.050	0.745			3.8123	1.3558
Column III	530.5	1.120	2.975	0.750	1.2838	1.6646	5.0333	1.7900
	688.0	1.590	4.975	0.770			6.3153	2.2459
	334.5	0.970	0.500	0.912			3.4378	1.2226
Column IV					239.23	4662.2		
	530.5	1.185	1.775	0.925			5.0333	1.7900

gas mixtures. The corresponding CSFs based on Maxwell-model-dependent and Slieker-model-independent methods are entered in table 3.

3. The theoretical formulation of the column calibration factor

The column parameters in cylindrical coordinates derived from the most elementary theory of the thermal diffusion column by Cohen [9] are

$$H = -2\pi \int_{r_h}^{r_c} \alpha_T \frac{\partial}{\partial r}(\ln T)\,\mathrm{d}r \left(\int_{r_h}^{r} \rho_{ij} v r\,\mathrm{d}r \right),$$

$$K_c = 2\pi \int_{r_h}^{r_c} \frac{\mathrm{d}r}{\rho_{ij} D_{ij} r} \left(\int_{r_h}^{r} \rho_{ij} v r\,\mathrm{d}r \right)^2$$

$$\text{and } K_d = 2\pi \int_{r_h}^{r_c} \rho_{ij} D_{ij} r\,\mathrm{d}r$$

which can, however, be approximated almost in the same manner as was done earlier by Slieker [8]. Here ρ_{ij} and D_{ij} are the density and diffusion coefficients of the gas mixture, r is the radial coordinate and T is the absolute temperature in kelvins.

Under the influence of the temperature gradient along the horizontal plane of the column, the convective velocity v of the molecule in the vertical direction is obtained from the Navier–Stokes equation in cylindrical coordinates:

$$\frac{\partial^3 v}{\partial r^3} + \frac{1}{r}\frac{\partial^2 v}{\partial r^2} - \frac{1}{r^2}\frac{\partial v}{\partial r} = \frac{\rho_{ij} g}{\eta_{ij} \overline{T}} \frac{\mathrm{d}T}{\mathrm{d}r}.$$

If we consider the rectilinear flow of heat from the hot wire or wall of temperature T_h to the cold wall of temperature T_c of a TDC, the temperature T is given by

$$T = T_h - \frac{\Delta T}{r_c - r_h}(r - r_h)$$

or

$$\frac{\mathrm{d}T}{\mathrm{d}r} = -\frac{\Delta T}{r_c - r_h}.$$

Putting $r = e^x$ and solving the above equation, we get

$$v = C_1 + C_2 \ln r + C_3 r^2 - \frac{\rho_{ij} g}{\eta_{ij} \overline{T}} \frac{\Delta T}{(r_c - r_h)} \frac{r^3}{9}$$

$$= G r_c^2 (K_1 + K_2 \ln \phi + K_3 \phi^2 + \phi^3) \qquad (8)$$

where

$$K_1 = \frac{C_1}{G r_c^2} + \frac{C_2}{G r_c^2} \ln r_c,$$

$$K_2 = \frac{C_2}{G r_c^2}, \qquad K_3 = C_3/G$$

$$\text{and } G = \frac{\rho_{ij} g}{\eta_{ij} \overline{T}} \frac{\Delta T}{(a-1)} \frac{1}{9}.$$

C_1, C_2 and C_3 being the integration constants, $\phi = r/r_c$ is the new variable and $a = r_h/r_c$. The boundary conditions are

(i) $v = 0$ at $r = r_c$ for which $\phi = 1$,

(ii) $v = 0$ at $r = r_h$ for which $\phi = a$ and since there is no transport of components of the gas mixture at equilibrium in the vertical direction up and down the column, we have

(iii) $r_c^2 \int_a^1 \rho v \phi\,\mathrm{d}\phi = 0$.

Here, K_1, K_2 and K_3 are dimensionless constants which are, however, given explicitly in terms of $a(= r_h/r_c)$ of a TDC by applying the boundary conditions mentioned above:

$$K_1 = \frac{5a^2(1-a)(1+2a^2\ln a - a^2) + \ln a}{5(a^2-1)^2 + 5(1-2a^4)\ln a},$$

$$K_2 = \frac{5a^2(1-a)(1-2a^2) - (1-a^2)}{5(a^2-1)^2 + 5(1-2a^4)\ln a}$$

$$\text{and } K_3 = -(K_1 + 1).$$

The column coefficients H, K_c and K_d are now derived as follows:

$$H = -2\pi r_c^2 \int_a^1 \alpha_T \frac{\partial}{\partial \phi}(\ln T)\,\mathrm{d}\phi \int_a^{\phi} \rho_{ij} v \phi\,\mathrm{d}\phi$$

$$= 2\pi\alpha_T \frac{\Delta T}{1-a}\rho_{ij} G r_c^4 \times \int_a^1 \frac{1}{T}\left(\frac{K_1\phi^2}{2} + \frac{K_2\phi^2}{2}\left(\ln\phi - \frac{1}{2}\right) + \frac{K_3\phi^4}{4} + \frac{\phi^5}{5} + K_4\right) d\phi$$

where

$$K_4 = -\frac{a^2}{2}\left[K_1 + K_2\left(\ln a - \frac{1}{2}\right) + \frac{K_3 a^2}{2} + \frac{2a^3}{5}\right].$$

Here, the temperature and composition dependences of η_{ij}, ρ_{ij}, D_{ij} and α_T are not taken into account [7–9] and the above equation for H becomes

$$H = 2\pi\alpha_T r_c^4 \frac{\rho_{ij}^2 g}{\eta_{ij}\overline{T}} \frac{\Delta T}{(a-1)} \frac{1}{9} G_1 \tag{9}$$

where

$$G_1 = \frac{\Delta T}{\overline{T}(1-a)}\left(\frac{2K_1 - K_2}{12}(1-a^3) - \frac{K_2}{18}(1-a^3) - \frac{K_2 a^3}{6}\ln a + \frac{K_3}{20} + K_4(1-a) + \frac{1}{30}\right) - \left(\frac{\Delta T}{\overline{T}(1-a)}\right)^2\left[\frac{2K_1 - K_2}{48} - \frac{K_2}{24}\left(\frac{7}{12} + a^4\ln a\right) + \frac{K_3}{120} + \frac{K_4}{2}(1-a^2) + \frac{1}{210}\right] + \left(\frac{\Delta T}{\overline{T}(1-a)}\right)^3\left(\frac{2K_1 - K_2}{240} - \frac{47K_2}{7200} + \frac{K_3}{840} + \frac{K_4}{6}(1-a^3) + \frac{1}{1680}\right) \tag{10}$$

retaining the term containing up to the third power of $\Delta T/[\overline{T}(1-a)]$ because the contributions of higher terms are negligibly small. Again, a^n is very small compared with unity for $n \geq 4$.

The coefficient K_c of a TDC is given by

$$K_c = 2\pi \int_a^1 \frac{d\phi}{\rho_{ij} D_{ij}\phi}\left(\int_a^\phi \rho_{ij} v\phi\, d\phi\right)^2 = \frac{2\pi\rho_{ij} G^2 r_c^8}{D_{ij}} \int_a^1 \frac{1}{\phi}\left(\frac{K_1\phi^2}{2} + \frac{K_2\phi^2}{2}\left(\ln\phi - \frac{1}{2}\right) + \frac{K_3\phi^4}{4} + \frac{\phi^5}{5} + K_4\right)^2 d\phi = \frac{2\pi\rho_{ij}^3 g^2}{\eta_{ij}^2 D_{ij}}\left(\frac{\Delta T}{\overline{T}}\right)^2 \frac{r_c^8}{81(1-a)^2} G_2 \tag{11}$$

where

$$G_2 = \frac{K_1^2}{16} + \frac{5K_2^2}{128} - K_4^2\ln a + \frac{K_3^2}{128} - \frac{3K_1K_2}{32} + \frac{K_1K_3}{24} + \frac{K_1K_4}{2}(1-a^2) - \frac{K_2K_3}{36} + \frac{K_3K_4}{8} - \frac{K_2K_4}{4}(2 + 2a^2\ln a - a^2) + \frac{K_1}{35} - \frac{9K_2}{490} + \frac{K_3}{90} + \frac{2K_4}{25} + \frac{1}{250} \tag{12}$$

and the coefficient K_d of a TDC is obtained from

$$K_d = 2\pi r_c^2 \int_a^1 \rho_{ij} D_{ij}\phi\, d\phi = \pi r_c^2 \rho_{ij} D_{ij}(1-a^2). \tag{13}$$

Thus the CCF per unit length, F_s/L, is finally obtained from equation (5) with the help of equations (9)–(13). It is given by

$$F_s/L = \frac{G_1}{r_c[2(1-a^2)G_2]^{1/2}}. \tag{14}$$

The theoretical CCF per unit length of any TD column can thus be approximated in terms of G_1, G_2, a and r_c of the column. The values of formulated F_s are placed in table 1 for columns I, II, III and IV. They are shown in figure 3 together with the experimental F_s/L obtained from $\ln q_{max}$ and known α_T values of Ne^{20}–Ne^{22} gas mixtures. F_s/L of equation (14) plays an important role in determining α_T of any binary gas mixture [1–4]. Because its model independence is well established [3], F_s/L can safely be used to concentrate impurities of any gas to any desired level in TDC experiments.

4. Force parameters from the TD factor

The theoretical α_T based on Chapman–Enskog gas kinetic theory [6] is given by

$$\alpha_T = g(6C_{ij}^* - 5) \tag{15}$$

where

$$g = \frac{1}{6\lambda_{ij}} \frac{S^{(i)}x_i - S^{(j)}x_j}{X_\lambda + Y_\lambda}$$

is a complicated function of the composition of the gas mixture and of the thermal conductivity λ_{ij} whereas $(6C_{ij}^* - 5)$ strongly depends on the temperature. The λ_{ij} terms are, however, obtained from the η_{ij} terms by using the relation

$$\lambda_{ij} = \frac{15}{4}\frac{R}{M}\eta_{ij}.$$

The experimental values of η_{ij} of the Ne^{20}–Ne^{22} gas mixture are taken from Yamamoto *et al* [10]. The estimated theoretical α_T values for Ne^{20}–Ne^{22} are shown by curve IV of figure 2, in which they are compared with α_T values obtained by the existing method, curve II and curve III, due to the Maxwell and Slieker CSFs as well as with α_T values of curve I obtained by the CCF method.

Now, the slowly varying function of temperature g is given by [3, 11]

$$g = \frac{A}{6C - 5}.$$

A and C are two arbitrary constants. A is determined from α_T of the CCF method at two available temperatures $\overline{T}$ in kelvins and C from the reported data of C_{ij}^* versus $\overline{T}^*$ [12]. Using the relation

$$(6C_{ij}^* - 5) = \frac{(\alpha_T)_{expt}}{g} \tag{16}$$

the collision integral C_{ij}^* at the experimental temperature is determined. Now C_{ij}^* fixes $\overline{T}^*$ [12] where $\overline{T}^* = \overline{T}/(\epsilon/k)$

and hence ϵ_{ij}/k of the molecule is located. Because the variation of g with the temperature is very slow, the entire procedure with the initially estimated ϵ_{ij}/k is repeated to get the exact value of ϵ_{ij}/k. The molecular diameter σ_{ij} is then determined from the viscosity data [10] with the estimated ϵ_{ij}/k. It is worthy of mention that, in the case of isotopic components, the force parameters due to binary interactions ϵ_{ij}/k and σ_{ij} become ϵ_{ii}/k or ϵ_{jj}/k and σ_{ii} or σ_{jj} respectively.

5. Results and discussion

The equations of $p^2/\ln q_e$ against p^4 of Ne^{20}–Ne^{22} gas mixtures were, however, worked out in terms of the measured values of H', K_c' and K_d' [5] from the pressure dependences of $\ln q_e$ in four columns of different column geometries and at various experimental temperatures. They are for column I:

$$\frac{p^2}{\ln q_e} = \begin{cases} 0.0305 + 1.9290p^4 & \text{at } \overline{T} = 530.5 \text{ K} \\ 0.0286 + 1.3574p^4 & \text{at } \overline{T} = 680.5 \text{ K} \end{cases}$$

for column II:

$$\frac{p^2}{\ln q_e} = \begin{cases} 0.0571 + 0.8346p^4 & \text{at } \overline{T} = 530.5 \text{ K} \\ 0.0629 + 0.4908p^4 & \text{at } \overline{T} = 680.5 \text{ K} \end{cases}$$

for column III:

$$\frac{p^2}{\ln q_e} = \begin{cases} 0.5309 + 0.9654p^4 & \text{at } \overline{T} = 380.5 \text{ K} \\ 0.2506 + 0.4247p^4 & \text{at } \overline{T} = 530.5 \text{ K} \\ 0.2703 + 0.2102p^4 & \text{at } \overline{T} = 688.0 \text{ K} \end{cases}$$

for column IV:

$$\frac{p^2}{\ln q_e} = \begin{cases} 1.9970 + 0.4298p^4 & \text{at } \overline{T} = 334.5 \text{ K} \\ 0.5129 + 0.0977p^4 & \text{at } \overline{T} = 530.5 \text{ K}. \end{cases}$$

The variation of $\ln q_e$ with p in atmospheres is found to increase with increasing length L and r_h/r_c of the TD columns as shown in figure 1. p_{opt}, the optimum pressure at which $\ln q_e$ becomes maximum as observed in figure 1, also increases on going from column I to column IV for increasing r_h/r_c. The variation of $p^2/\ln q_e$ against p^4 is governed by a' and b' of equation (3). a' and b' were, however, obtained by applying a least square fitting technique to equation (3) with the experimental data of H', K_c' and K_d' [5]. They are placed in the fifth and sixth columns of table 1. $\ln q_{max}$ in terms of a' and b' of equation (4) are also placed in the seventh column of table 1.

An approximate formulation of theoretical F_s with the column geometry has been derived by considering the convective velocity of the molecules in a TD column from the Navier–Stokes equation in cylindrical coordinates. Rectilinear flow of heat from a hot wire or wall to a cold wall seems to be a better choice, unlike Slieker's derivation. Although the temperature and composition dependences of the transport parameters like ρ_{ij}, η_{ij}, D_{ij}, λ_{ij} and α_T were not taken into account, the derived relationship of F_s with the column geometry and the temperature is nonetheless reliable, simple and straightforward. This is strictly valid in the case of a hot wire or cryogenic wall or even for a hot wall column.

The column constants G_1 and G_2 depending on the column geometry and wall temperatures were worked out for four columns and are placed in the eighth and ninth columns of table 1. F_s/L of each column at experimental temperatures were then determined using equation (14) and are placed in the tenth column of table 1. G_1 and G_2 of equations (10) and (12) are dimensionless column constants, suggesting the fact that these parameters are independent of the molecular model. G_1 depends on $\Delta T/\overline{T}$ and r_h/r_c of a TDC whereas G_2 is expressed in terms of r_h/r_c alone. The physical meanings of G_1 and G_2 can be realized from equations (9) and (11). G_1 is related to the column transport coefficient H which is involved in the process of thermal diffusion, whereas G_2 is related to K_c, called the convective remixing coefficient, for convection occurring in a TD process. However, K_p and K_d are the longitudinal and back diffusion coefficients in a TDC. Nevertheless, G_1 and G_2 are of much importance for locating the exact values of F_s, α_T and p_{opt} at which $\ln q_e$ becomes maximum. The available α_T values of Ne^{20}–Ne^{22} gas mixtures, which are 0.0250, 0.0258, 0.0270, 0.0276 and 0.0276 at 334.5 K, 380.5 K, 530.5 K, 680.5 K and 688 K respectively [5], help one to get experimental F_s at various values of $\overline{T}$ from estimated $\ln q_{max}$ of equation (4) of the TD columns. The experimental F_s when plotted against $\overline{T}$ in figure 3 are in close agreement with theoretical F_s derived from equation (14) at various $\overline{T}$.

Using equation (1) the α_T values of Ne^{20}–Ne^{22} gas mixtures are estimated through theoretical F_s by the CCF method. These α_T values are presented in the third columns of table 2 and plotted against $\overline{T}$ in figure 2. The experimental α_T values obtained by the CCF method from $\ln q_{max}$ and F_s are found to fall almost on the same curve I and increase slowly with $\overline{T}$.

The slight disagreement between the experimental and theoretical F_s seen in figure 3 and table 1 results in a slight difference between the theoretical α_T values and the experimental ones obtained by the CCF method. This may, perhaps, arise due to the effect of parasitic remixing in the thermal diffusion process.

The molecular force parameters of Ne^{20}–Ne^{22} were estimated from the slope and the intercept of the α_T against $1/\overline{T}$ equation. The α_T at 500.0 and 600.0 K from curve 1 of figure 2 were found to obey an equation of the form $\alpha_T = 0.029\,13 - 1.125\,01(1/\overline{T})$. The molecular force parameters ϵ_{ii}/k or ϵ_{jj}/k of Ne^{20}–Ne^{22} were thus determined as explained elsewhere [3, 11]. The η_{ij} [10] of Ne^{20}–Ne^{22} were then used to obtain the molecular diameter σ_{ii} or σ_{jj}. The close agreement of the estimated force parameters, placed in table 2 with the reported ones [13], establishes the reliability of α_T as obtained by CCF method.

The α_T due to Slieker's CSF, as seen in table 3, are calculated from equation (7) and are placed in the fourth column of table 2. These α_T values, although slightly higher in magnitude than the α_T values obtained by the CCF method, are plotted with $\overline{T}$ in figure 2 on curve II. The α_T

values from $\ln q_{max}$ of column IV are scattered (figure 2), but still maintain the same trend as that of the CCF method. The magnitudes of the Maxwell-model-dependent CSF are really very difficult to locate exactly. They were, however, obtained by interpolation and extrapolation from the data of Văsaru [7] and placed in table 3. The probable temperature dependence of α_T using the Maxwell-model-dependent CSF was then obtained from equation (6) and shown in the fifth column of table 2. They are plotted with $\overline{T}$ in figure 2 on curve III, showing both the trend and the magnitude of α_T against $\overline{T}$. It fails to accord with α_T obtained by the other methods. The theoretical α_T values based on elastic collisions among molecules were also calculated from equation (15) at 334.5 K, 380.5 K, 530.5 K, 680.5 K and 688.0 K for Ne^{20}–Ne^{22} and placed in the sixth column of table 2. These are plotted against $\overline{T}$ on curve IV of figure 2. Both the magnitudes and the trends of these α_T values are more or less the same as those of the α_T values obtained from the CCF. It is also interesting to note that the theoretical α_T values of curve IV exhibit the same trend of increasing with temperature as do the α_T values obtained by the CCF method.

In fact, asymmetry in column geometry is an inherent property and as such it invited remixing. Thus in the TD column theory Furry and Jones [14] added a term K_p called the remixing coefficient, proportional to p^4 in the denominator of equation (2). Obviously in an ideal column K_p is supposed to be zero. Leyarovski *et al* [15] had shown that K_p never exceeds 20% of K_c. Thus, owing to remixing effects, the maximum error that creeps into F_s and hence into α_T is 9.54%. In spite of that the excellent agreement of the experimental α_T (curve I) and the theoretical α_T (curve IV) in figure 2 right from $T = 2T_c$ and onwards (figure 2) is evidence that equation (14) is reliable for F_s/L. Moreover, it indicates that K_p decreases with $\overline{T}$ and vanishes at and after $\overline{T} = 2T_c$; that is, remixing stops from $\overline{T} = 2T_c$ in a TD column.

The discussion above makes it clear that the theoretical formulation of the CCF, which is the central point of study in this paper, is a model-independent parameter, as observed earlier [1–4, 8, 16]. Furthermore, the α_T values obtained from the CCF with $\overline{T}$ of a binary gas mixture are convenient means of estimating the molecular force parameters like ϵ_{ij}/k and σ_{ij} of the molecules. The subject in this paper is thus related to the efficiency of the gas separation using thermal diffusion column to throw some light on the basic physical properties of a gas mixture through the CCF and α_T.

6. Conclusions

In fact, the theoretical background of the process of thermal diffusion simultaneously involved with longitudinal and back diffusion in a TDC is much too complicated. The presented mathematical formulation of equation (14), achieved so far, seems to be a significant improvement over the existing theories. Determination of F_s/L appears to be an important means of estimating the experimental α_T through $\ln q_{max}$, particularly when $\Delta T/\overline{T}$ is close to unity or $\overline{T} = 2T_c$ and afterwards. When $\Delta T/\overline{T}$ is well below unity the experimental α_T obtained by the CCF method differs from the theoretical α_T. Again, experimental α_T values obtained by using Slieker-model-independent and Maxwell-model-dependent CSFs are low compared with theoretical α_T values in the lower temperature region. Asymmetry in column geometry through K_p may be a reason for such a deviation. The theoretical α_T derived from the elastic collision theory is not in good agreement with experimental α_T for the non-spherical molecules. Even in the cases of spherical molecules, the agreement is no better. The model-independent parameter F_s/L of equation (14) thus ought to be used to estimate α_T for the pair of molecules concerned through experimental $\ln q_{max}$ in the TDC. The procedure of determining α_T by the CCF method is, therefore, necessary in order to improve the theory for obtaining α_T for elastic or inelastic collisions among the molecules [17]. The simultaneous use of reliable α_T by the CCF method and C_{ij}^* against $1/\overline{T}$ and $1/\overline{T}^*$ respectively appears to be a unique method of locating the exact force parameters of the molecules too.

Acknowledgments

The authors are grateful to Professor I L Saha and S K Sit for many helpful discussions during this work.

References

[1] Acharyya S, Saha I L, Datta A K and Chattarjee A K 1987 *J. Phys. Soc. Japan* **56** 105
[2] Datta A K, Dasgupta G and Acharyya S 1990 *J. Phys. Soc. Japan* **59** 3602
[3] Dasgupta G, Ghosh N, Nandi N and Acharyya S 1997 *J. Phys. Soc. Japan* **66** 108
[4] Datta A K and Acharyya S 1993 *J. Phys. Soc. Japan* **62** 1527
[5] Rutherford W M and Kaminsky K J 1967 *J. Chem. Phys.* **47** 5427
[6] Chapman S and Cowling T G 1952 *The Mathematical Theory of Non-uniform Gases* (London: Cambridge University Press)
[7] Văsaru G, Thermal diffusion column. Supplied by S Raman (Bombay: BARC)
[8] Slieker C J G 1964 *PhD Diss.* Amsterdam University
[9] Cohen K 1951 *The Theory of Isotope Separation* (New York: McGraw-Hill)
[10] Yamamoto I, Makino H and Kanagawa A 1990 *J. Nucl. Sci. Technol.* **27** 156
[11] Dasgupta G, Ghosh N, Nandi N, Chattarjee A K and Acharyya S 1996 *J. Phys. Soc. Japan* **65** 2506
[12] Klein M and Smith F J 1968 Tables of collision integral for the $(m, 6)$ potential for the values of m, Arnold Engineering Development Centre, Air Force Systems Command, Arnold Air Force Station, Tennessee
[13] Maitland G C, Rigby M, Smith E B and Wakeham W A 1981 *Intermolecular Forces: their Origin and Determination* (Oxford: Clarendon)
[14] Furry W H and Jones R C 1946 *Phys. Rev.* **69** 459
[15] Leyarovski E I, Georgiev J K and Zahariev A L 1988 *Int. J. Thermophys.* **9** 391
[16] Madariaga J A, Navarro J L, Saviron J M and Brun J L 1983 *J. Phys. A: Math. Gen.* **16** 1947
[17] Chattopadhyay T K and Acharyya S 1974 *J. Phys. B: At. Mol. Phys.* **7** 2277

After publication of this paper some calculations were found in errors. The paper in its correct form is presented in the 9th chapter of this thesis.